



Thèse

2022

Open Access

This version of the publication is provided by the author(s) and made available in accordance with the copyright holder(s).

The Role and Regulation of the Transcription Factor SP5 in *Hydra* Patterning

Iglesias Olle, Laura

How to cite

IGLESIAS OLLE, Laura. The Role and Regulation of the Transcription Factor SP5 in *Hydra* Patterning. Doctoral Thesis, 2022. doi: 10.13097/archive-ouverte/unige:164530

This publication URL: <https://archive-ouverte.unige.ch/unige:164530>

Publication DOI: [10.13097/archive-ouverte/unige:164530](https://doi.org/10.13097/archive-ouverte/unige:164530)

THE ROLE AND REGULATION OF THE TRANSCRIPTION FACTOR SP5
IN *HYDRA* PATTERNING

THÈSE

présentée aux Facultés de médecine et des sciences de l'Université de Genève
pour obtenir le grade de Docteur ès sciences en sciences de la vie,
mention Biosciences moléculaires

par

Laura IGLESIAS OLLÉ

de

Valls (Espagne)

Thèse N° nnnn

GENÈVE

Atelier d'Impression REPROMAIL

2022

Acknowledgements

I would like to start by thanking my thesis supervisor, Prof. Brigitte Galliot, for providing me the opportunity to complete both my PhD and master's theses in her lab and for allowing me to work on this intriguing project. I am very grateful for her trust and support, as well as her ongoing encouragement to advance my scientific knowledge and skills.

Following that, I would like to express my gratitude to the members of my thesis committee Prof. Ivan Rodriguez and Dr. Charisios Tsiairis, for their interest in my work and willingness to participate on my thesis jury.

Next, I want to thank all the members of Brigitte Galliot's laboratory, both present and former. First to Chrystelle Perruchoud, for being the best lab friend ever and for being willing to help with anything; to Nenad Suknovic, for his fruitful discussions; to Sarah Al Haddad for her kindness and advice; to Wanda Buzgariu, for her willingness to help at all times, as well as to Amélie, Sasha, Denis, Delphine, Quentin, Szymon, Yvan, Laura, Kazadi and Salima for their excellent support over these years and for their great scientific and non-scientific discussions. It was a real pleasure to work with all of you guys!

Special thanks to Dr. Matthias Vogg, who guided me during my master's thesis and shared his enthusiasm for science with me, and for his fruitful discussions. In addition, to Dr. Paul Gerald Layague Sanchez, who joined the lab lately but greatly helped me with the project and provided me good advice.

To my boyfriend, for his unconditional support throughout these years and for being able to comprehend my work schedule even from a distance. Thank you for coming here over the past few months to help me physically and psychologically, but most importantly, for always being supportive and encouraging me to believe in myself.

To my parents and my little sister for always believing in me and being a pillar of support for each decision I make, for teaching me how to pursue my goals and for assisting me in accomplishing them. To my parents-in-law for their help and kindness.

To all my friends from "Mandanga" and from "Prioritats", especially Ada, Alba, Eva, Judit F, Judit M, Silvia and Sandra; thank you girls for your friendship and for constantly making me feel like practically nothing has changed despite the distance. I love you!

Finally, to the friends I met during my time in Geneva: Chrystelle, Sarah, Laura BN, Quentin, Yvan, Nenad, Szymon, Nikolai, Adai, Pau, Pearl, Jöel, Laura B, ... for all the great times we spent having a beer, climbing, hiking, skiing or simply chatting around. Last but not least, a very special thanks to Arielle, Audrey, Chloe, Ilaria, Mireia and Aurélie for coming across my life during the PhD and continuing to be there. I just met you, girls, a few years ago, yet I already feel like you are a part of me, and those years would not have been possible without you. Thanks for always listening to me without judging, for understanding me and offering me good advice, for sticking by me in any of my moods, and for all the coffee breaks, adventures and experiences we have shared; I really want to make many more memories with you girls! I love you!

<i>Acknowledgements</i>	3
ABSTRACT	7
RESUME	9
<i>List of Figures</i>	11
<i>List of Tables</i>	15
<i>List of Abbreviations</i>	17
INTRODUCTION	19
1. WHOLE-BODY REGENERATION: A PHENOMENON ACROSS METAZOAN	19
2. <i>HYDRA</i> AS A MODEL SYSTEM TO STUDY REGENERATION	21
I. <i>Anatomy and morphology</i>	21
II. <i>Homeostatic and developmental properties of Hydra</i>	23
i. Asexual (budding) and sexual reproduction	24
ii. Regeneration	25
iii. Reaggregation.....	27
3. <i>HYDRA</i> , A MODEL ORGANISM TO STUDY ORGANIZER ACTIVITY	28
I. <i>Discovery of the concept of organizer</i>	28
II. <i>The activator and inhibitor components of the Hydra head organizer</i>	29
III. <i>Modeling of the two components of the Hydra head organizer</i>	32
IV. <i>Hydra, a model organism to study the molecular components of the organizer activity</i>	33
V. <i>Molecular nature of the head activator and head inhibitor in Hydra</i>	34
VI. <i>The inhibitory component of the head organizer</i>	35
4. THE IMPORTANCE OF WNT/ β -CATENIN SIGNALING IN INTACT AND REGENERATING <i>HYDRA</i>	35
I. <i>The Wnt/β-catenin signaling pathway is evolutionarily-conserved</i>	36
II. <i>Wnt/β-catenin signaling during bilaterian homeostasis, development, regeneration and disease</i>	38
5. THE SP/KLF FAMILY OF TRANSCRIPTION FACTORS	40
I. <i>Developmental role(s) of the Sp5 transcription factor in bilaterians</i>	41
II. <i>Sp5 as a downstream target of Wnt/β-catenin and FGF signaling pathways</i>	46
III. <i>The regulation of the transcription factor Sp5</i>	46
6. METHODOLOGICAL TOOLS DEVELOPED FOR <i>HYDRA</i>	48
7. AIMS OF THIS STUDY.....	51
RESULTS	53
CHAPTER-1 IDENTIFICATION OF THE <i>HYDRA</i> HEAD INHIBITOR	55
CHAPTER-2 AUTO-REGULATION STUDY OF THE <i>HYDRA</i> HEAD INHIBITOR SP5	97

DISCUSSION	173
1. CHALLENGES AND LIMITATIONS OF THE PROJECT	173
2. IDENTIFICATION OF THE TRANSCRIPTION FACTOR <i>Sp5</i> AS THE <i>HYDRA</i> HEAD INHIBITOR	175
3. SPATIO-TEMPORAL GFP DISTRIBUTION IN THE <i>Sp5</i> TRANSGENIC LINES	177
4. THE 3169BP OF THE <i>HYDRA Sp5</i> PROMOTER RESPOND TO <i>WNT</i> / β -CATENIN SIGNALING.....	180
5. THE NEGATIVE AUTO-REGULATION OF <i>Sp5</i>	181
6. TEMPORAL EXPRESSION OF <i>Wnt3</i> AND <i>Sp5</i>	183
7. GENERATION OF TRANSGENIC LINES WITH UNSTABLE REPORTER GENES TO FOLLOW THE REGULATION IN THE EPIDERMAL AND THE GASTRODERMAL LAYER	185
8. <i>Sp5</i> BINDS TO THE <i>HYDRA Sp5</i> PROMOTER	186
CONCLUSIONS AND PERSPECTIVES.....	187
REFERENCES.....	189
APENDIX 1: CONSTRUCT MAPS	201

ABSTRACT

The Wnt/ β -catenin signaling pathway is highly conserved in all metazoans, involved in numerous developmental processes and regulating stem cell proliferation in adulthood. Disruption of the Wnt/ β -catenin signaling pathway induces a range of abnormalities in embryonic development as well as important adult pathologies such as cancer. In *Hydra*, the Wnt/ β -catenin signaling pathway plays a key role in the apical organizer that maintains apical patterning and allows the development of new heads. The objective of this PhD project is to better understand the regulation of the Wnt/ β -catenin pathway during *Hydra* regeneration and maintenance of the apical organizer. We designed strategies to understand the dialogue between Wnt/ β -catenin signaling and Sp5 in the maintenance of the apical organizer in adult animals and in the formation of a new organizer during developmental processes such as budding and regeneration.

We first identified the transcription factor Sp5 as an inhibitor of the apical organizing center in *Hydra*, and show that this gene fulfills the five conditions necessary for an apical inhibitor. Briefly, this *Sp5* gene is (1) predominantly expressed in the head, with a graded expression profile from apical to basal; (2) up-regulated during apical regeneration; (3) its expression is induced by the Wnt/ β -catenin signaling pathway; (4) Sp5 inhibits the expression of *Wnt3* and *β -catenin*, thereby inhibiting the activity of this signaling pathway; and (5) Sp5 restricts apical development.

In the following chapter, we focused on the study of *Sp5* regulation *in vivo*. We generated two transgenic lines, which constitutively express either in the epidermal layer or in the gastrodermal layer a unique construct, whose tandem structure allows the expression of the mCherry reporter gene under the control of the *Hydra actin* gene promoter on the one hand, and the eGFP reporter gene under the control of the *Hydra Sp5* promoter on the other. This approach revealed that in the intact animal, especially in the apical organizer region, *Sp5* has a distinct spatial regulation in the epidermis and in the gastrodermis. During apical regeneration, the difference in expression between epidermis and gastrodermis is mainly quantitative during the first 24 hours, very low in the epidermis and massive in the gastrodermis.

Following treatment with alsterpaullone, which constitutively activates Wnt/ β -catenin signaling, *Sp5* expression is suppressed in the apical region, while two belts of maximal epidermal expression are transiently formed below the apical region and near the basal region. In parallel, *Sp5* is globally upregulated in the gastrodermis. Furthermore, the production of transgenic animals silenced for the *β -catenin* or the *Sp5* genes suggest that a negative autoregulation of Sp5 takes place extensively in the epidermis, more restrictedly in the gastrodermis. Knowing the prominent role of gastrodermal epithelial cells in the activity of the apical organizer, these results raise the question of the role of interactions between Sp5 and the Wnt/ β -catenin signaling pathway within and between the epidermis and gastrodermis in the context of the homeostatic apical organizer and the developmental apical organizer.

In conclusion, this study highlights the fine regulation of *Sp5*, a target gene of the Wnt/ β -catenin signaling pathway, as well as the putative interactions between Wnt3 and Sp5 in the different cell layers of *Hydra*, either in intact or developing animals, or in animals subjected to pharmacological or genetic perturbations. It also highlights in the model organism of *Hydra* expression patterns of *Sp5* and *Wnt3* that are different in the two modes of functioning of the apical organizer, homeostatic in adult animals on the one hand, dynamic because in the process of formation or newly formed on the other hand.

RESUME

La voie de signalisation Wnt/ β -catenin est hautement conservée chez les métazoaires, impliquée dans de nombreux processus du développement et régulant la prolifération des cellules souches à l'âge adulte. La perturbation de la voie de signalisation Wnt/ β -catenin induit une série d'anomalies congénitales ainsi qu'à d'importantes pathologies adultes telles que le cancer. Chez l'*Hydre*, la voie de signalisation Wnt/ β -catenin joue un rôle clé dans l'organisateur apical qui maintient le patron apical et permet le développement de nouvelles têtes. L'objectif de ce projet de doctorat est de mieux comprendre la régulation du processus d'inhibition de la voie Wnt/ β -catenin pendant la régénération de l'*Hydre* et le maintien de l'organisateur de la tête. Nous avons établi des stratégies pour comprendre le dialogue entre Sp5 et Wnt/ β -catenin dans le maintien de l'organisateur apical chez l'animal adulte et dans la formation d'un nouvel organisateur lors des processus de développement tels que le bourgeonnement et la régénération.

Nous avons tout d'abord identifié le facteur de transcription Sp5 comme inhibant le centre organisateur de la tête chez l'*Hydre*, et nous montrons que ce gène remplit les cinq conditions nécessaires à un inhibiteur de la tête. En bref, ce gène *Sp5* est (1) principalement exprimé dans la tête, avec un profil d'expression gradué d'apical à basal; (2) son expression est activée pendant la régénération de l'extrémité apicale; (3) son expression est induite par la voie de signalisation Wnt/ β -catenin; (4) Sp5 inhibe l'expression de *Wnt3* et *β -catenin*, inhibant de ce fait l'activité de cette voie de signalisation et (5) Sp5 restreint le développement de la tête.

Dans le chapitre suivant, nous nous sommes concentrés sur l'étude de la régulation de *Sp5 in vivo*. Nous avons généré deux lignées transgéniques, qui expriment de façon constitutive soit dans la couche épidermique, soit dans la couche gastrodermique une construction unique, dont la structure en tandem permet l'expression d'une part du gène rapporteur mCherry sous le contrôle du promoteur du gène d'actine, d'autre part le gène rapporteur eGFP sous le contrôle du promoteur *Sp5* d'*Hydre*. Cette approche a révélé que dans l'animal intact, en particulier dans la région de l'organisateur apical, *Sp5* a une régulation spatiale distincte dans l'épiderme et dans le gastroderme. Au

cours de la régénération apicale, la différence d'expression entre épiderme et gastroderme est principalement quantitative au cours des premières 24 heures, très faible dans l'épiderme et massive dans le gastroderme.

Suite au traitement à l'alsterpaullone, qui active la signalisation Wnt/ β -catenin de manière constitutive, l'expression épidermique de Sp5 est supprimée dans la région apicale, tandis que se forment transitoirement deux ceintures d'expression maximale sous la région apicale et à proximité de la région basale. Parallèlement, *Sp5* est globalement régulé à la hausse dans le gastroderme. Par ailleurs, la production d'animaux transgéniques rendus silencieux pour le gène *b-catenin* ou pour le gène Sp5 suggèrent qu'une autorégulation négative de Sp5 a lieu de façon importante dans l'épiderme, de façon plus restreinte dans le gastroderme. Sachant le rôle prépondérant des cellules épithéliales du gastroderme dans l'activité de l'organisateur apical, ces résultats posent la question du rôle des interactions entre Sp5 et la voie de signalisation Wnt/ β -catenin au sein et entre l'épiderme et le gastroderme dans le contexte de l'organisateur apical homéostatique et de l'organisateur apical développemental.

En conclusion, cette étude met en lumière la régulation fine de *Sp5*, un gène cible de la voie de signalisation Wnt/ β -catenin, ainsi que les interactions putatives entre *Wnt3* et *Sp5* dans les différentes couches cellulaires de l'*Hydre* qu'il s'agisse d'animaux intacts, en cours de développement ou soumis à des perturbations pharmacologiques ou génétiques. Elle met également en évidence dans l'organisme modèle de l'*Hydre* des patrons d'expression distincts au cours des deux modes de fonctionnement de l'organisateur apical, homeostatique chez l'animal adulte d'une part, dynamique car en cours de formation ou nouvellement formé d'autre part.

List of Figures

Introduction

- Figure 1: The ability of various organisms to regenerate
- Figure 2: Phylogenetic tree of the Cnidarian phylum and the various *Hydra* species
- Figure 3: *Hydra* anatomy
- Figure 4: Illustration of the two layers that constitute the *Hydra* polyp
- Figure 5: *Hydra* regeneration after mid-gastric bisection
- Figure 6: The dissociation-aggregation process of *Hydra*
- Figure 7: Scheme of the grafting experiment performed by Ethel Browne
- Figure 8: Schematic representation of the experiment performed in *Hydra* to demonstrate the presence of the inhibitory component
- Figure 9: Schematic representation of *Hydra* transplantation experiments that were performed to determine the levels of head activation (left) and head inhibition (right)
- Figure 10: Illustration of the non-linear activation-inhibition model proposed by Gierer and Meinhardt
- Figure 11: An overview of the canonical Wnt/ β -catenin signaling mechanism
- Figure 12: Structure of the nine SP proteins identified in humans
- Figure 13: Alignment of Sp5 in the described organisms

Results

Chapter 1

- Figure 1: Screening strategy to identify candidate head inhibitor genes in *Hydra*
 - Figure 2: Knocking down *HySp5* leads to the formation of ectopic axes and ectopic heads
 - Figure 3: HySp5 antagonizes Wnt/ β -catenin signaling in *Hydra*
 - Figure 4: *Hydra* Sp5 and zebrafish Sp5 repress the *Wnt3* promoter activity
 - Figure 5: Wnt/ β -catenin signaling regulates *HySp5* expression
 - Figure 6: *Hydra* Sp5 acts as a transcriptional activator and repressor
 - Figure 7: Working model of the feedback loop involving Wnt/ β -catenin/TCF and Sp5
- Sup Figure 1: Upstream and coding *Sp5* sequences in *Hydra vulgaris* Hm-105 strain

- Sup Figure 2: Evolutionarily-conserved structure of Sp5 transcription factors
- Sup Figure 3: Three Sp families, Sp1-4, Sp5 and Sp6-9, already diversified in the last common ancestor of cnidarians and bilaterians
- Sup Figure 4: *HySp5* expression patterns in intact and regenerating animals
- Sup Figure 5: *HySp5* and *Wnt3* expression in *Hydra* stem cell populations
- Sup Figure 6: Kinetics of *HySp5* phenotype occurrence in intact animals
- Sup Figure 7: Kinetics of *HySp5* phenotype occurrence in head regenerating animals
- Sup Figure 8: Knockdown of β -*catenin* delays head regeneration
- Sup Figure 9: *HySp5* phenotype occurrence requires active Wnt/ β -catenin signaling
- Sup Figure 10: *HySp5* antagonizes Wnt/ β -catenin signaling
- Sup Figure 11: Knockdown of *Sp5* in reaggregation studies
- Sup Figure 12: Kinetics of *Wnt3* expression in *Sp5*(RNAi) animals
- Sup Figure 13: Mapping of putative Sp5 binding sites in the *Wnt3* and *Sp5* upstream sequences in *Hydra* and teleost fish
- Sup Figure 14: *HySp5* expression in Alsterpaullone-treated animals
- Sup Figure 15: Interactions between Sp5 and β -catenin or TCF1
- Sup Figure 16: Genome-wide mapping of putative Sp5 binding sites in human HEK293T cells and mouse ESCs
- Sup Figure 17: Direct transcriptional targets of HySp5 and ZfSp5a
- Sup Figure 18: Overexpressing HySp5 in zebrafish embryos induces Wnt-like phenotypes

Chapter 2

- Figure 1: Epidermal-specific and gastrodermal-specific patterns of GFP fluorescence and *GFP* expression in *HySp5*-3169:GFP transgenic animals
- Figure 2: Developmental regulation of epidermal and gastrodermal GFP fluorescence in budding and regenerating *HySp5*-3169:GFP_{ep} and *HySp5*-3169:GFP_{ga} animals
- Figure 3: Morphological changes and *GFP*, *Wnt3* and *Sp5* ectopic expression induced by alsterpaullone (ALP) treatment in *HySp5*-3169:GFP and *HyWnt3*-2149:GFP animals
- Figure 4: Modulations of GFP fluorescence and *GFP* expression in *HySp5*-3169:GFP_{ep} animals knocked-down for β -*catenin*
- Figure 5: Ectopic GFP fluorescence and *GFP* expression in *HySp5*-3169:GFP animals knocked-down for *Sp5*
- Figure 6: ChIP-qPCR identification of Sp5-binding sites in the *HySp5* promoter
- Figure 7: Summary view of the layer-specific regulation of *Sp5* in *Hydra*

- Sup Figure 1: Epidermal and gastrodermal eGFP and mCherry fluorescences detected in live *HySp5-3169:GFP-ep* and *HySp5-3169:GFP-ga* transgenic animals
- Sup Figure 2: GFP fluorescence detected in live *HySp5-3169:GFP_ep* (A) and *HySp5-3169:GFP_ga* animals undergoing apical or basal regeneration
- Sup Figure 3: *GFP* expression in *HySp5-3169:GFP_ep* and *HySp5-3169:GFP_ga* animals undergoing apical (A) or basal (B) regeneration
- Sup Figure 4: Alsterpaullone (ALP)-induced modulations of *Sp5*, *Wnt3* and *GFP* expression in *Hv_AEP* animals
- Sup Figure 5: (A, B) Co-detection of *Sp5* and *Wnt3* expression in *HySp5-3169:GFP-ep* (A) and *HySp5-3169:GFP-ga* (B) transgenic animals exposed to Alsterpaullone (ALP)
- Sup Figure 5: (C, D) Co-detection of *GFP* and *Wnt3* expression in *HySp5-3169:GFP-ep* (C) and *HySp5-3169:GFP-ga* (D) transgenic animals exposed to Alsterpaullone (ALP)
- Sup Figure 6: (A, B) Co-detection of *Sp5* and *Wnt3* expression in *HyWnt3-2149:GFP-ep* (A) and *HyWnt3-2149:GFP-ga* (B) transgenic animals exposed to Alsterpaullone (ALP)
- Sup Figure 6: (C, D) Co-detection of *GFP* and *Wnt3* expression in *HyWnt3-2149:GFP-ep* (C) and *HyWnt3-2149:GFP-ga* (D) transgenic animals exposed to Alsterpaullone (ALP)
- Sup Figure 7: Ectopic "bump" structures along the body column of *Hv-Basal* animals knocked-down for *β -catenin*
- Sup Figure 8: Ectopic epidermal GFP fluorescence in *HySp5-3169:GFP_ep* animals knocked-down for *β -catenin*
- Sup Figure 9: GFP fluorescence and *GFP* expression in *HySp5-3169:GFP_ep* animals knocked-down for *Sp5*
- Sup Figure 10: Ectopic epidermal *GFP* expression in *HySp5-3169:GFP_ep* animals knocked-down for *Sp5*
- Sup Figure 11: GFP fluorescence and *GFP* expression in *HySp5-3169:GFP_ga* animals knocked-down for *Sp5*
- Sup Figure 12: Gastroermal *GFP* expression in *HySp5-3169:GFP_ga* animals knocked-down for *Sp5*
- Sup Figure 13: Transient ectopic *GFP* expression in *HySp5-3169:GFP Sp5 (RNAi)* animals 2 days post-EP2
- Sup Figure 14: ChIP-qPCR analysis of the Sp5-binding sites in the *Hydra Sp5* promoter using anti Hydra-Sp5 antibodies
- Appendix 1: Mapping the Sp5 Transcriptional Start Sites (TSS)
- Appendix 2: *HyActin-1388:mCherry-HySp5-3169:eGFP* map and sequences (10533bp)

Discussion, Conclusions and Perspectives

Figure 14: *Sp5* and *GFP* expression patterns by ISH

Figure 15: The knockdown of *Sp5* results in a multiple headed phenotype in *Hv_AEP* animals

Figure 16: *Sp5* functions as a transcriptional repressor on its own promoter

List of Tables

Chapter 1

Sup Table 1: Cloning, siRNAs, qPCR and CHIP-qPCR primer sequences

Sup Table 2: DNA constructs used in this study

Chapter 2

Sup Table 1: List of primers, siRNAs and ds-oligonucleotides

Sup Table 2: List of plasmids

Sup Table 3: List of transgenic lines

List of Abbreviations

ALP – Alsterpaullone
AP – anterior – posterior
APC – Adenomatous polyposis coli
BTD – Buttonhead
bp – base pairs
CDS – coding sequence
ChIP – Chromatin Immunoprecipitation
dpEP – days post electroporation
Dvl - Dishebeled
Fzd - Frizzled
GFP – green fluorescent protein
GSK3 β – Glycogen synthase kinase 3 beta
hpa – hours post amputation
hpEP – hours post electroporation
hPSCs – human pluripotent stem cells
KLF – Krüppel - like factor
LRP – Lipoprotein receptor - related protein
mESC – mouse embryonic stem cells
mpb – millions of base pairs
PCP – planar cell polarity (pathway)
pEP – post electroporation
RNAi – RNA interference
shRNA – short hairpin RNA
siRNA – small interfering RNA
Sp – Specificity protein
Sp5l – Sp5-like
TSS – Transcription start site

INTRODUCTION

1. Whole-Body regeneration: a phenomenon across metazoan

Regeneration is the process of replacing or restoring damaged or missing cells, tissues, organs, appendages or any other lost body parts to the original tissue architecture with the purpose to recapitulate its full function (Bely and Nyberg, 2010; Gurtner et al., 2008; Poss, 2010). Nonetheless, in most of the cases, injuries lead to a non-functioning mass of fibrotic tissue known as a scar (Gurtner et al., 2008). From a classical point of view, regeneration can be divided into two types: morphallaxis, which occurs when active cell proliferation is absent or limited, and therefore it occurs thanks to the remodeling of existing tissue, or epimorphosis, which occurs when there is requirement of cell proliferation and the formation of a blastema, which is a mass of undifferentiated cells capable of regeneration (Thomas Hunt Morgan, 1901). However, it has been proposed that categorizing regeneration into two types may not be entirely correct because regeneration without any proliferation is extremely rare, and that categorizing regeneration into two types would simplify the process by eliminating the need to consider all of the different regenerative contexts (Galliot and Ghila, 2010). This phenomenon is common across the animal kingdom, although the regenerating potential varies widely between species and even between parts of the same organism. While certain metazoans, such as planarians and *Hydra*, display an extraordinary ability to regenerate, others, such as nematodes and birds, have lost this ability (Bely and Nyberg, 2010).

Regeneration has long been investigated in order to understand how tissue regeneration occurs, and it has captivated the attention of countless biologists since many centuries. Aristotle (around 350 B.C.) was the first one to report that lizards and snails were able to regenerate the tail. Since then, many regeneration events have been described among the different organisms (Sánchez Alvarado, 2000). In 1744, the Swiss zoologist Abraham Trembley revealed the amazing capacity of *Hydra* regeneration (Abraham Trembley, 1744); in 1766, Peter Simon Pallas reported the regenerative properties of planarian (Pallas, 1766), and in 1769, Lazzaro Spallanzani, made the first

discoveries that amphibian tadpoles were able to regenerate their tails and salamanders could regenerate their jaws, limbs, tails and eyes just to mention few examples (Spallanzani Lazzaro, 1768). Two centuries after, in 1987, a study was published showing that human liver is also capable of regenerating itself (Nagasue et al., 1987). Below there are examples of the regeneration capacities of different species that have been described (**Figure 1**).

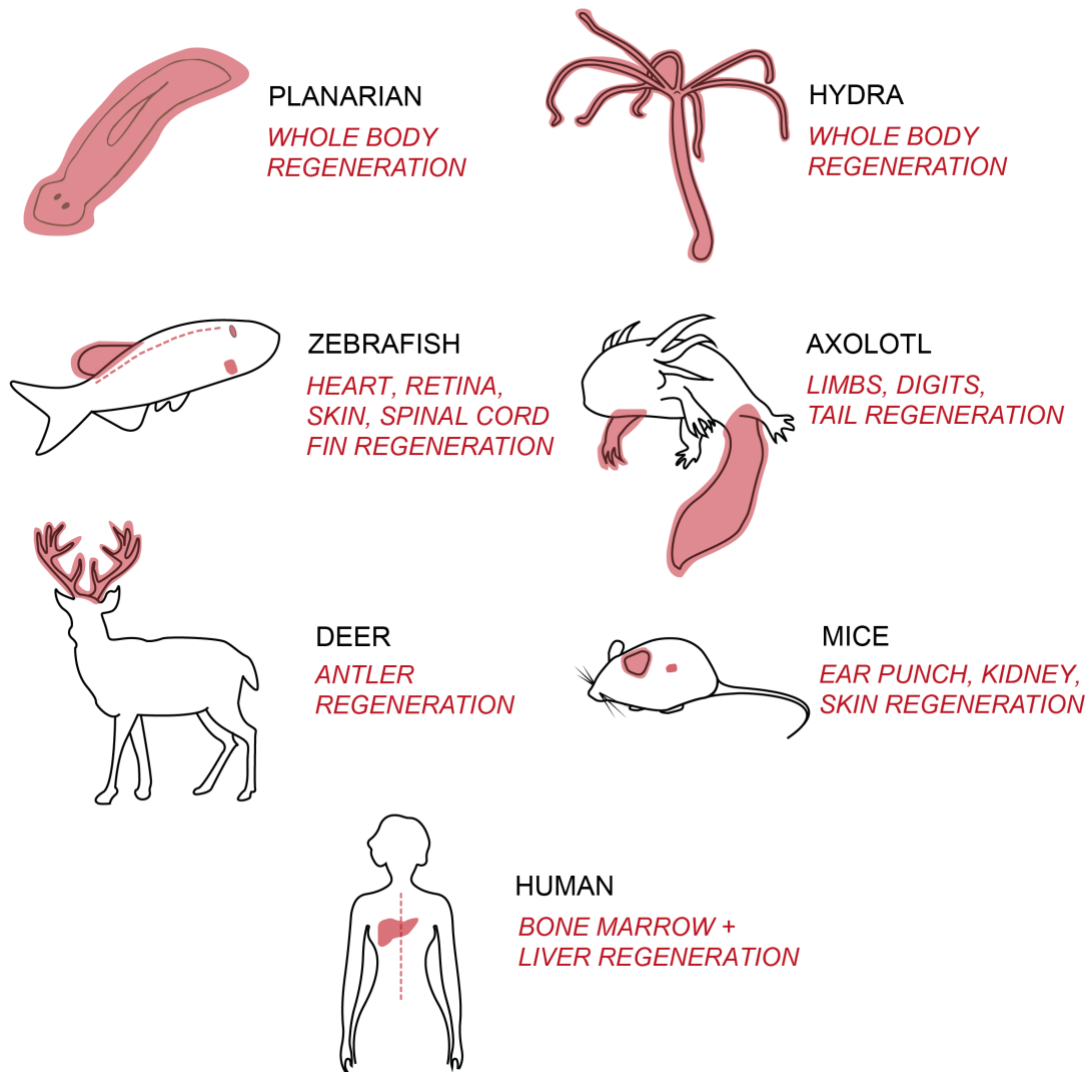


Figure 1. The ability of various organisms to regenerate.

Planarians and *Hydra* have the amazing capacity to regrow the head or tail after removing and regenerate the whole body from a body piece (Reddien and Sánchez Alvarado, 2004). Zebrafish can regenerate the retina, spinal cord and fin, as well as various organs such as the heart and skin (Marques et al., 2019). Axolotl is a well-studied salamander with the ability to regenerate limbs, digits and the tail (Joven et al., 2019; Kragl et al., 2009). Mammalian regeneration potential is less frequent; nonetheless, deers renew antlers (Price et al., 2005), *Acomys*

regenerate kidney, skin and ear (Okamura et al., 2021; Seifert et al., 2012), and humans have the ability to regenerate liver and bone marrow (Nagasue et al., 1987; Orlic et al., 2003).

Many episodes of gaining and losing regenerative ability have been described in various groups during evolution, but the cause of this occurrence is unknown (Bely and Nyberg, 2010). Nevertheless, it's possible that maintaining this favorable trait in some species is too energy demanding, and so incompatible with the species' long-term survival. As a result, an explanation for this variation remains a major challenge in regenerative biology.

2. *Hydra* as a model system to study regeneration

Hydra is an animal of about 1cm in length with some of the most remarkable regenerative abilities ever seen in the animal kingdom, such as the ability to completely regrow any missing body part after amputation or even reaggregate when dissociated into single cells. It is a member of the Cnidarian phylum which is the sister group of Bilaterian, and despite having diverged from the Bilaterian 740 million years ago (Park et al., 2012) and regarding its simple anatomy, share a large part of their gene repertoire with vertebrates, making it an excellent model system to study development, patterning, homeostasis, aging, regulation of stem cells and regeneration among many others (Galliot, 2012).

I. Anatomy and morphology

Hydra lives in fresh water, whereas practically all other cnidarians such as the starlet sea anemone *Nematostella vectensis* or the jellyfish are marine animals. This phylum is very diverse in morphology and is subdivided into four classes: Hydrozoa, Scyphozoa, Anthozoa and Cubozoa (**Figure 2**). *Hydra* genus can be classified in four distinct species, *H. viridissima*, *H. braueri*, *H. oligactis* and *H. vulgaris* (Martínez et al., 2010). Despite having a similar morphology, *Hydra* species differ in physiology and genome size; *H. viridissima* is the only one to live at all stages of its life cycle in permanent symbiosis with a unicellular algae named *Chlorella vulgaris*; moreover, it has the smallest genome size among all *Hydra* species with approximately 380 Mpb,

whereas the other species range from 1100 to 1450 Mbp (Hemmrich et al., 2007; Zacharias et al., 2004).

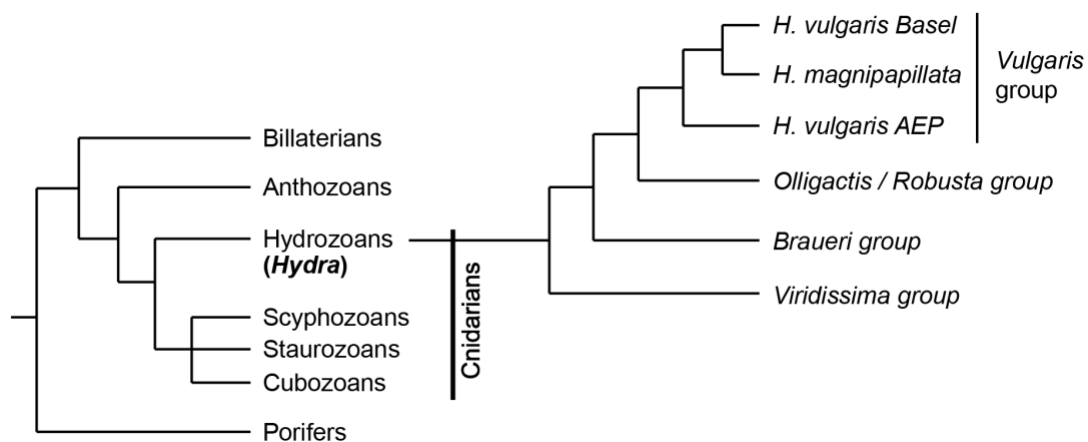


Figure 2. Phylogenetic tree of the Cnidarian phylum and the various *Hydra* species.

Among the various classes existing in Cnidarians, *Hydra* is a member of the Hydrozoa class. As represented, four different species of *Hydra* exist, with distinctions made in Basel, Magnipapillata, and AEP among the Vulgaris group (Vogg et al., 2019b; Wenger and Galliot, 2013).

Hydra anatomy is rather simple; it comprises of a single axis composed of the oral – aboral pole with radial symmetry. Along the axis of this animal, three major parts can be distinguished: the apical region, also named head, which is located in one extremity, the basal region, also named foot, which is positioned on the other side, and the gastric region, also called as the central body column, which connects both regions (Figure 3). At the oral pole, the head is surrounded by a ring of tentacles that are used to capture preys and bring them to the mouth opening located at the very apical tip (Galliot, 2012). The foot, also named basal disc is located at the aboral side and allows animals to attach to the different surfaces thanks to the production of mucus, produced by acid mucopolysaccharide droplets located in epidermal epithelial cells, which are terminally differentiated in this area (Rodrigues et al., 2016).

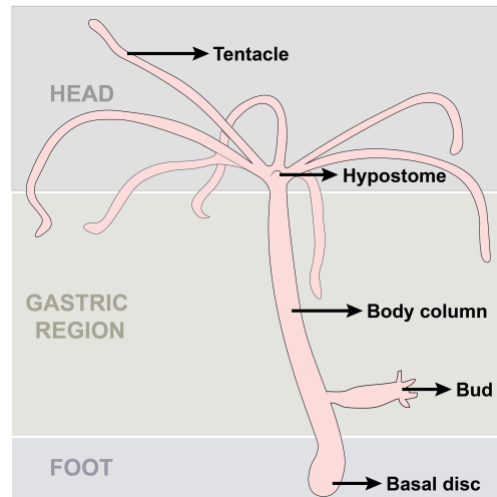


Figure 3. *Hydra* anatomy.

On the oral side, there is the head, which is surrounded by tentacles and contains the hypostome, which is positioned at the most apical region of the animal. The body column is positioned in the gastric area, and the budding process occurs in its lower part. The foot on the aboral side is where the basal disc is located.

Hydra consists of two epithelial cell layers, each of which is made up of a single cell thick and extends throughout the animal. The outer layer is called epidermis (also known as ectoderm) and the inner layer called gastrodermis (also known as endoderm). These layers are organized side by side to produce a two-layered tube that surrounds the gastric cavity and they are separated by a collagen-containing extracellular matrix called mesoglea (Galliot, 2012).

II. Homeostatic and developmental properties of *Hydra*

Hydra is characterized by three stem cell populations with a continuous self-renewal capacity that allow for continuous cell renewal in the polyp (Figure 4). The epidermal and gastrodermal epithelial cells in the *Hydra* body column are unipotent stem cells that are constantly proliferating and self-renewing, thus contribute to the budding process in intact animals, and to regeneration in amputated ones. In addition, these cells, when they reach the extremities, terminally differentiate and replace the terminally differentiated epithelial cells located at the extremities of the polyp, the tentacles and the foot that get sloughed off. Epithelial cells perform several functions

such as osmoregulation, food digesting (gastrodermal epithelial cells), and muscle-like contraction (Buzgariu et al., 2015).

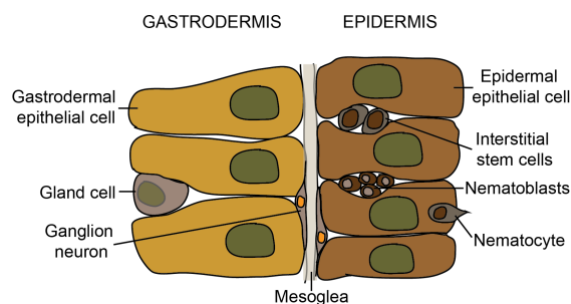


Figure 4. Illustration of the two layers that constitute the *Hydra* polyp.

The mesoglea (grey) separates the gastrodermis (left) and epidermis (right) layers, which are composed of gastrodermal and epidermal epithelial cells, respectively. The other non-epithelial cells types are also represented in the location where they are commonly found.

The third stem cell population in *Hydra* are the interstitial stem cells, which are highly proliferative, interspersed throughout the epithelial cells of the epidermal layer mainly in the central body column. Interstitial stem cells are multipotent stem cells that differentiate into neurons, secretory cells also named gland cells, nematocytes as well as germ cells (David, 2012). They do not, however, give rise to epithelial cells. Note that the various differentiated stem cells are also in a steady state of production and loss. The sustained proliferation of these three stem cell populations characterizes tissue dynamics in *Hydra*. However, epithelial and interstitial stem cells do not proliferate at the same rate; epidermal stem cells self-renew approximately every 3-4 days, whereas interstitial stem cells self-renew at a faster rate, every 24-30 hours (David, 2012; David and Campbell, 1972).

i. Asexual (budding) and sexual reproduction

Two different modes of reproduction coexist in this animal; sexual through gametogenesis and asexual through a process called budding. When the animals are fed on a regular basis, budding occurs by default. This process takes place in the budding zone, which is located in the lower part of the body column, but with certain distance from the foot. It takes about four days from the time a small bud begins to grow, recruiting cells from the parental animal, to develop all the different structures, and finally detach through the foot from the parental body column (Otto and

Campbell, 1977). Animals, on the other hand, undergo sexual reproduction when they are confronted to harsh conditions, such as temperature changes or a lack of food. When this occurs, some animals undergo sexual differentiation, differentiate testes or oocytes (or both) in the epidermal layer of the body column. The oocyte once fertilized will detach from the polyp and develops into an embryo, eventually giving rise to a new polyp (Bossert and Galliot, 2012).

ii. Regeneration

Head and foot regeneration in *Hydra* are two highly robust processes as a result of its tissue dynamics thanks to the continuous self-renewal of stem cells. It is a relatively quick procedure, as within 2-3 days after mid-gastric bisection, the upper body column will regenerate a foot at the basal end and the lower body column will regenerate a head at the apical end (**Figure 5**). After mid-gastric bisection, wound healing immediately takes place with epithelial cells extending to cover and close the wound within 3 to 6 hours. Concomitantly to wound healing, regeneration is initiated. Head regeneration proceeds from the lower half, and tentacles emerging within 40 to 46 hours after bisection, with head regeneration completing within 2 to 3 days. Foot regeneration from the upper part of the animal is faster, taking approximately 30 hours (Bode, 2003).

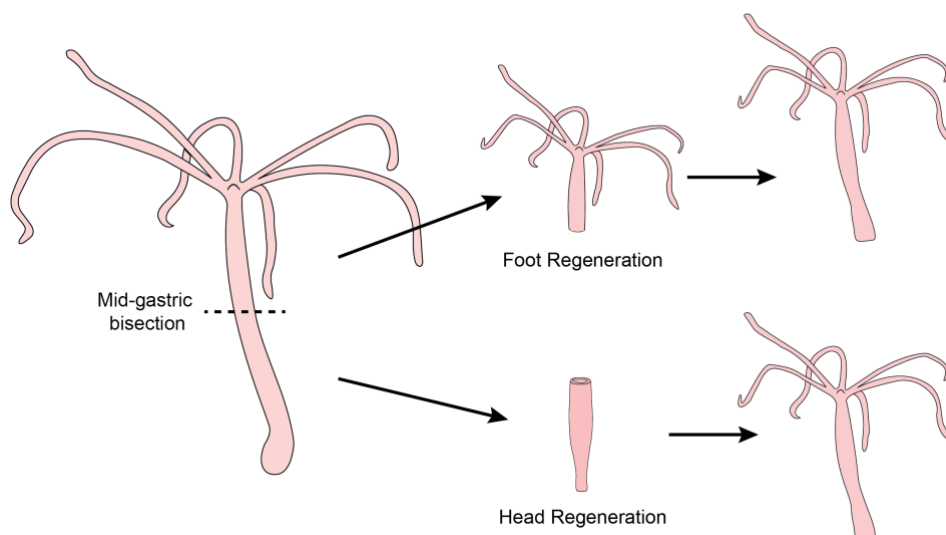


Figure 5. *Hydra* regeneration after mid-gastric bisection.

When a *Hydra* polyp is cut in half, each half has the capacity to fully regrow the missing section. As a result, the upper part will regenerate the foot, while the lower part, will fully regenerate the

entire head structure.

Regeneration is also efficient if a slice of the body column is isolated, it will heal into a small cylinder and subsequently regenerate into its normal size (Bode, 2003). If a polyp is bisected vertically, isolated sections of the body column form a head and a foot at the apical and basal ends respectively, indicating that there is an oral-aboral polarity, which is retained even after injury (Bode and Bode, 1980). The regeneration potential of *Hydra* is incredibly robust, as a whole animal can be formed from as little as 5% of the body column, where stem cells are located. That is, regeneration will not be achieved if the same percentage of tissue is taken from the tentacles or the foot region (Bode and Bode, 1980). Even though the three stem cell lineages are distributed along the body column, only the epithelial cells of both layers are involved in regeneration because animals can regenerate normally after interstitial stem cell depletion (Marcum and Campbell, 1978). Furthermore, in *Hydra*, where interstitial stem cells and thus the nervous system are depleted, epithelial cells take over the role by increasing their sensibility thanks to their plasticity (Wenger et al., 2016).

Since the cellular processes supporting head regeneration after decapitation (animal cut at 80% body length) seem to significantly differ from those underlying head regeneration following mid-gastric bisection (cut at 50%), two types of regeneration have been described in *Hydra* (Galliot and Chera, 2010). Regeneration occurs following head decapitation as inductive components from the amputated hypostome persist in the remaining tissue, and this region is already populated with apical progenitor cells, therefore resulting in a remodeling of the existing tissue. Head regeneration after mid-gastric bisection, on the other hand, relies on apoptosis-induced compensatory proliferation because the cells of this area are proliferating stem cells that have not yet acquired an apical destiny, resulting in an epimorphic process (Chera et al., 2009; Galliot and Chera, 2010). Furthermore, two proliferative waves in which several cell cycle genes are up-regulated occur more intensely during head regeneration after bisection than after decapitation (Buzgariu et al., 2018). Therefore, the initial homeostatic conditions appear have an impact on the type of regeneration that occurs in *Hydra*.

iii. Reaggregation

Self-organization during development is an important concern in animal development that can only be addressed experimentally in a few model systems. *Hydra* tissue can be dissociated, and subsequently the isolated cells can re-aggregate and form a complete animal by self-organization within three to five days (**Figure 6**) (Gierer et al., 1972). Self-organization in *Hydra* aggregates occurs via *de novo* pattern formation (Technau and Holstein, 1992). Cells are randomly distributed in a sphere-like structure after dissociation. Then, after 2-3 days, clusters of 5-15 epithelial cells with the appropriate head competence level form an activation center by *de novo* formation, and the surrounding tissue gets organized into a complete polyp. Thus, even if cells with different levels of head competence are dispersed in the aggregate after dissociation, head development is initiated by cells with highest levels of head competence, which becomes an activation center and operates as a classical organizer (Technau and Holstein, 1992).

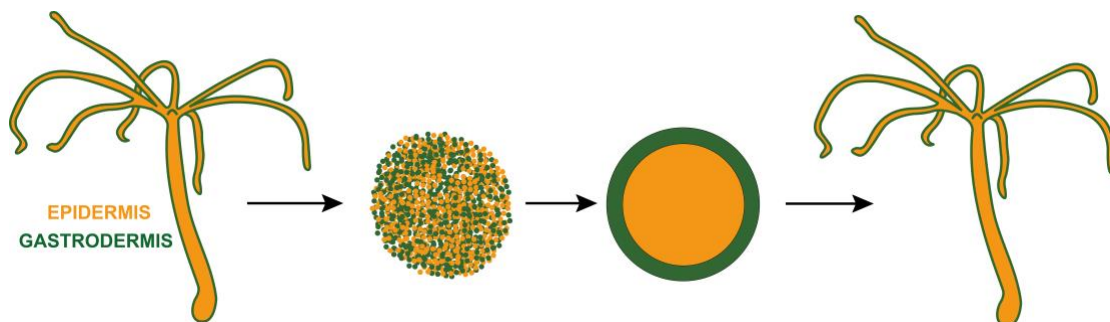


Figure 6. The dissociation-aggregation process of *Hydra*.

A *Hydra* polyp is macerated to the point where tissues are dissociated into single cells. When these cells are put in a close proximity, they form a sphere aggregate. Immediately, the epidermal and gastrodermal cells get separated from each other, with the epidermal cells sorted in the aggregate's outer layer and the gastrodermal cells in the aggregate's interior. Afterwards, developmental processes take place, culminating in the formation of one or several fully formed new polyp (Adapted from Cohen, 2017).

To sum up, the extraordinary regeneration capacity that *Hydra* constantly provides, offers a permanent access to study developmental and patterning mechanisms at cellular and molecular levels. As a result, even as an adult animal, it exhibits many embryonic characteristics as it seems to lack organismal aging. Furthermore, despite its simple anatomy, it has a well-defined body plan, making it a good model organism

for studying basic biological processes such as cell proliferation, migration and differentiation.

3. *Hydra*, a model organism to study organizer activity

I. Discovery of the concept of organizer

Ethel Browne was the first to discover the induction phenomena already in 1909 (Browne, 1909). By doing a series of transplantation studies in *Hydra*, she discovered that the tissue situated at the tip of the head, the hypostome, was capable of inducing the formation of a new axis when grafted laterally to another *Hydra*. She observed that grafted cells from an unpigmented hypostome were able to recruit green-pigmented cells from the host and induce the formation of another polyp (**Figure 7**). Similarly, tissue from the apical regenerating tip after (at least 10 hours following mid-gastric bisection) and tissue from the anterior end of a young bud were able to recruit cells from the host when grafted laterally to a host *Hydra*. Thus, tissue from the hypostome of the *Hydra*, apical regenerating tip and apical budding region has the properties of an organizer and thus produces substances that recruit cells from the host and stimulate the formation of the new axis.

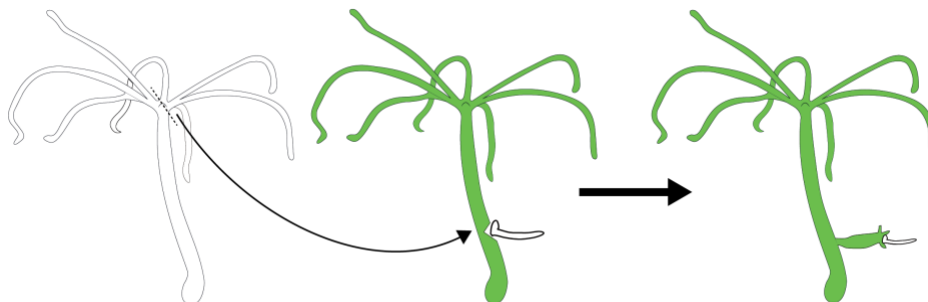


Figure 7. Scheme of the grafting experiment performed by Ethel Browne.

When a piece of the hypostome tissue together with a tentacle used as a marker from an unpigmented *Hydra* is grafted into the body column of a pigmented *Hydra*, the unpigmented piece is able to recruit cells from the body column and induce the formation of a secondary body axis in the pigmented one.

In 1924, Spemann and Mangold introduced the term “organizer”, defined as a “region or group of cells unique in being able both to induce and to pattern neighboring tissue”(Anderson and Stern, 2016). Spemann and Mangold were inspired by Ross

Harrison, who employed the lineage-tracing approach in 1903 (De Robertis, 2009), and grafted the dorsal blastopore lip of a non-pigmented salamander into the ventral side of a pigmented one. This experiment allowed them to observe how the various cells coming from the transplant or the host contribute to the formation of the new axis. They discovered that the dorsal lip of the blastopore was the only region that retained its original fate and gave rise to dorsal tissues when transplanted. As a result, they adopted the term “organizer” to describe the induced new axis since the transplanted tissue caused primary embryonic tissue to become divided in two. In 1932, Spemann was awarded with the Nobel Prize for the discovery of the induction phenomenon (Spemann and Mangold, 1924). Despite the fact that Spemann coined the term “organizer”, Ethel Browne was the first to discover the induction phenomenon by transplantation experiments. However, Spemann never cited her work despite having her manuscript (Lenhoff, 1991).

Since then, similar experiments in different organisms have revealed groups of cells with similar instructive potential, and thus other organizer centers have been described such as the Hensen’s node in the avian embryo, which induces and patterns the central nervous system; the notochord/floor-plate, which induces and organizes different sets of neurons in the neural tube; the zone of polarizing activity (ZPA) and apical ectodermal ridge (AER), which induces a patterns a set of limb elements, and the midbrain-hindbrain boundary, which specifies and patterns the adjacent regions of the midbrain/tectum and hindbrain/cerebellum (Anderson and Stern, 2016).

II. The activator and inhibitor components of the *Hydra* head organizer

Ethel Browne concluded in 1909 that tissue from the hypostome, head regenerating tip, and anterior region of a young bug has the ability to stimulate and thus positively dominate the development of specialized structures (Browne, 1909).

Later, in 1926, further grafting tests were carried out in *Hydra*, resulting in the identification of an inhibitory component also located in the head (Rand et al., 1926). Rand grafted the head of a *Hydra* laterally into the body column of a host. Once the

graft was attached to the host (one or two days later), the head of the host was amputated, and no regeneration of the host was observed (**Figure 8**). However, regeneration of the host occurred when grafting a piece that was headless. As a result, Rand concluded that inhibition was caused by the head or to something situated or generated by it.

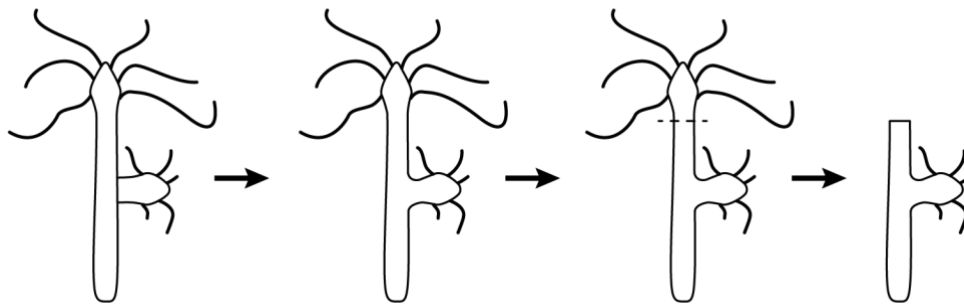


Figure 8. Schematic representation of the experiment performed in *Hydra* to demonstrate the presence of the inhibitory component.

When a head region is grafted laterally to a host and subsequently the head of the host is amputated, regeneration of the head does not occur due to the high inhibition level of the grafted head, which transmits to the host and disrupts its proper regeneration.

Following that, similar transplantation experiments were performed by several scientists in which brought to confirm that grafting a dominant region restricts the creation of another dominant region and that the distance between the laterally grafted hypostome (dominant region) and the host's amputation surface is critical for distal regeneration to occur or not (Rand et al., 1926; Webster, 1966; Webster and Wolpert, 1966). Thus, the frequency of head development is reduced at places close to an existing head.

After that, a series of transplantation experiments were carried out to assess the levels of head activation and head inhibition. Pieces from different regions were grafted below the budding region of a host to assess head activation levels, and the results showed that pieces obtained from regions close to the head are more likely to produce an ectopic head when transplanted than pieces obtained from more distal parts (**Figure 9**, left) (Webster and Wolpert, 1966). To assess the head inhibition level, a piece of the upper body column was grafted into several positions of the host (Webster, 1966). The

formation of an ectopic head occurred more frequently if the graft was made in the basal region because the host tissue capacity to inhibit the formation of an ectopic head is lower in this region compared to more apical regions. Overall, it shows that the head activator and head inhibitor are graded down the body column (**Figure 9**, right) (Shimizu, 2012; Takano and Sugiyama, 1983). *Hydra* has as well a foot organizer in the aboral pole that, similar to the head organizer, produces a foot activator and a foot inhibitor, both of whose activities are graded as well (MacWilliams and Kafatos, 1968).

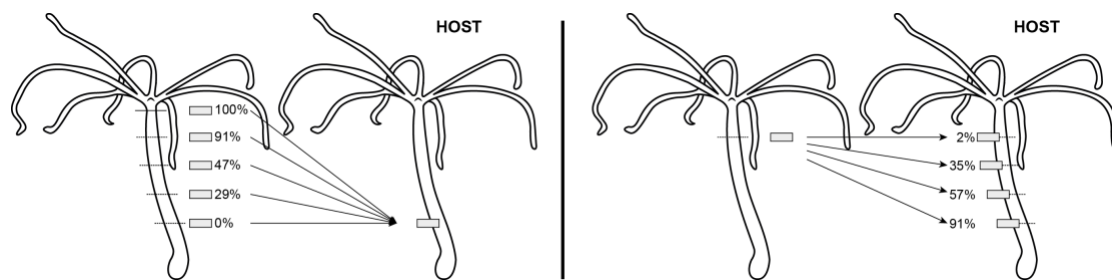


Figure 9. Schematic representation of *Hydra* transplantation experiments that were performed to determine the levels of head activation (left) and head inhibition (right).

On the left, a piece of tissue dissected from various regions along the body column is grafted into the lower part of the body column of a host animal. When pieces close to the head region are transplanted, the success rate of developing an ectopic axis through self-differentiation is higher, implying a higher activation. On the right, a piece of tissue dissected from a region close to the head is grafted at different levels along the body column of the host, ectopic axis formation is more successful when the graft is inserted at distance from the existing head, suggesting that the inhibitory activity is lower there (Adapted from Shimizu, 2012).

To summarize, transplantation is a powerful tool that provides basic understanding of various aspects of developmental biology allowing researchers to better understand embryonic development such as cell specification, cell fate determination, induction and plasticity. *Hydra* is a model organism with great potential because, as previously stated, transplantation can be done quickly and easily. In addition, thanks to the established organizer in homeostatic conditions as well as the potential organizers during developing conditions, is bringing a better understanding of the head activation and inhibition levels produced on the organizer in the different contexts. The head organizer produces morphogenic gradients and because of the tissue dynamics and regeneration capacity, morphogenesis and patterning are active and tightly regulated

throughout the entire life of this animal, making it an excellent model organism to study these concepts.

III. Modeling of the two components of the *Hydra* head organizer

The hypostome of the *Hydra* polyp produces a head activator gradient that is maximal in the head and graded down the body column as it has the characteristics of an organizer, and thus has the capacity to induce the host tissue and form a secondary axis by recruiting the cells from the host. Tissue from the body column, on the other hand, has self-organizing activity but not inductive activity. As a result, the head organizer features of the *Hydra* are quite similar to those previously reported in vertebrate embryos (Broun and Bode, 2002). The fact that this occurs in an adult *Hydra* polyp could reflect the fact that tissue dynamics are constantly engaged in this animal, implying that axial patterning processes are constantly active. The organizer, which as mentioned is located in the head, produces an activator and inhibitor signaling that is graded down the body column. The head organizer has to be constantly maintained in the scenario of tissue dynamics and thus constant cell replacement that occurs throughout the lifespan of *Hydra* (Bode, 2009).

The reaction-diffusion system proposed by Turing (Turing, 1952) to generate spatio-temporal patterns autonomously in which two substances that interact with each other and diffuse at different rates was later adopted by Gierer and Meinhardt in 1972 for *Hydra* patterning (Gierer and Meinhardt, 1972). Gierer and Meinhardt proposed a non-linear activation-inhibition paradigm in which the activator produced by a source might locally self-regulate and therefore activate the synthesis of the inhibitor, which in turn would repress the activator (**Figure 10**). The activation gradient with a short range would provide head formation capacity in the body column and during regeneration, whereas the inhibition gradient with a long range fast-diffusive would prevent head formation along the body column and restrict head formation during regeneration, distinguishing between the activator and inhibitor concentrations on one side, and the densities of their sources on the other. Gierer and Meinhardt used all of the quantitative data gathered from previous transplantation experiments performed in *Hydra* to develop this model.

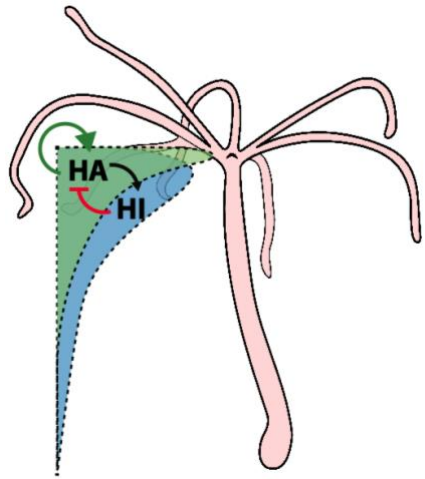


Figure 10. Illustration of the non-linear activation-inhibition model proposed by Gierer and Meinhardt.

The *Hydra* head activator, which operates in a positive feedback loop, activates the *Hydra* head inhibitor, which represses the head activator and thus prevents head formation throughout the body of the animal.

IV. *Hydra*, a model organism to study the molecular components of the organizer activity

The activities of the head activator and the head inhibitor were also assessed along the body column during head regeneration. To measure the activator properties, apical regenerating tips were transplanted laterally to a host at different time points during head regeneration to measure the frequency of head formation. The measurements revealed that the activity of the activator increases over time during head regeneration, that it is a local phenomenon limited to the head region, and that it is recovered within 12 hours post mid-gastric bisection (MacWilliams, 1983a). Regarding the activity of the inhibitor, which is also primarily produced in the head but also in the body in lesser amounts, it has a half-time of less than 6 hours after decapitation because transplantation of a body region into a decapitated host does not prevent head formation in the donor grafted piece because the head inhibition level of the host at 6 hours post amputation has not yet been restored. After that, the activity of the inhibitor is gradually restored in the regenerating head, but does not fully acquire its normal inhibition ability until 24 hours mid-gastric bisection (MacWilliams, 1983b).

V. Molecular nature of the head activator and head inhibitor in *Hydra*

As in organizer formation in zebrafish embryos (Kelly et al., 2000), β -catenin signaling also plays a critical role in setting up the *Hydra* head organizer (Gee et al., 2010). In the hypostome several members of the Wnt/ β -catenin signaling pathway are expressed in homeostatic conditions like *β -catenin* and *Tcf* (Hobmayer et al., 2000). They are expressed in a broad manner since very early budding stages in the budding zone, where later become restricted to the bud site and finally to the head of the bud. Similar spatio-temporal expression occurs during regeneration (Hobmayer et al., 2000). Nuclear β -catenin is found predominantly in the hypostome in homeostatic conditions (Broun et al., 2005) and loss-of-function assays using the β -catenin inhibitor iCRT14 shows that is indeed required for head and foot regeneration (Gufler et al., 2018) and gain-of-function assays by using a transgenic line where β -catenin is overexpressed, animals formed heads and secondary axes in several places of the body column and regenerated more head and feet (Gee et al., 2010; Gufler et al., 2018).

Eleven Wnts genes have been described in *Hydra*, seven of them being expressed in the adult hypostome, and re-expressed during regeneration (Lengfeld et al., 2009). *Wnt3* expression is restricted to the most apical region in homeostatic conditions and to the apical region in newly formed buds. In addition, is the first one to be expressed being up-regulated 1.5 hours post amputation (hpa) during head regeneration, exhibiting a broad expression pattern in the regenerating tip at early time points that is later restricted to the most apical region by 24hpa. Furthermore, the addition of recombinant HyWnt3 protein in the *Hydra* medium improves head regeneration in a head-regeneration deficient strain. (Hobmayer et al., 2000; Lengfeld et al., 2009). Taken together, these findings suggest that *Wnt3* may be the master regulator of axial patterning in *Hydra*. Indeed, two years later *Wnt3* was identified as the *Hydra* head activator being expressed in the most apical region of the animal, being rapidly up-regulated during regeneration and its activity relies on Wnt/ β -catenin-dependent regulation. In addition, to control the organizer activity, *Hydra Wnt3* promoter harbors two different cis-regulatory elements: an autoregulatory element that activates *Wnt3* transcription and a repressor element that restricts the activity of the autoregulatory

element, limiting the expression to the most apical region (Nakamura et al., 2011).

VI. The inhibitory component of the head organizer

Concerning the nature of the *Hydra* head inhibitor, several attempts were made to identify it. A protease inhibitor substance was suggested, but its nature was never determined (Berking, 1979). Among putative candidates, *Hydra* Dkk1/2/4 (*HyDkk1/2/4*) emerged as a putative candidate. The DKK gene family encodes secreted antagonists of Wnt signaling, however, *HyDkk* is not expressed in the head region and is negatively regulated by Wnt/ β -catenin signaling (Augustin et al., 2006; Guder et al., 2006). After, a Thrombospondin (*HmTSP*) was described as a Wnt signaling target being expressed in the hypostome region and being down-regulated after the knock-down of β -catenin by RNA interference (RNAi). However, the knock-down of *HmTSP* does not induce a multiple-headed phenotype in *Hydra* (Lommel et al., 2018). HAS-7, an astacin proteinase, was recently identified as a potential candidate for limiting head organizer formation (Ziegler et al., 2021). HAS-7 maintains a single head organizer via Wnt3 proteolysis, but it is not expressed in the head and thus is not in close proximity to the region where *Wnt3* is expressed. In 2019, the transcription factor *Sp5* was identified as the *Hydra* head inhibitor. This transcription factor, which is predominantly expressed in the head and at lower levels along the body column, meets all of the criteria for being the *Hydra* head inhibitor (Vogg et al., 2019a). *Sp5* has an apical-to-basal graded activity, is rapidly up-regulated during head regeneration, is under the control of Wnt/ β -catenin signaling, it inhibits Wnt/ β -catenin signaling, and prevents head formation along the body column since the knock-down of *Sp5* results in a multiple headed phenotype.

4. The importance of Wnt/ β -catenin signaling in intact and regenerating *Hydra*

The canonical Wnt/ β -catenin signaling is involved in axis formation in *Hydra* and in the reestablishment of the head organizer (Hobmayer et al., 2000). Moreover, ectopic activation of Wnt/ β -catenin signaling in *Hydra* by treating them with Alsterpaullone (ALP) (a GSK3 β kinase inhibitor) causes that tissue from the body column to acquire

the characteristics of the head organizer thus expressing genes that are normally expressed in the hypostome and the formation of ectopic tentacles along the body column, demonstrating the importance of Wnt/ β -catenin signaling in axis development (Broun et al., 2005; Gee et al., 2010).

Over the last 20 years, numerous experimental studies in the field of regeneration have uncovered signaling molecules associated with injured tissues that are necessary for successful regeneration (Tanaka and Reddien, 2011). Cell signaling, particularly Wnt and FGF signaling, is critical for regeneration initiation and blastema formation. Wnt/ β -catenin signaling is a highly conserved signaling pathway required for embryonic development, tissue regeneration, and a number of other biological processes. It has been revealed that Wnt/ β -catenin signaling plays a key role in the regeneration of a range of organisms, including *Hydra* and planarians, as well as limb regeneration in amphibians, fin regeneration in zebrafish and blastema production in various species (Gurley et al., 2008; Hobmayer et al., 2000; Kawakami et al., 2006; Li et al., 2015; Stoick-Cooper et al., 2007; Wehner et al., 2014).

I. The Wnt/ β -catenin signaling pathway is evolutionarily-conserved

The formation of the embryonic axis is one of the first and most critical events during the development of organisms. The canonical Wnt/ β -catenin signaling pathway has been strongly linked to axis formation across all phyla (Croce and McClay, 2006). The Wnt/ β -catenin signaling pathway is an ancient and evolutionarily conserved signaling pathway that regulates critical aspects of embryonic development such as cell fate determination, cell migration, cell polarity, proliferation, neural patterning, and organogenesis, as well as homeostasis. As a result, it is involved in nearly every aspect of embryonic development and also regulates homeostatic self-renewal of stem cells in a variety of adult tissues (Clevers, 2006). Unsurprisingly, changes in the Wnt pathway components generally cause growth-related pathologies, and thus mutations in the Wnt pathway can be found in a wide range of cancers (Nusse and Clevers, 2017). Mutations in various Wnt/ β -catenin pathway components, including *APC*, *β -catenin*, and *Axin* have been found in a large proportion of primary human tumours. Other components of this pathway, such as the transcription factor TCF, have been linked to

type II diabetes, and Wnt antagonists are being explored to treat osteoporosis, for example (MacDonald et al., 2009).

Wnt genes encode a large family of secreted protein growth factors found in all metazoan animals, from poriferans to humans (Lapébie et al., 2009; Miller, 2002). Wnt proteins contain a high number of conserved cysteine residues and an N-terminal signal peptide for secretion. Wnt3a, a Wnt molecule isolated in mice in 2003, was studied and it was discovered that Wnt proteins undergo a post-translation modification called palmitoylation, which involves the attachment of a palmitic acid molecule to a conserved cysteine. It was later discovered that all Wnts undergo this lipid modification caused by the porcupine enzyme, which would explain why these proteins are so insoluble (MacDonald et al., 2009; Willert et al., 2003).

There are three different Wnt signaling pathways, which include the canonical Wnt/ β -catenin pathway (**Figure 11**), the Wnt/ Ca^{2+} pathway, and the Wnt/polarity pathway, also known as the noncanonical planar cell polarity (PCP) pathway. Each of these pathways is activated by different sets of Wnt and Frizzled receptors (Clevers, 2006; Miller, 2002). Here I will focus on the canonical Wnt/ β -catenin signaling pathway since it is the most well studied and the most relevant for this study. The canonical Wnt/ β -catenin signaling pathway regulates the amount of the transcriptional co-activator β -catenin in the nucleus.

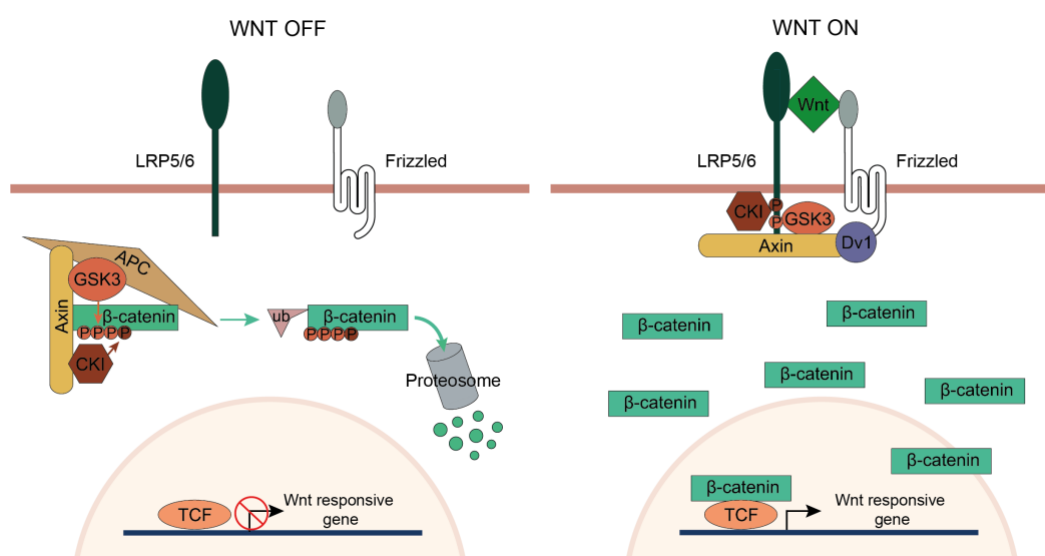


Figure 11. An overview of the canonical Wnt/ β -catenin signaling mechanism.

In the absence of Wnt ligands, the destruction complex phosphorylates β -catenin, which is then recognized and degraded by the proteasome. In the presence of Wnt ligands, its interaction with Frizzled and LRP5/6 receptors recruits Dvl and causes the destruction complex to dissociate. β -catenin is no longer phosphorylated and accumulates in the cytoplasm before being translocated to the nucleus to interact with TCF to activate gene expression (Adapted from MacDonald et al., 2009).

Binding of Wnt proteins to cell surface receptors of the Frizzled (Fzd) family and the LDL-receptor-related protein (LRP) family, is required for Wnt signaling (Miller et al., 2001). Frizzled proteins are seven-pass transmembrane cell-surface receptors with a conserved motif in their cytoplasmic tail that is required for pathway activation, while LRP proteins have a single-pass transmembrane co-receptor. When Wnt ligands bind to Fzd/LRP proteins, the physical interaction with Fzd activates cytoplasmic Disheveled (Dvl), which is then translocated to the membrane. There, Dsh inhibits Glycogen synthase kinase-3 beta (Gsk3 β), thus preventing the phosphorylation of β -catenin and its degradation. As a consequence, β -catenin is stabilized and translocates to the nucleus, where it interacts with a member of the TCF/LEF transcription factor family to modulate the transcription of Wnt signaling target genes. In the absence of Wnt ligands, this pathway is no longer activated, resulting in the formation of a cytoplasmic complex called the destruction complex, made up of the tumor suppressors adenomatous polyposis coli (APC) and Axin, as well as the kinases Gsk3 β and Casein Kinase 1 α (CK). The kinases phosphorylate β -catenin, which is then ubiquitinated and rapidly targeted for degradation by the proteasome (Clevers, 2006; Croce and McClay, 2006). The continuous proteasomal degradation of β -catenin prevents it from reaching the nucleus and thus activating the signaling pathway.

II. Wnt/ β -catenin signaling during bilaterian homeostasis, development, regeneration and disease

This signaling pathway dates back to when Wnt signals first appeared in the simplest multicellular organisms, when Wnts served as primordial symmetry-breaking signals that were critical for the formation of patterned tissues during embryogenesis (Clevers et al., 2014). These signals are also involved in pattern maintenance in vertebrates: they

promote tissue regeneration, thus allowing tissues to be refilled and maintained throughout time (Clevers et al., 2014).

Wnts determine polarity in bilaterian animals via β -catenin, the most important protein in the canonical Wnt signaling. β -catenin, in particular, defines the posterior nature of the anteroposterior axis throughout the bilaterians. Also, in pre-bilaterians (Cnidarians and Poriferans) Wnts are expressed in a polarized manner along the main axis. However, in bilaterians, Wnts are expressed at the oral pole, while Wnt inhibitors are expressed aborally (Petersen and Reddien, 2009). Perturbation of Wnt/ β -catenin signaling has significant axis defects throughout the animal kingdom. For example, *wnt3a* causes head enlargement and tail development failure in zebrafish (Shimizu et al., 2005) and *β -catenin* silencing causes ectopic head formation in planarians (Gurley et al., 2008). Overall, the canonical Wnt/ β -catenin signaling is widely used in all metazoans and has a conserved role in promoting the polarized features of head-to-tail or oral-aboral axis (Petersen and Reddien, 2009).

In addition to playing an important function throughout embryonic development and adult tissue homeostasis, Wnt/ β -catenin signaling appears to have an essential role during regeneration. In zebrafish for example, Wnt/ β -catenin signaling is required for zebrafish tail fin regeneration and is sufficient to increase regeneration (Stoick-Cooper et al., 2007). In Planarians, Wnt is expressed in the animals' posterior end, and β -catenin acts as a molecular switch to determine and preserve the anterior-posterior (AP) identity in homeostasis but also during regeneration. The knockdown of *β -catenin* through RNAi causes the regeneration of a head after tail amputation in regenerating animals and the formation of ectopic head on the posterior side in homeostatic animals. Thus, polarity is controlled by the anterior-posterior location of Wnt genes and Wnt signaling antagonists, which is also determinant for the polarity during regeneration (Gurley et al., 2008; Petersen and Reddien, 2008). Thus, Wnt coordinates repair after injury and imparts positional information crucial for shaping proper regeneration.

5. The Sp/KLF family of transcription factors

Krüppel-like factor (KLF) and Sp proteins are members of a family of transcription factors that play an important role in the development of a variety of organisms. These transcription factors bind to GC/GT-rich promoter sites via the characterized zinc finger DNA binding domain that contains several Cys(2)-His(2) at their C-terminal domain. These promoter regions are critical for the proper expression of ubiquitous and tissue-specific genes, particularly those involved in cell cycle regulation or developmental patterning (Black et al., 2001; Suske, 1999; Turner and Crossley, 1999).

The Specificity protein (Sp) transcription factor family is a subclass among the Sp/KLF family, characterized by the presence of a three zinc finger DNA-binding domain (Harrison et al., 2000; Kaczynski et al., 2003; Zhang et al., 2001). One distinguishing feature of Sp proteins is the presence of the Buttonhead (Btd) box, positioned right at the N-terminus of the zinc fingers and necessary for transactivation activity (Athaniar et al., 1997). Another trait of most Sp factors is the existence of a highly conserved amino acid sequence, called Sp box, located at the N-terminus, with an unknown function (Suske et al., 2005). *Sp1* was the first member of the family to be identified as well as one of the first transcription factors discovered in mammalian cells, in the early 1980s. Since then, nine distinct Sp proteins have been identified in humans (Kim et al., 2017) (**Figure 12**). Although the majority of members of this family have been discovered in mammals, these proteins have also been identified in a variety of vertebrates and invertebrate species, and they appear to have evolved through a series of gene-duplication events. Despite the significant overall sequence similarity of the zinc-finger motifs among the different members of this family, their capacity to regulate transcription varies greatly. Therefore, distinct members of the Sp/KLF family can operate as transcriptional activators or repressors depending on the promoter to which they bind as on the different cellular context. Additionally, there are multiple transcription-related domains in the amino-terminal of these proteins, and they are highly diverse. As a result, they may also be regulated by the interaction with coregulators through these domains, adding more complexity to the transcriptional regulation of this family of transcription factors (Kaczynski et al., 2003; Safe and

Abdelrahim, 2005). The analysis of the expression pattern and the results of loss-of-function assays of genes from the Sp/KLF family demonstrates that they are engaged in growth-regulatory and developmental processes in a wide range of tissues.

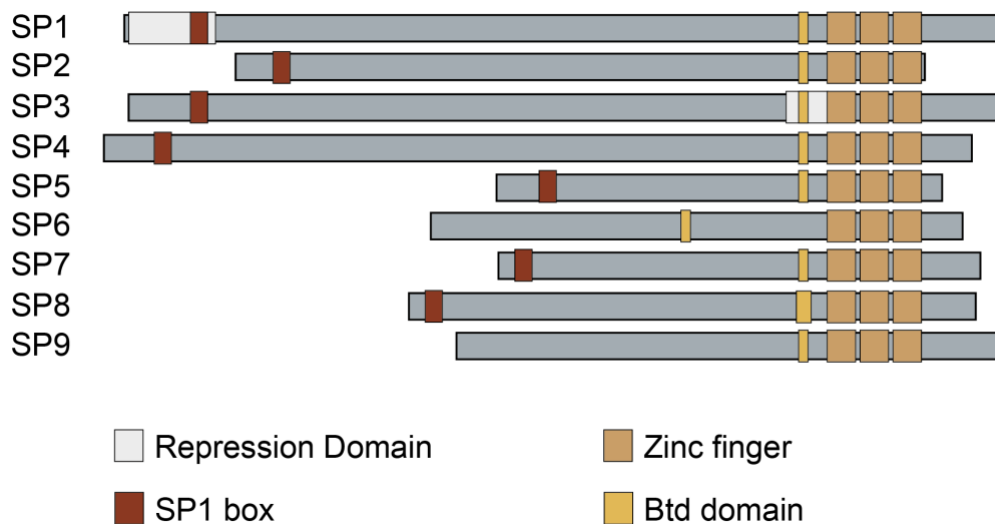


Figure 12. Structure of the nine SP proteins identified in humans.

The three zinc-finger domains as well as the Btd domain are found in all nine SP proteins. Except for the SP9 protein, all proteins contain the Sp box domain. A repression domain has also been identified in SP1 and SP3 proteins. (Adapted from Kim et al., 2017)

I. Developmental role(s) of the Sp5 transcription factor in bilaterians

Sp5 is a transcription factor that belongs to the Sp/KLP family. It encodes a protein containing a C2H2 zinc finger domain at the C-terminus that allows this transcription factor to bind to DNA. *Sp5* binds to the GC box of promoter elements in the same way that other Sp members do and it also contains a Btd box and a Sp box. *Sp5* has been identified in a variety of organisms (Figure 13), and in the majority of them, it is associated with a role in early development.

The *Sp5* transcription factor in mouse

Sp5, first discovered in mouse, is closely related to the previously identified Sp1 transcription factor. *Sp5* demonstrates a remarkably dynamic and limited pattern of expression throughout mouse embryogenesis (Harrison et al., 2000; Treichel et al., 2001). Moreover, there is an interaction between *Sp5* and *Brachyury*, implying that may

play a role in the coordination of changes in transcription to generate numerous tissue patterning events in the developing embryo, such as gastrulation and axial elongation; differentiation and patterning of the neural tube, pharyngeal region, and somites; and formation of skeletal muscle in the body and limbs (Harrison et al., 2000). Later on, it was demonstrated that the transcription factors *Sp5* and *Sp8* seem to have a redundant role in trunk and tail development because the generation of *Sp5;Sp8* double mutants exhibit a phenotype that is very similar to the *Wnt3a*^{-/-} phenotype, suggesting an essential role for the regulation of neuromesodermal stem cells (Dunty et al., 2014).

The *Sp5* transcription factor in humans

In human fetuses, *SP5*, is highly expressed in lungs, colon and stomach, as well as in the uterus and the skin (Chen et al., 2006). *SP5* is up-regulated in various human cancers, including hepatocellular carcinoma, gastric cancer and colon cancer. *SP5* expression appears to be restricted in fetal tissues, suggesting to play an important function in early development, similar to mouse *Sp5*. In addition, it may work to promote the growth of human tumor cells *SP5* was later discovered to be primarily activated in human pluripotent stem cells (hPSCs), with a critical paper for the correct differentiation of hPSCs confirming the important role in developmental environments (Huggins et al., 2017).

The *Sp5* transcription factor in chicken

Recently, during the characterization of the genetic circuit responsible for the developmental switch in neural crest, *Sp5* was identified in chick embryos (Azambuja and Simoes-Costa, 2021). Here, *SP5* is expressed during gastrula stages and stimulates the expression of genes produced during this stage, while restricting the expression of specification genes from being expressed (*AXUD1*). Later in the specification process, *Sp5* is rapidly downregulated in the neural crest lineage, allowing *AXUD1* to be transcribed in the neural crest. In conclusion, *Sp5* directly promotes neural plate border identity and, in collaboration with *AXUD1*, regulates the temporal activation of neural crest genes.

The *Sp5* transcription factor in *Xenopus*

The zinc finger clusters of *XSPR-1* and *XSPR-2* in *Xenopus laevis* are closely related to mouse *Sp5* as deduced from the sequence alignment (Ossipova et al., 2002). *XSPR-1/2* are dynamically expressed throughout *Xenopus* embryogenesis, mimicking several characteristics of *Sp5* expression in mouse. They are, however, distinctly expressed during development, indicating that they have varied functional roles (Elsy et al., 2019; Ossipova et al., 2002). *XSPR-1* is expressed in the non-involuting marginal zone during gastrulation and at later stages shows the expression in the neuroectoderm, forebrain and the midbrain/hindbrain boundary, whereas *XSPR-2*, is expressed in the presumptive mesoderm during gastrulation and subsequently in the tip of the tail (Ossipova et al., 2002). In 2005, *XSPR-1* was designated as the *Xenopus Sp5*, playing an important role in neural crest formation during early embryogenesis (Park et al., 2013), and *XSPR-2* as the *Sp5-like (Sp5l)*, and participating in posterior patterning. Furthermore, like the mouse *Sp5*, both *Xenopus Sp5* and *Sp5l* are regulators in the tail bud (Elsy et al., 2019).

The *Sp5* transcription factor in zebrafish

In zebrafish, two zinc-finger transcriptional activators of the Sp-1 family, initially termed *bts1* (Tallafuss et al., 2001) and *spr2* (Zhao et al., 2003) were identified. These two transcriptional activators have a similar expression pattern in early stages, but they differ in the expression at later time points. During gastrulation, *Bts1*, later renamed *Sp5*, is expressed in the presumptive midbrain/hindbrain area (Tallafuss et al., 2001). *Spr2*, later on renamed *Sp5-like*, was found to be expressed in hypoblast and epiblast cells in the late blastula and early gastrula suggesting that is involved in mesoderm induction (Zhao et al., 2003). Following that, it was demonstrated that *Sp5* and *Sp5l* are crucial mediators in mesoderm and neuroectoderm patterning in zebrafish (Weidinger et al., 2005) and that *Sp5l* is also required to govern tail formation (Thorpe et al., 2005).

The *Sp5* transcription factor in Cephalochordates

Three *Sp* genes were reported in *Branchiostoma*, a genus of lancelets in the subphylum Cephalochordata, among which, one is *Sp5* (Dailey et al., 2017). In this organism, *Sp5* is expressed in axial mesoderm and neuroectoderm, the brain vesicle and the tailbud,

which is consistent with the expression and the role of *Sp5* previously described in chordates.

The *Sp5* transcription factor in planarians and acoels

Sp5 is expressed in a variety of cells from the posterior pole in planarians and acoels (Tewari et al., 2019). In addition, *Sp5* is specifically upregulated at posterior-facing wounds of head and trunk regenerating fragments at 24 hours post-amputation (hpa) while broadly expressed at 0 hpa in tail fragments, where it shifts expression to the posterior end by 24 hpa, forming a gradient in tail fragments. Furthermore, after knocking-down *Sp5* by *RNAi*, a series of genes expressed in the tail become upregulated, indicating that *Sp5* contributes to regulate the posterior identity during both development and regeneration (Ramirez et al., 2020; Tewari et al., 2019)

The *Sp5* transcription factor in Panarthropoda

In *Drosophila melanogaster*, *Sp5* was first described as *Buttonhead (Btd)*, a gap-like segmentation gene involved in head development (Cohen and Jürgens, 1990). Following the gastrulation stage, *Btd* is also expressed during the formation of the peripheral nervous system, implying that *Sp5/Btd* contributes to several developmental processes (Wimmer et al., 1996). This role in head development is likely evolutionarily-conserved in arthropods, as the *Sp5/Btd* expression pattern is similar in *Tribolium castaneum*, *Thermobia domestica*, and *Folsomia candida* (Schaeper et al., 2010).

In the velvet worm *Euperopatoides kanangrensis*, which belongs to the phylum Onychophora, a sister group to arthropods, *Sp5/btd1* is expressed earlier in development, around the blastopore, and later in the transverse segmental stripes, which will subsequently pattern the tips of the appendages and the ventral nervous system. *Sp5/btd1* expression is very similar to that of *Sp6-9*, implying a putative redundancy between *Sp5/btd1* and *Sp6-9*. Overall, these findings point to *Sp5/btd1* as playing a conserved role in the development of appendages and the nervous system in arthropods and onychophorans (Janssen and Budd, 2020).

The Sp5 transcription factor in Cnidarians

In *Nematostella*, Sp5 mainly localized to the oral site and is target gene of Wnt/ β -catenin signaling (Bagaeva et al., 2020). *Sp5* was identified as the head inhibitor in *Hydra*, and thus plays an important role in both maintaining and establishing the head organizer during developmental processes (Vogg et al., 2019a). Is primarily expressed in the head and graded down the body column, and it is also regulated by Wnt/ β -catenin signaling.

	BTD Box	Zinc finger 1
Drosophila	FNF--DDIAFQTQLQRRSVRCTCPNCTNEMSGLPPIVGPDERGRK	CHICHIPGCKERLYGK
Planarian	LNLSSNRANIPQLGQRKQKCTCPNCHQGLNSRA--NL--NGAKKV	HICYI--CHKTYGK
Hofstania	LY--SQSAVAVPTTRRCRRRCPCNQNSSNSGTNNGG--VAKKKV	HVCHIAGCAKVVYK
Hydra	S---HA-VVPNSVATRRRCRCKPCNCSGQQ-----SE--PNKPK	QHVCHIPGCGKVYK
Zebrafish_1	L---QGTSGLLSSTRRCRCKPCNQQSTGNGGA-ALE--FGKKRI	HICHIPDCGKVYK
Branchiostoma	L---QK---PTIATARRCRRRCPCNQNSTAG-----S--PNKKK	HICHIPGCGKVYK
Tribolium	K---VE-YSNYSSKARRCIKQCPNQNVEEVG---LKK--PSSKKV	HVCHYQCGDKVYK
Chicken	L---QT-KSPLAATARRCRRRCPCNQAAGSAP-EAE--PGKKK	QHVCHIPGCGKVYK
Humans	L---QT-KAPLAATARRCRRRCPCNQAAGSAP-EAE--PGKKK	QHVCHVPGCGKVYK
Mouse	L---QT-KAPLAATARRCRRRCPCNQAAGSAP-EAE--PGKKK	QHVCHVPGCGKVYK
Zebrafish	L---HT-KSPLA-TARRCRRRCPCNQSSTSSS---SDE--PGKKK	HICHIPGCGKVYK
Xenopus	L---QT-KSPLA-TARRCRRRCPCNQTSSTSSG---PDE--VGKKK	HICHIPGCGKVYK
Xenopus_1	L---QT-KSPLA-TARRCRRRCPCNQTSSTSSG---PDE--AGKKK	HICHIPGCGKVYK
	* : . : * * * * *	: * * : : * : * *
	Zinc finger 2	Zinc finger 3
Drosophila	ASHLKTHLRWHTGEREFLC--LTCGRKFSRSDELQHRHGRTH	TNYRYPACPICSKKFMRSD
Planarian	TSHLKAHIRWHTNDRE FVCTYHLCSKSFTRSDELQHRMTRH	TGEKRFVCPFCRFRMRSD
Hofstania	TSHLKAHLRWHAGERE FVCNWLFCGKSFTRSDELQHRHTRH	TGEKRFVCDGCRFRMRSD
Hydra	TSHLKAHLRWHAGLRE FVCNWLFCNKSFTRSDELQHRHTRH	TGEKRFACQDCGCRFRMRSD
Zebrafish_1	TSHLKAHLRWHAGERE FICNWLFCGKSFTRSDELQHRHTRH	TGEKRFVCGQCGCRFRMRSD
Branchiostoma	TSHLKAHLRWHHTGERE FVCNWLFCGKSFTRSDELQHRHTRH	TGEKRFVCPDCGCRFRMRSD
Tribolium	TSHLQAHLRWHHTGERE FVCNWLFCGKSFTRSDELQHRHTRH	TGEKRFVACSVCTKFRMRSD
Chicken	TSHLKAHLRWHHTGERE FVCNWLFCGKSFTRSDELQHRHTRH	TGEKRFVCPCEGCRFRMRSD
Humans	TSHLKAHLRWHHTGERE FVCNWLFCGKSFTRSDELQHRHTRH	TGEKRFVACPEGCRFRMRSD
Mouse	TSHLKAHLRWHHTGERE FVCNWLFCGKSFTRSDELQHRHTRH	TGEKRFVACPEGCRFRMRSD
Zebrafish	TSHLKAHLRWHHTGERE FVCNWLFCGKSFTRSDELQHRHTRH	TGEKRFVCPDCCKRFRMRSD
Xenopus	TSHLKAHLRWHHTGERE FICNWLFCGKSFTRSDELQHRHTRH	TGEKRFVCPCEGCRFRMRSD
Xenopus_1	TSHLKAHLRWHHTGERE FICNWLFCGKSFTRSDELQHRHTRH	TGEKRFVCPCEGCRFRMRSD
	: * * * : * : * * * . * * * : * * * * * * * * * * : : * * * * * : * *	
Drosophila	HLSKHKKTHFKDKSKKVLAAEAKEQAAAAIKLEKKEKKS	GKPLTPVFEFKQEQPDTTFL
Planarian	HLAKHKKTHEGVDPIVLGTVISKDTN--SSIKS-----	PKALNPKDIYKQONVKKPR
Hofstania	HLSKHSKTHANRRNNNNNTSSKLTE----HSKE-----	E---LSSLLHTTDLITKPT
Hydra	HLSKHKKTHQNKKQENTFVKDVTIE---VIKD-----	N---VD-----
Zebrafish_1	HLSKHVKTQSRKSRSSQPPHSGTD---ALLS-----	N---I-----
Branchiostoma	HLAKHVKTQAQKRAKGPDSQTS---DIEN-----	N---N-----
Tribolium	HLAKHVKTQKNKSSDGV---KSEN---V-----	-----
Chicken	HLAKHVKTQNKKLKAAADAVKRED---G-----	-----
Humans	HLAKHVKTQNKKLKVAEAGVKRED---A-----	-----
Mouse	HLAKHVKTQNKKLKVAEAGVKREN---P-----	-----
Zebrafish	HLAKHVKTQNKKSKSHDKTSDYVK---R-----	-----
Xenopus	HLAKHVKTQENKKIKNVERTVKQEQ---N-----	-----
Xenopus_1	HLAKHVKTQENKKIKNVERTVKQEQ---N-----	-----
	* * : * * * * *	

Figure 13. Alignment of Sp5 in the described organisms.

The alignment of the protein sequences of transcription factor Sp5 from different organisms shows that, despite some differences, the BTB domain and the three zinc fingers domains are well conserved.

II. *Sp5* as a downstream target of Wnt/ β -catenin and FGF signaling pathways

Sp5 and *Sp5-like* genes act downstream of Wnt/ β -catenin signaling in vertebrates like zebrafish (Thorpe et al., 2005; Weidinger et al., 2005; Zhao et al., 2003), *Xenopus* (Park et al., 2013), humans (Huggins et al., 2017; Takahashi et al., 2005) and chick (Azambuja and Simoes-Costa, 2021). In mouse embryos, *Sp5* is up regulated after ectopic activation of β -catenin (Fujimura et al., 2007). Furthermore, the mouse *Sp5* promoter contains five TCF/LEF binding sites, which mediate the direct regulation of *Sp5* expression by Wnt/ β -catenin signaling (Fujimura et al., 2007; Kennedy et al., 2016). These results demonstrate that *Sp5* is a direct target gene of Wnt/ β -catenin signaling. In the same line, the human SP5 promoter region contains seven consensus TCF/LEF binding sites (Chen et al., 2006), *Sp5* also responds to Wnt/ β -catenin signaling in Branchiostoma (Dailey et al., 2017), as in *Hydra* (Vogg et al., 2019a), planarians and acoels (Tewari et al., 2019). *Sp5* and *Sp5-like* also function as downstream regulators of the FGF signaling pathway in zebrafish (Zhao et al., 2003) and *Xenopus* to regulate neural crest induction (Elsy et al., 2019; Park et al., 2013).

III. The regulation of the transcription factor Sp5

Sp5, like other members of the Sp/KLF family, appears to have distinct transcriptional activities and, as a result, functions as a transcriptional activator or repressor depending on the target genes as well as in a context-dependent manner. In mouse, for example, *Sp5* was initially discovered to be a transcriptional repressor, mediating the downstream responses to Wnt/ β -catenin signaling by directly repressing Sp1 target genes (Fujimura et al., 2007). However, it was later demonstrated that Sp5 and Sp8 directly bind to DNA via interactions with Tcf1/Lef1, thereby becoming new partners of the β -catenin-Tcf/Lef complex and thus promoting β -catenin association to activate selected Wnt target genes (Kennedy et al., 2016). SP5 is also recruited in close proximity

to β -catenin in humans, and more specifically in hPSCs, suggesting that the two proteins interact in this system as well. However, evidence suggests that in this case, SP5 acts to down regulate the expression of several genes that are activated by Wnt/ β -catenin signaling, including SP5 itself. As a result, SP5 would act as a transcriptional repressor on its own promoter (Huggins et al., 2017). *Sp5* appears to function as a transcriptional activator in zebrafish (Tallafuss et al., 2001), as does *Sp5-l*, which seems to bind promoters of Wnt target genes and enhance their activation (Thorpe et al., 2005). In *Branchiostoma*, on the other hand, it is hypothesized to function in a negative-feedback loop in the Wnt/ β -catenin signaling pathway (Dailey et al., 2017). Similarly, in planarians and acoels it acts to down-regulate the expression of Wnt-regulated trunk genes in the tail, promoting different spatial identities on the primary axis of these animals (Tewari et al., 2019). In *Hydra*, *Sp5* appears to function as both a transcriptional repressor by inhibiting Wnt/ β -catenin signaling and a transcriptional activator on its own promoter, as revealed by *in vitro* data (Vogg et al., 2019a). Finally, SP5 also plays a dual role in the chick; it activates neural plate border genes while also preventing premature expression of specification genes. In this system it is shown that it also regulates its own transcription (Azambuja and Simoes-Costa, 2021).

Overall, we can see that the DNA binding domain and the transactivation domain the Sp5 transcription factor are well conserved across the different organisms in which it has been identified. Furthermore, we can conclude that *Sp5* is primarily expressed during embryogenesis, playing a critical role in patterning during the early stages of development. Further to that, it is re-expressed when replicating developmental processes such as regeneration and during the development of many cancers. *Sp5* appears to function as a transcriptional activator or transcriptional repressor depending on the context, and because it is a target of the conserved Wnt/ β -catenin signaling pathway, we hope to elucidate the ancient regulation of this transcription factor by studying its regulation in *Hydra*.

6. Methodological tools developed for *Hydra*

Hydra is a model organism that is generally maintained in the laboratory at 18°C. They are usually kept in glass or plastic dishes and fed with freshly hatched *Artemia nauplii* twice to four times per week. They can also be easily kept at 4°C, where a feeding every two weeks is sufficient. Several cellular and molecular tools have become available for the *Hydra* model system over the last 20 years. The genome of *Hydra magnipapillata* was not made public available until 2010 (Chapman et al., 2010). The *Hydra* genome is (A+T)-rich and contains approximately 57% transposable elements, making this process more challenging. The *Hydra* genome was re-sequenced in 2015 using long-range sequencing approaches and *Hydra viridissima* genome became as well available in 2020 (Hamada et al., 2020). Later, thanks to the efforts of several laboratories other OMICS tools such as transcriptomics became available (Boehm et al., 2012; Hemmrich et al., 2012; Wenger and Galliot, 2013) and single-cell RNA sequencing was finally approached in 2019 (Siebert et al., 2019). In 2015 an extensive proteomic analysis was also made available (Petersen et al., 2015) and the *Hydra* 2.0 Genome Project Portal was released in May 2017. Furthermore, HydrATLAS, a very useful tool for blasting any sequence against the *Hydra* transcriptome, was launched (Wenger et al., 2019a). Gene expression along the *Hydra* axis, gene expression profile during regeneration, and gene expression at the different cell types can all be visualized here.

To study gene expression and regulation, stable transgenic animals can be generated (Wittlieb et al., 2006). Furthermore, it enables to study functional gene analysis because gene overexpression constructs (Gee et al., 2010) and gene knockdown via short hairpin RNA (shRNA) plasmids can be used to generate transgenic lines (Boehm et al., 2012; Franzenburg et al., 2012; Klimovich et al., 2019). In brief, transgenic *Hydra* are created by microinjecting the desired plasmid into an oocyte that will later be fertilized. Random genome integration, on one hand, occurs with low success rate and is highly variable from one plasmid to another. On the other hand, the rate of hatched polyps after injection is very low, as well as the rate of gametogenesis in terms of oocyte production in *Hydra* females is not very high. Finally, once a positive polyp hatches, only a few cells are usually positive, resulting in a chimeric animal from which a fully

stable transgenic line can be obtained by clonal propagation after several rounds of budding processes.

On one hand attempts were made to develop CRISPR-Cas9 in *Hydra* (Lommel et al., 2017). Transient gene knockdown by RNAi, on the other hand, is well established in *Hydra* (Watanabe et al., 2014). Gene silencing is accomplished through the electroporation of small interfering RNA (siRNAs) or shRNAs into the animals, and the efficiency varies depending on each gene, thus necessitating multiple electroporations for some genes (Klimovich et al., 2018; Vogg et al., 2019a).

7. AIMS of this study

Hydra is a well-known classic organism recognized for its exceptional ability to regenerate. Furthermore, regarding its simple anatomy, it contains a high percentage of conserved genes, particularly in signaling pathways such as the Wnt/ β -catenin signaling pathway. As a result, we chose this model organism to investigate the molecular mechanisms underlying head regeneration. During this process, a master regulator, Wnt3, initiates the process following mid-gastric amputation, thus acting as the head activator. The goal of this research is to identify and characterize the molecular nature of the *Hydra* head inhibitor, which is required to restrict head formation in intact and regenerating conditions. Furthermore, because *Hydra* is an excellent model for studying regulation not only regulation in homeostatic conditions but also during developmental contexts, we will investigate the regulation of the *Hydra* head inhibitor in both contexts. To do so, we compared planarian down-regulated genes after the silencing of *β -catenin* (Reuter et al., 2015) to *Hydra* genes with apical-to-basal graded expression as well as that are up-regulated during head regeneration. Once identified, we will create a *Hydra* transgenic line expressing the *Hydra* head inhibitor and we will develop antibodies against it to perform CHIP-sequencing assay in order to characterize its target genes.

- 1) Identification and characterization of the *Hydra* head inhibitor
- 2) Study the regulation of *Hydra Sp5 in vivo*
- 3) Identify and characterize direct *Hydra Sp5* target genes with a putative role in *Hydra* head inhibition

Finally, our study aims to acquire new insights into the developmental function of the evolutionarily conserved Wnt/ β -catenin/Sp5 signaling pathway.

RESULTS

Chapter-1 IDENTIFICATION OF THE *HYDRA* HEAD INHIBITOR

The results presented in this chapter correspond primarily to those obtained during my master's degree, which I completed in Galliot's laboratory under the supervision of Dr. Matthias Vogg, as well as the beginning of my doctoral thesis. The main goal was to identify and characterize the *Hydra* head inhibitor, which had remained unknown for long time despite the fact that an inhibitory head component had been mentioned in 1926 (Rand et al., 1926).

To find the head inhibitor, a planarian gene dataset was assessed, which included genes whose expression was down-regulated after the silencing of *β -catenin* (Reuter et al., 2015). To identify the corresponding genes in *Hydra*, the planarian dataset was blasted against the *Hydra* transcriptome (Wenger et al., 2019a). Among the 124 genes identified in *Hydra*, potential candidates were those whose expression was focused primarily in the head and transitioned down the body column. Another requirement was that the candidate was rapidly up-regulated during head regeneration. Among the remaining three candidates, the transcription factor *Sp5* meets all of the requirements for the *Hydra* head inhibitor. Once selected, the main goal was to demonstrate that this candidate met all of the previously established criteria for the head inhibitor gene.




This project was started by Dr. Matthias Vogg, so *Sp5* was already identified as a potential candidate when I joined this project. Nonetheless, I contributed to this work by performing the gene expression analysis with *In situ* hybridization, cell culture experiments to understand *Sp5 in vitro* regulation, loss-of-function assays that resulted in the characteristic multiple headed phenotype, and ALP drug treatments which lead to confirm that Wnt/ β -catenin positively regulates the expression of *Sp5*. I performed all the ISH of the paper and made supplementary figure 4, supplementary figure 14A.

ARTICLE

<https://doi.org/10.1038/s41467-018-08242-2>

OPEN

An evolutionarily-conserved Wnt3/ β -catenin/Sp5 feedback loop restricts head organizer activity in *Hydra*

Matthias C. Vogg ¹, Leonardo Beccari¹, Laura Iglesias Ollé¹, Christine Rampon^{2,3,4}, Sophie Vríz^{2,3,4}, Chrystelle Perruchoud¹, Yvan Wenger ¹ & Brigitte Galliot ¹

Polyps of the cnidarian *Hydra* maintain their adult anatomy through two developmental organizers, the head organizer located apically and the foot organizer basally. The head organizer is made of two antagonistic cross-reacting components, an activator, driving apical differentiation and an inhibitor, preventing ectopic head formation. Here we characterize the head inhibitor by comparing planarian genes down-regulated when β -catenin is silenced to *Hydra* genes displaying a graded apical-to-basal expression and an up-regulation during head regeneration. We identify Sp5 as a transcription factor that fulfills the head inhibitor properties: leading to a robust multiheaded phenotype when knocked-down in *Hydra*, acting as a transcriptional repressor of *Wnt3* and positively regulated by Wnt/ β -catenin signaling. *Hydra* and zebrafish Sp5 repress *Wnt3* promoter activity while *Hydra* Sp5 also activates its own expression, likely via β -catenin/TCF interaction. This work identifies Sp5 as a potent feedback loop inhibitor of Wnt/ β -catenin signaling, a function conserved across eumetazoan evolution.

¹Department of Genetics and Evolution, Institute of Genetics and Genomics in Geneva (iGE3), Faculty of Sciences, University of Geneva, 30 Quai Ernest Ansermet, CH-1211 Geneva 4, Switzerland. ²Centre Interdisciplinaire de Recherche en Biologie (CIRB), CNRS UMR 7241/INSERM U1050/Collège de France, 11, Place Marcelin Berthelot, 75231 Paris Cedex 05, France. ³Université Paris Diderot, Sorbonne Paris Cité, Biology Department, 75205 Paris Cedex 13, France. ⁴PSL Research University, 75005 Paris, France. Correspondence and requests for materials should be addressed to B.G. (email: brigitte.galliot@unige.ch)

The freshwater *Hydra* polyp, which belongs to Cnidaria, a sister group to Bilateria, has the remarkable talent to regenerate any lost body parts, including a fully functional head. *Hydra*, which is made of two cell layers, external named epidermis and internal named gastrodermis, shows a polarized tubular anatomy with a head at the apical/oral pole and a foot at the basal/aboral one, both extremities being enriched in nerve cells (Fig. 1a). Remarkably, the cnidarian oral pole has been proposed to correspond to the posterior end of bilaterians¹. Head regeneration relies on the rapid transformation of a piece of somatic adult tissue, the amputated gastric tube, into a tissue with developmental properties named head organizer, which directs the patterning of the regenerating tissue (reviewed in^{2–4}) (Fig. 1b). This process is highly robust in *Hydra*, occurring after bisection at any level along the body column. The concept of organizer was first discovered by Ethel Browne who performed lateral transplantation experiments between pigmented and depigmented *Hydra*⁵. By grafting a non-pigmented piece of head onto the body column of a pigmented host, she observed the development of an ectopic axis predominantly made of pigmented cells, demonstrating the recruitment of host cells by the graft. This discovery was later confirmed in hydrozoans^{6–10} but also in vertebrates where organizers play an essential role during embryonic development¹¹. In *Hydra* regenerating its head, the organizer gets established within 10 to 12 h after mid-gastric bisection, restricted to the head-regenerating tip within the first 24 h, remaining stable until the new head is formed and subsequently persisting as a homeostatic head organizer⁹.

The *Hydra* model also helped understand the dual structure of organizers. By comparing the efficiency of apical grafts to induce ectopic axis on intact or decapitated hosts, Rand et al. showed that the *Hydra* head organizer exerts two opposite activities, one activator that promotes apical differentiation, and another inhibitory that prevents the formation of supernumerary or ectopic heads¹². In *Hydra* the inhibitory activity is graded along the body axis, maximal at the apical pole⁸, and tightly modulated during head regeneration, rapidly decaying after amputation and slowly recovering¹³. Gierer and Meinhardt used the results obtained from a series of transplantation experiments to propose a general mathematical model of morphogenesis¹⁴. Their model revisits the Turing model based on the reaction-diffusion model, where two substances that exhibit distinct diffusion properties and interact with each other, form a minimal regulatory loop that suffices for de novo pattern formation¹⁵. Gierer and Meinhardt posed that the activation component acts over short-range distance and the inhibition one over long-range distance. They distinguished between “the effective concentrations of activator and inhibitor, on one hand, and the density of their sources on the other”¹⁴. These models proved to efficiently simulate basic properties of pattern formation and to fit molecular data in a variety of developmental contexts¹⁶.

In *Hydra*, the Holstein lab identified *Wnt3* as a growth factor fulfilling the criteria of the head activator, expressed locally at the tip of the head in intact *Hydra*, rapidly re-expressed in head-regenerating tips after amputation, and able to trigger an auto-catalytic feedback loop^{17–19}. Concerning the head inhibitor necessary to maintain a single head in homeostatic polyps and to develop a single head in budding and regenerating contexts, several attempts were made to characterize it, either biochemically or genetically. A protease-resistant small hydrophilic molecule was identified, exhibiting an apical to basal graded activity although with some activity also detected in the basal disc^{20,21}. This last property discouraged from any further characterization. A genetic screen identified a *Hydra* ortholog of the vertebrate Wnt dickkopf inhibitors, named *hyDkk1/2/4*, which efficiently antagonizes Wnt activity in *Xenopus*²². However, *Dkk1/2/4* is not

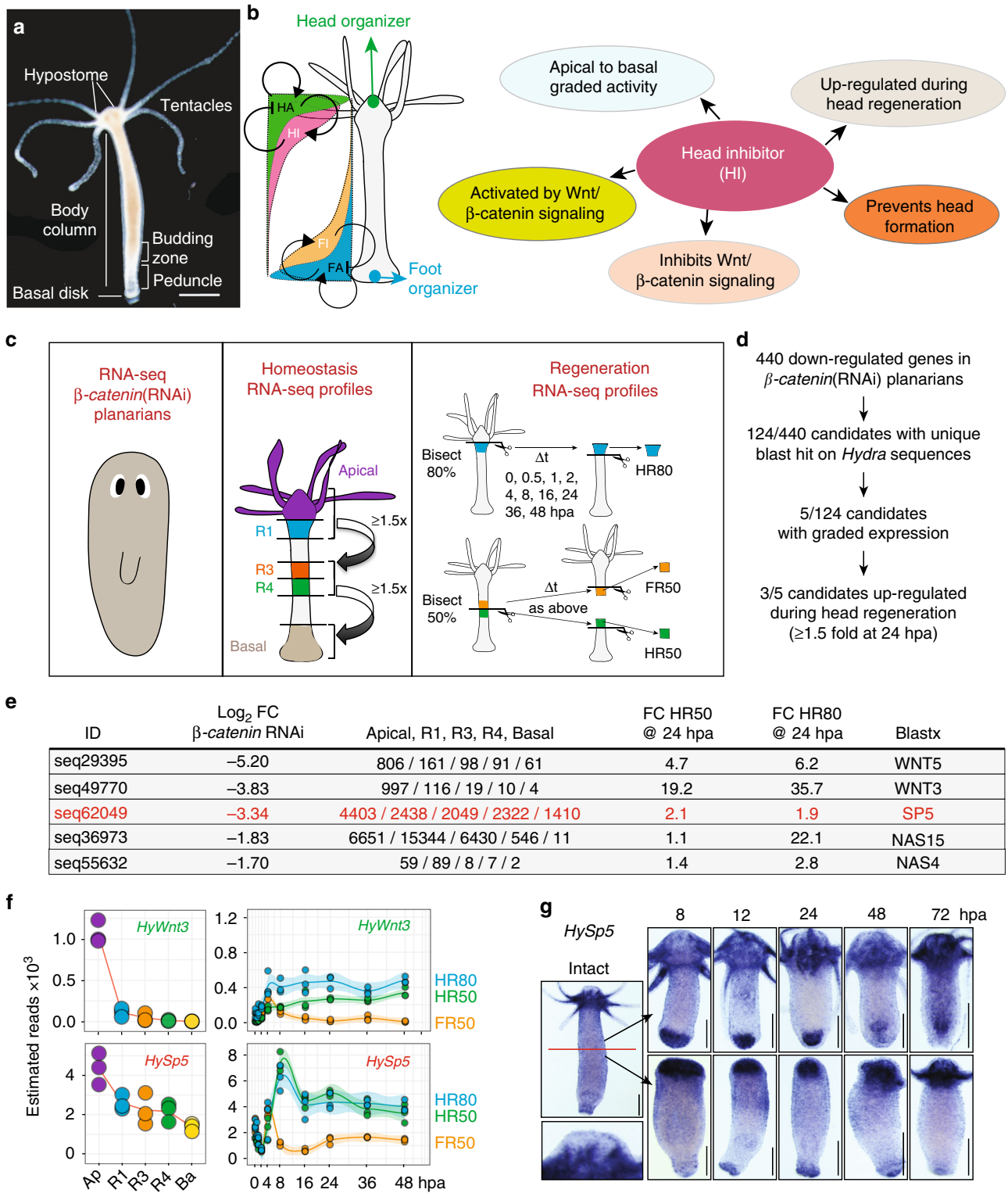
expressed apically, being negatively regulated by Wnt/ β -catenin signaling and its downregulation does not induce a multiheaded phenotype^{22,23}. A recent study suggests that *Hydra* Thrombospondin might be involved in head inhibition, however its downregulation does not lead to a multiheaded phenotype²⁴. Therefore, the molecular nature of the negative regulator(s) of the *Hydra* head organizer remains unknown. Here we used a strategy based on the evolutionarily conservation of Wnt/ β -catenin signaling to trace the *Hydra* head inhibitor. We identify the transcription factor *Sp5* as a transcriptional repressor of *Wnt3*, leading to a robust multiheaded phenotype when knocked-down in *Hydra*, while Wnt/ β -catenin signaling positively modulates *Sp5* expression. *Sp5* fulfills the requirements of a head inhibitor in *Hydra*, and we show that this feedback loop between *Sp5* and Wnt/ β -catenin signaling appears conserved across eumetazoan evolution.

Results

Identification of putative *Hydra* head inhibitors. To identify inhibitors of apical patterning that regulate the activity of the head organizer in both homeostatic and regenerative conditions, we established five criteria to be fulfilled by head inhibitor (HI) gene(s): (1) be controlled by Wnt/ β -catenin signaling, (2) display an apical-to-basal graded activity, (3) be upregulated within the first day of head regeneration, (4) inhibit Wnt/ β -catenin signaling, (5) prevent head formation (Fig. 1b). To select β -catenin target genes, we used a dataset of 440 genes downregulated in planarians silenced for *β -catenin*²⁵ to retrieve 124 *Hydra* cognate genes (Supplementary Data 1). We analyzed their spatial and temporal RNA-seq expression profiles and found 5/124 genes predominantly expressed in the head and 3/5 upregulated in head-regenerating tips at least 1.5 fold after 24 h of regeneration (Fig. 1c, d). Among these candidates, we found *Wnt3* and *Wnt5*, known as positive regulators of morphogenetic processes^{17,18,26} and *Sp5*, previously identified as a Wnt/ β -catenin target gene in vertebrates^{27–31}, thus a putative HI candidate (Fig. 1e). *Hydra Sp5* (*HySp5*) encodes a Sp/Klf-class transcription factor whose sequence clusters with the bilaterian *Sp5* ones in phylogenetic analyses (Supplementary Figs. 1–3).

Whole mount in situ hybridization confirmed the RNA-seq *Sp5* pattern in intact *Hydra*, predominantly expressed in the head although absent from the apical tip where *Wnt3* expression is maximal (Fig. 1f, g). After mid-gastric bisection, *Sp5* is rapidly upregulated in both head- and foot-regenerating tips but its expression is only sustained in head-regenerating ones (Fig. 1g, Supplementary Fig. 4) supporting the idea that *Sp5* is involved in head but not foot regeneration. We also performed a RNA-seq analysis of the cell-type expression³² and found that both *Sp5* and *Wnt3* are predominantly expressed in the gastrodermal epithelial stem cells (gESCs), a cell type associated with morphogenetic processes (Supplementary Fig. 5).

***Hydra Sp5* a robust head inhibitory component.** Next, we silenced *Sp5* by electroporating siRNAs in intact animals and observed that within two days following the third electroporation (RNAi3), *Sp5*(RNAi) animals develop ectopic axes, initially from the budding zone, few days later from the upper body column (Fig. 2a, Supplementary Fig. 6). These ectopic axes differentiate multiple heads when located in the basal half but not from the upper half. Both ectopic axes and ectopic heads express the apical markers *Wnt3*, *Bra1* and *Tsp1*, and the gland cell marker *Kazal1* in the gastric tissue (Fig. 2b). When single-headed animals silenced for *Sp5* are bisected after RNAi2, they all regenerate multiple heads that express *Wnt3* at the tip (Fig. 2c, Supplementary Fig. 7). This multiheaded phenotype is



robust, emerging quite synchronously in 50% uncut animals one day after RNAi2, in 100% two days after RNAi3 (Fig. 2d, Supplementary Fig. 6a–c). Furthermore, these ectopic heads express the neuropeptide RF-amide and are able to catch and ingest live *Artemia*, indicating that each ectopic head is functional (Fig. 2e, Supplementary Fig. 6d, Supplementary Movies 1–4). These results indicate that Sp5 acts as a strong inhibitor of head formation in *Hydra*.

Sp5 antagonizes Wnt/β-catenin signaling in *Hydra*. Next, we tested whether the multiheaded phenotype corresponds to a de-repression of *Wnt3*. To do this, we first tested whether the phenotype occurs when the Wnt/β-catenin pathway is inactive and thus knocked-down *Sp5* together with *β-catenin* (Fig. 3a). Silencing *β-catenin* on its own delays head regeneration (Supplementary Fig. 8) and causes the formation of ectopic bumps in intact animals (Fig. 3a, Supplementary Fig. 9). While knocking

Fig. 1 Screening strategy to identify candidate head inhibitor genes in *Hydra*. **a** Anatomy of an intact *Hydra*. The apical extremity (head) is composed of a dome-shaped structure called hypostome, surrounded by a ring of tentacles. At the other extremity (foot), the basal disk allows the animals to attach. **b** The five criteria used to identify HI candidate genes. **c, d** Screening procedure applied to identify HI candidate genes: An RNA-seq dataset of 440 downregulated genes in β -catenin (RNAi) planarians was used to retrieve through blastx on NCBI (E value $< 1e^{-10}$) 124 non-redundant *Hydra* sequences that correspond to 106 unique proteins (Supplementary Data 1). These candidates were next tested on RNA-seq data sets obtained in intact *Hydra* measured at five positions along the body axis (apical -Ap-, regions R1, R3, R4, basal -Ba-) to identify five apical-to-basal graded genes, which were tested on RNA-seq data sets obtained from regenerating tips taken at nine time points after a 50% or 80% bisection. Data available on HydrAtlas.unige.ch **e** Three genes downregulated after β -catenin(RNAi) in planarians, show an apical-to-basal graded expression in *Hydra*, and a minimal 1.5-fold upregulation in head-regenerating tips at 24 hpa. The 3rd column indicates the mean value of the number of reads measured in three biological replicates in the indicated regions. Fold Change (FC) measured in head-regenerating (HR) tips at 24 h post-amputation (hpa) over the values measured at time 0. **f** *Wnt3* and *HySp5* RNA-seq profiles in intact and regenerating animals. **g** *HySp5* expression patterns in intact and regenerating *Hydra* tested as indicated after mid-gastric bisection in two independent experiments. Inset: magnified view of the apex. Scale bars: 250 μ m

down *Sp5* causes the formation of multiple heads, the simultaneous knockdown of *Sp5* and β -catenin prevents the occurrence of the multiheaded phenotype (Fig. 3a, Supplementary Fig. 9), suggesting that an increase in Wnt/ β -catenin signaling activity is necessary to trigger multiple head formation when *Sp5* is knocked down.

To further demonstrate that *Sp5* represses Wnt/ β -catenin signaling via *Wnt3* repression, we knocked-down *Sp5* in combination with Alsterpaullone (ALP), a drug that activates the Wnt/ β -catenin pathway by antagonizing GSK3 β ^{33,34}. As anticipated this combination led to a significant increase in ectopic tentacle formation, while knocking down β -catenin provides the opposite effect (Fig. 3b, Supplementary Fig. 10a). In these *Sp5*(RNAi) animals, we could also detect an increase in *Wnt3* expression along the body column, indicating that *Sp5* does repress *Wnt3* expression (Fig. 3c, Supplementary Fig. 10b).

We also performed reaggregation experiments with cells coming from ALP-treated animals knocked-down either for *Sp5* or for β -catenin. In standard conditions of reaggregation, several head spots form, each of them containing 5–15 *Wnt3* expressing cells at 24 hours³⁵. When *Sp5* is knocked-down, we noted that the reaggregates tend to form multiple axes with a number of *Wnt3* expressing spots increased by two-fold (Fig. 3d, e, Supplementary Fig. 11). In contrast, when β -catenin is knocked-down, the reaggregation process proceeds slower with aggregates exhibiting only few tentacles at day-4, with a number of *Wnt3*-expressing clusters similar to that observed in scramble(RNAi) control animals (Fig. 3d). These results confirm that *Sp5* directly or indirectly represses *Wnt3* expression.

To test whether *Sp5* can directly repress the *Wnt3* promoter, we produced a transgenic strain expressing the *HyWnt3*-2149:GFP-*HyAct*:dsRed construct where 2'149 bp of the *Hydra Wnt3* promoter drives GFP expression and the *Hydra Actin* promoter drives dsRed expression¹⁹. We noted distinct levels of *Wnt3*-driven GFP fluorescence in control transgenic animals, maximal at the apex, intermediate in the adjacent region above the tentacle ring, and null at the level of the tentacle ring and along the body column (Supplementary Fig. 12a). In such transgenic animals knocked-down for *Sp5*, we did not record any body-wide GFP fluorescence but rather the appearance of patches of GFP + cells at the tip of the ectopic axes (Supplementary Fig. 12b). We could confirm this patchy *Wnt3* activation along the body column of *Sp5*(RNAi) animals by performing a detailed kinetic analysis of *Wnt3* expression (Supplementary Fig. 12c–d). This *Wnt3* ectopic expression pattern suggests that *Sp5* is silenced in restricted regions along the body column where *Wnt3* is de-repressed and enhances its own expression via β -catenin signaling as previously recorded.

***Sp5* represses the *Hydra* and zebrafish *Wnt3* promoter.** To further investigate the repressing activity of *HySp5* on the

HyWnt3 promoter, we performed luciferase reporter assays in human HEK293T cells (Fig. 4a–c). As the *HyWnt3*-2149:Luc construct shows a very low basal activity, we co-expressed a constitutively active form of β -Catenin (*CMV:hu $\Delta\beta$ -Cat*)³⁶ that enhances by ~10-fold the luciferase activity (Fig. 4b). In such conditions, the co-expression of *HySp5* significantly reduces the activity of the *HyWnt3* promoter (Fig. 4b). This effect was not observed when a partial version of *HySp5* lacking the DNA-binding domain was used, indicating that the repressive effect of *HySp5* is DNA-binding dependent (Fig. 4b). Two adjacent cis-regulatory modules were previously identified in the *HyWnt3* promoter, a 599 bp-long activator that contains three clustered TCF binding sites and a 386 bp-long repressor sequence¹⁹, located immediately downstream (Fig. 4a, Supplementary Fig. 13a). This repressor module, highly conserved across *Hydra* species (Fig. 4a), is necessary for the *Sp5*-mediated *Wnt3* repression, as the repression is no longer observed when this element is removed (Fig. 4b). Among the four constructs that harbor limited deletions within the *Wnt3* repressor element, the construct containing both the -386/-286 and the -95/-1 sequences is the only one repressed by *Sp5* (Fig. 4c), suggesting that the *Sp5*-dependent *Wnt3* repression requires the cooperative activity of these two elements.

To test whether *Sp5* also represses *Wnt3* transcription in vertebrates we tested the 4 kb promoter region of the zebrafish *Wnt3* locus in reporter assays where the zebrafish paralogs *ZfSp5a* and *ZfSp511* are expressed (Fig. 4d, e). As for the *HyWnt3*-2149 construct, the transcriptional activity of the *ZfWnt3*-3997 construct was strongly enhanced by *hu $\Delta\beta$ -Cat*, but repressed upon co-expression of *ZfSp5a* or *ZfSp511* (Fig. 4e). The repressor activity of *ZfSp5a* was abolished when the DNA-binding domain was deleted. Although the zebrafish *Wnt3* promoter does not share obvious sequence homologies with that of the *HyWnt3* promoter, we could identify regions evolutionarily-conserved across different teleost lineages as well as TCF binding sites (TCF-BS) (Fig. 4d, Supplementary Fig. 13b). ChIP-qPCR experiments performed in transfected HEK293T identified two evolutionarily-conserved elements within the *ZfWnt3* promoter directly bound by *ZfSp5a* (Fig. 4f).

Wnt/ β -catenin signaling regulates *HySp5* expression. In planarians as in zebrafish and mammals, the canonical Wnt/ β -catenin pathway positively regulates the expression of *Sp5*^{25,27,31,37}. In mammals, *Sp5* has also been reported to auto-regulate its expression, although studies in human and mouse embryonic stem cells (ESCs) differ on whether *Sp5* acts positively or negatively on its own promoter^{31,37}. In *Hydra*, a two days exposure to ALP suffices to upregulate *Sp5* expression along the body column (Fig. 5a, Supplementary Fig. 14), suggesting that *Sp5* regulation by the Wnt/ β -catenin pathway predates the divergence of cnidarians. To test this hypothesis, we cloned 2'992 bp of the

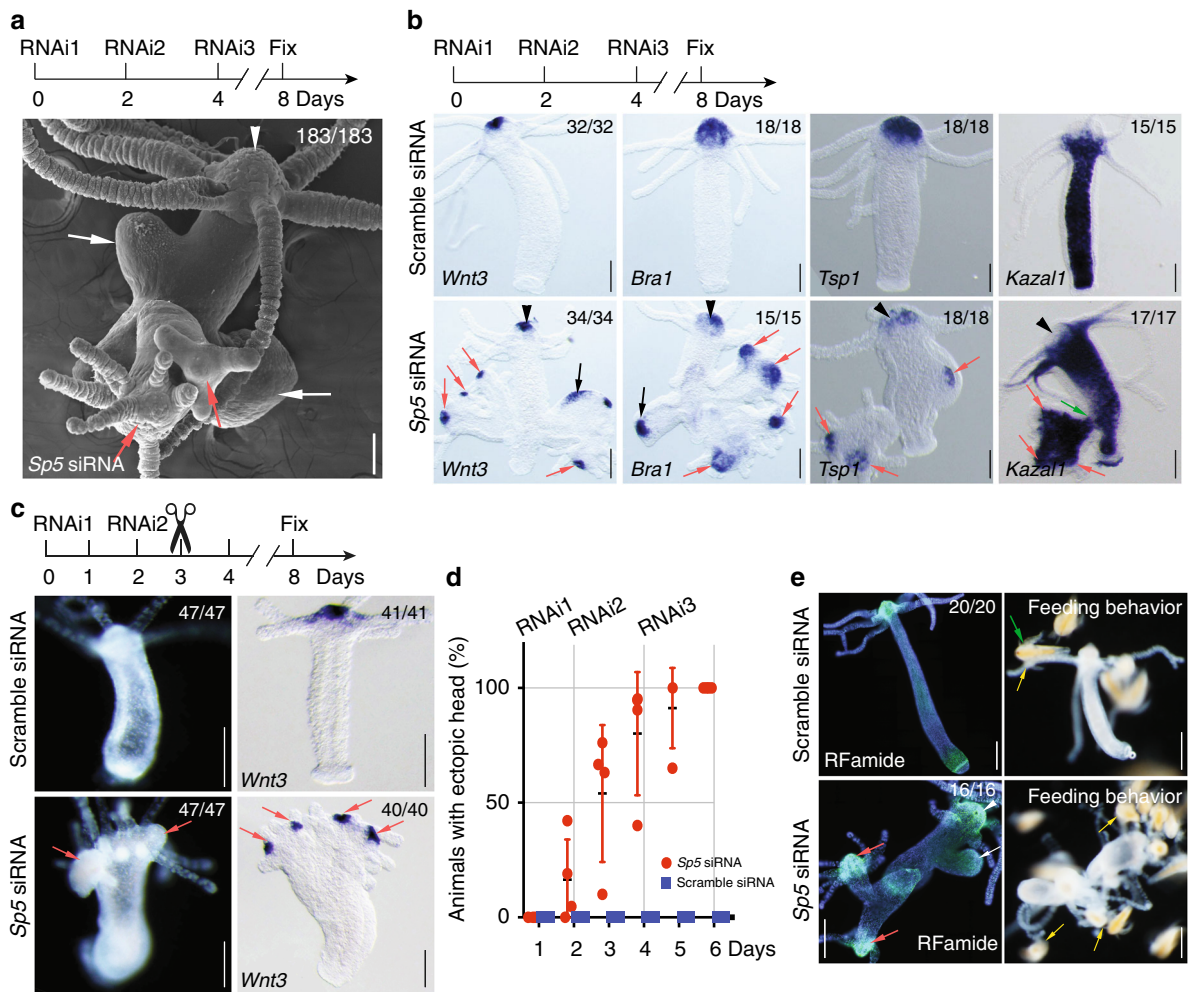


Fig. 2 Knocking down *HySp5* leads to the formation of ectopic axes and ectopic heads. **a, b** Morphological changes detected in intact *Hydra* exposed three times to *Sp5* or scramble siRNAs as indicated. In **a** SEM view four days after *Sp5* RNAi3. In **b** animals fixed and detected for *Wnt3*, *HyBra1*, *Tsp1* or *Kazal1* expression. White or black arrows: ectopic axes; red arrows: ectopic heads; arrowheads: parental heads; green arrow: connection between endodermal tissue of the secondary axis and the parental body column (3 independent experiments). **c** Morphological changes detected in head regenerating animals 5 days after mid-gastric bisection performed 24 h after two exposures to *Sp5* siRNAs (3 independent experiments). Arrows as in **a**. **d** Kinetics of morphological changes observed in intact *Sp5*(RNAi) *Hydra*. Each dot represents an independent experiment ($n = 4$). **e** RFamide expression and feeding response tested in ectopic heads of *Sp5*(RNAi) *Hydra* 4 days after RNAi3 (2 independent experiments). White arrow: ectopic axis; red arrows: ectopic heads; arrowhead: parental head; green arrow: *Artemia*; yellow arrows: *Artemia* caught by tentacles. Scale bars: 200 μ m. Error bars indicate SD

HySp5 promoter, a region that is evolutionarily-conserved across *Hydra* species and contains five putative TCF binding sites (Fig. 5b, Supplementary Fig. 13c). We evidenced its responsiveness to *Wnt*/ β -catenin signaling, as we recorded a significant upregulation of the activity of the *HySp5*-2992:Luc reporter construct when the human *WNT3*, *LRP6* or *hu $\Delta\beta$ -Cat* proteins were co-expressed (Fig. 5c). In addition, we found that *HySp5* can bind its own promoter as in ChIP-qPCR experiments *Sp5* binding is significantly enriched in two neighboring regions located immediately upstream of the *Sp5* Transcriptional Start Site (TSS) (Fig. 5d). Furthermore, co-expression of *HySp5*-2992:Luc and *HySp5*, alone or in combination with *hu $\Delta\beta$ -Cat* resulted in a strong increase in luciferase activity (Fig. 5e). In mouse ESCs, *Sp5* interacts with β -catenin and *Tcf-Lef1* to regulate gene expression³¹. As anticipated, we found in a ChIP-seq analysis the mouse *Sp5* and β -catenin proteins enriched in the same region of the *Sp5* promoter (Supplementary Fig. 15a), suggesting a possible cooperation to regulate *Sp5* transcription. We performed co-immunoprecipitation experiments with HEK293T cells co-transfected with *HySp5* and *hu $\Delta\beta$ -Cat* or *huTCF1* and

observed an interaction between *HySp5* and these factors (Fig. 5f, Supplementary Fig. 15b–c). These results indicate that *HySp5*, similarly to its mammalian cognates, can act as an activator or a repressor of transcription and that *Hydra* and vertebrate *Sp5* can interact with β -catenin or TCF1.

***Sp5* DNA-binding properties are evolutionarily-conserved.** To further compare the transcriptional activities of *HySp5* and *ZfSp5a*, we expressed *HySp5* or *ZfSp5a* in HEK293T cells and analyzed the genomic occupancies and the transcriptional changes induced by their overexpression (Fig. 6a). ChIP-seq analysis revealed that *HySp5* binds a much smaller fraction of sequences than *ZfSp5a* (Fig. 6b), while the number of genes bound by *HySp5* and *ZfSp5a* is not so different, 13'251 vs. 18'619, 99% of the *HySp5* bound genes are also *ZfSp5a* targets (Fig. 6c). Interestingly, *HySp5* and *ZfSp5a* differ in the spatial distribution of their target sequences: the majority of *HySp5* bound elements localize within the 5 kb proximal region of the assigned genes, while *ZfSp5a* proportionally binds more frequently elements

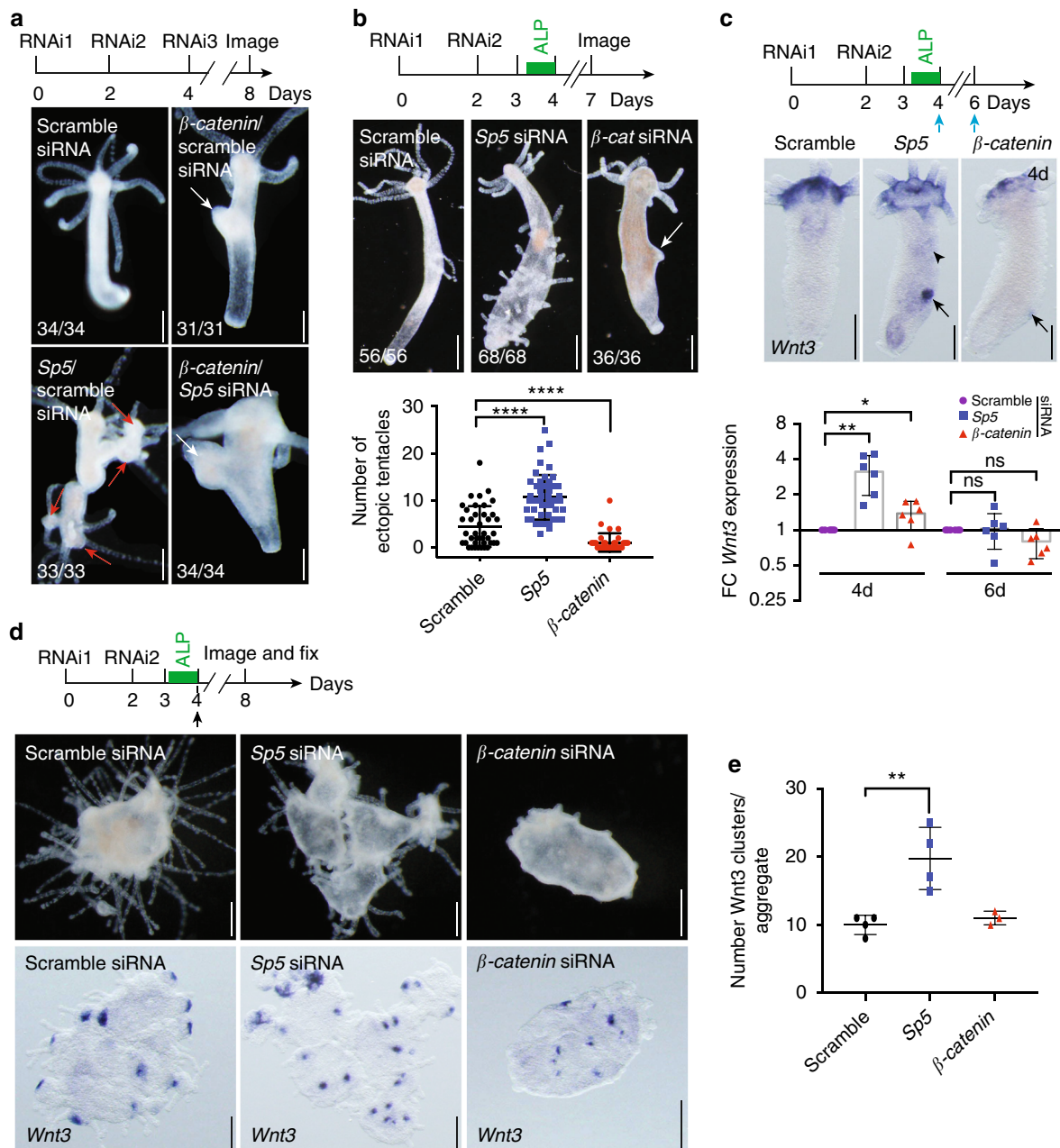


Fig. 3 HySp5 antagonizes Wnt/ β -catenin signaling in *Hydra*. **a** Double knockdown of *Sp5* and β -catenin. Animals were pictured live on day-8 in two independent experiments. RNAi: siRNA electroporation day. Red arrows: ectopic heads; white arrows: bumps. **b** Knockdown of *Sp5* and β -catenin in ALP-treated animals. Upper panel: Morphological changes observed in animals fixed at day-7. Lower panel: Quantification of ectopic tentacles formed at day-7. Each dot represents the number of ectopic tentacles in one animal (two biologically independent experiments). **c** Intact *Hydra* exposed to siRNAs and ALP as indicated and detected for *Wnt3* by WISH (upper panel) and qPCR (lower panel). Blue arrows: RNA extraction days; black arrows: local increase in *Wnt3*; black arrowhead: diffuse increase in *Wnt3* expression. Each data point represents one biologically independent experiment. **d** Effect of *Sp5* knockdown on head patterning during the process of reaggregation initiated on day-4 (black arrow). Aggregates were pictured live (upper row), then fixed to detect *Wnt3* expression (lower row) in two independent experiments. **e** Quantification of *Wnt3* expressing clusters. Each dot represents the number of *Wnt3*+ clusters in one aggregate. Statistical *p* values: **P* \leq 0.05, ***p* \leq 0.01, *****p* \leq 0.0001 (unpaired *t* test). Scale bars in panels **a–d**: 200 μ m. Error bars indicate SD

located in upstream sequences, above 10 kb from the TSS (Fig. 6d, e). This suggests that vertebrate Sp5 more readily recognizes sequences enriched in long-range regulatory elements, which are not recognized by the HySp5 protein.

Motif enrichment analysis of the HySp5 and ZfSp5a bound elements revealed that the two orthologs recognize both similar and divergent consensus binding sites (Fig. 6f). In both cases, the most enriched motif resembled the general SP/KLF consensus

sequence (GGGxGGG/A). We then used the enriched motifs to identify putative HySp5/ZfSp5a binding sites in the regulatory regions of *HyWnt3*, *ZfWnt3* and *HySp5*. We could identify putative HySp5 binding sites in the two regions of the *HyWnt3* repressor required to inhibit transcription (Supplementary Figs. 13). Similarly, we also found evolutionarily-conserved Sp5 binding sites in the regions of *ZfWnt3* and *HySp5* enriched in the ChIP-qPCR analysis, supporting the idea that *Hydra* and

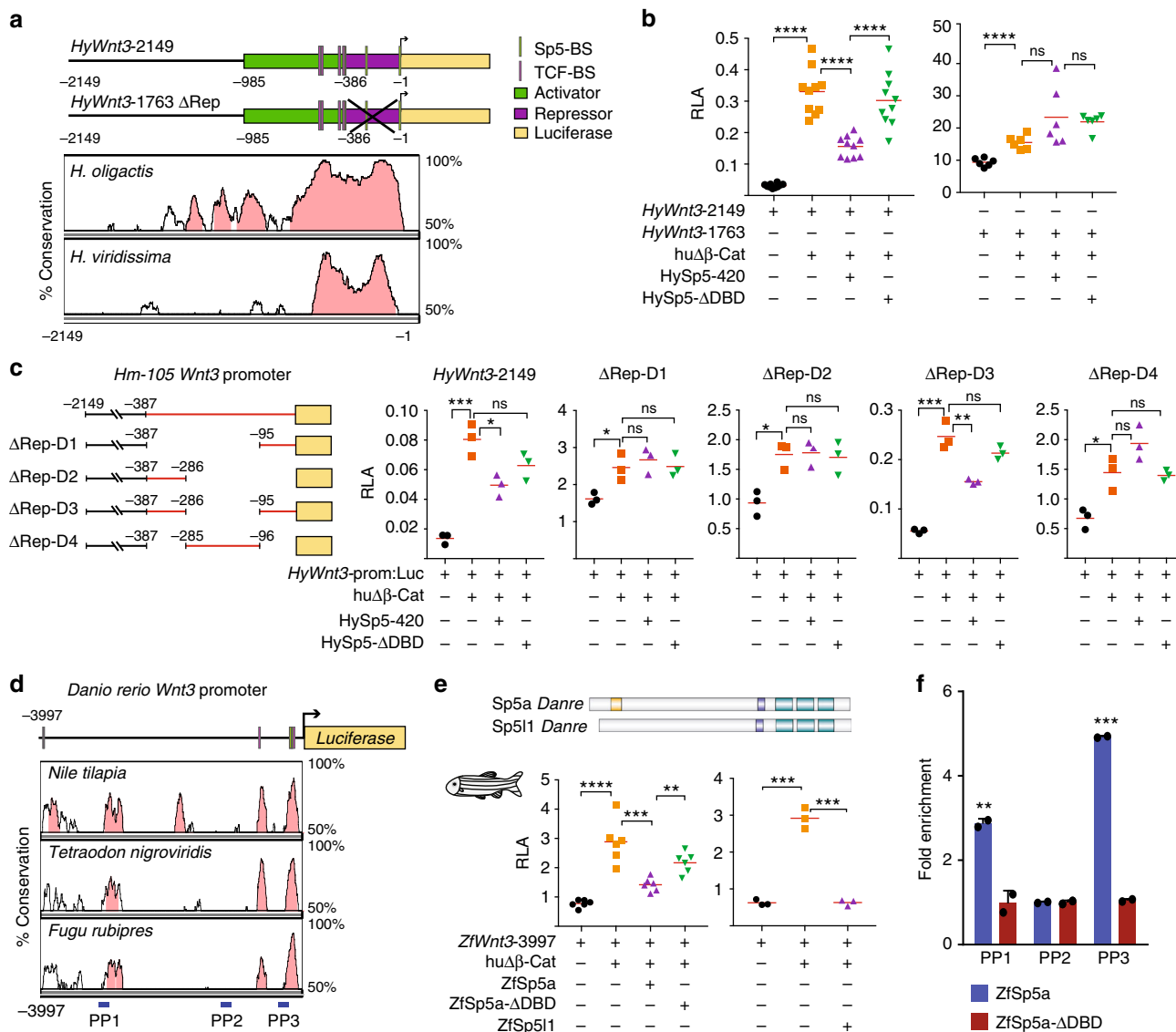


Fig. 4 *Hydra* Sp5 and zebrafish Sp5 repress the *Wnt3* promoter activity. **a** Map of the *HyWnt3* promoter and phylogenetic footprinting plot comparing the 2 kb genomic region encompassing the *H. magnipapillata* (*Hm-105*) *Wnt3* promoter with the corresponding regions in the *H. oligactis* and *H. viridissima* genomes. Green and magenta bars indicate the activator and repressor regions identified by (ref. 19). Conserved TCF binding sites (TCF-BS) are shown in magenta and putative Sp5-BS in green. Pink peaks in the Vista alignment plot represent evolutionarily-conserved modules (at least 70% base-pair identity over 100 bp sliding window). **b** Luciferase assays measuring the activity of the *HyWnt3-2149* (left) or *HyWnt3-1763-ΔRep* (right) promoters in HEK293T cells co-expressing a constitutively active human β-Catenin (*huΔβ-Cat*), *HySp5-420* (full-length Sp5) or *HySp5-ΔDBD* (Sp5 lacking the DNA-Binding Domain). Note the ~300x higher basal activity of *HyWnt3-1763-ΔRep:Luc* when compared to that of *HyWnt3-2149:Luc*. RLA: Relative Luciferase Activity. **c** Luciferase assays performed in HEK293T cells testing the *HyWnt3* promoter when deleted of different portions of the repressor. Note that the repressive effect of *HySp5* is only observed with the *HyWnt3-2149* and *HyWnt3-ΔRep-D3* constructs. **d** Phylogenetic footprinting plot comparing the 4 kb genomic region encompassing the zebrafish *Wnt3* promoter with the corresponding genomic regions of three teleost fish species. Pink peaks as in panel a; blue rectangles indicate regions of the *ZfWnt3* promoter tested for *ZfSp5a* binding in ChIP-qPCR assays. PP: Primer Pair. **e** Luciferase assays measuring the activity of the zebrafish *Wnt3* promoter in HEK293T cells, co-transfected with *huΔβ-Cat*, *ZfSp5a*, *ZfSp5a-ΔDBD* (left) or *huΔβ-Cat*, *ZfSp511* (right). **f** ChIP-qPCR assays performed with cells expressing *ZfSp5a* or *ZfSp5a-ΔDBD*. Note the significant enrichment in the PP1 and PP3 regions. Source Data are provided as a Source Data file. Each data point in **b**, **c**, **e**, **f** represents one biological independent experiment. Statistical *p* values: **p* ≤ 0.05; ***p* ≤ 0.01; ****p* ≤ 0.001; *****p* ≤ 0.0001 (unpaired *t* test). Error bars indicate SD

zebrafish Sp5 directly regulate the transcriptional activity of these promoters. Despite the similarity in the main consensus sites bound by *HySp5* and *ZfSp5a*, we also identified motifs differentially enriched among the elements bound by these two orthologs (Fig. 6f). Interestingly, *ZfSp5a* binds elements that display an over-representation of Tbx1 and Sox13 motifs, which were not identified in the pool of *HySp5* bound sequences (Fig. 6f). Members of the Tbx and Sox families are known to

interact with Sp1³⁸ and β-catenin³⁹ respectively, suggesting that they could also form transcriptional complexes with Sp5. Thus, the enrichment in Tbx/Sox consensus sequences suggests that vertebrate Sp5 but not *Hydra* Sp5 may regulate gene expression in complexes involving these transcription factors.

To further validate that *HySp5* has similar DNA-binding properties than its vertebrate orthologs, we inspected the *HySp5* genomic coverages in the proximities of genes identified as

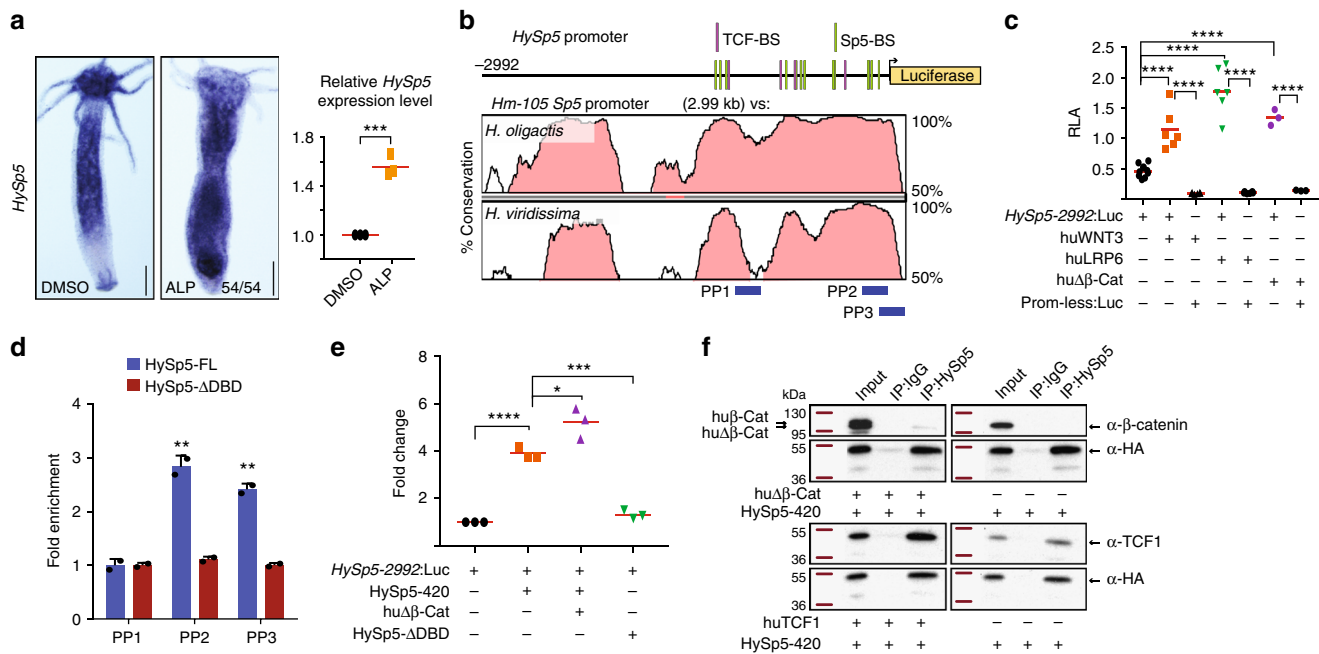


Fig. 5 Wnt/ β -catenin signaling regulates *HySp5* expression. **a** *HySp5* expression in intact *Hydra* exposed to ALP for two days, detected by WISH (left) (3 independent experiments) and qPCR (right). Each point represents an independent replicate. Scale bar: 250 μ m. **b** Map of the 2992 bp genomic region encompassing the *Sp5* promoter from the *Hm-105* strain and phylogenetic footprinting plot comparing this region in *Hm-105*, *H. oligactis* and *H. viridissima*. Pink peaks and binding sites as in Fig. 4. Blue rectangles: regions tested for *Sp5* binding in ChIP-qPCR assays. **c** *HySp5* promoter activity measured in HEK293T cells co-transfected with *HySp5*-2992:Luc and plasmids expressing activators of Wnt/ β -catenin signaling, human WNT3, LRP6, $\Delta\beta$ -Catenin. **d** ChIP-qPCR assays performed in HEK293T cells expressing *HySp5*-2992:Luc together with *HySp5*-420 or *HySp5*- Δ DBD. Source Data are provided as a Source Data file. **e** *HySp5* promoter activity measured in HEK293T cells expressing *HySp5*-2992:Luc with hu $\Delta\beta$ -Catenin, *HySp5*-420 or *HySp5*- Δ DBD. **f** Immunoprecipitation (IP) of HA-tagged *HySp5*-420 expressed in HEK293T cells together or not with hu $\Delta\beta$ -Catenin (upper) or huTCF1 (lower). IP was performed with an anti-HA antibody and Co-IP products were detected with the anti- β -catenin or anti-TCF1 antibodies. Same results were obtained in two independent experiments. Each data point in (c-e) represents one biological independent experiment. Statistical *p* values: **p* \leq 0.05, ***p* \leq 0.01, ****p* \leq 0.001, *****p* \leq 0.0001 (unpaired *t* test). Error bars indicate SD. PP primer pair, RLA relative luciferase activity

Wnt/ β -catenin targets in mouse and human ESCs^{31,37}. Comparable binding profiles of *HySp5* and *mSp5* were observed for the *Axin2*, *Bra* and *Lrg5* loci in human and mouse cells, while quite different at the *Nanog* and *Plk4* loci, the latter likely due to cell-type or species specific differences (Supplementary Fig. 16a). We also found a strong enrichment of *HySp5* and *ZfSp5a* binding in the *WNT3* intronic sequences, in the promoter and intronic sequences of the neighboring *WNT9B* locus and in the upstream and intronic sequences of *SP5* (Supplementary Fig. 16b). The GO term enrichment analysis actually identified the Wnt pathway as the most enriched category (Supplementary Fig. 16c, Supplementary Data 2).

All together, these results point to similar DNA-binding capacities between *HySp5* and *ZfSp5a* even though the latter recognizes a larger set of sequences, often located at mid-long distances upstream from the TSS, possibly acting in combination with Sox and/or Tbx proteins.

Conserved and divergent transcriptional functions of *Sp5*. To assess the transcriptional activity of *HySp5* and *ZfSp5a*, we measured by qRNA-seq the transcriptional changes induced by the overexpression of *HySp5* and *ZfSp5a* in HEK293T cells co-expressing or not the hu $\Delta\beta$ -Cat construct (Fig. 6a). As controls we used HEK293T cells transfected with a mock plasmid, the hu $\Delta\beta$ -Cat construct alone or the mutated *HySp5*- Δ DBD and *ZfSp5a*- Δ DBD constructs. Principal component analysis (PCA) showed that *HySp5* and *ZfSp5a* transfected samples, either alone or in combination with hu $\Delta\beta$ -Cat, segregated together, widely separated from the control or *HySp5*- Δ DBD/*ZfSp5a*- Δ DBD

values (Fig. 6g). This suggests that *HySp5* and *ZfSp5a* elicit overall similar transcriptional responses. Instead, the values obtained from hu $\Delta\beta$ -Cat transfected cells grouped together with the values from mock-transfected samples, while the values corresponding to cells co-expressing hu $\Delta\beta$ -Cat with *HySp5* or *ZfSp5a* do not substantially differ from those overexpressing *HySp5* or *ZfSp5a* alone (Fig. 6g, Supplementary Data 2). These results imply that HEK293T cells do not respond to hu $\Delta\beta$ -Cat overexpression, in agreement with previous reports showing that although HEK293T cells respond to Wnt signalling stimulation by translocating β -catenin to the nucleus^{40,41}, they display limited transcriptional responses of their endogenous Wnt target genes^{37,42}.

Next, we analyzed the genes whose expression is modulated upon *HySp5* or *ZfSp5a* overexpression but remains unaffected when their respective DNA-binding domain is deleted (Fig. 6h, Supplementary Data 2). We focused our analysis on the modulated genes that were associated to *HySp5*- or *ZfSp5a*-bound elements in ChIP-seq analysis, suggesting that these genes are directly activated or directly repressed targets. We identified downregulated genes, 153 upon *HySp5* expression, 113 by *ZfSp5a*, and 83 by both (Fig. 6i, Supplementary Fig. 17, Supplementary Data 3). This demonstrates that the cnidarian and vertebrate *Sp5* proteins have a similar repressive capacity. We also identified 137 and 23 genes upregulated upon *ZfSp5a* and *HySp5* overexpression, respectively. Of these, only 5 are activated by both *Sp5* orthologs (Fig. 6i, Supplementary Fig. 17, Supplementary Data 3), indicating that the activator function of the cnidarian and vertebrate *Sp5* transcription factors diverged

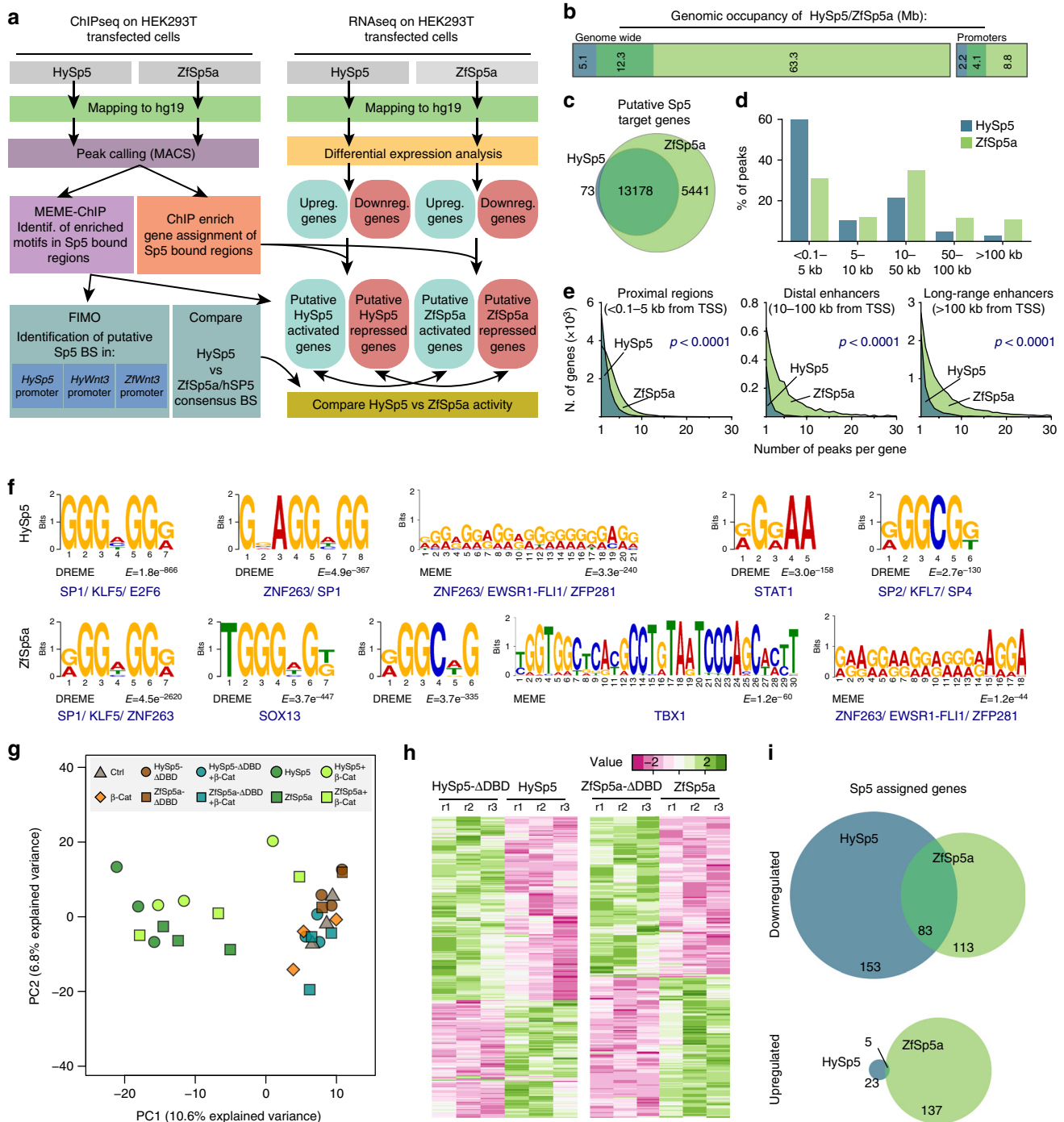


Fig. 6 *Hydra* Sp5 acts as a transcriptional activator and repressor. **a** Schematic representation of the workflow used for the analysis of the ChIP-seq and RNA-seq data in this study. Putative target genes were identified based on the identification of Sp5 bound elements using ChIPenrich. The consensus motifs enriched in Sp5 bound elements were identified using the MEME ChIP suite tool. Differential expression analysis was performed on RNA-seq samples to identify up- and downregulated genes. Those associated to a Sp5 bound element were considered as direct Sp5 up- or downregulated targets. **b** Bar graph representing the genomic coverage of HySp5 and ZfSp5a genome wide or in the promoters of Ensembl genes (defined as the 5 kb upstream of the gene TSS). Only autosomal chromosomes were used for this study. ZfSp5a coverages are considerably higher than those of HySp5. However, within gene promoters this difference is proportionally lower. **c** Venn diagram representing the number of genes assigned to HySp5 or ZfSp5a bound elements. Note the considerable overlap between HySp5 and ZfSp5a data sets. **d** Bar plot representing the percentage of Sp5 bound elements at different distances from the assigned gene TSS for HySp5 (blue) or ZfSp5a (green). **e** Frequency distribution of the number of peaks associated to each gene and located in the promoter region (left), 10–100 kb upstream of gene TSS (middle) or at long genomic distances (> 100 kb) from the gene body. **f** Enriched transcription factor consensus matrix identified in HySp5 and ZfSp5a bound elements. **g** Principal component analysis showing the segregation of RNA-seq samples across the two main principal components. **h** Heat map plots showing the z score value of genes significantly up- or downregulated (based on Wald test $p < 0,05$) in HySp5 or ZfSp5a transfected HEK293T cells compared to their respective control conditions (HySp5- Δ DBD or ZfSp5a- Δ DBD). **i** Venn diagrams showing the number of HySp5 and ZfSp5a direct transcriptional targets (see description in **a**) significantly up- or downregulated

during evolution. This is surprising, since both HySp5 and mammalian orthologs can interact with β -catenin (Fig. 5f) to promote target gene activation. As the HEK293T cells are largely insensitive to hu $\Delta\beta$ -Cat overexpression (Fig. 6g), the observed upregulation of HySp5 and ZfSp5a direct targets relies on mechanisms largely independent of β -catenin signaling. By contrast, the overexpression of HySp5 and ZfSp5a in zebrafish embryos leads to similar developmental alterations, which resemble those produced by the over-activation of Wnt/ β -catenin signaling (Supplementary Fig. 18, Supplementary Data 4).

Discussion

Studies performed in developing vertebrates show that *Sp5* is a target of Wnt/ β -catenin signaling as recorded in zebrafish^{27,28}, mice²⁹, *Xenopus*³⁰, as well as in self-renewing mouse and human ESCs^{31,37}. In line with these results, we show that in *Hydra*, *Sp5* is positively regulated by Wnt/ β -catenin signaling as evidenced by its upregulation when Wnt/ β -catenin signaling is pharmacologically enhanced. These results illustrate the deep conservation of the Wnt/ β -catenin-dependent regulation of *Sp5* across eumetazoans. Wnt5, another candidate identified in the screen might also play a role in head inhibition, as a putative inhibitor of the canonical Wnt pathway^{43,44} and a possible HySp5 target gene. By contrast, secreted Wnt antagonists such as Dickkopf (Dkk)⁴⁵ or Notum⁴⁶, both expressed in *Hydra*, were not identified in this screen.

Wnt3 and *Sp5* upregulations in head-regenerating tips are consistent with a rapid head organizer formation after bisection. *Sp5* is re-expressed early during head regeneration, although as expected, later than *Wnt3*. This temporal parameter is indeed essential for the establishment of a de novo head organizer as demonstrated by transplantation experiments that accurately measured the successive re-activation of the two head organizer components, with head activation restored within 12 hpa and head inhibition coming back later, detectable at 24 hpa^{9,13}. Here we used the qRNA-seq data to compare the respective regulations of *Wnt3* and *Sp5* in regenerating tips after decapitation or mid-gastric bisection. While *Wnt3* is rapidly upregulated to reach a plateau value at 4 hpa, *Sp5* shows an initial drop in expression within the first two hours following bisection, then an upregulation and a peak of expression detected at 8 hpa, four hours after that measured for *Wnt3*. If one assumes that the reestablishment of active Wnt3 and Sp5 proteins follows similar kinetics, then this four hour time window corresponds to a period when Wnt3/ β -catenin signaling is active but Sp5 still inactive as *Wnt3* repressor, leaving sufficient time to instruct tissues to form a head.

A recent observation suggested that human SP5 can directly repress the *WNT3* promoter in human ESCs³⁷. Here we demonstrate that indeed Sp5 from *Hydra* and zebrafish inhibit Wnt/ β -catenin signaling by repressing the activity of the *Wnt3* promoter. Both the RNA-seq and the ChIP-seq data presented here confirm this view, by showing firstly that HySp5 and ZfSp5a when overexpressed in HEK293T cells repress largely overlapping sets of genes and secondly that both *Hydra* and zebrafish Sp5 preferentially bind genes of the Wnt/ β -catenin signaling pathway, as observed in the promoter and intronic regions of the human *WNT3* and *WNT9B* genes. The studies performed in HEK293T cells also highlighted the fact that HySp5 and ZfSp5a, as transcriptional repressors, likely bind to regulatory elements located in the proximity of the TSS of their target genes. All together, these results highlight the similarity between the repressor effect of cnidarian and vertebrate Sp5 transcription factors, which predominantly affects genes of the Wnt/ β -catenin signaling pathway but is not restricted to it. It is thus tempting to speculate that the Sp5-dependent inhibition of Wnt/ β -catenin

signaling originated early in metazoan evolution and was maintained across eumetazoans. By contrast, the properties of HySp5 and ZfSp5a as transcriptional activators appear quite different: both can promote gene activation through β -catenin interaction, but they largely differ in their capacity to activate target genes in a β -catenin-independent mode. Therefore, we speculate that Sp5 possibly evolved the capacity to interact with partners not previously identified such as Tbx or Sox, and/or acquired the capacity to bind consensus motifs such as those enriched in the vertebrate long-range enhancers, after Cnidaria divergence.

Consistent with its *Wnt3* repressor function, *HySp5* silencing triggers in a highly robust way the ectopic formation of clusters of *Wnt3*-expressing cells, followed by the formation of multiple heads along the body column of intact animals, in head-regenerating regions and in reaggregates (Fig. 7). This phenotype is different from the ones obtained with pharmacological treatments, either with the GSK3- β inhibitor ALP^{22,23,33} or recombinant *Wnt3* that directly enhances β -catenin signaling^{18,47}, where ectopic tentacles form first, and heads appear several days later. In intact animals, the knockdown of *HySp5* leads to the direct and rapid formation of fully functional ectopic heads, preferentially in the budding zone, a region that is developmentally competent in adult animals where the expression of both *Wnt3* and β -catenin is quite dynamically regulated^{17,18}. By increasing the number of dsRNA electroporations, we noted the formation of ectopic heads in the apical half of the body column, even though the development of these heads remained incomplete. Nevertheless, we never observed supernumerary heads at the apex of homeostatic *HySp5*(RNAi) animals, likely reflecting the difficulty to obtain a significant silencing in the apical region where *Sp5* expression is high. In the peduncle and basal part of the animal, ectopic head formation upon *HySp5*(RNAi) does not occur either, most likely as the physiological activity of Wnt3/ β -catenin signaling is too low in this region to elicit ectopic head formation when *Sp5* is silenced. In head-regenerating animals or reaggregates, the *Sp5*(RNAi) phenotype is readily observed as, similarly to the budding zone, the expression of *Wnt3*, β -catenin and *Sp5* is quite dynamically regulated.

To further investigate these dynamic modulations, we designed strategies to modulate the *Sp5*(RNAi) phenotype. We first noticed that when β -catenin is silenced, the *Sp5*(RNAi) phenotype is greatly reduced, indicating that an active Wnt3/ β -catenin signaling is necessarily required for ectopic head formation. We also measured the spatial spreading of the ALP-induced phenotype when *Sp5* is knocked-down, with ectopic *Wnt3* expression and ectopic tentacle formation all along the body column. This last result indicates that the constitutive activation of Wnt3/ β -catenin signaling by ALP is significantly enhanced upon *Sp5* silencing. These modulations of the *Sp5*(RNAi) phenotype in response to β -catenin(RNAi) or the ALP-induced phenotype in response to *Sp5*(RNAi) again confirm the intimate dynamic cross-talk that takes place between *Sp5* regulation, Sp5 activity and the Wnt3/ β -catenin signaling activity.

The observed *Sp5*(RNAi) phenotypic modulations indicate that *Sp5* silencing cannot be easily maintained stable along the mid-gastric region, namely because its regulation is quite dynamic in response to the level of Wnt3/ β -catenin signaling. Therefore, we interpret the homeostatic *HySp5*(RNAi) phenotype in the budding region as the consequence of the transient downregulation of *HySp5* activity in tissues that have the highest potential for setting up an organizer as evidenced by the transient upregulation of β -catenin in the budding zone¹⁷. As an evidence of this dynamic cross-talk, we noticed that a transient drop in *HySp5* expression suffices to rapidly induce a de-repression of *Wnt3* expression, which leads to an upregulation of β -catenin activity, and in turn

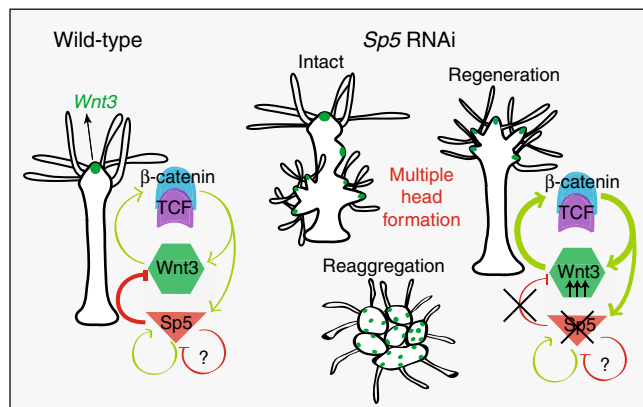


Fig. 7 Working model of the feedback loop involving Wnt3/β-catenin/TCF and Sp5. Wnt3/β-catenin signaling positively regulates Wnt3 expression via β-catenin stabilization as well as Sp5 expression. Head organizer activity is restricted by Sp5 that positively auto-regulates its own expression, likely by interacting with the β-catenin/TCF complex, but also represses the expression of Wnt3 through the Wnt3 repressor element. Depending on the level of Sp5 in a cell, Sp5 might also repress its own expression. This tight transcriptional control mechanism might then ensure a stable repression of the Wnt3 promoter. In the absence of Sp5, the repressing effect on the Wnt3 promoter is lost and Wnt3 is no longer restricted to the head organizer. The release of Wnt3 expression is sufficient to trigger multiple head formation in intact and regenerating conditions as well as in reaggregates

to Wnt3 upregulation followed by that of Sp5 (Fig. 7). The oscillatory nature of HySp5 and β-catenin expression in regions competent for head organizer formation suggests a bistability state relying on an auto-regulatory loop involving two transcription factors⁴⁸. This bistability as a prerequisite to head organizer induction and/or head organizer maintenance remains to be explored.

This study identifies the transcription factor Sp5 as a key inhibitory component of the *Hydra* head organizer. Indeed Sp5 fulfills the five criteria we initially fixed, derived from the predicted properties of the head inhibitor and from the previous identification of Wnt/β-catenin signaling as the head activator¹⁹. Sp5 globally fits the Turing/Gierer-Meinhardt model as HySp5 expression is controlled by Wnt3/β-catenin signaling, predominantly expressed in the head, reactivated during head regeneration, while HySp5, as a Wnt3 repressor, represses ectopic head formation (Fig. 7). However, several features diverge from the expected properties of the head inhibitor predicted by the Gierer-Meinhardt model.

Firstly, we noted the lack of Sp5 expression at the very apical tip of the hypostome in intact animals, the region where Wnt3 expression, and most likely Wnt3 activity, is maximal. Two distinct cis-regulatory elements in the Wnt3 promoter were previously identified, an activator and a repressor element, the latter restricting Wnt3 expression to the distal tip of the head¹⁹. The Sp5 pattern is thus consistent with the prediction that the inhibitor should be absent or unable to repress Wnt3 in this area. As Sp5 appears as a direct target of Wnt3/β-catenin signaling (see below), an additional negative regulation has to take place in this most apical area, to prevent Sp5 expression. This local regulation remains to be identified.

Secondly, this study supports a scenario where Wnt3 acts as a short-range activator to sustain its own activity in the head organizer, while Sp5 prevents the expression of Wnt3 and possibly other Wnt genes in non-apical tissues. The Gierer-Meinhardt model, proposed at a time when the concept of transcription factor

was still unknown, predicts that the head inhibitor is a diffusible substance, acting non-cell autonomously across the tissue layers. As a transcription factor, HySp5 is suspected to act cell-autonomously and thus not diffusible. However, some transcription factors can be secreted, as reported for the helix-turn-helix transcription factor EspR in bacteria⁴⁹ or for some homeoproteins that exert non-cell autonomous functions in the mammalian brain⁵⁰. Also, Sp5 might upregulate target genes that encode secreted peptides or proteins that diffuse in the extra-cellular space and exert head inhibitory functions. Such target genes, possibly taxon-specific, remain to be identified.

Thirdly, we cannot exclude that Wnt signals, which are numerous to be emitted from the apical region¹⁸ are not short-range signals but rather act over long-range distances to activate HySp5 expression with lipid-binding proteins or cytonemes modulating the spread of Wnt proteins as observed in *Drosophila*, *Xenopus* and zebrafish^{51–53}. The inhibition of Wnt3/β-catenin signaling along the *Hydra* body axis might thus solely be mediated by transcriptional repression, with Sp5 regulating its own expression and tightly tuning the level of Wnt signals.

As a fourth divergence with the Gierer-Meinhardt model, we found that HySp5 activates its own promoter. Both the reporter assays and the ChIP-qPCR data demonstrate that HySp5 directly binds its own promoter, while the ChIP-seq data also suggest that HySp5 is able to bind the human SP5 promoter. These observations are consistent with a study showing that the mouse Sp5 protein directly binds and activates its own promoter³¹. In addition, β-catenin slightly enhances the activating effect of HySp5 on its promoter, likely through direct interaction between HySp5, TCF1 and/or β-catenin as observed in vitro. A recent study demonstrates a direct interaction between the zinc finger domain of mouse Sp5 and the HMG domain of Tcf/Lef1, while no direct interaction was observed for β-catenin³¹. Also the formation of active Tcf/Lef1-β-catenin complexes appears necessary for Sp5 DNA-binding in mouse ESCs³¹. In contrary, in human ESCs, SP5 could directly repress the human SP5 promoter³⁷. Thus, currently we cannot exclude that besides its auto-activating effect, HySp5 might also have an auto-repressing effect when it reaches high intracellular levels for example. Further studies should evidence this putative auto-repressing effect as well as the interactions between HySp5 and TCF/β-catenin that favor the switch from Sp5 auto-activation to Sp5 auto-repression.

Methods

Animal culture and drug treatment. All experiments were carried out with *Hydra vulgaris* (*Hv*) from the Basel, AEP or *Hm-105* strains. Cultures were maintained in Hydra Medium (HM: 1 mM NaCl, 1 mM CaCl₂, 0.1 mM KCl, 0.1 mM MgSO₄, 1 mM Tris pH 7.6) or in Volvic water, supplemented with 0.5 mM CaCl₂. Animals were fed two to three times per week with freshly hatched *Artemia* nauplii and starved for four days before any experiment. For drug treatments *Hv*_{Basel} were treated for two days with 5 μM Alsterpaullone (ALP, Sigma) diluted in HM, 0.015% DMSO then rinsed 3x in fresh HM. All animals were selected randomly for experiments.

Generation of the HyWnt3:GFP-HyAct:dsRED transgenic strain. To induce gametogenesis, *H. vulgaris* of the strain AEP were fed with freshly hatched *Artemia* nauplii 7x per week for three weeks and then 1x per week for 1 week. Thereafter, male and female animals were cultured together, resulting in fertilized embryos. The hoTG-HyWnt3FL-EGFP-HyAct:dsRED plasmid (kind gift from T. Holstein, Heidelberg)¹⁹ was injected into one-cell stage embryos. Out of 504 injected eggs, 104 embryos hatched and 7/104 embryos exhibited GFP fluorescence in the hypostome.

RNA interference. In short, intact *Hydra* were briefly washed and incubated for 45 min in Milli-Q water⁵⁴. 20 animals per condition were placed in 200 μl 10 mM sterilized HEPES solution (pH 7.0) and then transferred into a 0.4 cm gap electroporation cuvette (Cell Projects Ltd). Animals were electroporated with 4 μM of Sp5 (siRNA-1+siRNA-2+siRNA-3) or scramble siRNAs (Supplementary Table 1b) using the Biorad GenePulser Xcell electroporation system. For double knockdown experiments 2 μM of Sp5 siRNAs were mixed with 2 μM of scramble of

β -catenin siRNAs. The conditions of electroporation were: Voltage: 150 Volts; Pulse length: 50 milliseconds; Number of pulses: 2; Pulse intervals: 0.1 s. For subsequent ALP treatment, RNAi animals that did not show any phenotypic signs were kept for 18 h in HM containing 5 μ M ALP. The animals were then relaxed in 2% urethane/HM for one minute, fixed in 4% PFA prepared in HM (pH 7.5) for 2 h at RT and either processed for WISH, or directly mounted with Mowiol for picturing.

Reaggregation. Animals were electroporated twice (RNAi1, RNAi2) with siRNAs and treated with ALP as described above. Next, 50–60 animals of the same size that did not show any phenotypic signs, were dissociated in 10 mL of dissociation medium (DM) (3.6 mM KCl, 6 mM CaCl₂, 1.2 mM MgSO₄, 6 mM Na-Citrate, 6 mM Pyruvate, 4 mM Glucose and 12.5 mM TES; pH 6.9)⁵⁵ and the cell suspension was centrifuged at 1'400 rpm for 30 min at 4 °C. The pellet was resuspended in 1 mL DM and 450 μ L of the cell suspension equally distributed into 1.5 mL tubes, followed by centrifugation at 1'400 r.p.m. for 30 min. After detachment, the aggregates were kept for one hour at 18 °C in 75% DM/HM and overnight in 50% DM/HM. On the next day, the aggregates were transferred into HM.

Quantitative RT-PCR. Total RNA was extracted using the E.Z.N.A.[®] Total RNA kit (Omega) and cDNA synthesized using the qScript[™] cDNA SuperMix (Quanta Biosciences). qPCR was performed in a 96-well format using the SYBR[™] Select Master Mix for CFX (Thermo Fisher Scientific) and a Biorad CFX96[™] Real-Time System. The *TBP* gene was used as an internal reference gene. HySp5 and TBP primer sequences are listed in Supplementary Table 1c. For ChIP-qPCR, DNA was prepared as below (ChIP-seq section) and qPCR performed as above with primer sequences listed in Supplementary Table 1d.

Whole mount In Situ Hybridization and immunodetection. *Hydra* were relaxed in 2% urethane/HM for one minute, fixed in 4% PFA prepared in HM (pH 7.5) for 4 h at RT and stored in MeOH at –20 °C for at least one day. Samples were rehydrated through a series of EtOH, PBSTw (PBS, Tween 0.1%) washes (75%, 50%, 25%) for 5 min each, washed 3 \times with PBSTw for 5 min, digested with 10 μ g/mL Proteinase K (PK, Roche) in 0.1% SDS, PBSTw for 10 min, stopped by adding Glycine (4 mg/mL) and incubated for 10 min. Samples were washed 2 \times in PBSTw for 5 min, treated with 0.1 M TEA for 2 \times 5 min, incubated 5 min after adding acetic anhydride 0.25% (v/v), 5 min after adding again acetic anhydride 0.25% (final concentration 0.5% v/v). Samples were then washed in PBSTw 2 \times 5 min, post-fixed in 4% formaldehyde, PBSTw for 20 min, washed in PBSTw 4 \times 5 min before adding the pre-warmed pre-hybridization buffer (PreHyb: 50% Formamide, 0.1% CHAPS, 1 \times Denhardt's, 0.1 mg/mL Heparin, 0.1% Tween, 5 \times SSC) and incubated for 2 h at 58 °C. Next, 350 μ L hybridization buffer (PreHyb containing 0.2 mg/mL t-RNA, 5% Dextran) containing 200 ng DIG-labeled riboprobe was heated 5 min at 80 °C, then placed on ice for 2 min. This mix was added onto the samples, then incubated for 19 h at 58 °C. Next, the samples were rinsed 3 \times in pre-warmed PostHyb-1 (50% formamide, 5 \times SSC) and successively incubated for 10 min at 58 °C in PostHyb-1, PostHyb-2 (75% PostHyb-1, 25% 2 \times SSC, 0.1% Tween), PostHyb-3 (50% PostHyb-1, 50% 2 \times SSC, 0.1% Tween) and PostHyb-4 (25% PostHyb-1, 75% 2 \times SSC, 0.1% Tween). Samples were then washed 2 \times 30 min in 2 \times SSC, 0.1% Tween, 2 \times 30 min in 0.2 \times SSC, 0.1% Tween, 2 \times 10 min in MAB-Buffer1 (1 \times MAB, 0.1% Tween), blocked in MAB-Buffer2 (20% sheep serum, MAB-Buffer1) for 1 h and incubated with anti-DIG-AP antibody (1:4000, Roche) in MAB-Buffer2 overnight at 4 °C. Next, the samples were washed in MAB-Buffer1 for 4 \times 15 min, then in NTMT (NaCl 0.1 M, Tris-HCl pH 9.5 0.1 M, Tween 0.1%) for 5 min and finally in NTMT, levamisole 1 mM for 2 \times 5 min. The colorimetric reaction was started by adding staining solution (Tris-HCl pH 9.5 0.1 mM, NaCl 0.1 mM, PVA 7.8%, levamisole 1 mM) containing NBT/BCIP (Roche). The background color was removed by a series of washes in EtOH/PBSTw (30%/70%, 50%/50%, 70%/30%, 100% EtOH, 70%/30%, 50%/50%, 30%/70%), PBSTw 2 \times 10 min. Samples were post-fixed for 20 min in FA 3.7% diluted in PBSTw, washed in PBSTw 3 \times 10 min and mounted with Mowiol. All steps were performed at RT unless indicated otherwise. Whole mount immunofluorescence with the anti-RFamide antibody (kind gift of C. Grimmelikhuijzen, 1:1000) was performed as in ref. ³².

Peroxidase assay. *Hydra* were relaxed in 2% urethane/HM for one minute and fixed in 4% PFA prepared in HM (pH = 7.5) for 2 h at RT. Samples were washed 3 \times 10 min with PBS, followed by adding 500 μ L DAB (SIGMAFAST[™] 3,3'-Diamino-benzide) solution. The DAB solution was prepared as follows: 1 tablet of DAB was dissolved in 10 mL of PBS and filtered with a 0.22 μ m filter. 5 mL of the filtered solution was added to 5 mL of PBS together with 20 μ L of Triton X-100 (0.2%) and 1 μ L of a 30% H₂O₂ solution. The animals were incubated for 10 min in DAB solution and the reaction stopped by washing the samples 3 \times 10 min with PBS.

Plasmid constructions. To generate the *HyWnt3*:Luc construct 2149 bp of the *Hydra Wnt3* promoter were transferred from the hoTG-HyWnt3FL-EGFP construct (kind gift from T. Holstein, Heidelberg)¹⁹ into the pGL3 reporter construct (kind gift from Z. Kozmik, Prague)²⁹. For the *HyWnt3*: Δ Rep:Luc construct, the whole *HyWnt3*:Luc plasmid sequence was PCR-amplified except the 386 bp

corresponding to the repressor element. For the *ZfWnt3*:Luc construct 3997 bp of the zebrafish *Wnt3* promoter were transferred from pEGFP-Wnt3 (kind gift of Cathleen Teh, Singapore) into pGL3. For the *HySp5*:Luc construct, 2'992 bp of the *Hydra Sp5* promoter were PCR-amplified from *Hm-105* genomic DNA and sub-cloned into pGL3. To express HA-tagged HySp5, ZfSp5a, ZfSp5l1 proteins, a C-terminal HA-tag was introduced into the pCS2+ constructs encoding the *Hydra Sp5* (human codon-optimized), zebrafish *Sp5a* and *Sp5l1* full-length coding sequences. The HySp5- Δ SP construct was produced by inserting a human codon-optimized *HySp5* sequence lacking 110 amino acids of the N-terminal end together with a C-terminal HA-tag into pCS2+. The HySp5- Δ DBD and HySp5- Δ SP- Δ DBD constructs were generated using the QuikChange Lightning Multi Site-Directed Mutagenesis Kit (Agilent Technologies), following the manufacturer's instructions. To generate the ZfSp5a- Δ DBD construct, the ZfSp5a-FL plasmid sequence was PCR-amplified except the DNA-binding domain. For preparing riboprobes, the *HyWnt3*, *HyBra1*, *HyTsp1*, *HyKazal1* and *HySp5* PCR products were cloned into pGEM-T-Easy (Promega). All constructs were verified by sequencing. All plasmids are listed in Supplementary Table 2 and primer sequences in Supplementary Table 1a.

Reporter assays in human HEK293T cells. HEK293T cells were maintained in DMEM High Glucose, 1 mM Na pyruvate, 6 mM L-glutamine, 10% fetal bovine serum. For the luciferase assays HEK293T cells were seeded into 96-well plates (5000 cells/well) and transfected 18 h later with X-tremeGENE[™] HP DNA transfection reagent (Roche). The plasmids listed in Supplementary Table 2 were transfected as follows: pGL4.74(hRLuc/TK) (Promega): 1 ng, luciferase reporter constructs: 40 ng, *CMV:hu Δ -Cat*: 10 ng, Sp5 expression constructs: 20 ng, huWnt3 and huLRP6: 40 ng. Total DNA amount was adjusted with pTZ18R to 100 ng per well. To measure Firefly and *Renilla* luciferase activities, the samples were prepared using the Dual-Luciferase Reporter Assay System (Promega), transferred to a white OptiPlate[™]-96 (PerkinElmer) and measured with a multilabel detection platform (CHAMELEON[™]).

ChIP-seq sample preparation. 920'000 HEK293T (92 cells/ μ L) cells were seeded into a 10 cm dish containing 10 mL of cell culture medium and transfected as described above with HySp5 or ZfSp5a, both containing a C-terminal HA tag (3'666 ng). Twenty-four hours later, cells were collected, washed twice in pre-warmed culture medium, fixed in 1% formaldehyde (FA) solution (Sigma) for 15 min until Glycine was added (final 125 mM) for 3 more minutes. In subsequent steps numerous reagents were from Active Motif[™] (AM). The cells were washed once in ice-cold PBS and re-suspended in 5 mL chromatin prep buffer (AM), containing 0.1 mM PMSF and 0.1% protease inhibitor cocktail (PIC). The sample was transferred into a pre-cooled 15 mL glas Douncer, dounced with 30 strokes and incubated on ice for 10 min. Nuclei were centrifuged at 1250 g for 5 min at 4 °C, resuspended in 500 μ L sonication buffer (1% SDS, 50 mM Tris-HCl pH 8.0, 10 mM EDTA pH 8.0, 1 mM PMSF, 1% PIC), incubated on ice for 10 min. Next, the chromatin was sonicated with a Bioblock Scientific VibraCell 75042 sonicator (Amplitude: 25%, Time: 12 min, 30 s on, 30 s off, 24 cycles), in conditions optimized to have a fragmentation size of ~250 bp. Then 100 μ L of the sonicated chromatin was added to 900 μ L ChIP dilution buffer (0.1% NP-40, 0.02 M HEPES pH 7.3, 1 mM EDTA pH 8.0, 0.15 M NaCl, 1 mM PMSF, 1% PIC) and incubated with 4 μ g anti-HA antibody overnight at 4 °C on a rotator. Next, the sample was loaded on a ChIP-IT ProteinG Agarose Column (AM), incubated for 3 h at 4 °C on a rotator, washed 6 \times with 1 mL AM1 buffer and the DNA eluted with 180 μ L pre-warmed AM4 buffer. The sample was decrosslinked by adding 100 μ L high salt buffer (1 M NaCl, 3 \times TE buffer) and incubated for 5 h at 65 °C. RNase A (10 μ g/ μ L) was added and the sample incubated at 37 °C for 30 min before adding PK (10 μ g/ μ L) and further incubated for 2 h at 55 °C. The DNA was purified with the MiniElute PCR purification kit (Qiagen). For preparing the Input DNA, 5 μ L sonicated chromatin was diluted in 45 μ L 0.5 M NaCl, incubated for 15 min at 95 °C, then transferred to 37 °C, incubated for 5 min with RNase A (10 μ g/ μ L), adding PK (10 μ g/ μ L) and incubated at 55 °C for 30 min. 10 μ L were taken for purification (MiniElute PCR purification kit from Qiagen).

RNA-seq sample preparation. 156'500 HEK293T (78.25 cells/ μ L) cells were seeded into a 6-well plate containing 2 mL of cell culture medium and transfected as described above with 626 ng of HySp5, ZfSp5a, HySp5- Δ DBD, ZfSp5a- Δ DBD and 313 ng of human Δ β -Catenin. RNA was extracted with the E.Z.N.A. total RNA kit 1 from OMEGA following the manufacturer's instructions.

Co-immunoprecipitation assay and Western blotting. 920'000 HEK293T cells (92 cells/ μ L) were seeded into a 10 cm dish containing 10 mL of cell culture medium and transfected with hu Δ -Cat (1830 ng), huTCF1 (1830 ng) and HySp5 (3660 ng). 24 h later, Co-IP samples were prepared using the nuclear complex Co-IP kit from Active Motif, following the manufacturer's instructions (all steps at 4 °C with ice-cold buffers). 100 μ g nuclear extracts were then diluted in 500 μ L Co-IP incubation buffer containing 4 μ g anti-HA antibody or 4 μ g rabbit IgG (12–370, Merck Millipore) and incubated overnight on a rotator. The Co-IP reaction was then loaded on a Protein G Agarose column (AM) and incubated one hour on a rotating wheel. The column was washed 3 \times in 500 μ L Co-IP wash buffer

supplemented with 1 mg/mL BSA, 3x in 500 μ L of Co-IP wash buffer supplemented with 300 mM NaCl. The column was centrifuged at 1250 \times g for 3 min and 25 μ L 2x reducing buffer directly added onto the column. After 60 s incubation and 3 min centrifugation at 1250 \times g, 5 μ L glycerol (Sigma) was added and the sample boiled for 5 min at 95 °C before loading on a 8% SDS-PAGE gel, electrophoresed and transferred onto PVDF membrane (Bio-Rad). Then all steps were performed at RT unless specified. The membrane was blocked with M-TBS-Tw (TBS containing 0.1% Tween, 0.5% dry milk) for one hour until primary antibodies diluted 1:2000 in M-TBS-Tw were added for overnight incubation at 4 °C. The membrane was then washed 4 \times 10 min in TBS-Tw, incubated in anti-rabbit (ab99697, Abcam) or anti-mouse (W402B, Promega) IgG horseradish peroxidase antibody (1:5000) for one hour, visualized with Western Lightning[®] Plus-ECL reagent (PerkinElmer). 10 μ g extract were used as Input sample. Antibodies: anti-HA antibody (NB600–363, Novus Biologicals), anti- β -catenin antibody (610153, BD Biosciences), anti-TCF1 (sc-271453, Santa Cruz Biotechnology). All uncropped western blots can be found in Supplementary Fig. 15.

ChIP-seq data analysis. Demultiplexed ChIP-seq reads from our sequenced samples were mapped onto the Human GRCh37 (hg19) genome assembly using bowtie2, version 2.2.6.2⁵⁶, implemented in galaxy⁵⁷. Significantly enriched regions were identified using MACS2⁵⁸ (version 2.1.0.20151222.0). Coverage files were normalized by the millions of mapped reads in each sample using a manually created R script. Normalized bedgraph files were converted to bigwig using the Wig/BedGraph-to-bigWig converter tool (version 1.1.1) implemented in the public Galaxy server (<https://usegalaxy.org/>) and visualized with UCSC genome browser. The fastq files from the two biological replicates of each condition were merged and remapped in order to obtain the average coverage profile. Only autosomal chromosomes were analysed in this study. MACpeaks regions were either extended or cropped from their respective center to match a final size of 500 bp using a personalized R script based on the GenomicRanges package (version 1.32.6). Fasta files containing the DNA sequences corresponding to the coordinates of the MACpeaks regions were obtained using the UCSC table browser tool. These files were used to identify enriched motifs for transcription factor binding sites using the MEME-ChIP Suite⁵⁹ (<http://meme-suite.org/tools/meme-chip>) in classic mode. Significantly enriched motifs were identified and compared to previously described TF weight matrixes from the JASPAR CORE 2014 database⁵⁹ using the TOMTOM tool of the MEME-ChIP suite. Significantly enriched motifs were used to scan the *HySp5*, *HyWnt3* and *ZfWnt3* promoters, using the FIMO tool (<http://meme-suite.org/tools/fimo>)⁶⁰ to identify putative Sp5 binding sites. Gene assignment of the identified MACpeak region was performed using the ChipEnrich Package in R (version 2.4.0; locus definition: nearest TSS; gene set: gene ontology biological process; method: polyenrich). Calculations of the total *HySp5* and *ZfSp5a* coverages (in Mb) and of the frequency distribution of the number of Sp5-enriched regions per gene were performed in R using personalized scripts. ChIP-seq data sets for the Sp5 and β -catenin occupancies in mouse ES cells^{31,61} were, respectively, downloaded from the GEO subseries GSE72989 and GSM1065517 and re-mapped on the mouse mm10 genome assembly using the same workflow describe above.

RNA-seq data analysis. Demultiplexed RNA-seq reads from our sequenced samples were mapped onto the Human GRCh37 (hg19) genome assembly using the STAR RNA-seq aligner⁶² workflow implemented in Galaxy. The fastq files from the three biological replicates of each condition were merged and remapped in order to obtain the average coverage profile. Coverage files were normalized by the millions of mapped reads in each sample using a manually created R script. Normalized bedgraph files were converted to bigwig using the Wig/BedGraph-to-bigWig converter tool implemented in the public Galaxy server (<https://usegalaxy.org/>) and visualized with UCSC genome browser. We used Htseq⁶³ implemented in the Galaxy server to count the number of uniquely mapped reads attributable to each gene (based on human genomic annotations from Ensembl release 82⁶⁴). We used DESeq2⁶⁵ to perform differential expression analyses. Specifically, we contrasted a generalized linear model that explains the variation in read counts for each gene, as a function of the different transfection conditions, to a null model that assumes no effect of the *HySp5*/*HySp5*- Δ DBD, *ZfSp5a* or *ZfSp5a*- Δ DBD. We ran the Wald test and the *P* values were corrected for multiple testing with the Benjamini–Hochberg approach. We computed reads per kilobase of exon per million mapped reads gene expression levels using Cufflinks⁶⁶.

FPKM levels were Log₂-transformed, after adding an offset of 1 to each value. The Log₂-transformed values were centered across samples before Principal Component Analysis (PCA); no variance scaling was performed. Heatmap plots were produced using the gplot package (version 3.0.1 in R). For this we computed the Z score $((X - \mu)/\sigma)$, where for each gene μ and σ are respectively the average and standard deviation of all the replicates of the two conditions being compared and *X* is the FPKM value of each sample) based on the FPKM value of each gene differentially expressed between *HySp5* vs *HySp5*- Δ DBD or between *ZfSp5a* vs *ZfSp5a*- Δ DBD. Up- and downregulated genes from this analysis were considered as *HySp5* and/or *ZfSp5a* putative targets if they were associated with a MACpeak enriched region for these proteins (based on the chipenrich analysis described above).

GO term enrichment analysis. We used the GOrilla tool⁶⁷ to search for enriched GO term categories associated with *HySp5*/*ZfSp5a* bound genes and with upregulated or downregulated *HySp5*/*ZfSp5a* putative targets using a threshold of $p < 10^{-3}$ (FDR < 0.05). In the latter case, when more than 10 significantly enriched GO term categories were identified, we used the REVIGO tool⁶⁸ using 0.7 as threshold for allowed similarity between related GO term classes.

Hydra genome assembly. Five clonal animals of the species *Hydra viridissima* and *Hydra oligactis* were sampled independently to extract DNA material using the DNeasy Blood & Tissue kit (Qiagen). Sequencing libraries were prepared using the TruSeq Nano DNA kit (Illumina), with 350 bp insert sizes, and sequenced paired-end using 150 cycles on an Illumina HiSeq X Ten sequencer by Macrogen Inc. Average and standard deviations of insert sizes of the sequenced reads were measured using 10 mio reads mapped to a preliminary assembly of each genome, then the two genomes were assembled using MaSuRCA v3.2.1⁶⁹. All scaffolds (>300 bp) and unplaced contigs (>500 bp) were retained in the final set of sequences. The redundancy of each assembly was reduced by using CD-HIT-est v4.7⁷⁰ with a 100% identity threshold. Sequencing depth was evaluated from the number of reads and expected genome length: *Hydra viridissima*: 120x; *Hydra oligactis*: 50x. Scaffolds assembly statistics in bp: number of scaffolds: 85677 for *viridissima* and 447337 for *oligactis*; N50: 11871 for *viridissima* and 5391 for *oligactis*.

Hydra RNA-seq transcriptomics. For spatial and cell-type RNA-seq transcriptomics, see ref. ³². All profiles publicly available on the HydrATLAS server (<https://HydrATLAS.unige.ch>).

Multiple sequence alignment and phylogenetic analysis. For Supplementary Figure 2, the multiple sequence alignment was generated using T-Coffee⁷¹. The conserved zinc finger domains, SP and Btd boxes were visualized by IBS⁷². For the phylogenetic analysis of the Sp5, Sp-related and Klf-related gene families (Supplementary Figure 3), sequences from *Hydra* as well as from other cnidarian, ecdysozoans, lophotrochozoans and deuterostomes representative species were retrieved from Uniprot or NCBI, aligned with Muscle align (www.ebi.ac.uk/Tools/msa/muscle/)⁷³ or MAFFT (<https://mafft.cbrc.jp/alignment/server/>) and tested in iterative PhyML 3.0 analyses using the LG substitution model, 8 substitution rate categories and 100 bootstraps⁷⁴.

Sp5 expression in zebrafish embryos. For all zebrafish experiments, colonies of the strain AB-Tu or Nacre were used, with animals maintained at 28 °C with a maximal density of five fish per liter in a 14 h light–10 h dark cycle. The fish were fed twice a day with 2-day-old *Artemia* and fish embryos incubated at 28 °C. For overexpression experiments, capped sense mRNAs were synthesized using the mMESSAGE mMACHINE[®] Transcription Kit from Ambion (Ambion, Austin, TX USA) and 400 pg of *HySp5*, *HySp5*- Δ DBD, *HySp5*- Δ SP or *HySp5*- Δ SP- Δ DBD mRNAs injected into one cell stage embryos. For mRNA co-injection experiments, injected amounts were as follows: 400 pg of *HySp5* and 4 pg of *ZfWnt8* mRNA. All embryos were scored for phenotypes 48 h post fertilization.

Statistical analyses. All statistical analyses were performed with the software GraphPad Prism7. The statistical tests were two-tailed unpaired.

Reporting Summary. Further information on experimental design is available in the Nature Research Reporting Summary linked to this article.

Data availability

The *Hydra Sp5* sequence has been deposited in GenBank under: MG437301. The genome assemblies and reads have been deposited in the BioProject under: PRJNA419866. RNA-seq and ChIP-seq data have been deposited in the GEO database under accession code GSE121321 [<https://www.ncbi.nlm.nih.gov/geo/query/acc.cgi?acc=GSE121321>]. The authors declare that all data supporting the findings of this study are available within the article and its supplementary information files or from the corresponding author upon reasonable request. The Source Data underlying Figs. 4f, 5d and Supplementary Figs. 6b, 12d are provided as a Source Data file.

Received: 20 March 2018 Accepted: 17 December 2018

Published online: 18 January 2019

References

- Petersen, C. P. & Reddien, P. W. Wnt signaling and the polarity of the primary body axis. *Cell* **139**, 1056–1068 (2009).
- Bode, H. R. The head organizer in Hydra. *Int. J. Dev. Biol.* **56**, 473–478 (2012).

3. Shimizu, H. Transplantation analysis of developmental mechanisms in Hydra. *Int. J. Dev. Biol.* **56**, 463–472 (2012).
4. Vogg, M. C., Wenger, Y. & Galliot, B. How somatic adult tissues develop organizer activity. *Curr. Top. Dev. Biol.* **116**, 391–414 (2016).
5. Browne, E. N. The production of new hydranths in hydra by the insertion of small grafts. *J. Exp. Zool.* **7**, 1–37 (1909).
6. Mutz, E. Transplantationsversuche an Hydra mit besonderer Berücksichtigung der Induktion, Regionalität, Polarität. *Arch. EntwMech Org.* **121**, 210–271 (1930).
7. Yao, T. Studies on the organizer problem in Pelmatohydra oligactis. I. The induction potency of the implants and the nature of the induced hydranth. *J. Exp. Biol.* **21**, 145–150 (1945).
8. Webster, G. Studies on pattern regulation in hydra. II. Factors controlling hypostome formation. *J. Embryol. Exp. Morphol.* **16**, 105–122 (1966).
9. MacWilliams, H. K. Hydra transplantation phenomena and the mechanism of Hydra head regeneration. II. Properties of the head activation. *Dev. Biol.* **96**, 239–257 (1983).
10. Broun, M. & Bode, H. R. Characterization of the head organizer in hydra. *Development* **129**, 875–884 (2002).
11. Spemann, H. & Mangold, H. Über die induktion von embryonalanlagen durch implantation artfremder organisatoren. *Wilhelm. Roux's Arch. Entw Mech.* **100**, 599–638 (1924).
12. Rand, H. W., Bovard, J. F. & Minnich, D. E. Localization of formative agencies in Hydra. *Proc. Natl Acad. Sci. USA* **12**, 565–570 (1926).
13. MacWilliams, H. K. Hydra transplantation phenomena and the mechanism of hydra head regeneration. I. Properties of the head inhibition. *Dev. Biol.* **96**, 217–238 (1983).
14. Gierer, A. & Meinhardt, H. A theory of biological pattern formation. *Kybernetik* **12**, 30–39 (1972).
15. Turing, A. M. The Chemical Basis of Morphogenesis. *Philos. T Roy. Soc. B* **237**, 37–72 (1952).
16. Kondo, S. & Miura, T. Reaction-diffusion model as a framework for understanding biological pattern formation. *Science* **329**, 1616–1620 (2010).
17. Hobmayer, B. et al. WNT signalling molecules act in axis formation in the diploblastic metazoan Hydra. *Nature* **407**, 186–189 (2000).
18. Lengfeld, T. et al. Multiple Wnts are involved in Hydra organizer formation and regeneration. *Dev. Biol.* **330**, 186–199 (2009).
19. Nakamura, Y., Tsiarris, C. D., Ozbek, S. & Holstein, T. W. Autoregulatory and repressive inputs localize Hydra Wnt3 to the head organizer. *Proc. Natl Acad. Sci. USA* **108**, 9137–9142 (2011).
20. Berking, S. Bud formation in Hydra: Inhibition by an endogenous morphogen. *Wilhelm Roux's Arch. Entw Mech.* **181**, 215–225 (1977).
21. Schaller, H. C., Schmidt, T. & Grimmelikhuijzen, C. J. P. Separation and specificity of action of four morphogens from hydra. *Roux Arch. Dev. Biol.* **186**, 139–149 (1979).
22. Guder, C. et al. An ancient Wnt-Dickkopf antagonism in Hydra. *Development* **133**, 901–911 (2006).
23. Augustin, R. et al. Dickkopf related genes are components of the positional value gradient in Hydra. *Dev. Biol.* **296**, 62–70 (2006).
24. Lommel, M. et al. Hydra mesoglea proteome identifies thrombospondin as a conserved component active in head organizer restriction. *Sci. Rep.* **8**, 11753 (2018).
25. Reuter, H. et al. Beta-catenin-dependent control of positional information along the AP body axis in planarians involves a teashirt family member. *Cell Rep.* **10**, 253–265 (2015).
26. Philipp, I. et al. Wnt/beta-catenin and noncanonical Wnt signaling interact in tissue evagination in the simple eumetazoan Hydra. *Proc. Natl Acad. Sci. USA* **106**, 4290–4295 (2009).
27. Weidinger, G., Thorpe, C. J., Wuennenberg-Stapleton, K., Ngai, J. & Moon, R. T. The Sp1-related transcription factors sp5 and sp5-like act downstream of Wnt/beta-catenin signaling in mesoderm and neuroectoderm patterning. *Curr. Biol.* **15**, 489–500 (2005).
28. Thorpe, C. J., Weidinger, G. & Moon, R. T. Wnt/beta-catenin regulation of the Sp1-related transcription factor sp5l promotes tail development in zebrafish. *Development* **132**, 1763–1772 (2005).
29. Fujimura, N. et al. Wnt-mediated down-regulation of Sp1 target genes by a transcriptional repressor Sp5. *J. Biol. Chem.* **282**, 1225–1237 (2007).
30. Park, D. S. et al. Role of Sp5 as an essential early regulator of neural crest specification in xenopus. *Dev. Dyn.* **242**, 1382–1394 (2013).
31. Kennedy, M. W. et al. Sp5 and Sp8 recruit beta-catenin and Tcf1-Lef1 to select enhancers to activate Wnt target gene transcription. *Proc. Natl Acad. Sci. USA* **113**, 3545–3550 (2016).
32. Wenger, Y. & Buzgari, W. & Galliot, B. Loss of neurogenesis in Hydra leads to compensatory regulation of neurogenic and neurotransmission genes in epithelial cells. *Philos. Trans. R. Soc. Lond. B. Biol. Sci.* **371**, 20150040 (2016).
33. Broun, M., Gee, L., Reinhardt, B. & Bode, H. R. Formation of the head organizer in hydra involves the canonical Wnt pathway. *Development* **132**, 2907–2916 (2005).
34. Leost, M. et al. Paullones are potent inhibitors of glycogen synthase kinase-3beta and cyclin-dependent kinase 5/p25. *Eur. J. Biochem.* **267**, 5983–5994 (2000).
35. Technau, U. et al. Parameters of self-organization in Hydra aggregates. *Proc. Natl Acad. Sci. USA* **97**, 12127–12131 (2000).
36. Melotti, A. et al. The river blindness drug Ivermectin and related macrocyclic lactones inhibit WNT-TCF pathway responses in human cancer. *EMBO Mol. Med.* **6**, 1263–1278 (2014).
37. Huggins, I. J. et al. The WNT target SP5 negatively regulates WNT transcriptional programs in human pluripotent stem cells. *Nat. Commun.* **8**, 1034 (2017).
38. Chen, G. Y., Osada, H., Santamaria-Babi, L. F. & Kannagi, R. Interaction of GATA-3/T-bet transcription factors regulates expression of sialyl Lewis X homing receptors on Th1/Th2 lymphocytes. *Proc. Natl Acad. Sci. USA* **103**, 16894–16899 (2006).
39. Zorn, A. M. et al. Regulation of Wnt signaling by Sox proteins: XSox17 alpha/beta and XSox3 physically interact with beta-catenin. *Mol. Cell* **4**, 487–498 (1999).
40. Tan, C. W., Gardiner, B. S., Hirokawa, Y., Smith, D. W. & Burgess, A. W. Analysis of Wnt signaling beta-catenin spatial dynamics in HEK293T cells. *BMC Syst. Biol.* **8**, 44 (2014).
41. Tan, C. W. et al. Wnt signalling pathway parameters for mammalian cells. *PLoS ONE* **7**, e31882 (2012).
42. Li, Z., Nie, F., Wang, S. & Li, L. Histone H4 Lys 20 monomethylation by histone methylase SET8 mediates Wnt target gene activation. *Proc. Natl Acad. Sci. USA* **108**, 3116–3123 (2011).
43. Nemeth, M. J., Topol, L., Anderson, S. M., Yang, Y. & Bodine, D. M. Wnt5a inhibits canonical Wnt signaling in hematopoietic stem cells and enhances repopulation. *Proc. Natl Acad. Sci. USA* **104**, 15436–15441 (2007).
44. Mikels, A. J. & Nusse, R. Purified Wnt5a protein activates or inhibits beta-catenin-TCF signaling depending on receptor context. *PLoS Biol.* **4**, e115 (2006).
45. Glinka, A. et al. Dickkopf-1 is a member of a new family of secreted proteins and functions in head induction. *Nature* **391**, 357–362 (1998).
46. Kakugawa, S. et al. Notum deacylates Wnt proteins to suppress signalling activity. *Nature* **519**, 187–192 (2015).
47. Chera, S. et al. Apoptotic cells provide an unexpected source of Wnt3 signaling to drive hydra head regeneration. *Dev. Cell.* **17**, 279–289 (2009).
48. Widder, S., Macia, J. & Sole, R. Monomeric bistability and the role of autoloops in gene regulation. *PLoS ONE* **4**, e5399 (2009).
49. Raghavan, S., Manzanillo, P., Chan, K., Dovey, C. & Cox, J. S. Secreted transcription factor controls Mycobacterium tuberculosis virulence. *Nature* **454**, 717–721 (2008).
50. Bernard, C. et al. A Mouse model for conditional secretion of specific single-chain antibodies provides genetic evidence for regulation of cortical plasticity by a non-cell autonomous homeoprotein transcription factor. *PLoS Genet.* **12**, e1006035 (2016).
51. Stanganello, E. et al. Filopodia-based Wnt transport during vertebrate tissue patterning. *Nat. Commun.* **6**, 5846 (2015).
52. Mulligan, K. A. et al. Secreted Wingless-interacting molecule (Swim) promotes long-range signaling by maintaining Wingless solubility. *Proc. Natl Acad. Sci. USA* **109**, 370–377 (2012).
53. Mii, Y. & Taira, M. Secreted Frizzled-related proteins enhance the diffusion of Wnt ligands and expand their signalling range. *Development* **136**, 4083–4088 (2009).
54. Watanabe, H. et al. Nodal signalling determines biradial asymmetry in Hydra. *Nature* **515**, 112–115 (2014).
55. Gierer, A. et al. Regeneration of hydra from reaggregated cells. *Nat. New Biol.* **239**, 98–101 (1972).
56. Langmead, B. & Salzberg, S. L. Fast gapped-read alignment with Bowtie 2. *Nat. Methods* **9**, 357–359 (2012).
57. Blankenberg, D. et al. Galaxy: a web-based genome analysis tool for experimentalists. *Curr. Protoc. Mol. Biol.* **Chapter 19**(Unit 19 10), 11–21 (2010).
58. Feng, J., Liu, T., Qin, B., Zhang, Y. & Liu, X. S. Identifying ChIP-seq enrichment using MACS. *Nat. Protoc.* **7**, 1728–1740 (2012).
59. Bailey, T. L. et al. MEME SUITE: tools for motif discovery and searching. *Nucleic Acids Res.* **37**, W202–W208 (2009).
60. Grant, C. E., Bailey, T. L. & Noble, W. S. FIMO: scanning for occurrences of a given motif. *Bioinformatics* **27**, 1017–1018 (2011).
61. Zhang, X., Peterson, K. A., Liu, X. S., McMahon, A. P. & Ohba, S. Gene regulatory networks mediating canonical Wnt signal-directed control of pluripotency and differentiation in embryo stem cells. *Stem Cells* **31**, 2667–2679 (2013).
62. Dobin, A. et al. STAR: ultrafast universal RNA-seq aligner. *Bioinformatics* **29**, (15–21) (2013).
63. Anders, S. & Huber, W. Differential expression analysis for sequence count data. *Genome Biol.* **11**, R106 (2010).
64. Yates, A. et al. Ensembl 2016. *Nucleic Acids Res.* **44**, D710–D716 (2016).
65. Love, M. I., Huber, W. & Anders, S. Moderated estimation of fold change and dispersion for RNA-seq data with DESeq2. *Genome Biol.* **15**, 550 (2014).

66. Roberts, A., Trapnell, C., Donaghey, J., Rinn, J. L. & Pachter, L. Improving RNA-Seq expression estimates by correcting for fragment bias. *Genome Biol.* **12**, R22 (2011).
67. Eden, E., Navon, R., Steinfeld, I., Lipson, D. & Yakhini, Z. GOrilla: a tool for discovery and visualization of enriched GO terms in ranked gene lists. *BMC Bioinforma.* **10**, 48 (2009).
68. Supek, F., Bosnjak, M., Skunca, N. & Smuc, T. REVIGO summarizes and visualizes long lists of gene ontology terms. *PLoS ONE* **6**, e21800 (2011).
69. Zimin, A. V. et al. The MaSuRCA genome assembler. *Bioinformatics* **29**, 2669–2677 (2013).
70. Li, W. & Godzik, A. Cd-hit: a fast program for clustering and comparing large sets of protein or nucleotide sequences. *Bioinformatics* **22**, 1658–1659 (2006).
71. Notredame, C., Higgins, D. G. & Heringa, J. T-Coffee: a novel method for fast and accurate multiple sequence alignment. *J. Mol. Biol.* **302**, 205–217 (2000).
72. Liu, W. et al. IBS: an illustrator for the presentation and visualization of biological sequences. *Bioinformatics* **31**, 3359–3361 (2015).
73. Edgar, R. C. MUSCLE: multiple sequence alignment with high accuracy and high throughput. *Nucleic Acids Res.* **32**, 1792–1797 (2004).
74. Guindon, S. et al. New algorithms and methods to estimate maximum-likelihood phylogenies: assessing the performance of PhyML 3.0. *Syst. Biol.* **59**, 307–321 (2010).

Acknowledgements

This work was supported by the Swiss National Foundation (SNF 31003A_149630; 31003_169930), the Canton of Geneva, the Human Frontier Science Program (grant no. RGP0016/2010), the NCCR 'Frontiers in Genetics', the Claraz donation and the de Staël foundation. The authors warmly thank Denis Duboule and Claude Desplan for valuable inputs on the manuscript, Ariel Ruiz I Altaba and Charisios Tsiariris for discussions and reagents, Carol Gauron for excellent technical assistance, Nenad Suknovic and Szymon Tomczyk for help with image acquisition and the IGe3 Genomic Platform for ChIP-seq and RNA-seq library preparation and sequencing.

Author contributions

M.C.V. performed *Hydra* and cell culture experiments, performed biochemical assays and prepared ChIP-seq and RNA-seq samples; L.B. analyzed ChIP-seq and RNA-seq

data. M.C.V. and L.B. performed ChIP-qPCRs. L.I.O. contributed to plasmid constructions, knockdown experiments and in situ hybridizations; C.R. and S.V. performed zebrafish experiments; Y.W. and B.G. designed the *Hydra* high-throughput transcriptomics, Y.W. produced and processed the *Hydra* high-throughput transcriptomics as well as the genome data; C.P. produced the transgenic line; M.C.V. and B.G. conceived the study, M.C.V., L.B. and B.G. wrote the manuscript.

Additional information

Supplementary Information accompanies this paper at <https://doi.org/10.1038/s41467-018-08242-2>.

Competing interests: The authors declare no competing interests.

Reprints and permission information is available online at <http://npg.nature.com/reprintsandpermissions/>

Journal peer review information: *Nature Communications* thanks the anonymous reviewers for their contribution to the peer review of this work. Peer reviewer reports are available.

Publisher's note: Springer Nature remains neutral with regard to jurisdictional claims in published maps and institutional affiliations.



Open Access This article is licensed under a Creative Commons Attribution 4.0 International License, which permits use, sharing, adaptation, distribution and reproduction in any medium or format, as long as you give appropriate credit to the original author(s) and the source, provide a link to the Creative Commons license, and indicate if changes were made. The images or other third party material in this article are included in the article's Creative Commons license, unless indicated otherwise in a credit line to the material. If material is not included in the article's Creative Commons license and your intended use is not permitted by statutory regulation or exceeds the permitted use, you will need to obtain permission directly from the copyright holder. To view a copy of this license, visit <http://creativecommons.org/licenses/by/4.0/>.

© The Author(s) 2019

An evolutionarily-conserved Wnt3/ β -catenin/Sp5 feedback loop restricts head organizer activity in *Hydra*

Matthias C. Vogg¹, Leonardo Beccari¹, Laura Iglesias Ollé¹, Christine Rampon^{2,3,4}, Sophie Vríz^{2,3,4}, Chrystelle Perruchoud¹, Yvan Wenger¹, and Brigitte Galliot^{1*}

Supplementary Figures	2
Supplementary Figure 1. Upstream and coding <i>Sp5</i> sequences in <i>Hydra vulgaris</i> Hm-105 strain .2	
Supplementary Figure 2. Evolutionarily-conserved structure of Sp5 transcription factors	3
Supplementary Figure 3. Three Sp families, Sp1-4, Sp5 and Sp6-9, already diversified in the last common ancestor of cnidarians and bilaterians.....	4
Supplementary Figure 4. <i>HySp5</i> expression patterns in intact and regenerating animals.....	6
Supplementary Figure 5. <i>HySp5</i> and <i>Wnt3</i> expression in <i>Hydra</i> stem cell populations	6
Supplementary Figure 6. Kinetics of <i>HySp5</i> phenotype occurrence in intact animals	7
Supplementary Figure 7. Kinetics of <i>HySp5</i> phenotype occurrence in head regenerating animals.	8
Supplementary Figure 8. Knockdown of β -catenin delays head regeneration.....	9
Supplementary Figure 9. <i>HySp5</i> phenotype occurrence requires active Wnt/ β -catenin signaling.	10
Supplementary Figure 10. <i>HySp5</i> antagonizes Wnt/ β -catenin signaling	11
Supplementary Figure 11. Knockdown of <i>Sp5</i> in reaggregation studies	12
Supplementary Figure 12. Kinetics of <i>Wnt3</i> expression in <i>Sp5</i> (RNAi) animals	13
Supplementary Figure 13. Mapping of putative Sp5 binding sites in the <i>Wnt3</i> and <i>Sp5</i> upstream sequences in <i>Hydra</i> and teleost fish	15
Supplementary Figure 14. <i>HySp5</i> expression in Alsterpaullone-treated animals	17
Supplementary Figure 15. Interactions between Sp5 and β -Catenin or TCF1.....	18
Supplementary Figure 16. Genome-wide mapping of putative Sp5 binding sites in human HEK293T cells and mouse ESCs	19
Supplementary Figure 17. Direct transcriptional targets of <i>HySp5</i> and <i>ZfSp5a</i>	20
Supplementary Figure 18. Overexpressing <i>HySp5</i> in zebrafish embryos induces Wnt-like phenotypes.....	21
Supplementary Tables	22
Supplementary Table 1. Cloning, siRNAs, qPCR and ChIP-qPCR primer sequences	22
Supplementary Table 2. DNA constructs used in this study	23
Supplementary References	24

Supplementary Figures

1.....10.....20.....30.....40.....50.....60.....70.....80.....90.....

-2965 ctagttctaatattgacctattacgttcgcaaaagttgacaaagtcgcaaatTTTTTCTTTTCA - 2901

aaagacctcccattcattttaataaagactggttctaattttgctttatcagcttataaaaattgacaaagtcgcaagctattggttttttaaaagacc - 2801

tcccattcattgagataaactagttattttcatgtatcattgaaatagtaaacattcattctagttttatttctgctaggcagattttcacacct - 2701

ccacaagtcgcaaacgcttttatttactgattgagtaaatatttataaaataaaataaaaaataagaacttaattgtgaaaaaaacaaacaaac - 2601

aataaaaaaaacaatgtaaaatatttctcatagctggtgaaatattaaaaagcgaaggaataataacgcaaaagctaaattctttctgctgta - 2501

ttgctttttctctttattgtctggttggcttttctcactgattctattttgtgcttaataaatctcaatcgattttaaaggaatgactaggatggttc - 2401

atTTTGTATATATCAATAACTGAAATATAAAATCTCCTCAGTGCATCCGTCGTTAGACAATGGGGGATTAACTCAATTATTCTCTGAATATAAC - 2301

tcaacaagtaaaaaagtttcatccgtaagcaagaataacgacactgtttacatttaagaatttcttaactttatgtaaaaaacaattcttagtta - 2201

aaaaagaaagtaaaaggttttaatttttggtttttagttgaaacaaattgctaataaaacttaatttaaaaaaaacaaatattttaaagat - 2101

aaactggtttaaataatagattatacaaacattgtgaagcatttaaaacaattttttttataaaaaacaacaaaaaaatttcacctaatctctc - 2001

cgctttgtaataaaacctccgttttacagttaaaagtaattgtatgaaccgtaacccctattcaaaaaaaaggtatattggtttataagacgttttga - 1901

tgattgtagcttattttatatttttggcttttggcttttccctgtgtgtttttaaattgattgattatattcttacgacctacgaccagcttt - 1801

gctgttttaaatcggcagcgttctgttactttacacgaagcctctaaacaaacataaaagagaattcgcgaaagtaaaaaaatcatgctgacctctg - 1701

gtgactccgtaattgaaattgatataattttctccctattttgacataaaatggttaaagtaattcttttataaaactcaatcatttcaacaaata - 1601

agtgtcaagtttactgcttatttcaagtaacaaataagctctattgttaaaatgaaatttgggttaaaagggattgaaactcaatcattattgtaataa - 1501

gaagaatttcatgtaagattgtatttataaaataaaactaaatgaacaaagcgtcactcaaatttatatttggattataagaggaaattt - 1401

ttaccctaagttaaaactactgtaaaatcgaactgaatcaataaggtcagagagactaggtcagcaggtttggatcattaaactcgataacaaataa - 1301

cgataatggttataatgataggaaccttacactgacatttaaatggaagcctgaggctataacgctcgtttgctgctgggtagataagcaacttgaca - 1201

aaacatcatcttattttttatggcgccaaatggttatctgttttaattcttttataataatgataaaaaacatttaaccacaaatattttttttat - 1101

ctccaaatgaaatcaagaacttttaagctataaaaagtagcagcagcagctgataatcatagacaaggtgtacacattagcttatcaaaagtagctga - 1001

gagtaagctttataatgattggttaggataatccttctcgttaaaatattgtgctacttttatatcagatattcatttttagtttctgtg - 901

tctgatatataatatttctgattgtttgtatgtatattgtttgtgtatgtatgtaaaaaatgaaatatacttttgcaaatctttgttag - 801

aagtttaataaaatgattcaagttttaaatactcctcgtatattttaaagcttcaatttgggtggcgtagacacattagtaattgcggtaaagatca - 701

gtaagaatttcaatagacgttaattttaaacctggcctgcccctgattatttaatttgaatttttaagctgtctcatttcaaccacagatcaat - 601

gggtcggcaaaaaaagaaagattgaaactgtttatcaattttaccacgaaacaaacttaacaaatattgtagtacttttttaagtttaaatgtttttgt - 501

aaaactggtatttttaaaataaaaccttttactcttttttttttttttggaaactggttttaaaactgatatttaataaaagctaaatataaatgtggtaa - 401

agttcgtaaaaacaaatgagcaggtgccgcatagatgaaagtgaagaacaaatttttttatgaaactcacaatttactgtggattgtcggaatgttt - 301

actattaagttgatttgaagtcaaaaaaaataacaaatacaacaaatgaaactccttagaagattgttaatacaaaacaaatcaaatagcgttttata - 201

tcttttaacaaataagatacaatatttattgtttgtcggcactttaaagatttaaatcttttccgcttacgtattctgtttatcaccgcc - 101

tcttagaccatcccattgtacgtaaacagagaaatgatcgcaacgcccatttctcagtcagaggcgtgacattaaccccttatcaagaagcga - 1

AGCTATTAAAGATAAGATGGCGGTTTCTTCTGATGCTGAATGAATTGTTTCGGTTTTTTTTGAAGTAAGGATAACGTTAAGAACGATTGAAATGCCCA 100

GCTGATTTAAATAGAATTGAAGTAGAAGCATTTCAGTTAAACTTTCTACTTTAAAGTGCAAAGACGTTTCAAGAAATACATTTTCAGTAAAATTAAGTAA 200

AAATGTCACCTCCAAGTCGTGTTCCAACAACAATCAGCCCAAACCTTTAAAGTCAACATCATTTGCTTAAAGAACATATTAAGTATTACCCTGGCATTAA 300

M S P P S R V P T T I S P N F K S Q H H C L K E H I K Y S P L A L 33

CTTGACGAACTGTAATAAAATTTGGACGGCCTATCAGCCCATAGAACAAACATCTCCTAAAAAAATTTTCAACCATGGAATCACACGTTTGAATCAC 400

L A A T T C K K I G R P I S P L E Q T S P K K I F Q P W N H T F E S H 67

ACAATTGACACACCTATTTCACCAATAGCAAAGTGAGACACTTCTGAGACAAATTTCTCGCTTCCACCAAGTCTCCATTAATAATCAGAGTAGT 500

N Y D T P I S P N S K V R H F L E T N P S L P P S P P L K S E I V 100

Sp5-For1->

AAAAGTTCCCCCAACAAATAAGACCAATGCGCATGACGAATGTAATGCAAGAAAAAGCGACTTTAAATTAACCTCACAAAAACTTTCTCCACCTCCGTTGCTC 600

K V P P T I R P M P M T N V M Q E K A T L N Y S Q K L S P P P C L 133

GCATGTTAGTGGTCAAAAAGTGAATGGAATAAATAAATAATCTCCAGTTTTGCTTCTCCGCTGCCTCGCCAATCTCATGTTATTCTCTCAAAATA 700

A C S A G Q K C N G I N K I S P V L L S P P A S P I S W L F P Q N I 167

siRNA1

TTATTCAATCTCATCTTCTTAAAGTATCAA**TTAACGAGCCACATATA**AGAATATTCCGAACATTCTCAAGCTGATCCAACGCGTTTGTAAACTACGT 800

I Q S H P S K V S I N E H H I K E Y S E H S Q A D P T R F V N Y V 200

TTACAAAAACGTCGACTTCTTCAAGCAAAACCTAATCTAATAATTCGACACGATAACATGATCTCCTCTACACAATCGTATAAACAATCGTATATTCTCA 900

Y K N V D S S Q A K P N L I I R H D N M I S S T Q S Y N N R I F S 233

siRNA2

TCTTCGCCACATTTAA**CTACAACATCCACATATA**TTCAATGTCTACATCAATTCCTGCTCAATCGCATGCAGTTATACCGAACAGCGTTGCAACCCGAA 1000

S S P H L T T T S H I Y S M S T S I P A Q S H A V I P N S V A T R R 267

siRNA3

GATGTCGTCGTTGTAATGCCAAACTGCATATCAGGACAACAATCTGAGCCAAATAAACCCCA**AGCAGCACGATGTCATAT**TCCAGGGTGCAGAAAGGT 1100

C R R C K C P N C I S G Q Q S E P N K P K Q H V C H I P G C G K V 300

<- Sp5-Rev1

TTATGGTAAACTGACCTTAAAGCTCAITTAAGATGGCATGCTGATTGCGTCCATTCGTTTGTAAATTGGTTATTGCAACAAATCCTTTACTCTGT 1200

Y G K T S H L K A H L R W H A G L R P F V C N W L F C N K S F T R 333

TCTGATGAACCTCAACGTCACCTTGCAGAACACATACGGGCGAAAAGCGATTTCGCTGTCAAGATTGCGGCAACGTTTACTCGTCCGACCATTTATCGA 1300

S D E L Q R H L R T H T G E K R F A C Q D C G K R F T R S D H L S K 367

AACATATGAAACACACCAAAAATAAAACAAGAAAACACATTTGTAAAGATACTGTCTAGAAAGTGAATTAAGACAAATGTCGATGAAAATTGCGATGA 1400

H M K T H Q N K K Q E N T F V K D T V I E V I K D N V D E N C D E 400

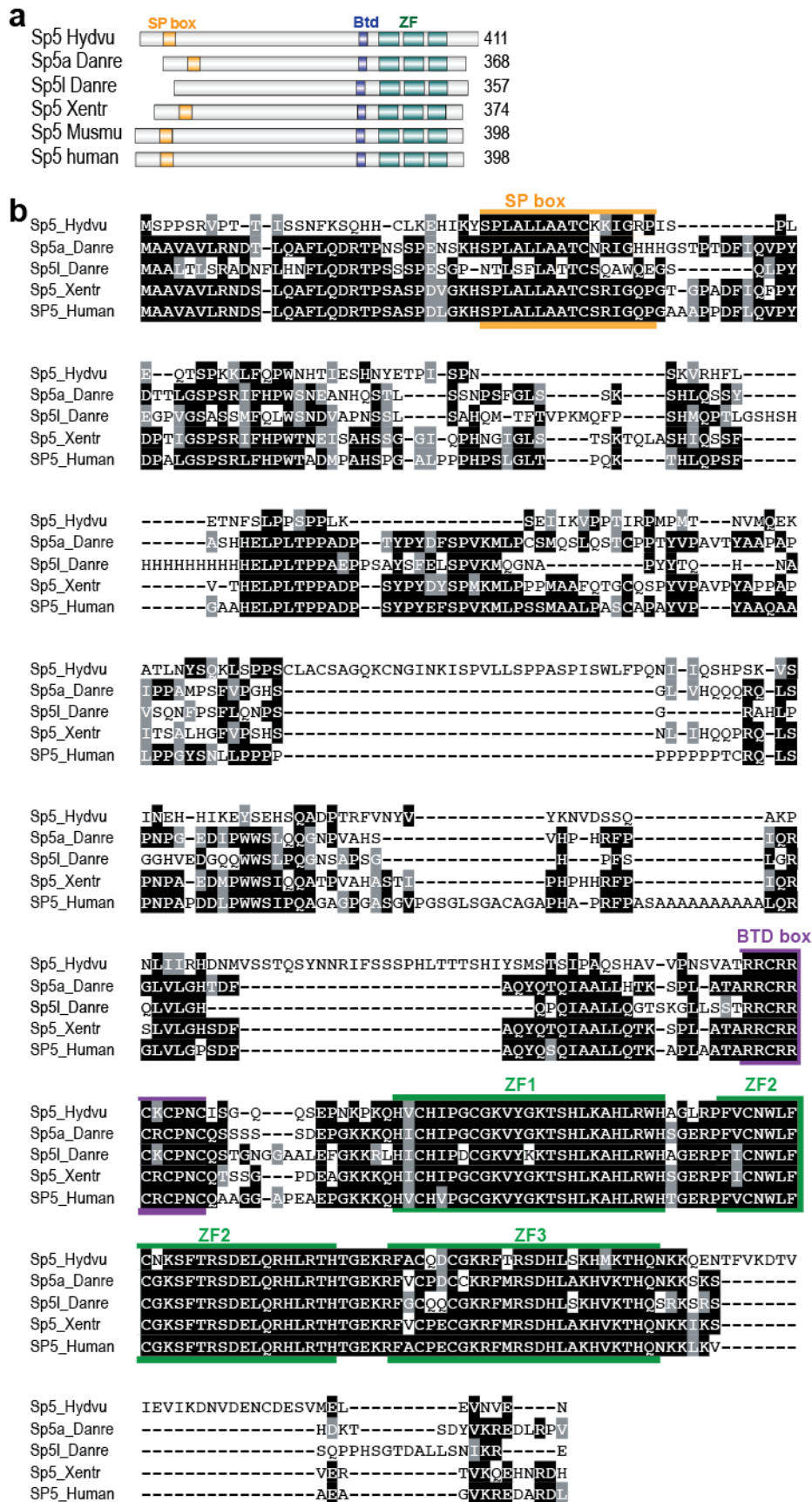
1.....10.....20.....30.....40.....50.....60.....70.....80.....90.....

GAATGTTATGGAACCTGAAGTAAACGTTGAAAACATAAATTTAAATTTGTTATTATAGCTTTATAGTATATCTTCTTTTAAATGTCTAATGTATATAA 1500

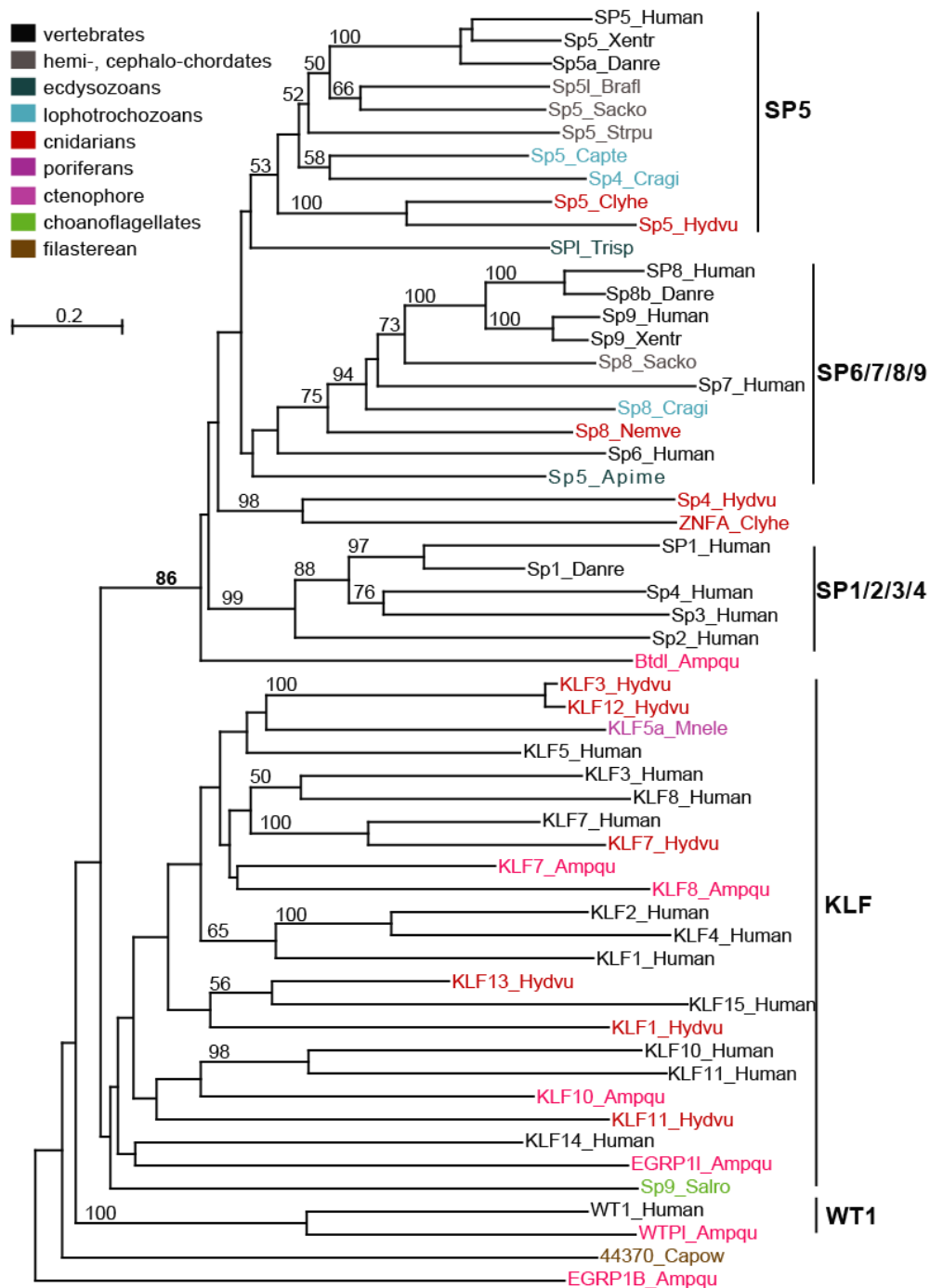
N V M E L E V N V E N * 411

CTTCAGTTTGTAAATATTGTACGTATGTAATATTACTCTCAATAATCGAAAAGTTTTTAATACTCTCTGTTTTTAATAACGATAAAAAATAAATTAACC 1599

Supplementary Figure 1. Upstream and coding *Sp5* sequences in *Hydra vulgaris* Hm-105 strain
Sp5 genomic sequence is written lowercase, *Sp5* transcribed sequence (c16537_g1) upper case. The deduced protein sequence is highlighted in green. DNA sequences highlighted in yellow correspond to the regions used to design siRNAs, underlined DNA stretches correspond to the primers used for subcloning and riboprobe preparation.

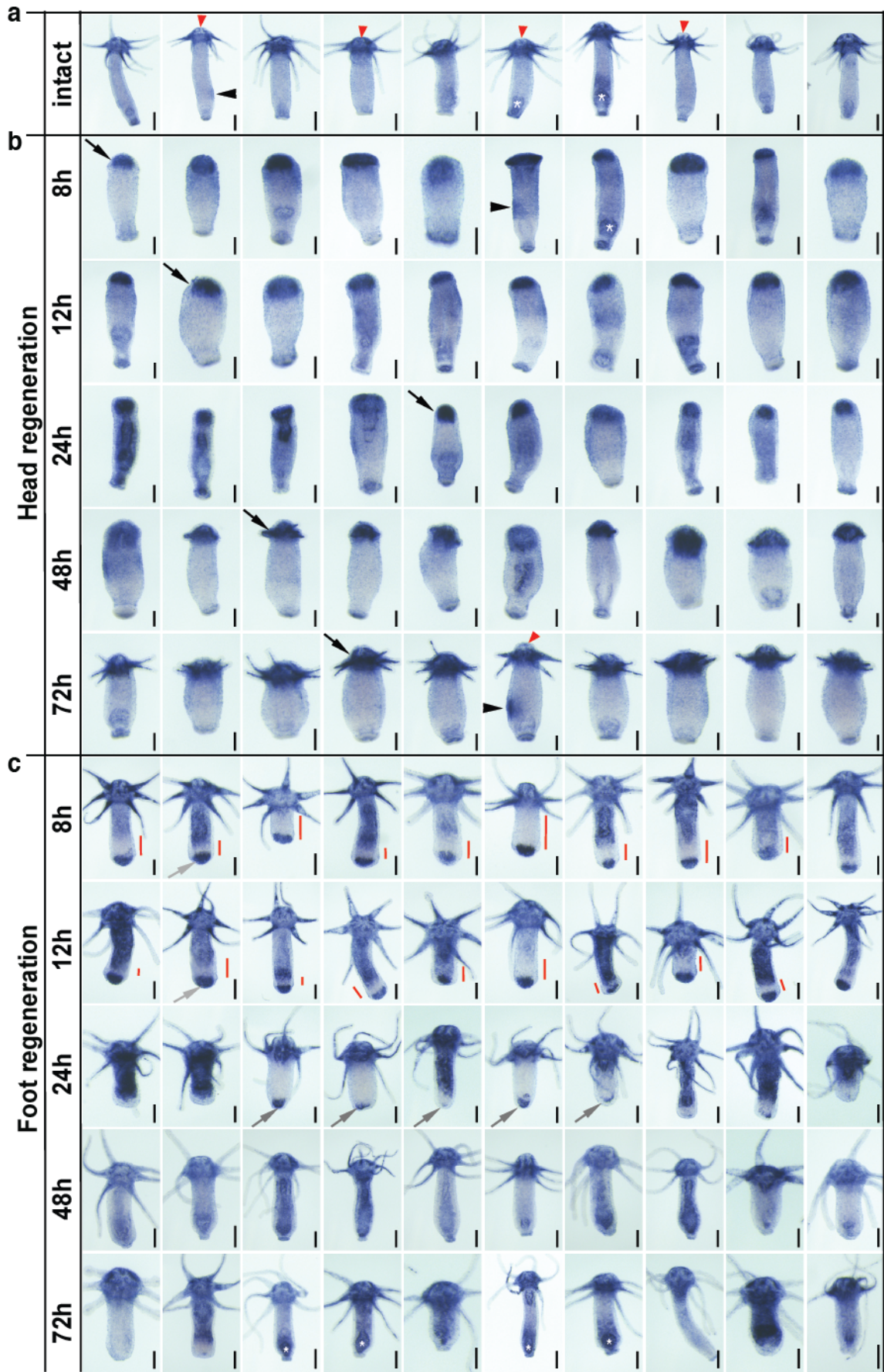


Supplementary Figure 2. Evolutionarily-conserved structure of Sp5 transcription factors
(a) Sp5 transcription factors contain a SP box (orange), a buttonhead box (Btd, purple) and a DNA-binding domain formed of three zinc finger domains (ZF, green). **(b)** Alignment of the Sp5 protein sequences from *H. vulgaris* (*Hydvu*), *Danio rerio* (*Danre*, zebrafish), *Xenopus tropicalis* (*Xentr*) and human.



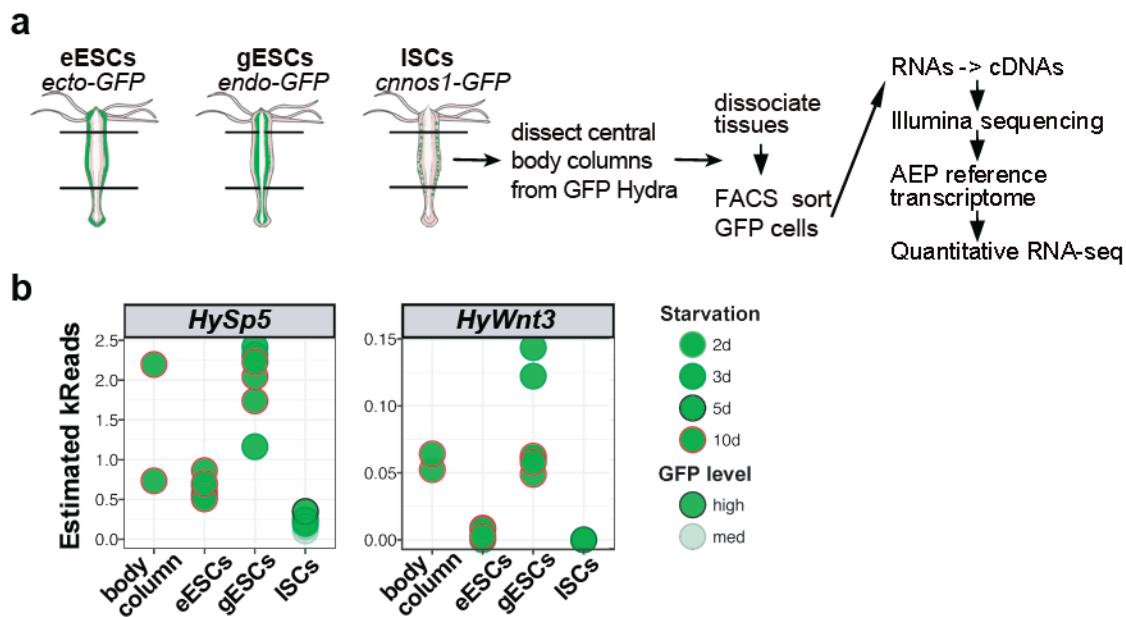
Supplementary Figure 3. Three Sp families, Sp1-4, Sp5 and Sp6-9, already diversified in the last common ancestor of cnidarians and bilaterians

The PhyML tree built on a MAFFT alignment of 56 full-length protein sequences of the Sp and KLF families tested with 100 bootstraps and rooted with two WT1 sequences. Note that a single Sp-related gene, *Btdl*, was found in the sponge *Amphimedon*, does not group with any of the three eumetazoan Sp super families. Species code: *Amphimedon queenslandica* (Ampqu, demosponge), *Apis mellifera* (Apime, honeybee), *Branchiostoma floridae* (Brafl, amphioxus), *Capitella telata* (Capte, annelid worm), *Capsaspora owczarzakii* (Capow, filasterean), *Clytia hemisphaerica* (Clyhe, jellyfish), *Crassostrea gigas* (Cragi, oyster), *Danio rerio* (Danre, zebrafish), *Hydra vulgaris* (Hydvu), *Mnemiopsis leidyi* (Mnele, ctenophore), *Nematostella vectensis* (Nemve, sea anemone), *Saccoglossus kowalevskii* (Sacko, acorn worm), *Salpingoeca rosetta* (Salro, choanoflagellate), *Strongylocentrotus purpuratus* (Strpu, sea urchin), *Xenopus tropicalis* (Xentr, clawed frog). Note that the two major Sp families identified in bilaterians, Sp5 and Sp6-9¹ can be traced in cnidarians, whereas the unique Sp sequence identified in *Amphimedon queenslandica* cannot be affiliated to any of these, and no typical Sp sequence could be found in non-metazoan species. Therefore, the most parsimonious scenario is that a unique Sp gene arose at the base of metazoans to duplicate in eumetazoan ancestors.



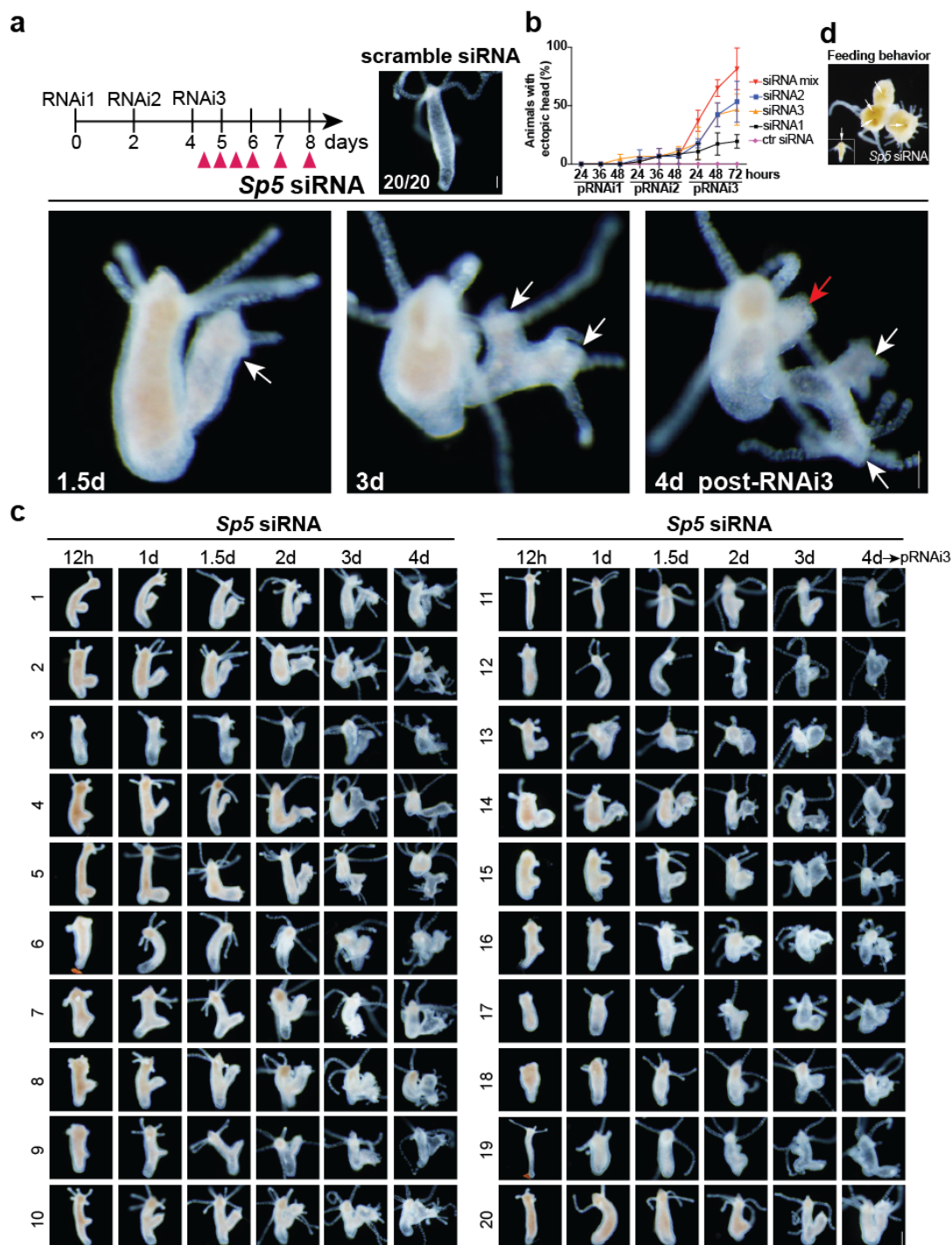
Supplementary Figure 4. *HySp5* expression patterns in intact and regenerating animals

(a) *HySp5* expression in intact *Hydra* (*Hv-Basel*) starved for 4 days is predominantly apical, although absent or strongly reduced at the most distal tip (red arrowheads). (b, c) *HySp5* expression in head- (b) and foot- (c) regenerating halves fixed 8, 12, 24, 48 and 72 hours after amputation (hpa, mid-gastric bisection). During head regeneration, *HySp5* expression is sustained, maximal in head-regenerating tips (black arrows), graded towards the basal end. Note the presence of a bud spot in some animals (black arrowheads). During foot regeneration, *HySp5* expression is strong at 8 and 12 hpa in foot-regenerating tips (light grey arrows) but restricted to this area as the adjacent region does not express *HySp5* (red bars); it is also transient, partially or totally lost at 24 hpa (darker grey arrows). In several animals equipped with a basal disc, the staining inside the lower part of the gastric cavity is artefactual (white asterisks). Shown are representative images of an experiment performed in duplicate. Scale bars: approximately 200 μ m.



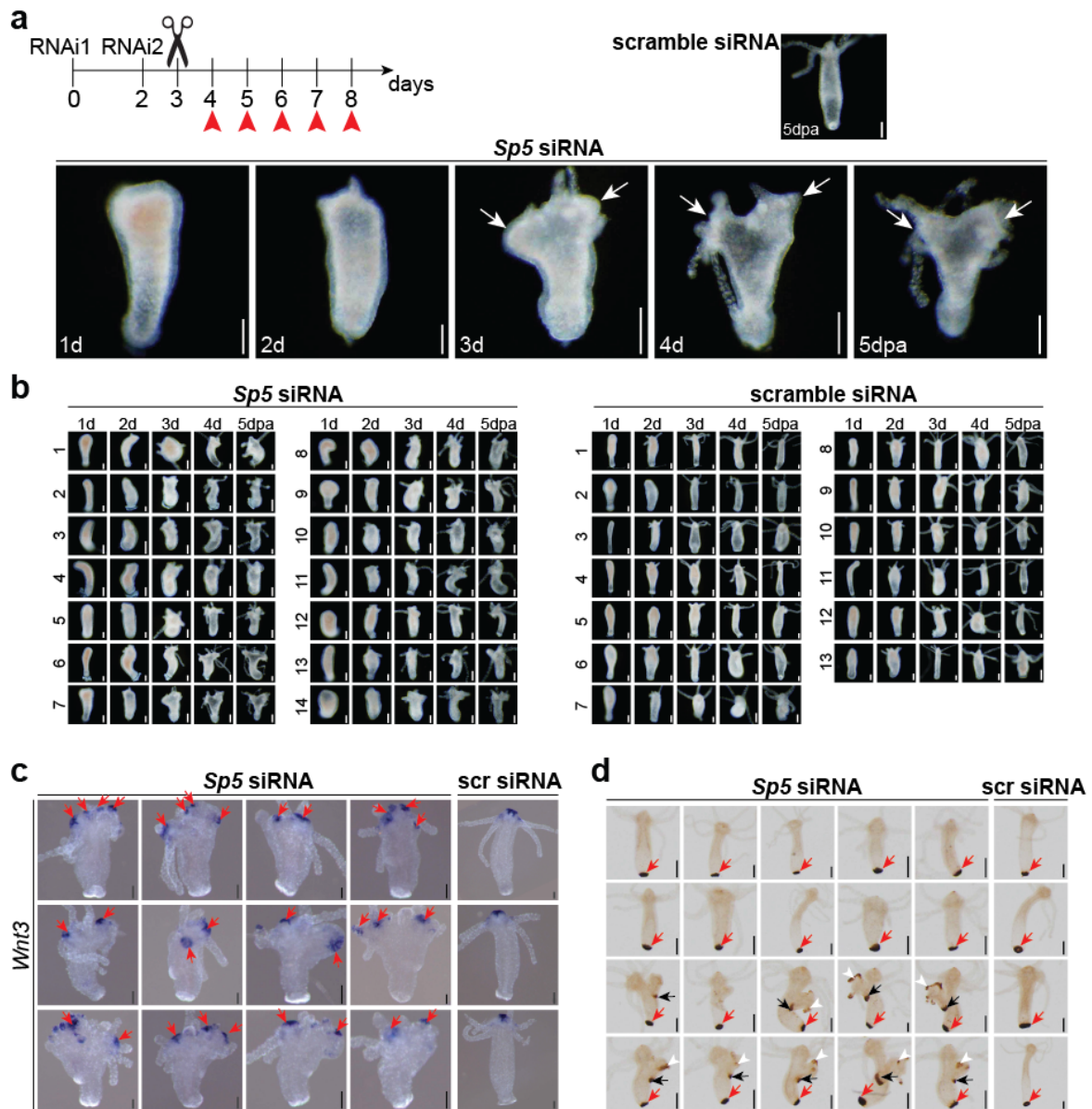
Supplementary Figure 5. *HySp5* and *Wnt3* expression in *Hydra* stem cell populations

(a) Procedure applied to perform qRNA-seq analysis of each specific stem cell population in *Hydra* (see details in ²). We used three transgenic AEP strains that were produced and kindly provided to us by the laboratory of Thomas Bosch (Kiel). In each strain one stem cell population constitutively expresses GFP, either epidermal epithelial stem cells (eESCs, Ecto-GFP³), gastrodermal epithelial stem cells (gESCs, Endo-GFP⁴), or interstitial stem cells (ISCs, Cnnos1-GFP⁵). Note that only GFP-expressing cells from the central body column were sorted by flow cytometry and analyzed for transcriptomics. (b) Cell type RNA-seq profiles of *HySp5* and *Wnt3*. The graphs depict the number of sequenced reads ($\times 10^3$) for *HySp5* and *HyWnt3* in the intact body column (no sorting), or in each stem cell population at different time points of starvation. Four biological replicates were tested for each condition.



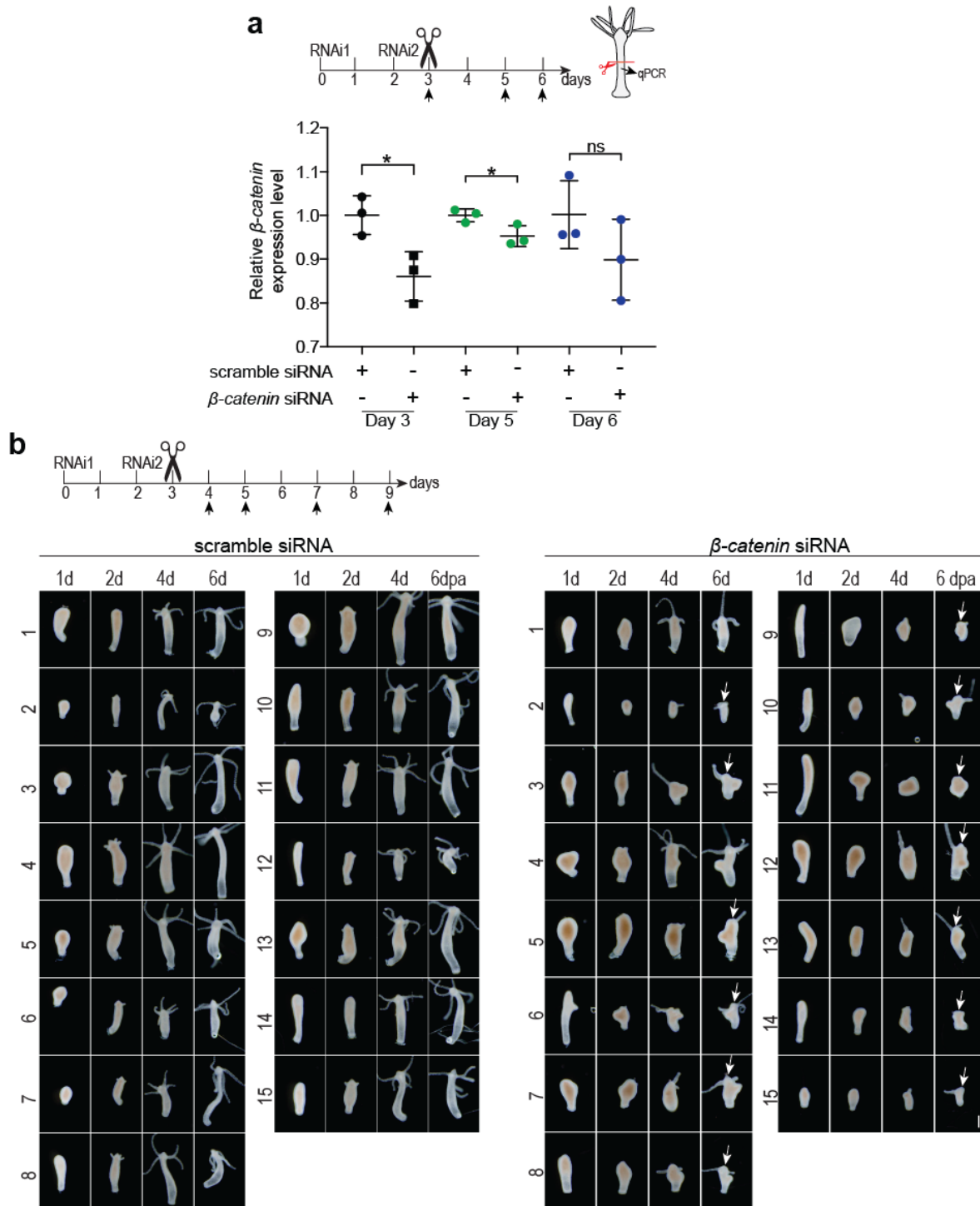
Supplementary Figure 6. Kinetics of *HySp5* phenotype occurrence in intact animals

Intact *Hydra* were electroporated three times every other day (RNAi1, RNAi2, RNAi3) either with a scramble siRNA (control) or with a mix of *HySp5* siRNAs and imaged live at various time-points after RNAi3 (red arrowheads). **(a)** Three successive views of a representative animal developing ectopic axes, first in the budding zone where they differentiate heads (white arrows), later in the upper body column where they remain headless (red arrow). **(b)** Kinetics of *Sp5* phenotype occurrence after testing *Sp5* siRNAs separately or in a mix (pool of siRNA 1-3). Note that the single siRNAs induced a multi-headed phenotype, however with a lower efficiency than the siRNA mix (3 independent experiments). Source data are provided as a Source Data file. **(c)** Multiheaded phenotype observed in 20 representative *Sp5*(RNAi) animals. Note the synchronous emergence of an ectopic axis in the budding zone of 12/20 *Sp5*(RNAi) animals already 12 hours after RNAi3, 1.5 day later in the remaining 8 animals. Ectopic axes/heads were never observed in control(RNAi) animals. **(d)** Feeding response tested in ectopic heads of *Sp5*(RNAi) animals 4 days after RNAi3. Inset: *Artemia*; white arrows: *Artemia* eyes. Shown are representative animals of an experiment performed in triplicate. Scale bars: approximately 200 μ m. Error bars indicate SD.



Supplementary Figure 7. Kinetics of *HySp5* phenotype occurrence in head regenerating animals

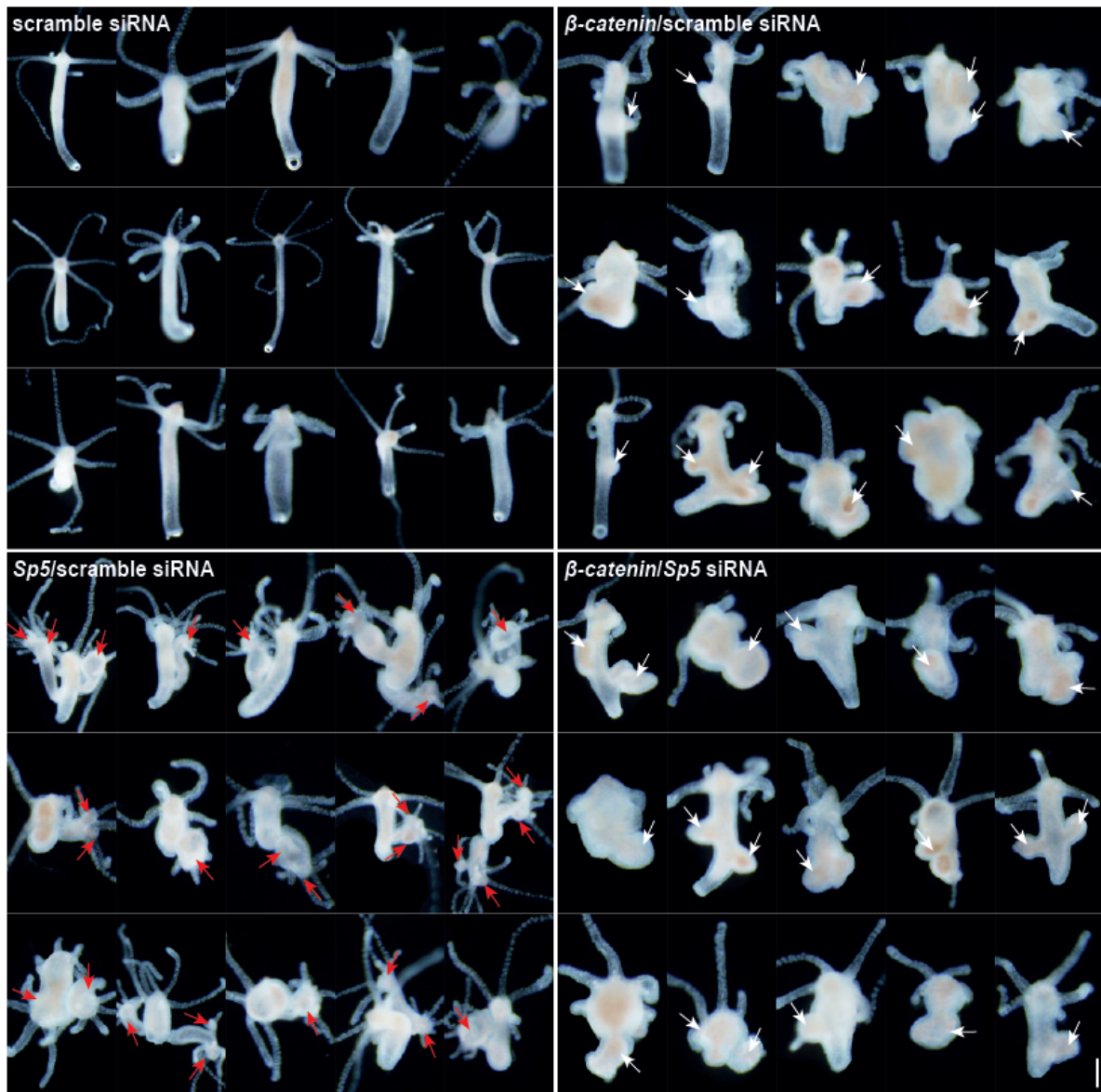
(a) Morphological changes detected in head regenerating *Sp5*(RNAi) animals after two exposures to *Sp5* siRNAs as indicated. Animals were imaged live at various time-points after mid-gastric bisection (red arrowheads). Five successive views of a representative animal regenerating multiple heads. **(b)** Multi-headed phenotype in 14 representative head regenerating *Sp5*(RNAi) animals. Note that control RNAi animals never regenerated multiple heads. **(c)** *Wnt3* expression in head regenerating *Sp5*(RNAi) animals on day 5 after mid-gastric bisection. Note the emergence of multiple *Wnt3* expressing clusters in the apex of *Sp5*(RNAi) animals (red arrows). **(d)** Detection of foot-specific peroxidase in foot regenerating *Sp5*(RNAi) animals 5 days after mid-gastric bisection. Note that foot regenerating *Sp5*(RNAi) animals never regenerated multiple heads. Red arrows: Regenerated foot; black arrows: foot of ectopic axis; white arrowheads: unspecific signal. Shown are representative animals of an experiment performed in triplicate. Scale bars: approximately 200 μ m.



Supplementary Figure 8. Knockdown of β -catenin delays head regeneration

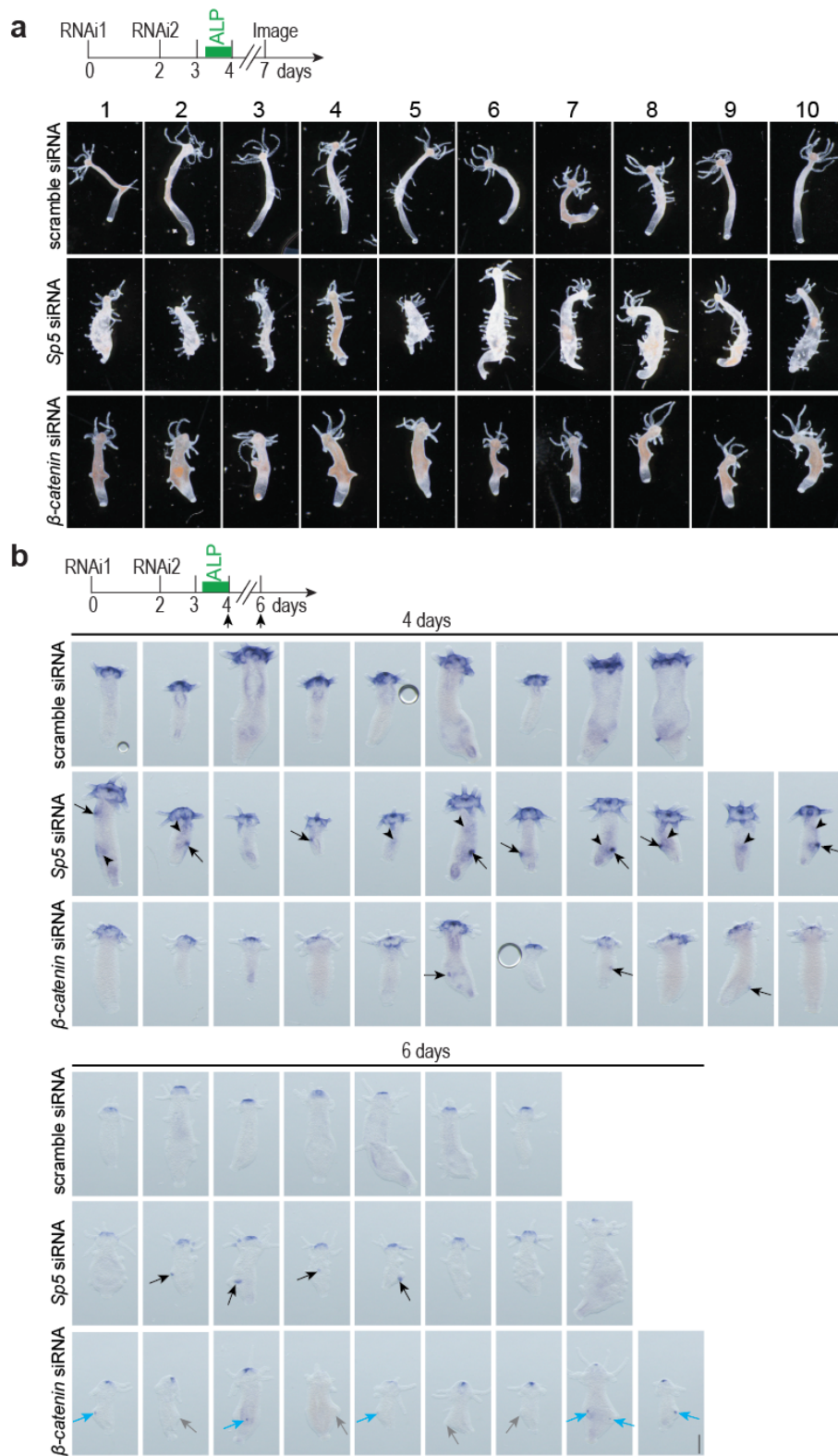
Intact *Hydra* were electroporated twice (RNAi1, RNAi2), either with a scramble siRNA or with a mix of β -catenin siRNAs. Head regeneration was induced by mid-gastric bisection 24 hours after RNAi2. **(a)** β -catenin expression detected by qPCR. Black arrows: Time points of RNA extraction. Note the significant down-regulation of β -catenin on day 3 and 5. Each data point represents an independent replicate. Statistical p-values: ≤ 0.05 (unpaired t test). **(b)** Scramble and β -catenin(RNAi) animals were imaged live at day 1, 2, 4, 6 post-amputation (black arrows). Note the delay in head regeneration after the knockdown of β -catenin as illustrated by a reduced number of tentacles on day 6 post-amputation (white arrows). Shown are representative animals of an experiment performed in triplicate. Scale bar: 200 μ m. Error bars indicate SD.

RNAi1 RNAi2 RNAi3 Image
 0 2 4 // 8 → days



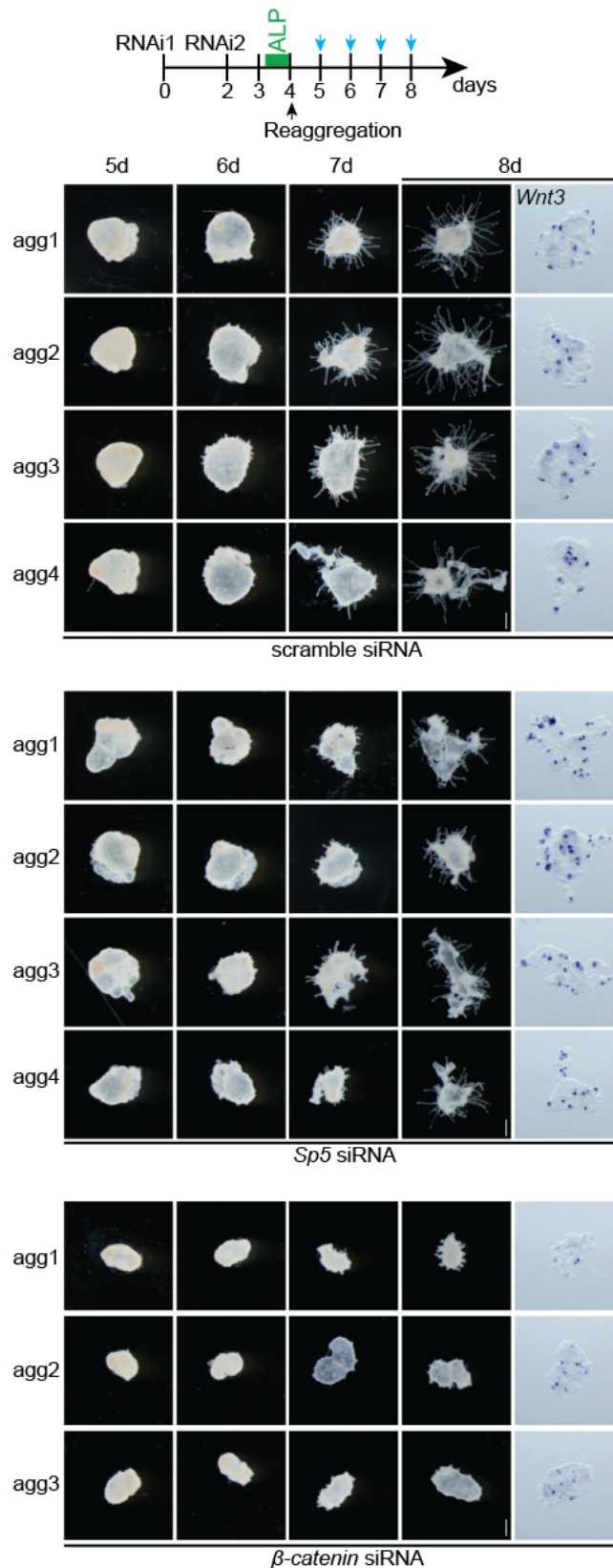
Supplementary Figure 9. *HySp5* phenotype occurrence requires active Wnt/ β -catenin signaling

Intact *Hydra* were electroporated three times every other day (RNAi1, RNAi2, RNAi3) either with a scramble siRNA or a mix of β -catenin/scramble, *Sp5*/scramble or β -catenin/*Sp5* siRNAs. Shown are live animals on day 4 after RNAi3. Note that β -catenin/scramble RNAi animals developed ectopic bumps (white arrows) while *Sp5*/scramble RNAi animals developed ectopic heads (red arrows). Ectopic heads did no longer occur when *Sp5* was knocked-down together with β -catenin. Shown are representative animals of an experiment performed in duplicate. Scale bar: approximately 200 μ m.



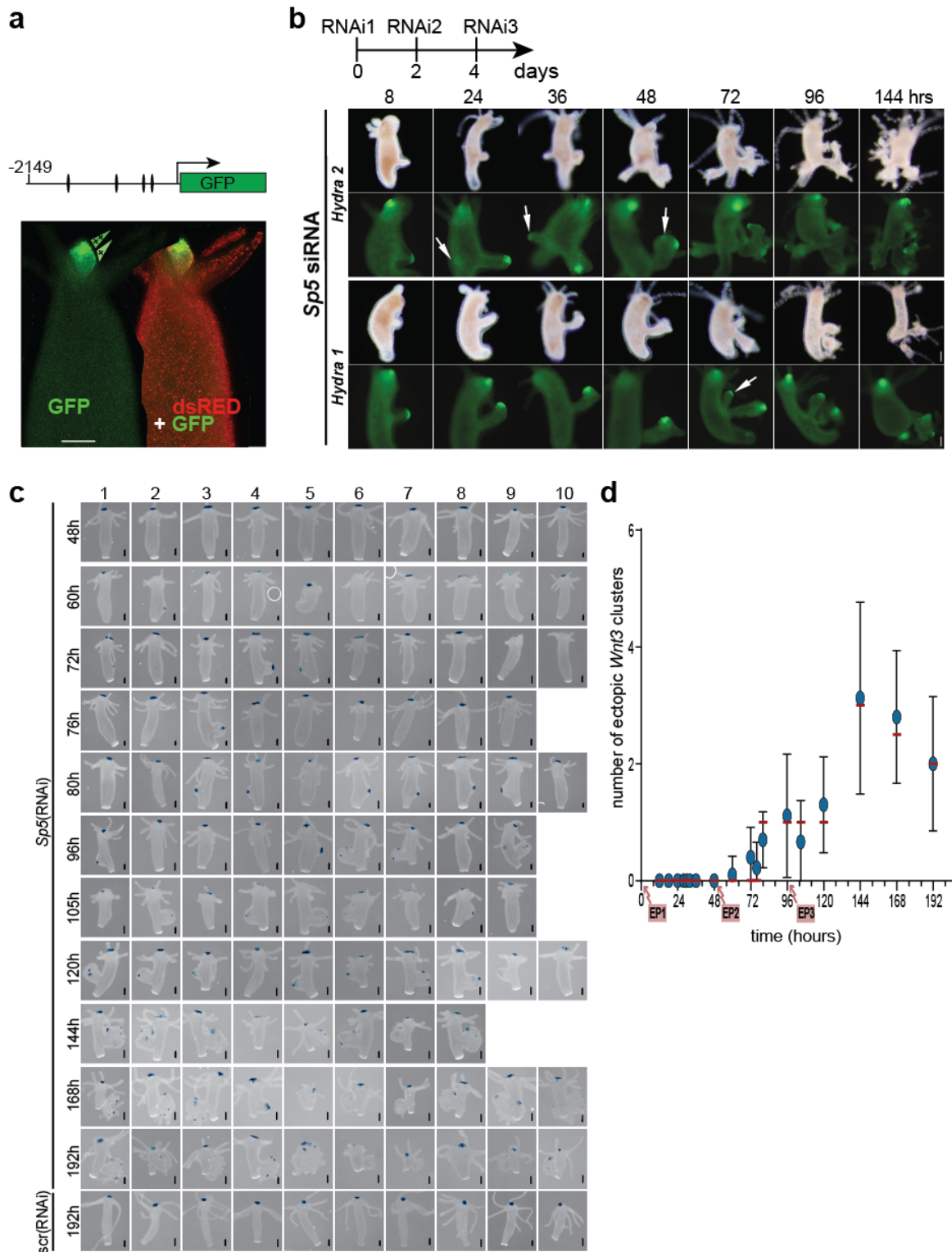
Supplementary Figure 10. *HySp5* antagonizes Wnt/ β -catenin signaling

Intact *Hydra* were electroporated two times (RNAi1, RNAi2) either with a scramble, *Sp5* or β -catenin siRNA, followed by treatment with Alsterpaullone (ALP). **(a)** Shown are ten representative animals of an experiment performed in duplicate. Animals were fixed on day 3 after the end of the treatment with ALP. Note that the knockdown of *Sp5* enhanced ectopic tentacle formation, while the knockdown of β -catenin reduced ectopic tentacle formation. **(b)** Shown are representative animals fixed and detected for *Wnt3* expression either immediately (Day 4) or 2 days after the end of the treatment with ALP (Day 6). Note that the knockdown of *Sp5* increases the expression of *Wnt3* throughout the body column. Black arrows: local increase in *Wnt3* expression; black arrowheads: diffuse increase in *Wnt3*; grey arrows: *Wnt3*-negative bumps; blue arrows: *Wnt3*-positive bumps. Scale bars: approximately 200 μ m.



Supplementary Figure 11. Knockdown of *Sp5* in reaggregation studies

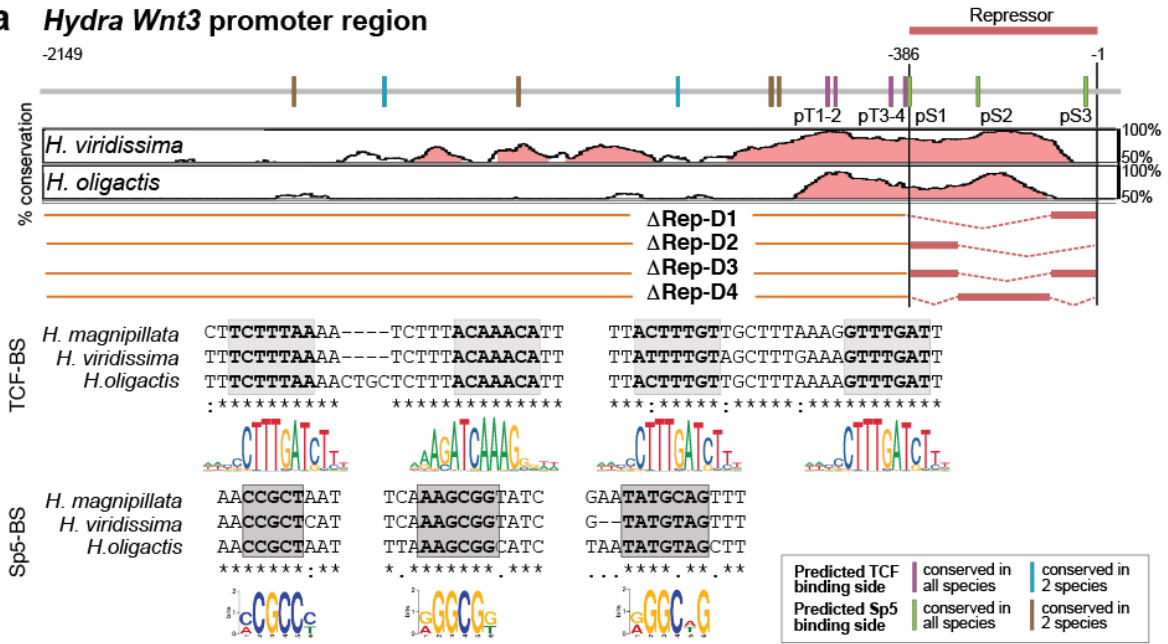
Intact *Hydra* electroporated twice (RNAi1, RNAi2) with scramble, *Sp5* or β -catenin siRNAs were treated with Alsterpaullone (ALP) for 18 hours and dissociated immediately after the ALP treatment to be reaggregated. Reaggregates (agg1, agg2, agg3, ...) were imaged live 1, 2, 3 or 4 days after reaggregation and then fixed four days post-dissociation (day-8) to be detected for *Wnt3* expression. Note the increased number of *Wnt3* expressing clusters in *Sp5*(RNAi) reaggregates. Shown are representative images of an experiment performed in duplicate. Scale bars: 200 μ m.



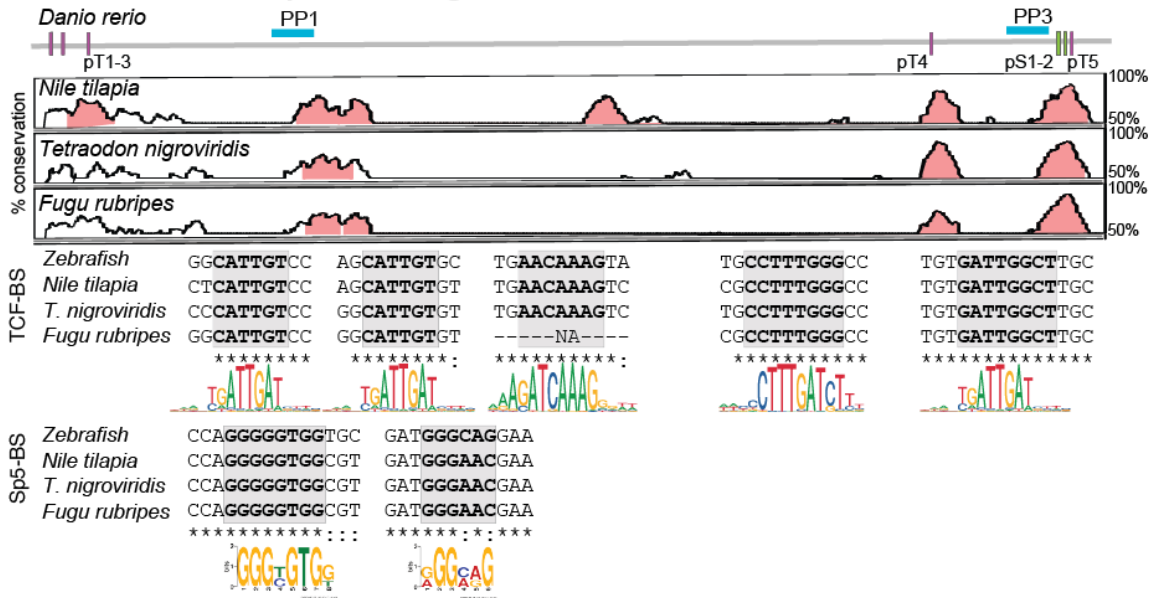
Supplementary Figure 12. Kinetics of *Wnt3* expression in *Sp5*(RNAi) animals

(a) Live transgenic *Hydra* expressing a *HyWnt3*:GFP-*HyAct*:dsRED construct where GFP expression is driven by the *Wnt3* promoter and dsRED by the ubiquitous *HyActin* promoter. Vertical bars: TCF binding sites. “++” and “+” indicate the maximal and intermediate GFP levels respectively. The same animal is shown in the GFP and dsRED channel. **(b)** Bright field and GFP fluorescence views of two *HyWnt3*:GFP-*HyAct*:dsRED animals (*Hydra* 1 and 2) knocked-down for *HySp5* and pictured at indicated time-points after RNAi3. Arrows: clustered GFP+ cells at the tip of ectopic axes. **(c)** Ten representative *Sp5*(RNAi) animals fixed and detected for *Wnt3* at different time points after RNAi1. Scale bars: 200 μ m. **(d)** Quantification of *Wnt3*-expressing clusters for animals shown in (c). Round circles: average number of ectopic *Wnt3*-expressing clusters; red horizontal lines: median. Arrow bars indicate SD. Source data are provided as a Source Data file. (a-b) Shown are representative animals of an experiment performed in duplicate. (c) Shown are animals analyzed in one experiment.

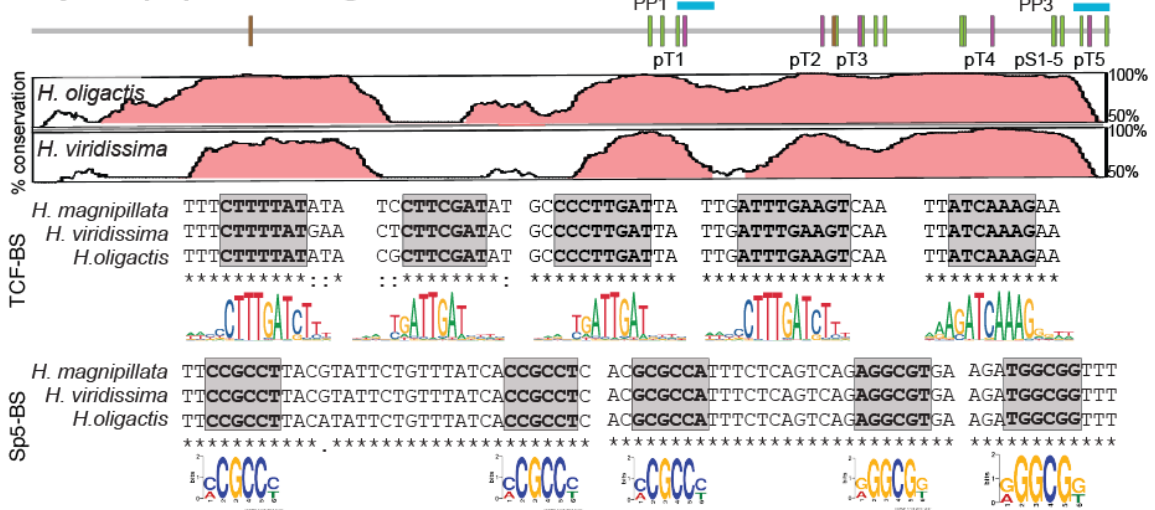
a Hydra Wnt3 promoter region



b Teleost fish Wnt3 promoter region

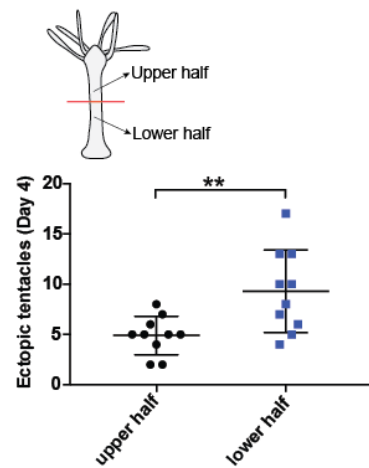
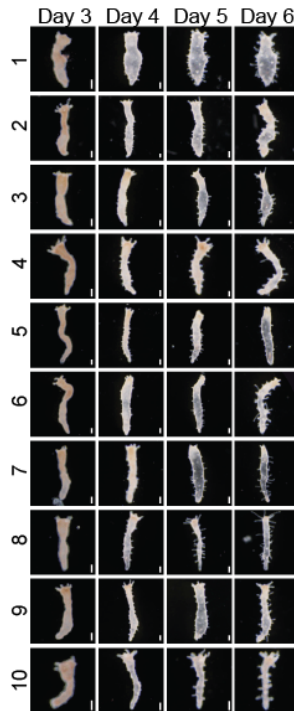
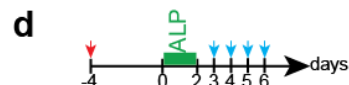
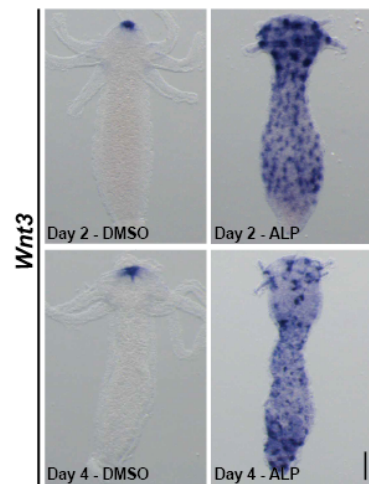
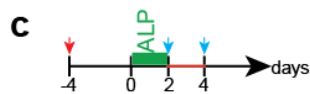
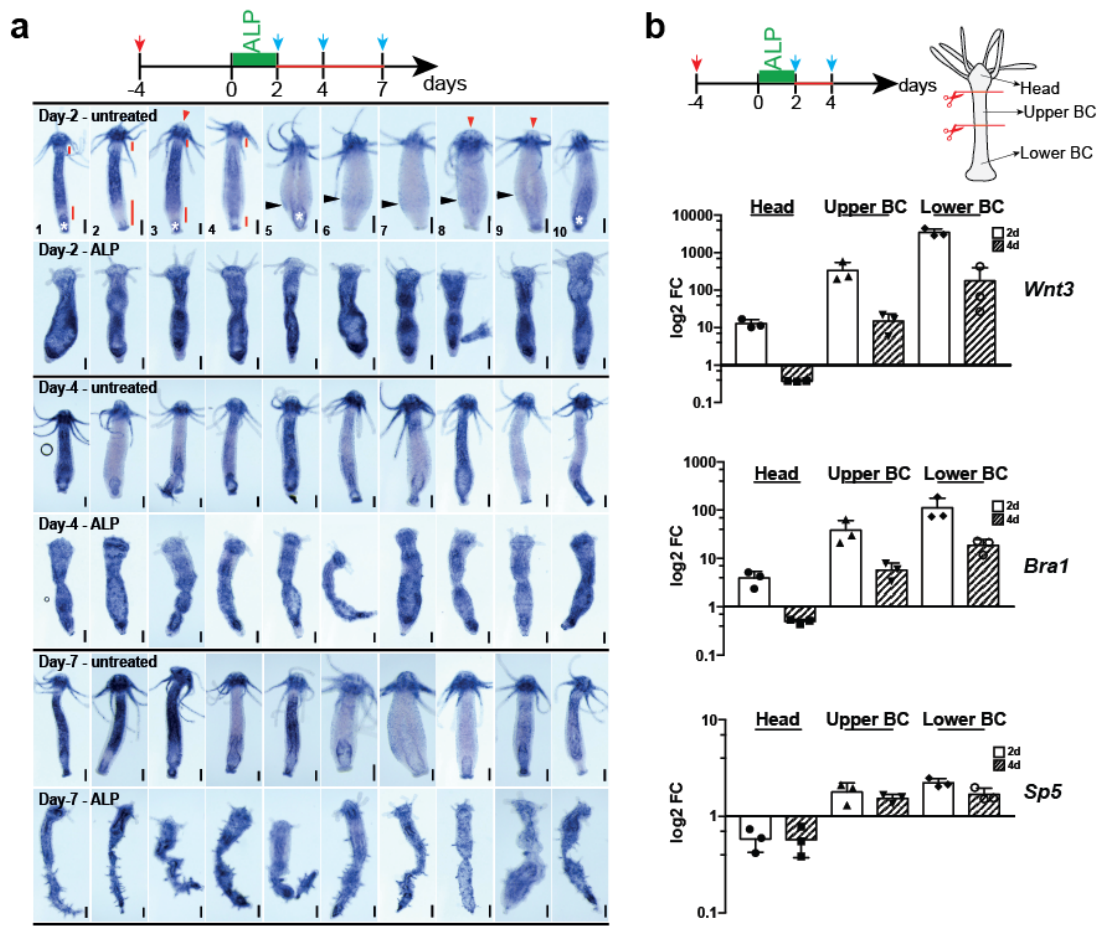


c Hydra Sp5 promoter region



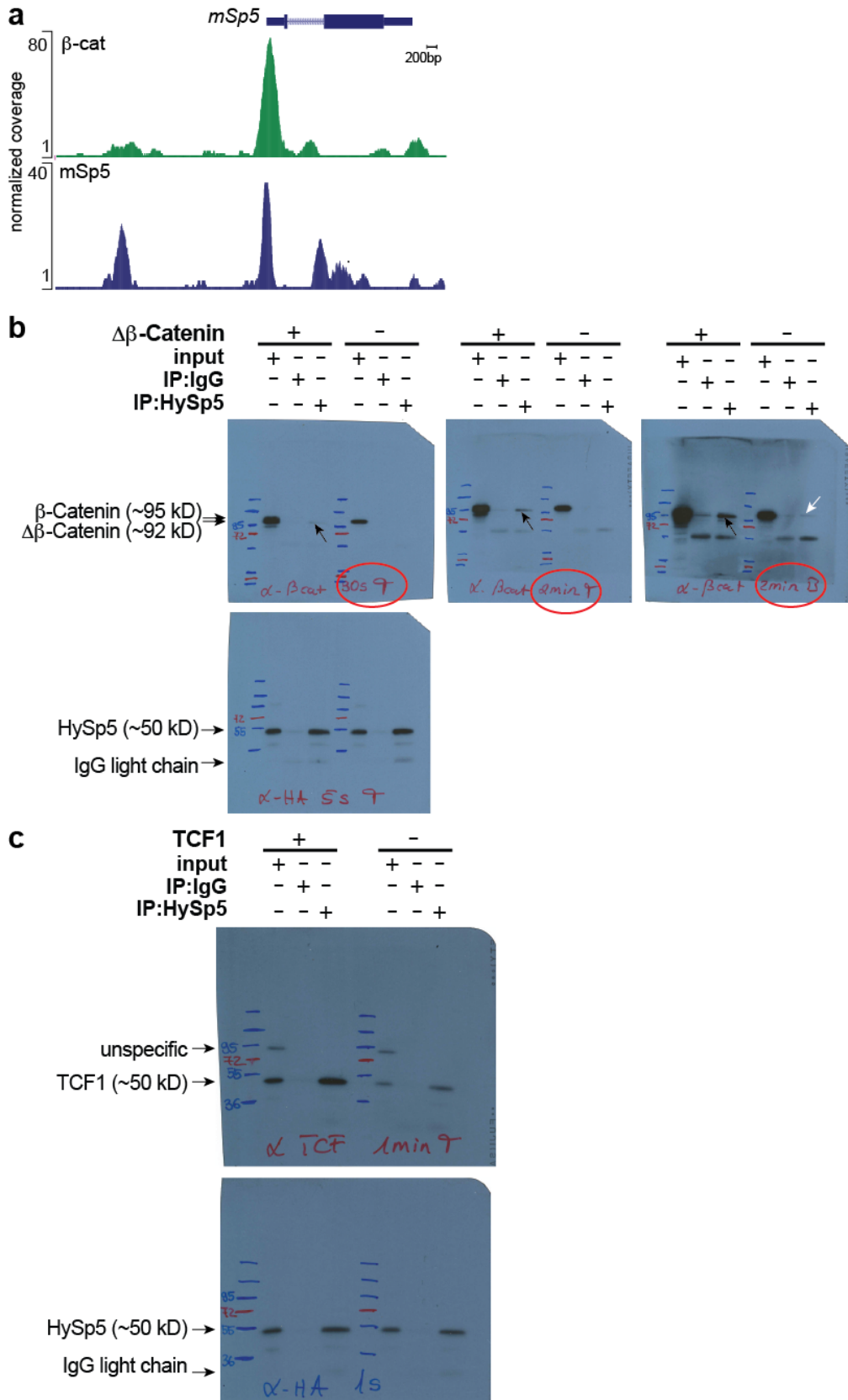
Supplementary Figure 13. Mapping of putative Sp5 binding sites in the *Wnt3* and *Sp5* upstream sequences in *Hydra* and teleost fish

Map showing the location of the putative Sp5 (pS) and TCF (pT) binding sites along the upstream sequences of *Hydra Wnt3* (a), zebrafish *Wnt3* (b) and *Hydra Sp5* (c). Sp5 binding sites were identified using the FIMO tool (see material and methods) and the consensus matrixes identified from the analysis of the HySp5 and ZfSp5a ChIP-seq dataset using MEME ChIP suite (see Methods). TCF binding sites (TCF-BS) were identified using the TCF1-LEF1 and TCF4 consensus matrixes available from the MultiTF tool implemented in Ecr browser. The evolutionary conservation of the putative Sp5 binding sites (Sp5-BS) was determined by comparing their sequence across three *Hydra* or four teleost fish species using the Vista alignment tool. Green bars: Sp5-BS conserved in all analyzed species, brown bars: Sp5-BS conserved in only two species, magenta bars: TCF-BS conserved in all analyzed species, blue bars : TCF-BS conserved in only two species ; Blue boxes: PP (primer pairs) regions tested in ChIP-qPCR experiments. A multispecies alignment of the sequences corresponding to each predicted TCF-BS (upper row) or Sp5-BS (lower row) is shown below the Vista plot (pink peaks) with the corresponding consensus matrix. The predicted BS sequences are written bold on a gray background. Stars mark nucleotides identical in all species, semi-columns the nucleotides conserved in 2/3 or 3/4 species. When the putative BS is located in the negative strand the reverse complement version of the corresponding matrix is shown. In the case of the *HySp5* promoter only the putative Sp5-BS located within the regions enriched in the ChIP-qPCR analysis (PP1, PP2, PP3) are shown. In (a) the *Wnt3* promoter sequences tested in deletion reporter constructs are schematized.



Supplementary Figure 14. *HySp5* expression in Alsterpaullone-treated animals

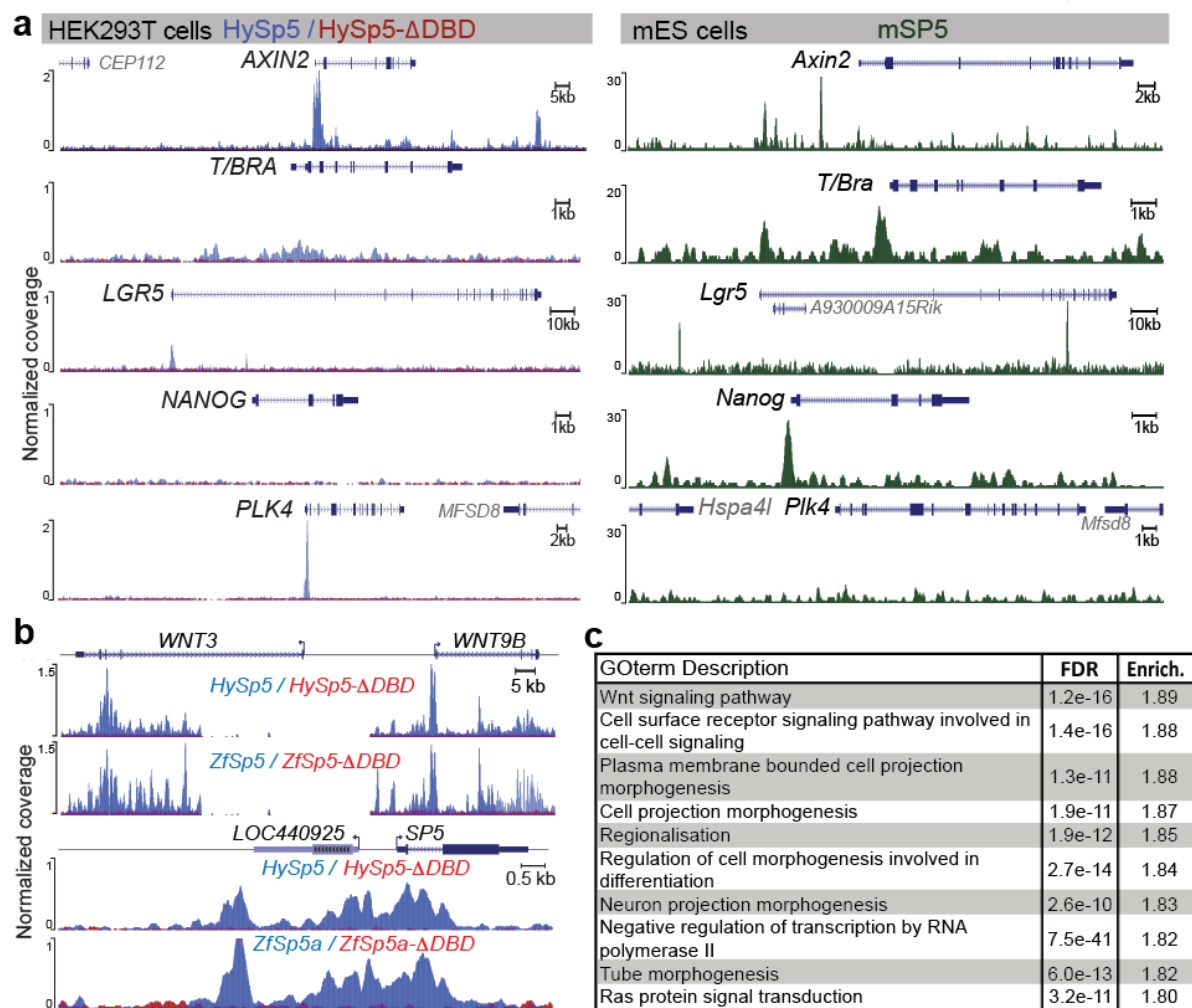
(a) *HySp5* expression in intact animals exposed for two days to Alsterpaullone (ALP) and fixed either immediately (Day 2), or transferred to HM and fixed two and five days later (Day 4, Day 7). Red arrow: last feeding, blue arrows: fixation days. Note that in all animals *HySp5* expression is high in the head region but low at the very apical tip (red arrowheads). In animals 1-4 (Day 2 untreated animals) *HySp5* expression is high in the body column with two adjacent regions where *HySp5* expression is low (red bars); in animals 5-10, *HySp5* expression is low in the body column and several show a higher level of *HySp5* expression in the budding zone (black arrowheads). Upon ALP treatment, *HySp5* is increased in the body column of all animals, and ectopic tentacles form dots of enhanced *HySp5* expression at Day 4, and become visible at Day 7. Shown are representative animals of an experiment performed in triplicate. **(b)** Treatment of intact *Hydra* with ALP for 2 days followed by detection of *Wnt3*, *Bra1* and *Sp5* expression by qPCR in head as well as upper and lower body column tissue. Blue arrows: Days of RNA extraction. Note the up-regulation of *Wnt3*, *Bra1* and *Sp5* in body column tissue on Day 2 and Day 4, the up-regulation of *Wnt3* and *Bra1* in head tissue on Day 2 and down-regulation on Day 4 as well as the down-regulation of *Sp5* in head tissue at both time points. Each point represents an independent replicate. **(c)** Treatment of *Hydra* with ALP for 2 days and detection of *Wnt3* on Day 2 and Day 4 (blue arrows). Note the reduction of *Wnt3* expression on Day 4 compared to Day 2 in head and body column tissue. Shown are representative animals of an experiment performed in triplicate. **(d)** Intact *Hydra* were treated with ALP for 2 days and imaged on Day 1-4 (blue arrows) after the end of the ALP treatment (left panel). Shown are representative animals of an experiment performed in triplicate. Quantification of ectopic tentacles in the upper and lower body column two days after the end of the ALP treatment (Day 4) (right panel). Note that ectopic tentacles first occurred in the lower half, which is consistent with a higher expression of *Wnt3* in lower than upper body column tissue (see panel b). Each data point represents one animal. Statistical p-values: ** ≤ 0.01 (unpaired t test). Scale bars: approximately 200 μm . Arrow bars indicate SD.



Supplementary Figure 15. Interactions between Sp5 and β -Catenin or TCF1

(a) ChIP-seq profile showing the genomic occupancies of the mouse Sp5 and β -catenin over the genomic region encompassing the *Sp5* locus in mouse ES cells. The profiles were obtained by re-mapping publicly available datasets^{6,7}. Note the overlap in the occupancies of Sp5 and β -catenin in the vicinity of the *Sp5* transcriptional start site. **(b-c)** Nuclear extracts were prepared from HEK293T cells transiently expressing HySp5_HA protein or not, in

the presence of a constitutively active form of human β -Catenin (hu $\Delta\beta$ -Cat) (b) or human TCF1 (c). **(b)** HySp5 and β -Catenin interaction after anti-HA immunoprecipitation, Western blotting and immunodetection with the anti- β -Catenin antibody (upper, at two distinct exposure times), or the anti-HA antibody (lower). Note that HySp5 interacts with exogenous (black arrows) and endogenous (white arrow) β -Catenin. T: Top; B= Bottom. **(c)** HySp5 and TCF1 interaction detected after anti-HA immunoprecipitation, Western blotting and immunodetection with the anti-TCF1 antibody. Note that HySp5 interacts with exogenous and endogenous TCF1. All Co-IP experiments were performed twice with extracts prepared independently.

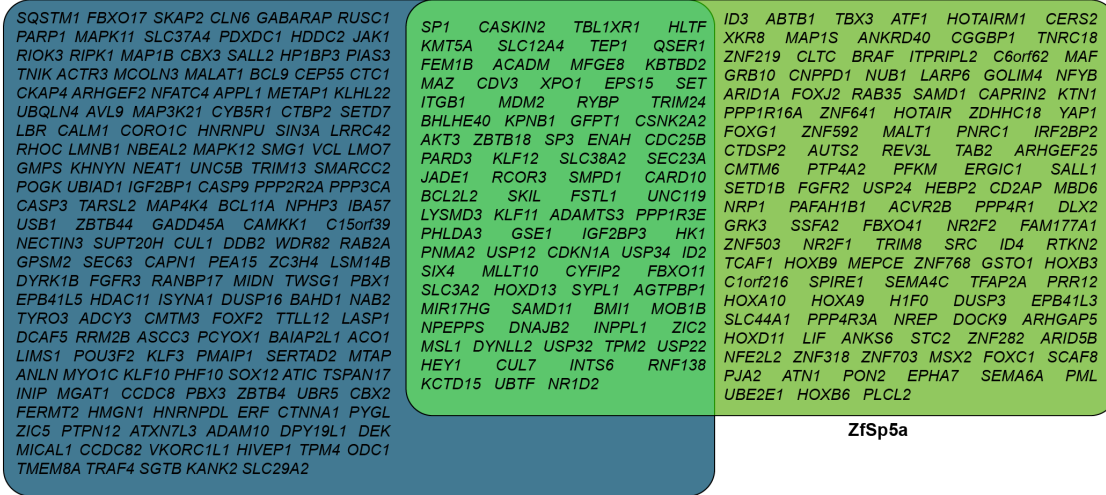


Supplementary Figure 16. Genome-wide mapping of putative Sp5 binding sites in human HEK293T cells and mouse ESCs

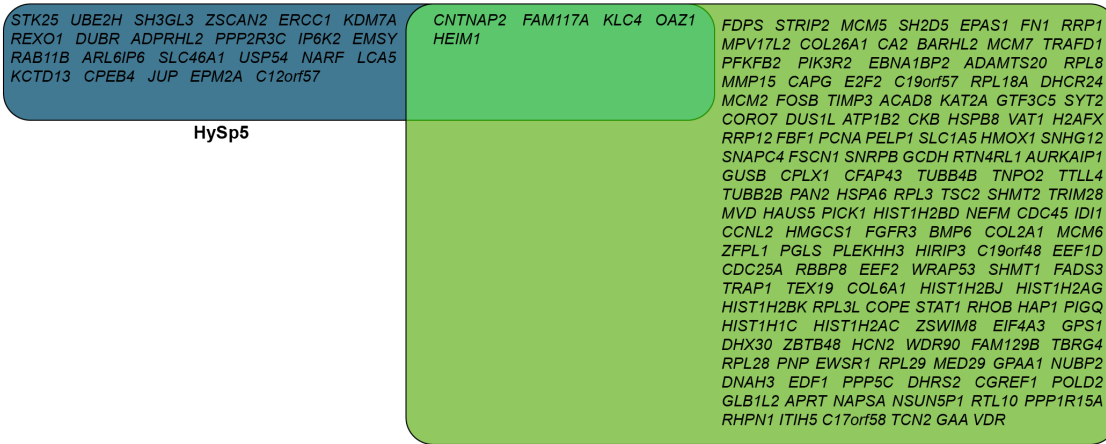
(a) ChIP-seq analysis showing the binding profiles of HySp5 expressed in HEK293T cells (left panels) within the genomic regions of known Wnt target genes, compared to the previously reported genomic occupancies of the mouse Sp5 in the corresponding mouse ortholog loci⁷ (right panels). The control recombinant protein HySp5- Δ DBD does not show any significant enrichment over the same genomic regions. **(b)** ChIP-seq analysis showing the genomic occupancies of the HySp5 and ZfSp5a proteins (blue) in the genome of HEK293T cells expressing these proteins. No enrichment is scored when HEK293T cells express Sp5 proteins lacking the DBD (red). **(c)** Table summarizing the 10 most enriched GO terms associated with the genes assigned to the Sp5-enriched regions in HEK293T cells expressing HySp5 and ZfSp5a. GO term search was performed using the Gorilla software to compare the genes assigned to Sp5 bound regions in both HySp5 and ZfSp5a ChIP-seq experiments versus the full list of human genes.

a

Downregulated genes -putative direct targets



Upregulated genes -putative direct targets

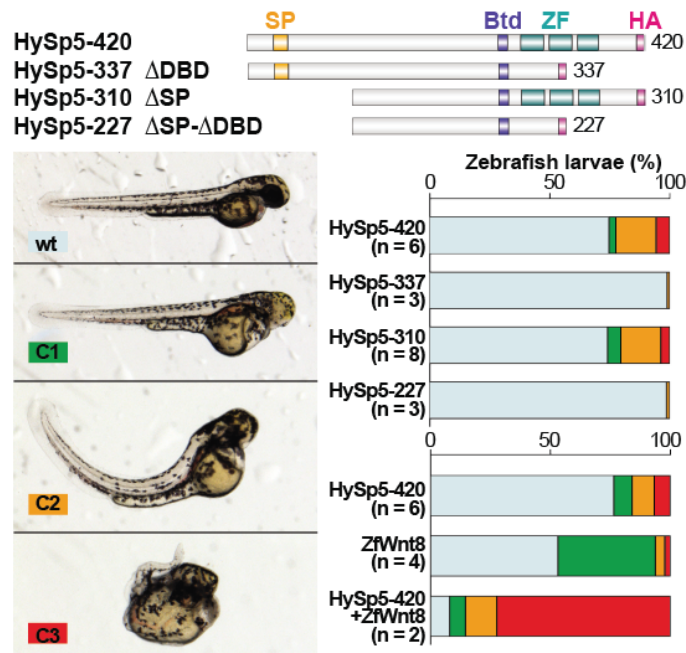


b

	GO term description	FDR	GO term description	FDR
ZfSp5a downreg. targets	Positive regulation of cellular process	3.4E-04	Organic cyclic compound metabolic process	2.5E-04
	Negative regulation of transcription, DNA-templated	5.9E-04	Nucleobase-containing compound metabolic process	6.6E-04
	Regulation of metabolic process	1.7E-03	Heterocycle metabolic process	7.7E-04
	Positive regulation of biological process	2.3E-03	Cellular aromatic compound metabolic process	7.9E-04
	Cellular macromolecule metabolic process	2.9E-03	Cellular nitrogen compound metabolic process	2.0E-03
HySp5 downreg. targets	Cellular response to stimulus	1.1E-04		
	Regulation of cellular process	1.6E-04		
	Cellular response to stress	2.5E-04		
	Regulation of cellular metabolic process	2.6E-04		
	Positive regulation of macromolecule metabolic process	6.1E-04		
HySp5-ZfSp5a downreg. targets	Regulation of transcription, DNA-templated	9.5E-08		
	Negative regulation of transcription, DNA-templated	1.0E-07		
	Regulation of transcription by RNA polymerase II	7.1E-07		
	Regulation of metabolic process	8.4E-07		
	Anatomical structure morphogenesis	8.7E-07		

Supplementary Figure 17. Direct transcriptional targets of HySp5 and ZfSp5a.

(a) Venn diagram showing the genes repressed (Top) or activated (Bottom) upon HySp5 or ZfSp5a overexpression in HEK293T cells and associated with HySp5 or ZfSp5a bound elements. (b) Summary of the 5 most significantly enriched GO term categories (based on their FDR value) for the different subset of genes represented in the Venn diagram in (a). No significantly enriched GO term categories were identified for the HySp5 specific and HySp5-ZfSp5a common upregulated targets. When more than 10 significantly enriched GO term categories were identified (FDR<0,05) the REVIGO tool was used to group related GO term classes using 0.7 as threshold for allowed similarity.



mRNA	[conc] pg	N	†% (n)	Sn	wt % (n)	class1 % (n)	class2 % (n)	class3 % (n)	Total % of abnormal embryos
HySp5-420	400	79	10.1% (8)	71	74.7% (53)	2.8% (2)	16.9% (12)	5.6% (4)	25.3%
HySp5-420	400	128	7.0% (9)	119	76.5% (91)	7.6% (9)	9.2% (11)	6.7% (8)	23.5%
HySp5-337 ΔDBD	400	96	2.1% (2)	94	98.9% (93)	0.0% (0)	1.1% (1)	0.0% (0)	1.1%
HySp5-310 ΔSP	400	56	3.6% (2)	54	74.1% (40)	5.5% (3)	16.7% (9)	3.7% (2)	25.9%
HySp5-227 ΔSP-ΔDBD	400	74	4.1% (3)	71	98.6% (70)	0.0% (0)	1.4% (1)	0.0% (0)	1.4%
HySp5-420	400	128	7.0% (9)	119	76.5% (91)	7.6% (9)	9.2% (11)	6.7% (8)	23.5%
ZfWnt8	4	138	7.3% (10)	128	53.1% (68)	40.6% (52)	3.9% (5)	2.3% (3)	46.9%
HySp5-420 + ZfWnt8	400+4	155	11.6% (18)	137	8.0% (11)	6.6% (9)	13.1% (18)	72.3% (99)	82%

Supplementary Figure 18. Overexpressing HySp5 in zebrafish embryos induces Wnt-like phenotypes

To test whether HySp5 is a mediator of the Wnt pathway, we injected *HySp5* mRNAs, either full-length (HySp5-FL) or lacking the SP box (HySp5-ΔSP) into zebrafish embryos and looked at larval morphology on day-2 post-fertilization (dpf). **(upper panel)** Wnt-like phenotypes detected in 2 days old zebrafish larvae overexpressing HySp5 (HySp5-420). These phenotypes were scored in three classes: no eyes (C1); no eyes + curly axis (C2); no eyes, underdeveloped axis and curly tail (C3). The HySp5 constructs lacking the DNA-binding domain do not affect embryonic development, whereas co-injecting ZfWnt8 with HySp5-420 increases the phenotypic penetrance. The number of independent experiments (n) is indicated for each construct and the graphs show one representative experiment. **(lower panel)** Table showing the scoring of the embryonic phenotypes identified in zebrafish overexpressing HySp5 or ZfWnt8. One representative experiment is shown. All embryos were produced from wild-type parental strains and analyzed at 48 hpf. N = number of injected embryos; †%(n) = percentage (number) of dead embryos; Sn = number of surviving embryos. Given the similarities with the morphological defects obtained when the zebrafish β-catenin or Wnt8 are overexpressed during development^{8,9}, we deduced that HySp5 can mediate at least some effects of Wnt/β-catenin signaling during zebrafish gastrulation, a mediation that requires its DNA-binding activity.

Supplementary Tables

Supplementary Table 1. Cloning, siRNAs, qPCR and ChIP-qPCR primer sequences

(a) List of cloning primers

	Primer name	Sequence
HySp5:Luc	HySp5 promoter Forward	CTAGTTCTAATTTAGCTCTATTACGTTCCG
	HySp5 promoter Reverse	GAAACCGCCATCTTATCTTAAATAGCTTCGG
ZfSp5a-ΔDBD	ZfSp5a-ΔDBD Forward	CAGAACAAGAAGAGCAAAAGTCACG
	ZfSp5a-ΔDBD Reverse	CTGTTTCTTCTTTCCGGGCTCA
HyWnt3-ΔRep:Luc	HyWnt3-ΔRep:Luc Forward	CTCGAGATCTGCGATCTAAG
	HyWnt3-ΔRep:Luc Reverse	GCGGTTAGTTAAATCAAACC
pGEM-T-Easy-HySp5	HySp5 Forward (Sp5-For1)	AATTACTCACAAAACTTT
	HySp5 Reverse (Sp5-Rev1)	TAAGGTGACTAGTTTTACC
pGEM-T-Easy-HyWnt3	HyWnt3 Forward	ATGGGCACGACGCGTTATAA
	HyWnt3 Reverse	CTATTTACAGGTGTATTCCAG
pGEM-T-Easy-HyBra1	HyBra1 Forward	TGGAAGGCGAATGTTTCCTG
	HyBra1 Reverse	TTCGGTGATACGGTGATGGA

(b) List of siRNAs

HySp5 siRNA-1	UUA ACG AGC ACC ACA UAA A
HySp5 siRNA-2	CUA CAA CAU CCC ACA UAU A
HySp5 siRNA-3	GCA GCA CGU AUG UCA UAU U
β-catenin siRNA-1	UCA ACC UAA CAG ACA ACA A
β-catenin siRNA-2	UGA GGA GCU AUA CUU AUG A
β-catenin siRNA-3	ACG ACU CUC UGU UGA AUU A
scramble siRNA	AGGUAGUGUAAUCGCCUUG

(c) List of qPCR primers

HySp5 Forward	CCAGGGTGCGGAAAGGTT
HySp5 Reverse	CCAGCATGCCATCTTAAATGAG
Wnt3 Forward	GAGTTGACGGTTGCGAACTT
Wnt3 Reverse	ACATGAAACCTTGCAACACCA
β-catenin Forward	TACGCAATGTTGTTGGTGCT
β-catenin Reverse	GCTTCAATTCGATGGCCTAA
Bra1 Forward	ATAGATTGGTATCCGTGCGG
Bra1 Reverse	GGAAACTGAGGCGGATACCA
TBP Forward	AAGCGATTTGCAGCAGTTAT
TBP Reverse	GCTCTTCACTTTTTGCTCCA

(d) List of ChIP-qPCR primers

HySp5 promoter (Hm-105)

PP1-F	TAAGCTGTCTCCATTTCAACCA
PP1-R	AATATTTGTTAAGTGTTCGTTGG
PP2-F	TATCTTTTCCGCCTTACGTATTC
PP2-R	ACTGAGAAATGGCGCGTTG
PP3-F	CAGAGAAAATATGATCGCAACG
PP3-R	GAAACCGCCATCTTATCTTAAA

ZfWnt3 promoter

PP1-F	TCTGAAGAGAAAGGGGCAAA
PP1-R	ACCCTCTCCTCACACACGTC
PP2-F	GCAAGCAACATGGGACAATA
PP2-R	ATGTAGGTTCCGGCCAATTT
PP3-F	ACAGCTGGGTTTCCTTGATG
PP3-R	AGGCTGGGAGGGAATAAGAA

Supplementary Table 2. DNA constructs used in this study

Name	Abbreviation	Reference	Source
pGL3- <i>HySp5</i> -2992	HySp5:Luc	/	This study
pGL3- <i>HyWnt3</i> -2149	HyWnt3:Luc	/	This study
pGL3- <i>HyWnt3</i> -1763	HyWnt3-ΔRep:Luc	/	This study
pGL3- <i>HyWnt3</i> -1858	HyWnt3-ΔRep-D1:Luc	/	This study
pGL3- <i>HyWnt3</i> -1864	HyWnt3-ΔRep-D2:Luc	/	This study
pGL3- <i>HyWnt3</i> -1959	HyWnt3-ΔRep-D3:Luc	/	This study
pGL3- <i>HyWnt3</i> -1953	HyWnt3-ΔRep-D4:Luc	/	This study
pEGFP- <i>ZfWnt3</i> -3997	ZfWnt3-promoter	Ref. ¹⁰	Cathleen Teh (gift)
pGL3- <i>ZfWnt3</i> -3997	ZfWnt3:Luc	/	This study
pGL3	no-prom:Luc	Ref. ¹¹	Zbynek Kozmik (gift)
pCS2+		www.addgene.org/vector-database/2295/	
pCS2+- <i>HySp5</i> -FL	HySp5-420	/	This study
pCS2+- <i>HySp5</i> -ΔDBD	HySp5-337	/	This study
pCS2+- <i>HySp5</i> -ΔSP	HySp5-310	/	This study
pCS2+- <i>HySp5</i> -ΔSP-ΔDBD	HySp5-227	/	This study
pCS2+- <i>ZfSp5a</i> -FL	ZfSp5a-337	/	This study
pCS2+- <i>ZfSp5a</i> -ΔDBD	ZfSp5a-289	/	This study
pCS2+- <i>ZfSp5l1</i> -FL	ZfSp5l1	/	This study
ZE14 pCS2P+ <i>wnt8</i> ORF1	ZfWnt8	Ref. ⁹	Addgene # 17048
pcDNA-Wnt3	huWnt3	Ref. ¹²	Addgene # 35909
pcDNA6- <i>huLRP6</i> -v5	huLRP6	Ref. ¹³	Bart Willimans (gift)
pFLAG-CMV- <i>hu-β-Catenin</i> Δ45	huΔβ-cat	Ref. ¹⁴	Ariel Ruiz i Altaba (gift)
pCAG-FLAG-TCF-1	TCF1	Ref. ¹⁵	Junichiro Yasunaga (gift)
pGEM-T-Easy- <i>HyWnt3</i> -1092	/	/	This study
pGEM-T-Easy- <i>HyBra1</i> -635	/	/	This study
pGEM-T-Easy- <i>HySp5</i> -557	/	/	This study
pGL4.74[hRluc/TK]		www.promega.com/-/media/files/resources/protocols/product-information-sheets/a/pgl474-vector.pdf?la=en	

Supplementary References

- 1 Schaeper, N. D., Prpic, N. M. & Wimmer, E. A. A clustered set of three Sp-family genes is ancestral in the Metazoa: evidence from sequence analysis, protein domain structure, developmental expression patterns and chromosomal location. *BMC Evol Biol* **10**, 88, doi:10.1186/1471-2148-10-88 (2010).
- 2 Wenger, Y., Buzgariu, W. & Galliot, B. Loss of neurogenesis in Hydra leads to compensatory regulation of neurogenic and neurotransmission genes in epithelial cells. *Philos Trans R Soc Lond B Biol Sci* **371**, 20150040, doi:10.1098/rstb.2015.0040 (2016).
- 3 Anton-Erxleben, F., Thomas, A., Wittlieb, J., Fraune, S. & Bosch, T. C. Plasticity of epithelial cell shape in response to upstream signals: a whole-organism study using transgenic Hydra. *Zoology (Jena)* **112**, 185-194, doi:10.1016/j.zool.2008.09.002 S0944-2006(09)00002-6 [pii] (2009).
- 4 Wittlieb, J., Khalturin, K., Lohmann, J. U., Anton-Erxleben, F. & Bosch, T. C. Transgenic Hydra allow in vivo tracking of individual stem cells during morphogenesis. *Proc Natl Acad Sci U S A* **103**, 6208-6211 (2006).
- 5 Hemmrich, G. *et al.* Molecular signatures of the three stem cell lineages in hydra and the emergence of stem cell function at the base of multicellularity. *Mol Biol Evol* **29**, 3267-3280, doi:10.1093/molbev/mss134 (2012).
- 6 Zhang, X., Peterson, K. A., Liu, X. S., McMahon, A. P. & Ohba, S. Gene regulatory networks mediating canonical Wnt signal-directed control of pluripotency and differentiation in embryo stem cells. *Stem Cells* **31**, 2667-2679, doi:10.1002/stem.1371 (2013).
- 7 Kennedy, M. W. *et al.* Sp5 and Sp8 recruit beta-catenin and Tcf1-Lef1 to select enhancers to activate Wnt target gene transcription. *Proc Natl Acad Sci U S A* **113**, 3545-3550, doi:10.1073/pnas.1519994113 (2016).
- 8 Pelegri, F. & Maischein, H. M. Function of zebrafish beta-catenin and TCF-3 in dorsoventral patterning. *Mech Dev* **77**, 63-74 (1998).
- 9 Lekven, A. C., Thorpe, C. J., Waxman, J. S. & Moon, R. T. Zebrafish wnt8 encodes two wnt8 proteins on a bicistronic transcript and is required for mesoderm and neurectoderm patterning. *Dev Cell* **1**, 103-114 (2001).
- 10 Teh, C., Sun, G., Shen, H., Korzh, V. & Wohland, T. Modulating the expression level of secreted Wnt3 influences cerebellum development in zebrafish transgenics. *Development* **142**, 3721-3733, doi:10.1242/dev.127589 (2015).
- 11 Fujimura, N. *et al.* Wnt-mediated down-regulation of Sp1 target genes by a transcriptional repressor Sp5. *J Biol Chem* **282**, 1225-1237, doi:10.1074/jbc.M605851200 (2007).
- 12 Najdi, R. *et al.* A uniform human Wnt expression library reveals a shared secretory pathway and unique signaling activities. *Differentiation* **84**, 203-213, doi:10.1016/j.diff.2012.06.004 (2012).
- 13 Holmen, S. L., Salic, A., Zylstra, C. R., Kirschner, M. W. & Williams, B. O. A novel set of Wnt-Frizzled fusion proteins identifies receptor components that activate beta-catenin-dependent signaling. *J Biol Chem* **277**, 34727-34735, doi:10.1074/jbc.M204989200 (2002).
- 14 Melotti, A. *et al.* The river blindness drug Ivermectin and related macrocyclic lactones inhibit WNT-TCF pathway responses in human cancer. *EMBO Mol Med* **6**, 1263-1278, doi:10.15252/emmm.201404084 (2014).
- 15 Ma, G., Yasunaga, J., Fan, J., Yanagawa, S. & Matsuoka, M. HTLV-1 bZIP factor dysregulates the Wnt pathways to support proliferation and migration of adult T-cell leukemia cells. *Oncogene* **32**, 4222-4230, doi:10.1038/onc.2012.450 (2013).

Chapter-2 AUTO-REGULATION STUDY OF THE *HYDRA* HEAD INHIBITOR

SP5

The results presented in this chapter correspond to the main research conducted during the doctoral thesis. After identifying *Sp5* as the *Hydra* head inhibitor and confirming that this gene met the criteria for being the right candidate, many questions remained regarding its *in vivo* regulation as well as the identification of *Sp5* putative target gene candidates that could be involved during the inhibition of the head activator and thus patterning the established head organizer as well as the putative developing head organizers and thus contribute to the axial patterning of this animal.

To study the regulation of *Sp5 in vivo*, we decided to generate transgenic *Hydra* lines with a tandem reporter construct in which the *Hydra Sp5* promoter (*HySp5-3169*) drives the expression of a reporter gene, in this case GFP. By performing gain- and loss-of-function analysis on *Sp5* transgenic lines, we aim to decipher the *in vivo* auto-regulation of *Sp5*. We obtained two *Sp5* transgenic lines, one that expresses the reporter construct in the epidermis and the other one in the gastrodermis. Thus, by using different assays, we were able to not only demonstrate that *Sp5* has a negative auto-regulation in both layers, but also to better understand how each layer could contribute to the *Sp5* phenotype as well as how each layer plays a role when we ectopically activate Wnt/ β -catenin signaling and thus contribute to pattern the different ectopic structures caused by Wnt/ β -catenin signaling overexpression.

For this chapter I carried out all the experiments, analyzed the results and created all of the figures. With the additional help of Chrystelle Perruchoud, I injected myself the construct for the production of the *Sp5* transgenic lines. The project was developed in cooperation with Brigitte Galliot, with meaningful insights from Dr. Matthias Vogg and Dr. Paul Gerald Sánchez.

Finally, Dr. Leonardo Beccari supported in developing the ChIP optimization protocol for this paper using *Hydra* tissue.

Differential negative autoregulation of *Sp5* in the epidermal and gastrodermal epithelial layers in *Hydra*

Laura Iglesias Ollé¹, Matthias Christian Vogg¹, Paul Gerald Layague Sanchez¹,
Chrystelle Perruchoud¹, Brigitte Galliot^{1,*}

¹Department of Genetics and Evolution, Institute of Genetics and Genomics (iGE3), Faculty of Sciences, University of Geneva; 30 Quai Ernest Ansermet, 1211 Geneva 4, Switzerland.
*Corresponding author. Email: brigitte.galliot@unige.ch

ABSTRACT

The *Sp5* transcription factor was identified as a negative regulator of Wnt/ β -catenin signaling, the activator component of the *Hydra* apical organizer. Here we investigate how *Sp5* expression is regulated in the two *Hydra* epithelial layers, epidermis and gastrodermis. We generated two *Hv_AEP2* transgenic lines that constitutively express either in the gastrodermis or in the epidermis, a tandem reporter construct where the *Hydra actin* promoter and the *Hydra Sp5* promoter drive mCherry and eGFP expression respectively (*HyAct-1388:mCherry_HySp5-3169:eGFP*). That way we could monitor in each layer mCherry and GFP fluorescence, as well as *GFP*, *Sp5* and *Wnt3* expression. In intact and apical-regenerating animals, we recorded distinct spatial regulations of *Sp5* and *Wnt3* in the epidermis and the gastrodermis, suggesting that the cellular and molecular interactions are not identical in homeostatic and developmental apical organizers. Upon alsterpaullone treatment, Wnt/ β -catenin signaling is constitutively activated, maximal apically where epidermal *Sp5* expression is suppressed while in the upper and lower body column *Sp5* transiently forms two zones of maximal expression; in parallel *Sp5* is globally upregulated in the gastrodermis. Both, β -catenin and *Sp5* silencing lead to paradoxal epidermal *Sp5* expression along the body column, suggesting a *Sp5* promoter activation resulting from the suppression of a negative *Sp5* autoregulation. By contrast, in the gastrodermis, *Sp5* silencing leads to restricted spots of *Sp5* expression. The proximal *Sp5* promoter contains clustered *Sp5* binding-sites, recognized by *Sp5* in ChIP-PCR assay. We propose that *Sp5* autoregulation with layer-specific modulations impacts the cross-talk between the different components of the apical organizer.

Keywords: *Sp5* transcription factor, inhibitor of *Hydra* apical organizer, tandem reporter constructs, *Hydra* transgenic lines, epidermis and gastrodermal layers, *Sp5* promoter sequences

INTRODUCTION

Appendage and whole-body regeneration are amazing biological processes that offer the possibility to study in a juvenile or adult context how developmental genetic programs that took place during embryogenesis but at a much smaller scale, can possibly be reactivated and what are the specific biophysical, biochemical and cellular processes involved in this reactivation (Tanaka and Reddien, 2011). *Hydra* is an organism that, even in adulthood, allows to study morphogenesis and *de novo* pattern formation due to its specific tissue dynamics and the presence of organizers, apical and basal, that generate morphogenetic factors that tightly regulate the 3D reconstruction occurring during regeneration but also budding (Galliot, 2012; Vogg et al., 2019b). *Hydra* is a cnidarian freshwater polyp of about one cm long organized around a single oral-aboral axis. The apical extremity (also named “head”) is centered around the mouth (the unique opening of the animal) and surrounded by a ring of tentacles, while the basal extremity is a basal disc also named foot that can attach to substrates. The central region of the animal, named body column, is basically a gastric tube that connects the apical region to the basal one at the aboral side. All along its body, the animal is composed of two myoepithelial layers known as the epidermis and gastrodermis, which correspond to the inner and outer layers respectively. The animal is populated by a dozen of distinct cell types that derive from three stem cell populations, epithelial epidermal, epithelial gastrodermal and interstitial, which constantly self-renew in the body column to maintain *Hydra* homeostasis (Vogg et al., 2021a).

Hydra is known for its exceptional regenerative capacities, capable to regenerate any missing part of its body, such as a new fully functional head in three to four days after mid-gastric bisection. This developmental process relies on the activation of an apical organizer in the regenerating tip (also named head organizer) whose activity relies on two main regulators : *Wnt3*, which acts as an activator, is required to maintain apical differentiation and initiate apical regeneration (Hobmayer et al., 2000; Lengfeld et al., 2009; Nakamura et al., 2011), and the transcription factor *Sp5*, which in a negative feedback loop, restricts the activity of the activator, thus considered as a key inhibitor of the apical organizer (Vogg et al., 2019a). *Wnt3* is predominantly expressed in the gastrodermal epithelial cells of the apical region, specifically in the tip of the hypostome, the most apical region of the animal where the apical organizer is located (Lengfeld et al., 2009).

In intact animals, *HySp5* is predominantly expressed apically, in both the hypostome and the tentacle ring but not at the tip where *Wnt3* expression is maximal, and at a lower level along the body column. *HySp5* is expressed in the epithelial cells, at higher levels in the gastrodermis than in the epidermis (**Figure 1A**). After mid-gastric bisection, *Sp5* and *Wnt3* are specifically up-regulated in the apical-regenerating tips, within two to three hours for *Wnt3*, after eight

hours for *Sp5*, and they remain expressed at high levels throughout the entire regenerative process. Knocking down *Sp5* shows that *Sp5* prevents ectopic head formation along the body column in homeostatic conditions and restricts apical regeneration after bisection.

Three distinct experimental approaches bring evidence that the body column can acquire the properties of an apical organizer: (i) the pharmacological activation of Wnt/ β -catenin signaling by the drug alsterpaullone (ALP) that leads to the ectopic expression of *Wnt3* along the body column and the rapid formation of ectopic tentacles (Broun et al., 2005; Gee et al., 2010); (ii) the exposure to the HyWnt3 or human Wnt3 recombinant protein, which improves head regeneration (Chera et al., 2009; Lengfeld et al., 2009); (iii) the silencing of *Sp5* that triggers a multiheaded phenotype in both homeostatic and regenerating animals (Vogg et al., 2019a). Hence, the crosstalk between *Wnt3* and *Sp5* plays a critical role in the maintenance of apical patterning in *Hydra* and in the apical developmental processes as observed during regeneration and budding. However, the precise way this crosstalk is regulated in each tissue layer remains unclear. With this study we wanted to uncover whether *HySp5* auto-regulation plays a role *in vivo* (**Figure 1A**).

In *Hydra*, the *Wnt3* promoter contains an auto-regulatory element that positively activates *Wnt3* (Nakamura et al., 2011); similarly, data obtained in mammalian cells transiently co-expressing HySp5 together with a reporter construct driven by *HySp5* promoter, suggest a positive *Sp5* auto-regulation (Vogg et al., 2019a). *Hydra Sp5* is a downstream target of the evolutionarily conserved Wnt/ β -catenin signaling pathway, as is *Sp5* in other vertebrate organisms such as zebrafish (Weidinger et al., 2005), *Xenopus* (Park et al., 2013) and humans (Takahashi et al., 2005). Regarding the regulation, in human pluripotent stem cells (hPSCs) *Sp5* down-regulates genes activated by Wnt/ β -catenin signaling including *SP5* (Huggins et al., 2017), whereas in mouse embryonic stem cells (mESCs), *Sp5* selectively activates Wnt/ β -catenin target genes (Kennedy et al., 2016), suggesting that *Sp5* may act as a transcriptional activator or a transcriptional repressor depending on the context.

To test the homeostatic as well as developmental regulation of *Sp5* in each epithelial layer, we produced transgenic lines that constitutively express the tandem reporter construct either in the epidermis or in the gastrodermis a tandem reporter construct where the *Hydra actin* promoter drives mCherry expression and the *Hydra Sp5* promoter eGFP expression. We monitored GFP fluorescence and *GFP*, *Sp5*, *Wnt3* expression in intact, budding and regenerating transgenic animals, after either pharmacological activation of Wnt/ β -catenin signaling, or *b-catenin* silencing, or *Sp5* silencing. The results show distinct spatial regulations of *HySp5* expression in the epidermis and the gastrodermis as well as a negative auto-regulation of the *Hydra* head inhibitor *Sp5*.

RESULTS

GFP fluorescence in *HySp5-3169:GFP* epidermal and *HySp5-3169:GFP* gastrodermal transgenic animals mimics endogenous spatial *Sp5* expression

To monitor the regulation of *Sp5* expression, we designed a tandem reporter construct where 3169 bp of the *HySp5* promoter drive eGFP expression and 1388 bp of the *HyActin* promoter drive mCherry expression, used here as a gene ubiquitously expressed (**Figure 1B**). After injecting the reporter construct into *Hv_AEP* one or two cell stage embryos, two *Sp5* reporter lines were obtained: *HySp5-3169:GFP_ep* and *HySp5-3169:GFP_ga* and clonal populations were amplified. We first performed a q-PCR analysis of *Sp5*, *GFP* and *Wnt3* expression in the apical, central body column and basal regions to compare endogenous *Sp5* expression and *GFP* expression in each of the two transgenic lines (**Figure 1C, 1D**). This analysis confirmed the expected *Sp5* and *Wnt3* expression profiles in both transgenic lines, exclusively apical for *Wnt3*, with highest levels apically for *Sp5*, and showed that *GFP* is also expressed at highest levels apically in *HySp5-3169:GFP_ep* animals (**Figure 1C**) but at similar levels apically and along the body column in *HySp5-3169:GFP_ga* animals (**Figure 1D**). This result indicates that *Sp5* expression driven by the 3169 bp sequences of the *Sp5* promoter is strikingly different between the epidermal and gastrodermal layers both in the apical and the body column regions.

In *HySp5-3169:GFP_ep* animals, eGFP expression recorded in live animals through fluorescence (**Figure 1E**) or in fixed animals after immunodetection (**Figure 1G**) is restricted to the epithelial cells of the epidermal layer, present over the whole hypostome, the proximal part of the tentacles, the tentacle ring with a rather sharp boundary below the tentacle ring. In *HySp5-3169:GFP_ga* animals, eGFP expression recorded in live animals through fluorescence (**Figure 1F**) or in fixed animals after immunodetection (**Figure 1H**) is restricted to the epithelial cells of the gastrodermal layer, showing a broad domain of expression that extends from the apical region throughout the body column. However, the tip of the hypostome is free of GFP fluorescence and GFP protein (see enlarged head in Figure 1F, arrows in Figure 1H), an area where *Wnt3* expression is maximal and endogenous *Sp5* expression minimal (Nakamura et al., 2011; Vogg et al., 2019a). This analysis of GFP expression shows that 3169 bp sequences of the *Sp5* promoter are sufficient to recapitulate the endogenous *Sp5* expression pattern previously identified in the apical region and along the body column (Vogg et al., 2019a).

From the eGFP and mCherry fluorescence profiles obtained from live or fixed animals, we produced a relative GFP intensity profile for each animal that corresponds to the eGFP/mCherry ratio at all points along the body axis (**Figure 1E, 1F, FigS1**). By grouping the relative GFP intensity profiles of 10 animals, we concluded that GFP fluorescence in live

HySp5-3169:GFP_ep animals is graded apical-to-basal, from 100% to 70% body length, then maintained at low levels between positions 70% to 10% (**Figure 1I, FigS1B**). By contrast, the same analyses performed in *HySp5-3169:GFP_ga* animals, shows that GFP levels are low at the tip (position 100%-90%), reach a plateau from position 90% up to 40% body-length, then declines towards the basal extremity (**Figure 1J, FigS1D**). The profiles obtained after immunodetection of GFP and mCherry in the two *HySp5-3169:GFP* transgenic strains are highly similar to the patterns obtained by analysis of GFP fluorescence (**Figure 1K, 1L**). In summary, the analysis of the level of GFP transcripts, GFP protein and GFP fluorescence identify distinct spatial patterns along the body axis in the epidermis and the gastrodermis, suggesting that *Sp5* regulation is not identical in these two layers.

Developmental regulation of *Sp5* in the epidermal and gastrodermal layers

During budding, GFP fluorescence is detected throughout the whole process in *HySp5-3169:GFP_ep* and *HySp5-3169:GFP_ga* animals (**Figure 2A, 2B, 2C**). GFP fluorescence is first detected on the parental polyp as a patch in the epidermal layer (stage-1) as well as in the budding zone with well-defined boundaries (see stages 3 and 4 in **Figure 2A, 2C**). In the growing bud, GFP fluorescence is ubiquitously expressed in both layers, becoming from stage 6 restricted to the presumptive head only in the epidermal layer. At stages 9 and 10, the bud is mature, ready to detach, and spatial patterns of epidermal and gastrodermal GFP fluorescences correspond to those observed in adult polyps.

During apical regeneration after mid-gastric bisection, a strong GFP fluorescence can be detected at 8 hours post-amputation (hpa), similar in both layers, broadly distributed along the lower half except in the peduncle region, subsequently maintained during the first 24 hours (**Figure 2D, 2E, FigS2**). Subsequently, when tentacle rudiments appear, the epidermal GFP fluorescence becomes restricted to the apical region while the gastrodermal one remains broadly distributed, and within three days, the adult homeostatic patterns are reestablished. During basal regeneration, no GFP fluorescence is observed in the upper regenerating halves of *HySp5-3169:GFP_ep* animals except the original GFP fluorescence of the apical region (**Figure 2D, FigS2A**). In *HySp5-3169:GFP_ga* animals, the GFP fluorescence is broadly distributed along the body axis, becoming excluded from the basal disc when it gets differentiated after 24 hpa (**Figure 2E, FigS2B**).

The analysis of *GFP* transcripts by *WMISH* reveals that in *HySp5-3169:GFP_ep* animals, *GFP* expression is low in apical-regenerating tips at 8 hpa, progressively increased at 12 and 24 hpa (**FigS3A**). At 48 hpa, tentacle rudiments that emerge do not express *GFP* whereas the apical region strongly expresses *GFP*; at 72 hpa, the epidermal *GFP* pattern is typical, with maximal expression at the root of tentacles. In *HySp5-3169:GFP_ga* animals, *GFP* is first detected immediately after bisection, possibly artefactual in the injured tissues, then at high

levels in a broad domain encompassing the apical-regenerating tips at 8, 12 and 24 hpa, with in some but not all animals some expression in lower regions of the body column. At 48 hpa, while tentacle rudiments emerge, *GFP* expression becomes restricted to the apical area surrounding the tentacles, leaving the tentacles and the tip of the future hypostome free of expression. Most animals also show some *GFP* expression along the body column, including in the peduncle area. At 72 hpa, *GFP* expression is predominantly apical at the level of the tentacle ring but absent from the tentacles and the hypostome, with some low level of expression in the peduncle region. The analysis of the gastrodermal *GFP* pattern during apical regeneration identifies modulations of the *GFP* pattern along the gastrodermis, some animals showing stripes of high expression levels and others exhibiting a diffuse expression throughout the animal.

During basal regeneration, *GFP WMISH* reveals that *GFP* expression is excluded from the basal-regenerating half in *HySp5-3169:GFP_ep* animals at all time-points (**FigS3B**). At 48 hpa, most animals have differentiated a new basal disc and *GFP* expression is slightly up-regulated in the peduncle region. In *HySp5-3169:GFP_ga* animals, the *GFP* up-regulation observed immediately after bisection in the basal-regenerating tip might be artefactual, linked to injury as in apical-regenerating tips artefactual. At 8 hpa, *GFP* expression is quite strong in the body column, in continuity with the apical domain. *GFP* is also expressed in the regenerating-tips, in continuity or not with the body column domain. At 12 hpa, three domains of high levels of *GFP* expression can be identified in most animals: the apical region, the central body column domain and the regenerating tips; at 24 hpa, the central body column domain and the regenerating tip domain appear weaker. At 48 and 72 hpa, the basal disc has formed in most animals, free of *GFP*, whereas the peduncle domain is visible, which in half of the animals extends towards the apical extremity. In summary, the epidermal and gastrodermal *HySp5-3169:GFP* transgenic lines provide the means to deduce the layer-specific temporal regulations of *Sp5* linked to regeneration. As deduced from the observed layer-specific *GFP* modulations, *Sp5* is up-regulated at an immediate-early phase in the gastrodermis and at an early-late phase in the epidermis during apical regeneration; while during basal regeneration, *Sp5* is not expressed in the epidermis except at the apical extremity, and is strongly expressed in the regenerating tip and highly modulated in the gastrodermis of the whole regenerating half.

Layer-specific modulations of *Sp5* expression upon pharmacological activation of Wnt/ β -catenin signaling

In *H. vulgaris*, the pharmacological activation of Wnt/ β -catenin signaling by the GSK3 β inhibitor Alsterpaullone (ALP), causes the formation of ectopic tentacles along the body column after a two-day treatment (Broun et al., 2005). In *Hv_AEP* animals, a two-day ALP treatment does not lead to the formation of ectopic tentacles along the body column (**Figure 3A, 3B, FigS4**), which

is not surprising as this strain is known to be less sensitive to drug treatments (Suknovic et al., 2021). However, when ALP treatment is prolonged for at least four days, morphogenetic changes take place such as the size reduction of the original tentacles together with the enlargement of the original hypostome region that appears “swollen”, the progressive transformation of the basal extremity already visible after a four-day treatment. After a 14-day treatment, the tentacle ring is duplicated, and the peduncle and basal regions become dramatically thinned, the two extremities expressing *Wnt3* at high levels while ectopic tentacles along the body column are not visible (**Figure 3C**). The monitoring of GFP fluorescence in *HySp5-3169:GFP_ep*, *HySp5-3169:GFP_ga* animals shows a global up-regulation in the body column after a two-day and four-day ALP exposure. A seven-day treatment results in a complete shift of GFP fluorescence to the basal region in *HySp5-3169:GFP-ga* animals while in *HySp5-3169:GFP-ep* animals, GFP fluorescence is only visualized at the apical and basal extremities (**Figure 3A**).

To further investigate how *Sp5* expression is regulated in this context, we analyzed the parallel modulations of *GFP* and *Wnt3*, or *Sp5* and *Wnt3* expression in wt *Hv_AEP*, *HySp5-3169:GFP_ep*, and *HySp5-3169:GFP_ga* animals exposed to a two- or four-day ALP treatment (**Figure 3B**, **FigS4**, **FigS5**). Given the feedback regulatory loop between *Sp5* and *Wnt3* expression, we also included in this analysis animals from the two transgenic lines *HyWnt3-2149:GFP_ep* and *HyWnt3-2149:GFP_ga* where GFP expression is driven by 2149 bp of the *Wnt3* promoter (Nakamura et al., 2011; Vogg et al., 2019a). The analysis of *GFP* expression in these four transgenic lines helps identify the layer-specific regulations of *Sp5* (**FigS5**) and *Wnt3* (**FigS6**) respectively.

After a two-day ALP treatment, animals exhibit an expansion of the *Wnt3* apical domain with large spots at the level of the tentacle ring, some dots of expression in the upper and lower body column, which are well visible in *HyWnt3-2149:GFP-ep* animals. Some animals also show some *Wnt3* expression at the basal extremity. By contrast, *Sp5* expression, normally at highest levels at the base of the hypostome and in the tentacle ring, vanishes from these two locations and seems shifted towards the upper body column where it forms a belt of strong expression detected in both the epidermis and the gastrodermis. In parallel, in the epidermis *Sp5* also forms a second belt of high expression close to the basal extremity and in some animals, small circular figures along the body column, which likely correspond to regions where ectopic tentacles could emerge (**Figure 3B**, **FigS4A**, **FigS5**). In *HySp5-3169:GFP_ga* animals *GFP* expression is up-regulated along the body column, reflecting the ALP-dependent up-regulation of the diffuse gastrodermal *Sp5* pattern. After a four-day ALP treatment, the endogenous *Wnt3* is expressed in a dotted pattern all along the body column (**Figure 3B**, **FigS4**); in *HyWnt3-2149:GFP-ep* and *HyWnt3-2149:GFP-ga* animals this dotted pattern is well visible together with a diffuse up-regulation of *GFP* (**Figure 3B**, **FigS6**). As observed in

Hv_Basel animals, this *Wnt3* dotted pattern in the central body column is transient, no longer observed after a 14-day ALP treatment (**Figure 3C**). In parallel to this *Wnt3* up-regulation, we noted in all lines a global down-regulation of *Sp5* after a 4-day ALP treatment when compared to the 2d-ALP pattern (**Figure 3B, FigS5**).

In summary, *Wnt3* and *Sp5* show quite distinct regulations in response to ALP-dependent activation of Wnt/ β -catenin signaling: firstly, an expansion of the *Wnt3* apical expression domain that excludes *Sp5* expression from this region while *Sp5* is transiently up-regulated in the body column, and secondly, a *Wnt3* dotted pattern along the body column accompanied by a global down-regulation of *Sp5* expression. Even after prolonged ALP treatment, wt and transgenic *Hv_AEP* animals do not develop the previously described phenotype of ectopic tentacle formation but exhibit a shift of apical markers to the basal region.

Modulations of epidermal *GFP* expression upon β -catenin (RNAi)

Altering Wnt/ β -catenin signaling by knocking-down β -catenin triggers the formation of “bumps” along the body column, e-g lateral structures looking like buds but never form a head or differentiate tentacles (Vogg et al., 2019a) although these bumps express *Sp5* in *Hv_Basel* (**FigS7**). Here, we knocked-down β -catenin expression by submitting *HySp5-3169:GFP_ep* transgenic animals to repeated electroporations (EP) of scramble and β -catenin dsRNAs. To monitor GFP expression, animals were pictured live at indicated time-points after EP2 and EP3, and RNAs were prepared from the apical (100% - 80% body length) and body column (80%-0% body length) at same time points (**Figure 4A**). Concerning the live picturing of animals, we first noted in control animals a stable epidermal GFP pattern in the apical region as previously described (**Figure 4A, FigS8A**). In β -catenin (RNAi) animals, we noted two days post-EP2 and three days post-EP3 a loss of GFP fluorescence in large parts of the apical region and along the body column including the bump structures that never show any GFP fluorescence. Unexpectedly, we also detected two days post-EP2 in half of the animals, areas along the body column where GFP fluorescence is strongly up-regulated (**Figure 4A, FigS8A**).

The anti-GFP immunodetection performed three days post-EP3 confirmed these findings: the loss of epidermal GFP expression in a large part of the apical region in most animals, the lack of GFP expression in bump structures, the localized epidermal GFP ectopic expression along the body column of some animals (**Figure 4B, FigS8B**). The qPCR analysis detects a modest decrease in the levels of β -catenin transcripts in the apical region after EP1, EP2 and EP3 after β -catenin (RNAi) and a two-fold reduction in the body column (**Figure 4C**). Concerning *GFP* expression, we observed an up-regulation, about two-fold, in the body column of animals electroporated with scramble siRNAs, supporting the hypothesis that the stress of the electroporation suffices to activate the *Sp5* regulatory sequences. This *GFP* up-regulation is no longer observed in animals exposed to β -catenin (RNAi), likely as a result of the global *GFP*

down-regulation along the body column even though some areas overexpress GFP. In parallel, we found endogenous *Sp5* expression slightly reduced in the apical region and the body column, a result that was expected since *Sp5* is supposed to be a direct downstream target of Wnt/ β -catenin signaling (Vogg et al., 2019a).

From the observed modulations of GFP fluorescence and *GFP* expression in response to β -catenin (RNAi), we can draw two conclusions, (i) the *HySp5-3169:GFP* reporter construct contains the necessary *Hydra Sp5* regulatory sequences to respond positively to Wnt/ β -catenin signaling, (ii) the localized areas of GFP overexpression along the body column suggest a negative auto-regulation of *Sp5*, as β -catenin (RNAi) leads to *Sp5* downregulation. The up-regulation of *HySp5-3169:GFP* expression in β -catenin (RNAi) animals might result from the lower Wnt3/ β -catenin activity, a positive regulator of *Sp5* expression, and the subsequent down-regulation of *Sp5* levels and *Sp5* activity, including the transcriptional repressor activity on *Sp5* promoter.

Evidence for a negative regulation of *Sp5* on its own promoter.

To further evidence whether *Sp5* negatively regulates its own expression in the epidermis and/or the gastrodermis, we silenced *Sp5* in *HySp5-3169:GFP_ep* and *HySp5-3169:GFP_ga* animals and monitored the changes in GFP fluorescence *in vivo*, as well as the changes in *GFP*, *Wnt3* and *Sp5* expression 8, 16 and 24 hours post-EP1 (h-pEP1) and post-EP2 (h-pEP2, **Figure 5A**). In *HySp5-3169:GFP_ep* in *Sp5* (RNAi) animals, we noted a marked increase in GFP fluorescence along the body column already 16 h-pEP1, maintained high at subsequent time-points (**FigS9A**). Soon after electroporation (8h-pEP1, 8h-pEP2), some weak GFP fluorescence is visible in the epidermal layer of the upper body column of some control and *Sp5*(RNAi) animals, possibly linked to the stress of the electroporation.

GFP expression detected by WMISH in *HySp5-3169:GFP_ep* animals is moderately increased along the body column at 8 h-pEP1, then enhanced at 16 and 24 h-pEP1 (**Figure 5B, FigS10**). Eight hours after EP2, epidermal *GFP* expression along the body column is rather low, up-regulated again at 16 and 24 h-pEP2. The quantification by qPCR of epidermal *GFP* transcripts in the apical region and the body column confirms the up-regulation in *GFP* expression in these two regions after EP1 and EP2 (**Figure 5C, FigS9B**). The quantification of *Sp5* and *Wnt3* transcript levels does not reveal any significant modulations except an increase in *Wnt3* transcripts after EP2, similarly visible in the body column samples of scramble and *Sp5* (RNAi) animals, therefore possibly linked to a stress response.

In *HySp5-3169:GFP_ga* in *Sp5* (RNAi) animals, no notable increase in *GFP* expression can be detected in the body column, most likely because these animals constitutively express *GFP* in the gastrodermis (**Figure 5B**). However, after EP2 some animals show ectopic spots of GFP

fluorescence in the lowest body column (**Figure 5A, FigS11A**), these spots are also detected in the WMISH analysis (**Figure 5B, FigS12**). The q-PCR analysis does not detect any significant up-regulation of *GFP* or *Sp5* but shows the unspecific *Wnt3* up-regulation, particularly in the body column of scramble and *Sp5*(RNAi) animals (**Figure 5D, FigS11B**).

We also analyzed the GFP fluorescence at a later stage, two days after the second electroporation (2d-pEP2). We found the increase in GFP fluorescence still visible in the body column of *HySp5-3169:GFP_ep* animals while some GFP spots are visible in the tentacles of *HySp5-3169:GFP_ga* animals (**Figure 5E, FigS13**). Nevertheless, the analysis of the *GFP*, *Sp5* and *Wnt3* transcript levels in the apical region, the central body column and the basal region shows that in *HySp5-3169:GFP_ep* animals *GFP* expression is significantly lower in the body column and basal region two days post-EP2 while the expression of *β-catenin* is up-regulated in the body column and that of *Sp5* and *Wnt3* are not significantly modified (**Figure 5F**). In *HySp5-3169:GFP_ga* animals, none of these genes show a significant modulation upon *Sp5* (RNAi), except an increase in *β-catenin* expression in the body column of *Sp5* (RNAi) animals (**Figure 5G**).

These results indicate that knocking-down *Sp5* induces a 24 hour-long up-regulation of *Sp5-3169:GFP* expression along the epidermis of the body column and in some restricted areas of the gastrodermis, while an up-regulation of *β-catenin* transcripts can be detected 24 hours later in the body column and the basal region. Concomitantly, between 24 and 48 hours pEP2, the *GFP* up-regulation induced by *Sp5* (RNAi) ceases and *GFP* transcript levels go back to basal expression levels in the gastrodermis or even lower in the epidermis, even though ectopic GFP fluorescence is still visible in the epidermis, in line with the long life of GFP protein (Corish and Tyler-Smith, 1999).

Identification of *Sp5*-binding sites in *Hydra Sp5* promoter sequences

The *Hydra Sp5* transcription factor belongs to the Sp/KLF family, a class of DNA-binding proteins that bind GC-rich boxes or GT/CACC elements through their three zinc finger domains (Harrison et al., 2000; Kennedy et al., 2016). Among the 2'966 bp of the *Sp5* promoter, we previously identified by ChIP-seq analysis performed with extracts from HEK293T cells five *Sp5* binding sites (*Sp5*-BS) and five TCF binding sites (TCF-BS), clustered in two adjacent regions PPA and PPB in the vicinity of the *Sp5* transcriptional start site (**Figure 6A, 6B**) (Vogg et al., 2019a). To test whether these putative *Sp5*-BS are functional in *Hydra*, we designed double-stranded oligonucleotides (ds-oligos) encompassing these sequences to perform EMSA. When *Hydra* NEs were incubated with biotin-labeled *Sp5* ds-oligos, we noticed a mobility shift, while in competition conditions, i.e. in the presence of a 200x excess of unlabeled oligonucleotides, the shift was no longer visible (**Figure 6C**). Mutation of the *Sp5*-BS of the PPA region did not cancel the shift, but rather accentuated it; in contrast, when the *Sp5*-BS of

the PPB region were mutated, the shift virtually disappeared. This result indicates that Sp5 likely binds the presumptive Sp5-BS of regions PPA and PPB, the latter with higher specificity. Next, we produced two anti *Hydra* Sp5 antibodies with the aim to reproduce with *Hydra* extracts the ChIP-seq analysis of Sp5-BS previously performed with extracts from mammalian cells expressing HySp5 (Vogg et al., 2019a). We raised two antibodies against HySp5, one monoclonal and one polyclonal, designed to target regions that do not overlap with the evolutionarily-conserved Sp5 domains previously identified, i.e. the Sp box, the Buttonhead (Btd) box and the DNA-binding domain (**Figure 6D**, **FigS14A**). The two Sp5 antibodies specifically recognize the Sp5 protein either synthesized as a fragment (24 kDa) to raise the Sp5 monoclonal antibody, or produced *in vitro* with the TNT reticulocyte transcription-coupled-translation system, or produced in transfected mammalian HEK293T cells. The monoclonal anti-Sp5 specifically detects the Sp5 protein contained in *Hv_AEP2* extracts, at higher levels in the apical region than in the body column as expected (**Figure 6E**, **FigS14B-C**). Surprisingly, the polyclonal anti-Sp5 antibody recognizes a band at the appropriate size but exclusively in extracts prepared from the lower body column and not from the apical region (a result obtained in three independent experiments) (**FigS14C**). As a control experiment, we produced the *Hydra* Sp4 protein in TNT and tested the polyclonal α -Sp5 antibody that did not detect any band. These results suggests that the polyclonal α -Sp5 antibody detects with a higher affinity a Sp/KLF protein predominantly expressed in the basal half of *Hydra*.

Next, we decided to use both the monoclonal and the polyclonal α -Sp5 antibodies for ChIP-qPCR analysis. We first used *Hv_magnipapillata* extracts to assay the amplification of 15 regions along the 3'169 bp of the Sp5 promoter and 5'UTR sequences after ChIP (**Figure 6F**, **FigS14D**). Among these 15 regions, we found only two regions specifically enriched with one or the other antibody but not by the pre-immune serum, the regions PP4 and PP5, similarly to the results obtained with extracts from mammalian cells expressing HySp5 (Vogg et al., 2019a). Both regions contain three Sp5-BS; Sp5-BS1, Sp5-BS2, Sp5-BS3 for PP4, and Sp5-BS3, Sp5-BS4, Sp5-BS5 for PP5 (**Figure 6A**). A similar enrichment in regions PP4 and PP5 was observed when extracts from *Hv_AEP2* animals were used for the ChIP-qPCR (**Figure 6G**, **FigS14D**). These results confirm that in *Hydra*, two locations within the proximal *Sp5* promoter can bind the *Sp5* transcription factor, thus possibly involved in *Sp5* autoregulation. Further experiments testing this region *in vivo* when it is either deleted or mutated should clarify this hypothesis.

DISCUSSION

Technical considerations might impact levels of gene silencing or transcript detection between epidermis and gastrodermis

The observed differences in *Sp5* regulation between the epidermal and gastrodermal layers were confirmed by different methods applied to the transgenic *HySp5-3961:GFP* strains (*in vivo* fluorescence, immunodetection, qPCR, WMISH) and we consider the obtained results as robust and reliable. Nevertheless, some technical limitations might interfere with these results. First of all, the gene silencing obtained by electroporation of siRNAs is not homogenous along the surface of the animal given the short exposure to a polarized current. For this reason, electroporations are repeated two to three times. Second, the gastrodermis, which is the inner layer of the animal, is more difficult to penetrate upon electroporation and consequently, gene silencing is likely more limited in this layer. This problem was solved when RNA interference was obtained by feeding the animals with dsRNAs (Chera et al., 2006); unfortunately, the efficiency of this approach dramatically varies with *Hydra* strains and RNAi by feeding is poorly efficient in *Hv_AEP2*.

Similarly, when considering the analysis of gene expression on whole mount animals, transcripts expressed in the gastrodermis are more difficult to detect than transcripts expressed in the epidermis. Moreover, in experiments where we detected transcripts from two distinct genes, we combined two methods to detect the riboprobes, one of which is NBT/BCIP for the DIG-labeled riboprobe, and the other is Fast Red for the fluorescein-labeled riboprobes. The former is far more sensitive than the later, but at the same time, the NBT/BCIP detection is less efficient when tissues are treated for Fast Red. Consequently, the co-detection of two genes is highly informative when each expression pattern was analyzed independently and when variations within a given context (such as different time-points after gene silencing or pharmacological treatment) are analyzed. These two conditions were fulfilled when we analyzed the expression of *Wnt3* and *Sp5* or *Wnt3* and *GFP* after ALP treatment.

Wnt3/β-catenin signaling and *Sp5* crosstalk in the homeostatic and developmental apical organizers

In intact animals, Lengfeld et al. (2009) and Nakamura et al. (2011) have shown that *Wnt3* is predominantly expressed in gastrodermal epithelial cells at the tip of the hypostome, while cells from this area do not express endogenous *Sp5* (Vogg et al., 2019a). The generation of the gastrodermal and epidermal *HyAct-1388:mCherry_HySp5-3169:eGFP* transgenic lines opened the possibility to produce a comparative analysis of the *in vivo* regulation of *HySp5* in each animal layer. In intact transgenic animals, GFP fluorescence and *GFP* expression are primarily detected in the apical region, although with noticeable differences between the two layers as in the epidermal line, the whole hypostome does express GFP, while in the

gastrodermal one, the tip of the hypostome is free of GFP, as expected from the fact that *Sp5* transcripts are hardly detected in this area (Vogg et al., 2019) (**Figure 7A**). This result indicates that, in homeostatic context, *Sp5* regulatory sequences are not activated in gastrodermal epithelial cells where *Wnt3* expression is maximal. We also recorded marked differences along the body column, with *GFP* expression and GFP fluorescence restricted to the apical region in the epidermis, while similarly distributed along the body column down to the peduncle in the gastrodermis (**Figure 7A**).

During apical regeneration, GFP fluorescence in *HySp5-3169:GFP_ep* transgenic animals is detected in a broad apical domain during the first three days after mid-gastric bisection, although *GFP* expression is rather low in the epidermis at early time-points. *GFP* expression is up-regulated from 24 hpa and gets restricted to the newly formed apex at 72 hpa, while the GFP fluorescence pattern does not get restricted before 5 dpa, reflecting the high stability of GFP protein when compared to *Sp5* and *GFP* regulation. During budding, GFP fluorescence in the epidermis highlights the budding belt on the parental polyp and is visible in the whole growing bud up to stage 5, becoming progressively restricted to the apical region from stage 6. In *HySp5-3169:GFP_ga* animals undergoing budding or regeneration, *GFP* expression is massive in apical regenerating tips, initially present in the whole area corresponding to the presumptive apical region, but at late stages excluded from the tip of the forming hypostome (from 48 hpa in apical regeneration, or from stage 6 of budding). The immediate and early spatio-temporal pattern of gastrodermal *GFP* expression and GFP fluorescence during regeneration suggests a critical role of these gastrodermal epithelial cells in the regenerative process, which might be considered as blastema cells that undergo cycling once before head formation (Buzgariu et al., 2018).

It is important to note that a single word is commonly used in the field for the head organizer, which actually covers two distinct structures with distinct biological activities, one located at the apex of an intact animal that carries a function related to the maintenance of patterning (homeostatic apical organizer), the second located in the presumptive apical region of a bud or a regenerating tip, which carries a function related to the reactivation of the patterning process (developmental apical organizer). The results obtained here show that this distinction is supported by the comparative analysis of the *Sp5* and *Wnt3* regulation. In contrast to the homeostatic context where the *Wnt3* and *Sp5* domains at the hypostome tip do not overlap, at least in the gastrodermal layer, the *Wnt3* and *Sp5* gastrodermal domains do overlap during at least the first 24 hours post-amputation (the early and early-late phases of regeneration), when the gastric tissue acquires the properties of an apical organizer capable of shaping a new head. Given the key role played by the gastrodermis in the formation and maintenance of the apical organizer, these results suggest that the cross-talk between *Wnt3*/b-catenin signaling and *Sp5* is distinct in the homeostatic apical organizer and the developmental apical organizer.

ALP exposures highlight the plasticity of the regulation between the activator and inhibitor components of the apical organizer

Surprisingly, in *Hv_AEP2* animals exposed to alsterpaullone (ALP), we did not observe the typical ALP-induced phenotype recorded in *Hv_Basel* or *Hm105*, i.e. multiple ectopic tentacles along the body column. Instead, we noted after a four-day treatment, a modification of the apical extremity with an enlargement of the hypostome together with the shortening of the tentacles, while the basal region gets transformed with the basal disc rapidly losing its typical anatomy and the peduncle area undergoing thinning. After prolonged treatments (7 or 14 days), ectopic tentacles were still not visible along the body column but additional tentacle rings develop at the apical extremity. This difference in ALP-induced phenotypes between *Hv_Basel* or *Hm105* and *Hv_AEP2* suggest that the activator (Wnt/ β -catenin signaling) and inhibitor (Sp5 activity) activities of the apical organizer are differentially distributed along the body axis, resulting in a balance differentially regulated in these strains.

The comparative analysis of *Wnt3*, *Sp5* and *GFP* expression in ALP-treated animals, shows the good correlation between the endogenous *Sp5* expression and the *Sp5*-driven *GFP* expression, indicating that the 2'966 bp-long upstream *Sp5* sequences suffice to respond to Wnt/ β -catenin signaling. After an expansion of the *Wnt3* domain in the tentacle ring, in the tentacles and along the body column, a typical *Wnt3* dotted expression pattern can be detected along the body column in both layers after a four-day exposure (**Figure 7A**). Gastrodermal *Sp5*, which is initially broadly up-regulated along the body column, is subsequently excluded from the apical region where *Wnt3* expression is high, and reduced along the body column. We suspect that along the body column of *Hv_AEP2* animals the balance between the global upregulation of *Sp5* and the ectopic *Wnt3* expression allows the formation of regular dots after four days, but in contrast to *Hv_Basel* or *Hm105* strains, these dots never support the ectopic formation of tentacles. In the basal region where *Sp5* transiently forms a belt of epidermal expression after a 2-day ALP treatment, *Wnt3* is expressed at high levels in both layers, supporting the observed morphological transformation of the aboral pole, which however does not differentiate apical structures.

The distinct ALP-induced phenotypes in different *Hv* strains highlights the plasticity of the regulation between the activator and inhibitor components of the apical organizer. Among these components, it would be of interest to monitor *Zic4* expression, a *Sp5* target gene involved in tentacle formation and tentacle maintenance (Vogg et al., 2021b). Two types of approaches are needed to better understand the regulation of the cross-talk between Wnt3/ β -catenin signaling and *Sp5* activity, firstly experiments that would identify the other partners of this crosstalk, secondly experiments that would precisely quantify the drug-induced modulations of activity of each component.

Aberrant growth and paradoxal *Sp5* up-regulation upon β -catenin silencing

When Wnt/ β -catenin signaling is altered as after knocking-down β -catenin by RNAi, *Sp5*-driven GFP expression is down-regulated as revealed by the decrease in GFP fluorescence in the apical region but also by qPCR in the apical and body column regions, whereas the levels of endogenous *Sp5* expression are not modified. The loss of GFP fluorescence in the apical region is rather sustained, as not restored three days after the third exposure to β -catenin siRNAs. The phenotype induced by β -catenin (RNAi) is characterized by “bump” structures that form along the body axis but, contrary to buds, do not differentiate apical or basal extremities (Vogg et al., 2019a). After three electroporations, such bumps are observed in all *Hv_Basel* animals and in half of *Hv_AEP2* animals.

Preliminary experiments had shown that in these bumps, β -catenin protein is mostly nuclear, as if a β -catenin down-regulation would lead to a massive translocation of the stock of β -catenin protein available (Luiza Ghila, unpublished). We suspect that this sudden nuclear translocation of β -catenin leads to a transient transactivation of β -catenin target genes and to the fast growth of this aberrant growth zone along the body column. In agreement with this scenario, we found *Wnt3* but also *Sp5* expressed at high levels in these bump structures (Vogg et al., 2019a; this work). However, we never detected a bump structure with a high level of GFP fluorescence, at least in the *HySp5-3169:GFP_ep* transgenic animals, indicating that the *HySp5-3169:GFP* construct does not contain the necessary regulatory sequences, or that the observed *Sp5* up-regulation does not rely on a transcriptional mechanism.

By contrast, we noticed regions of high GFP fluorescence along the body column of *HySp5-3169:GFP_ep* β -catenin (RNAi) animals, in all animals showing the “bump” phenotype, always on the opposite side of the bump, as well as in some animals without bumps. One possible scenario would be that this localized up-regulation reflects a loss of negative autoregulation of *Sp5* on its own promoter, most likely transient, but still visible during several days given the high stability of the GFP protein. Indeed, regions of high *Sp5* expression facing the bump structures on β -catenin (RNAi) *Hv_Basel* animals were visible only in few animals. This hypothesis of a β -catenin (RNAi) induced release of *Sp5* negative autoregulation pushed us to test whether *Sp5* (RNAi) would also lead to some paradoxal *HySp5-3169:GFP* overexpression.

Sp5 (RNAi) supports the hypothesis of a negative *Sp5* auto-regulation

By knocking-down *Sp5* in the *HySp5-3169:GFP* transgenic lines, we were able to monitor *Sp5* regulation *in vivo* and identify an up-regulation of *Sp5*, as evidenced by the massive increase in GFP fluorescence along the body column of epidermal *HySp5-3169:eGFP* animals when compared to scramble (RNAi) control animals (**Figure 7B**). In gastrodermal *HySp5-3169:GFP*

animals, we could also detect some spots of ectopic GFP fluorescence in the peduncle region and in tentacles. The analysis of *GFP* expression confirmed this up-regulation in both *Sp5* transgenic lines, although more extensive in the epidermal transgenic line. This increased level in *GFP* expression was confirmed by qPCR, specifically at 16 hours after EP1 and EP2 in the body column (80%-0%), and we interpreted it as a release of the negative autoregulation played by *Sp5* on its own promoter. This release is only transient as *Sp5* as well as *GFP* expression returned to baseline by two days post-EP2. At this stage, GFP fluorescence is still enhanced over the body column, as expected given the long life of GFP protein. The higher upregulation of *GFP* in the body column when compared to the apical region is reasonable as the initial level of *Sp5* expression is significantly lower in the body column than in the apical region. As previously shown, *Sp5(RNAi)* in *Hv_Basel* animals easily triggers a multiheaded phenotype along the body column, in regenerating tips or in growing buds. But it does not affect the initial apical morphology, implying that gene regulations are highly robust in this area. We cannot rule out that the negative *Sp5* autoregulation is taking place in both layers, as modulations in GFP fluorescence are easier to visualize in the epidermis than in the gastrodermis. Also as discussed above, gene silencing upon siRNA electroporation is more efficient in the epidermis. However, the few GFP positive spots that are visible in the peduncle or in the tentacles support the hypothesis of a negative *Sp5* autoregulation in the gastrodermis. The hypothesis of a *Sp5* negative autoregulation is supported by the presence of clustered *Sp5* binding-sites in the proximal *Sp5* promoter. The two α -HySp5 antibodies that we developed allowed us to reproduce with *Hydra* extracts the ChIP-qPCR results we previously obtained with mammalian cell extracts (Vogg et al., 2019a). The enrichment we detected in two locations of the proximal *Sp5* promoter among 2'966 bp, indicates that *Sp5* can bind the *Sp5* promoter. The next step will be to perform a genomic ChIP-seq analysis with the *Sp5* antibodies in specific regions along the body axis, mainly the apical region and the body column, as well as in the apical-regenerating tips to identify in each context the *Sp5* target genes that contribute to Wnt3/ β -catenin inhibition and to characterize the conditions when the *Sp5* negative auto-regulation takes place.

In conclusion, the generation of *HySp5-3169:eGFP* epidermal and gastrodermal transgenic lines made possible the analysis of GFP expression after ALP treatment, β -catenin (RNAi) or *Sp5* (RNAi), which supports the possibility of an *in vivo* negative auto-regulation of *HySp5*. If confirmed, this would mean that in contrast to the *Hydra* head activator *Wnt3/b-catenin*, which autoregulates positively, the head inhibitor operates in a negative feedback loop.

MATERIALS AND METHODS

Animal culture and drug treatment: *Hydra vulgaris* from the Basel, magnipapillata or AEP2 strains (Schenkelaars et al., 2020) were cultured in Hydra Medium (HM: 1 mM NaCl, 1 mM CaCl₂, 0.1 mM KCl, 0.1 mM MgSO₄, 1 mM Tris pH 7.6) at 18°C and fed two to three times a week with freshly hatched *Artemia nauplii* (Sanders, Aqua Schwarz). For regeneration experiments, animals were starved for four days, then bisected at mid-gastric bisection. To activate Wnt/ β -catenin signaling, *Hv_Basel* or *Hv_AEP2* animals were starved for three or four days, then treated with 5 μ M Alsterpaullone (ALP, Sigma-Aldrich A4847) or 0.015% DMSO for the indicated periods of time, and subsequently washed with HM.

Mapping of the transcriptional start site (TSS): *Sp5* cDNAs sequences obtained by high throughput sequencing, available either on [HydrAtlas](#) (Wenger et al., 2019) for Cold Sensitive or Cold Resistant *H. oligactis* (*HoICS*, *HoICR*) and *Hv_AEP* strains, or on NCBI for the *Hm105* strain were aligned to the *Sp5 H. magnipapillata* genomic sequence (*Sp5_Hmgen*) with the [Muscle Align](#) software selecting a ClustalW output format. Next, the alignment was visualized with the [MView](#) tool (Madeira et al., 2022). Three transcriptional start sites were identified: TSS1 for *Hv_AEP Sp5* (position +1), TSS2 for *Hm105 Sp5* (position -149) and TSS3 for *H. oligactis Sp5* (position -192).

Production of the *Sp5* reporter construct: To produce the *HyAct-1388:mCherry_HySp5-3169:eGFP* construct, a block of 3'194 bp *HySp5* sequences were amplified from *Hm105* genomic DNA including 2'966 bp promoter sequences, 203 bp 5'UTR sequences and 25 bp coding sequences. The sequences of the *HySp5* promoter Forward and Reverse primers are given in Supplementary Table 1. The hoTG-HyWnt3FL-EGFP-HyAct:dsRED plasmid (kind gift from T. Holstein, Heidelberg) (Nakamura et al., 2011) was then digested with the EcoRV and AgeI enzymes to remove the HyWnt3FL promoter region and insert the *Sp5* 3'194 bp region. Next, dsRED sequence was replaced by the mCherry sequence by GenScript. The sequences of the final construct were verified by sequencing.

Generation of the transgenic lines: To generate the *Sp5* transgenic lines, gametogenesis was induced in *Hv_AEP2* strain by alternating the feeding rhythm from four times per week to once a week consequently. The *HyAct-1388:mCherry-HySp5-3169:eGFP* construct was injected into one- or two-cell stage *Hv_AEP2* embryos as described in (Wittlieb et al., 2006). Out of 330 injected eggs, 27 embryos hatched and 3/27 embryos exhibited GFP and mCherry fluorescence. The two lines analyzed in this work were obtained through clonal propagation from one epidermal-positive embryo for *HySp5-3169:GFP_ep* and one gastrodermal-positive embryo for *HySp5-3169:GFP_ga*, in which only a few cells were positive after hatching. By asexual reproduction of the original animal, i.e. budding, we obtained two transgenic animals

with a complete set of mCherry-eGFP positive epithelial cells, either epidermal or gastrodermal. The generation of the epidermal and gastrodermal *HyAct-1388:mCherry_HyWnt3-2149:eGFP* transgenic lines is described in (Vogg et al., 2019a).

RNA interference: For gene silencing experiments, we applied the procedure reported in (Vogg et al., 2019a). Briefly, four-day starved budless animals were selected from the *Hv_AEP2* culture, rinsed 3x in water, incubated for 45-60 minutes in Milli-Q water and electroporated with 4 μ M siRNAs, either targeting *Sp5* or *β -catenin* or scramble as negative control. For *Sp5* and *β -catenin* an equimolecular mixture of three siRNA was used (siRNA1+siRNA2+siRNA3, see sequences in Supplementary Table 1).

Quantitative RT-PCR: RNA extraction was performed using the E.Z.N.A.® Total RNA kit (Omega) and cDNA was synthesized with the qScript™ cDNA SuperMix (Quanta Biosciences). Quantitative RT-PCR was performed using the SYBR Select Master Mix for CFX and a Biorad CFX96™ Real-Time System. Primer sequences to amplify the *Sp5*, *Wnt3*, *β -catenin*, *GFP* and *TBP* genes are noted in Supplementary Table 1. When using distinct regions, 20 animals per condition were amputated either at 80% level to obtain the apical region (100%-80%) and the body column (80%-0%), or at 80% and 30% levels to obtain the apical region as above, the central body column (80%-30%) and the basal region (30%-0%). The different parts of the animals were transferred to RNA-later (Sigma-Aldrich R0901) immediately after amputation and kept at 4°C prior to RNA extraction.

Whole mount *In situ* hybridization (WMISH): The animals were allowed to relax in 2% urethane/HM for 1 minute, and fixed in 4% PFA prepared in HM for 4 hours at room temperature (RT). The animals were washed several times with MeOH before being stored in MeOH at -20°C. WMISH was performed as described in (Vogg et al., 2019a). For double WMISH, the *Wnt3* riboprobe was labeled with DIG (Sigma-Aldrich, Roche-11277073910) and the *Sp5* and *GFP* riboprobes labeled with fluorescein (Sigma-Aldrich, Roche-11685619910); the *Wnt3*-DIG riboprobe was co-incubated with either *Sp5*-FLUO or *GFP*-FLUO riboprobe during the hybridization step. At the development stage, the *Wnt3*-DIG riboprobe was first detected with NBT/BCIP (Sigma-Aldrich, Roche-11383213001) and the FLUO-labeled riboprobe subsequently detected with Fast Red. To stop NBT/BCIP reaction, samples were washed several times in NTMT, then incubated in glycine 100 mM, 0.1% Tween (pH 2.2) for 10 minutes and washed in Buffer I (1x MAB; 0.1% Tween). Next, samples were incubated in Buffer I containing 10% sheep serum (Buffer I-SS) for 30 min at RT, prolonged for 1 hour with fresh Buffer I-SS at 4°C. Incubation with anti-FLUO-AP antibody (1:4000, Roche-1142638910) was done at 4°C overnight. The next day, samples were briefly washed in Buffer I then in 0.1M Tris/HCl (pH 8.2) 3x10min. Samples were developed with Fast Red (SigmaFAST Fast Red TR/Naphtol AS-MX kit, F4648). To stop the reaction, samples were washed several times in

0.1M Tris/HCl (pH 8.2) and fixed in 3.7% formaldehyde for 10 min at RT, rinsed in water and mounted in Mowiol.

Immunofluorescence: Animals were fixed and subsequently rehydrated as for WMISH with repeated washes in successive dilutions of EtOH in PBST (PBS, 0.5% Triton). Blocking was performed with 2% BSA in PBST for 1-2 hours at RT. For immunostaining, samples were incubated overnight at 4°C with an anti-GFP antibody (1:400, Novus NB600-308) in 2% BSA. Then, after several washes in PBST, the secondary antibody anti-rabbit coupled to Alexa 488 (1:600, Invitrogen A21206) was added in 2% BSA for 4 hours. For double immunofluorescence, the anti-mCherry antibody (1:400, Abcam ab125096) and the secondary antibody anti-mouse coupled to Alexa 555 (1:600, Invitrogen A31570) were used.

Nuclear extracts (NEs): NEs were prepared according to (Galliot et al., 1995). Briefly, 100 *H. magnipapillata* or *Hv_AEP2* were washed rapidly in HM and once in Hypotonic Buffer (HB: 10 mM Hepes pH7.9, 2 mM MgCl₂, 5 mM KCl, 0.5 mM spermidine, 0.15 mM spermine), then placed in a 1 ml glass douncer with 1ml of HB and 20 strokes were given. After adding slowly (drop by drop) 210 µl of 2 M sucrose, 15 more strokes were given. The extract was centrifuged for 10 min at 3'200 rpm at 4°C, the pellet was washed twice with 800 µl Sucrose Buffer (0.3 M sucrose in HB) and resuspended in 50 µl Elution Buffer (glycerol 10%, 400 mM NaCl, 10 mM Hepes pH 7.9, 0.1 mM EDTA, 0.1 mM EGTA, 0.5 mM spermidine, 0.15 mM spermine) and incubated for 45 min. The eluate was centrifuged at 4°C for 20 min at 13'000 rpm, and the supernatant aliquoted, and stored at -80°C. All manipulations were carried out on ice and all buffers contain a mix of protease inhibitor cocktail (Bimake B14012).

Production of anti-Sp5 antibodies: Two anti-Sp5 antibodies were generated. A rabbit polyclonal antibody was produced by Covalab (Bron, France) against three peptides P1 (178-191): NEHHIKEYSEHSQA, P2 (398-411): CDENVMELEVNVEN and P3 (155-175). After four immunizations the sera were collected from a single rabbit and ELISA test was performed to check immunoreactivity. After, purification with P1 and P2 to remove P3 cross-reactivity was performed by Covalab. The mouse monoclonal antibody was produced by Proteogenix (Schiltigheim, France) against a 6His-tag (MGSHHHHHHSG) coupled to a 218 AA-long *Hydra* Sp5 fragment (see sequence in FigS14A) produced by Proteogenix. The partial recombinant Sp5 protein (24.5 kDa) was expressed in *E. coli* and injected to the animals. After four immunizations, spleen cells collected from two mice were fused to myeloma cells. The antibody was produced from one selected clone and validated by IP analysis.

Electro-Mobility Shift Assay (EMSA) or band-shift assay: The LightShift Chemiluminescent EMSA Kit (Thermo-Scientific, 89880) was used to perform EMSA with *Hydra* NE and biotinlabeled double-stranded oligos described in the Supplementary Table 1. Briefly, 3 µl of *Hydra* NEs per 20 µl binding reaction were incubated for 20 minutes with the double-stranded

oligos (20 fmol), then loaded on a 6% polyacrylamide gel (PAGE) in TBE 0.5x, electrophoresed and transferred onto a nylon membrane (BrightStar-Plus Invitrogen AM10102). Crosslink was done by exposing the membrane to UV-light 120 mJ/cm² for 30-50s (Marshall Scientific, SS-UV1800) and the samples fixed on the membrane were blocked for 15 minutes with Blocking Buffer (Thermo-Scientific 89880A). The membrane was then conjugated with Stabilized Streptavidin-Horseradish Peroxidase (1:300 dilution, Thermo-Scientific, 89880D) and developed by adding Luminol/Enhancer solution (Thermo-Scientific 89880E/F).

Cell culture and whole cell extracts (WCEs): HEK293T cells were cultured in DMEM High Glucose, 10% fetal bovine serum (FBS), 6 mM L-glutamine, and 1 mM NA pyruvate in 10 cm diameter cell culture dishes (CellStar, Greiner Bio-One 664160). After a two-day growth, the cells were collected by scraping, counted and 15x 10⁴ cells per well were seeded in 6-well plates and grown for 19 hours. Next, cells were transfected with 2 µg of pCS2+empty or pCS2+HySp5 plasmid using the X-tremeGENE HP DNA transfection reagent (Sigma, 6366546001) and cell extracts were prepared 24 hours later. Cells were resuspended in PBS 1x before being centrifuged for 3 minutes at 3'000 rpm at 4°C and the supernatant was discarded. The pellet was resuspended in fresh Lysis Buffer (50 mM Hepes pH 7.6, 150 mM NaCl, 2.5 mM MgCl₂, 0.5 mM DTT, 10% glycerol, 1% Triton 100x, 0.1 mg/ml PMSF, 10% protease inhibitor cocktail (Bimake, B14012) and a lab-made phosphatase inhibitors cocktail (8 mM NaF, 20 mM β-glycerophosphate, 10 mM Na₃VO₄) and incubated on ice for 30 minutes. Centrifugation was performed 14'000 rpm for 10 minutes at 4°C, the supernatant was aliquoted, and kept at -80°C.

Western blotting: 20 µg extracts, either WCEs or NEs, were diluted with Loading Laemmli buffer and then boiled for 5 minutes at 95°C before being loaded onto a 10% SDS-PAGE, then electrophoresed and transferred onto a PVDF membrane (Bio-Rad 162-0177). Next, the membrane was blocked for 2 hours at RT with 5% dry milk in TBS 1x, 0.1%Tween (TBS-T). Anti-Sp5 antibodies were added at a 1:500 dilution and incubated overnight at 4°C. The membranes were washed 3x 10 minutes in TBS-T before being incubated for 2 hours with the secondary anti-mouse-HRP- or anti-rabbit HRP antibody (1:5000, Promega anti-mouse, W4021; anti-rabbit W4011)). The membranes were washed in TBS-T for 3x 10 minutes and developed with Western Lightning Plus-ECL reagent (Perkin Elmer NEL104). To produce *in vitro* the Sp5 protein, the pCS2+empty and pCS2*HySp5 plasmids were incubated using the TNT Quick Coupled Transcription/Translation Systems (Promega L2080) as described in the guidelines and 1 µl was loaded on 10% SDS-PAGE.

ChIP-qPCR: 300 *H. magnipapillata* or *Hv_AEP2* animals were fixed in 1% Formaldehyde Solution (Thermo-Scientific 28906) for 15 minutes, followed by 3 minutes in Stop Solution (Active Motif 103922), then briefly washed in cold HM before being resuspended in 5 ml

Chromatin prep buffer containing 0.1 mM PMSF, 0.1% protease inhibitor cocktail (Active Motif 103923). The sample was transferred to a pre-cooled 15 ml glass douncer and 30 strokes were performed. The sample was incubated on ice for 10 minutes before being centrifuged at 4°C for 5 minutes at 1'250 rcf. The pellet was resuspended in 1 ml Sonication Buffer (SB: 1% SDS, 50 mM Tris-HCl pH 8.0, 10 mM EDTA pH 8.0, 1 mM PMSF, 1% protease inhibitor cocktail) and incubated on ice for 10 minutes. The chromatin was then sonicated with a Diagenode Bioruptor Cooler (sonication conditions: Amp: 25%, Time: 20s on, 30s off, 2 cycles). The samples were centrifuged at 14'000 rpm for 10 minutes at 4°C, the supernatant was sonicated (sonication conditions as above but 3 cycles), centrifuged 14'000 rpm for 10 minutes at 4°C, and the supernatant recovered. After measuring DNA with Qubit, 10 µg of the sonicated chromatin were diluted (1:5) in ChIP Dilution Buffer (DB: 0.1% NP-40, 0.02 M Hepes pH 7.3, 1 mM EDTA pH 8.0, 0.15 M NaCl, 1 mM PMSF, 1% protease inhibitor cocktail) and incubated with 1 µg of either monoclonal or polyclonal α -Sp5 antibody or pre-immune serum antibody overnight at 4°C on a rotating wheel. The sample was then loaded onto a ChIP-IT ProteinG Agarose Column (Active Motif 53039), incubated on a rotating wheel for 3 hours at 4°C, washed 6 times with 1 ml Buffer AM1 before being eluted with 180 µl Buffer AM4. After, 1M NaCl and 3x TE buffer were added to perform decrosslinking overnight at 65°C. The next day, RNase A (10 µg/µl) was added for 30 min at 37°C followed by Proteinase K (10 µg/µl) for 2 hours at 55°C. Finally, the MiniElute PCR purification kit (Qiagen, 28004) was used to purify the samples. DNA was eluted in 30 µl and 1 µl per condition was used for qPCR.

Imaging: Live imaging to analyze the dynamics of mCherry and GFP fluorescence was performed on the Leica DM5500 microscope using the Leica software. To quantify GFP fluorescence, the acquired data were analyzed with Fiji (ImageJ). The same microscope was used to image immunofluorescence on whole animals. A confocal LSM780 microscope was used to image with high magnification the immunostained hypostome region of transgenic animals, as well as the budding region of live transgenic animals. In this latter case, animals were incubated in 1 mM linalool, HM for 10 min prior to imaging, then kept in the linalool solution between two coverslips separated by a 0.025 mm spacer. WMISH pictures were acquired with the Olympus SZX10 microscope.

Statistical analyses: The statistical analyses were two-tailed unpaired and were carried out using the GraphPad Prism software. P values are for **** ≤ 0.0001 , *** > 0.0001 and ≤ 0.001 , ** > 0.001 and ≤ 0.01 , * > 0.01 and ≤ 0.05 , ns ≥ 0.05 .

Acknowledgements

The authors thank Leo Beccari for excellent advice, Denis Benoni for animal care, and all members of the Galliot lab for discussions. Laura Iglesias Ollé was supported by an iGE3 doctoral fellowship. This work was supported by the Canton of Geneva, the Swiss National Science Foundation (SNSF grants 31003A_149630, 31003_169930), the Claraz donation and by the Swiss Government for an Excellence Scholarship for Foreign Scholars given to GPLS.

Contributions

Conceptualization: LIO, MCV, PGLS, BG; Methodology: LIO, MCV, CP, PGLS, BG; Investigation: LIO, CP, PGLS; Visualization: LIO, CP, PGLS, BG; Funding acquisition: BG; Supervision: BG, MCV; Writing – original draft: LIO, BG; Writing – review & editing: BG

REFERENCES

- Broun, M., Gee, L., Reinhardt, B. and Bode, H. R.** (2005). Formation of the head organizer in hydra involves the canonical Wnt pathway. *Development* **132**, 2907–2916.
- Buzgariu, W., Wenger, Y., Tcaciuc, N., Catunda-Lemos, A.-P. and Galliot, B.** (2018). Impact of cycling cells and cell cycle regulation on Hydra regeneration. *Dev Biol* **433**, 240–253.
- Chera, S., de Rosa, R., Miljkovic-Licina, M., Dobretz, K., Ghila, L., Kaloulis, K. and Galliot, B.** (2006). Silencing of the hydra serine protease inhibitor Kazal1 gene mimics the human SPINK1 pancreatic phenotype. *J Cell Sci* **119**, 846–857.
- Corish, P. and Tyler-Smith, C.** (1999). Attenuation of green fluorescent protein half-life in mammalian cells. *Protein Eng* **12**, 1035–1040.
- Galliot, B.** (2012). Hydra, a fruitful model system for 270 years. *Int J Dev Biol* **56**, 411–423.
- Galliot, B., Welschhof, M., Schuckert, O., Hoffmeister, S. and Schaller, H. C.** (1995). The cAMP response element binding protein is involved in hydra regeneration. *Development* **121**, 1205–1216.
- Gee, L., Hartig, J., Law, L., Wittlieb, J., Khalturin, K., Bosch, T. C. G. and Bode, H. R.** (2010). beta-catenin plays a central role in setting up the head organizer in hydra. *Dev Biol* **340**, 116–124.
- Harrison, S. M., Houzelstein, D., Dunwoodie, S. L. and Beddington, R. S.** (2000). Sp5, a new member of the Sp1 family, is dynamically expressed during development and genetically interacts with Brachyury. *Dev Biol* **227**, 358–372.
- Hobmayer, B., Rentzsch, F., Kuhn, K., Happel, C. M., von Laue, C. C., Snyder, P., Rothbacher, U. and Holstein, T. W.** (2000). WNT signalling molecules act in axis formation in the diploblastic metazoan Hydra. *Nature* **407**, 186–189.
- Huggins, I. J., Bos, T., Gaylord, O., Jessen, C., Lonquich, B., Puranen, A., Richter, J., Rossdam, C., Brafman, D., Gaasterland, T., et al.** (2017). The WNT target SP5 negatively regulates WNT transcriptional programs in human pluripotent stem cells. *Nat Commun* **8**, 1034.
- Kennedy, M. W., Chalamalasetty, R. B., Thomas, S., Garriock, R. J., Jailwala, P. and Yamaguchi, T. P.** (2016). Sp5 and Sp8 recruit β -catenin and Tcf1-Lef1 to select enhancers to activate Wnt target gene transcription. *Proc Natl Acad Sci U S A* **113**, 3545–3550.
- Lengfeld, T., Watanabe, H., Simakov, O., Lindgens, D., Gee, L., Law, L., Schmidt, H. A., Özbek, S., Bode, H. and Holstein, T. W.** (2009). Multiple Wnts are involved in Hydra organizer formation and regeneration. *Dev Biol* **330**, 186–199.
- Madeira, F., Pearce, M., Tivey, A. R. N., Basutkar, P., Lee, J., Edbali, O., Madhusoodanan, N., Kolesnikov, A. and Lopez, R.** (2022). Search and sequence analysis tools services from EMBL-EBI in 2022. *Nucleic Acids Res* gkac240.
- Nakamura, Y., Tsiairis, C. D., Özbek, S. and Holstein, T. W.** (2011). Autoregulatory and repressive inputs localize Hydra Wnt3 to the head organizer. *Proc Natl Acad Sci U S A* **108**, 9137–9142.

- Park, D.-S., Seo, J.-H., Hong, M., Bang, W., Han, J.-K. and Choi, S.-C.** (2013). Role of Sp5 as an essential early regulator of neural crest specification in xenopus. *Dev Dyn* **242**, 1382–1394.
- Schenkelaars, Q., Perez-Cortes, D., Perruchoud, C. and Galliot, B.** (2020). The polymorphism of Hydra microsatellite sequences provides strain-specific signatures. *PLoS One* **15**, e0230547.
- Suknovic, N., Tomczyk, S., Colevret, D., Perruchoud, C. and Galliot, B.** (2021). The ULK1 kinase, a necessary component of the pro-regenerative and anti-aging machinery in Hydra. *Mech Ageing Dev* **194**, 111414.
- Takahashi, M., Nakamura, Y., Obama, K. and Furukawa, Y.** (2005). Identification of SP5 as a downstream gene of the beta-catenin/Tcf pathway and its enhanced expression in human colon cancer. *Int J Oncol* **27**, 1483–1487.
- Tanaka, E. M. and Reddien, P. W.** (2011). The cellular basis for animal regeneration. *Dev Cell* **21**, 172–185.
- Vogg, M. C., Beccari, L., Iglesias Ollé, L., Rampon, C., Vríz, S., Perruchoud, C., Wenger, Y. and Galliot, B.** (2019a). An evolutionarily-conserved Wnt3/ β -catenin/Sp5 feedback loop restricts head organizer activity in Hydra. *Nat Commun* **10**, 312.
- Vogg, M. C., Galliot, B. and Tsiairis, C. D.** (2019b). Model systems for regeneration: *Hydra*. *Development* **146**, dev177212.
- Vogg, M. C., Buzgariu, W., Suknovic, N. S. and Galliot, B.** (2021a). Cellular, Metabolic, and Developmental Dimensions of Whole-Body Regeneration in Hydra. *Cold Spring Harb Perspect Biol* **13**, a040725.
- Vogg, M. C., Ferenc, J., Buzgariu, W. C., Perruchoud, C., Papasaikas, P., Sanchez, P. G. L., Nuninger, C., Delucinge-Vivier, C., Rampon, C., Beccari, L., et al.** (2021b). *The transcription factor Zic4 acts as a transdifferentiation switch*. *Developmental Biology*.
- Weidinger, G., Thorpe, C. J., Wuennenberg-Stapleton, K., Ngai, J. and Moon, R. T.** (2005). The Sp1-related transcription factors sp5 and sp5-like act downstream of Wnt/ β -catenin signaling in mesoderm and neuroectoderm patterning. *Curr Biol* **15**, 489–500.
- Wenger, Y., Buzgariu, W., Perruchoud, C., Loichot, G. and Galliot, B.** (2019). *Generic and context-dependent gene modulations during Hydra whole body regeneration*. *Developmental Biology*.
- Wittlieb, J., Khalturin, K., Lohmann, J. U., Anton-Erxleben, F. and Bosch, T. C. G.** (2006). Transgenic *Hydra* allow *in vivo* tracking of individual stem cells during morphogenesis. *Proc. Natl. Acad. Sci. U.S.A.* **103**, 6208–6211.

SUPPLEMENTARY TABLE 1: List of primers, siRNAs and ds-oligonucleotides

Cloning primers	HySp5 promoter Forward	CCGGATATCCTAGTTCTAATTTAGCTCTATTACGTTCCGC
	HySp5 promoter Reverse	AACCCCTTATCAAAGAAGCCACCGGTCTAG
siRNAs	HySp5 siRNA-1	UUA ACG AGC ACC ACA UAA A
	HySp5 siRNA-2	CUA CAA CAU CCC ACA UAU A
	HySp5 siRNA-3	GCA GCA CGU AUG UCA UAU U
	β -catenin siRNA-1	UCA ACC UAA CAG ACA ACA A
	β -catenin siRNA-2	UGA GGA GCU AUA CUU AUG A
	β -catenin siRNA-3	ACG ACU CUC UGU UGA AUU U
	Scramble siRNA	AGG UAG UGU AAU CGC CUU G
qPCR primers	HySp5 Forward	CCAGGGTGC GGAAAGGTT
	HySp5 Reverse	CCAGCATGCCATCTTAAATGAG
	HyWnt3 Forward	GAGTTGACGGTTGCGAACTT
	HyWnt3 Reverse	ACATGAAACCTTGCAACACCA
	β -catenin Forward	TACGCAATGTTGTTGGTGCT
	β -catenin Reverse	GCTTCAATTCGATGGCCTAA
	GFP Forward	TGGAAGCGTTCAACTAGCAG
	GFP Reverse	AAAGGGCAGATTGTGTGGAC
	TBP Forward	AAGCGATTTGCAGCAGTTAT
TBP Reverse	GCTCTTCACTTTTTGCTCCA	
qPCR primers for ChIP	Sp5prom_F_1	TAAGCTGTCTCCATTTCAACCA
	Sp5prom_R_1	AATATTTGTTAAGTGTITTCGTTGG
	Sp5prom_F_2	AATTGCGGTAAAGATCAGTAAGAA
	Sp5prom_R_2	TGGTTGAAATGGAGACAGCTT
	Sp5prom_F_3	AAGTATCAAGTTTAAAAATTCCTTCG
	Sp5prom_R_3	ATTTAGAATTCCTACTGATCTTTACCG
	Sp5prom_F_4	TATCTTTCCGCCTTACGTATTC
	Sp5prom_R_4	ACTGAGAAATGGCGCGTTG
	Sp5prom_F_5	CAGAGAAAATATGATCGCAACG
	Sp5prom_R_5	GAAACCGCCATCTTATCTTAAA
	Sp5prom_F_6	AACCAAATATTTAAAATGATAAACTGG
	Sp5prom_R_6	CAAAGGCGGAGTAATTAGGTG
	Sp5prom_F_7	TGATTTGAAGTCAAAAACAAAATAACA
	Sp5prom_R_7	TGGTAAAAGATATAAACGCTATTTG
	Sp5prom_F_8	TGGTAAAGTTCGTAACCAATGA
	Sp5prom_R_8	AAACATTCCGACAATCCACAG
	Sp5prom_F_9	AAGTAGCGACAGCGCCAGT
	Sp5prom_R_9	ATATCCTAGCCAAAACAAAACAA
	Sp5prom_F_10	GGTCAGCGAGTTTGGATCAT
	Sp5prom_R_10	AGCCTCAGGACTTCCCATT
	Sp5prom_F_11	CGAGCGTTGCTTTGACTTTA
	Sp5prom_R_11	CAATTACGGATCACCGAAGG
	Sp5prom_F_12	CTCAGTGCATCCGTTTCGTT
	Sp5prom_R_12	TCTTGCTTGCTTACGGATGA
	Sp5prom_F_13	TGAAATATTA AAAAGACGGAAGGAA
	Sp5prom_R_13	TGCAGTAAAAGCAACAAAACA
	Sp5prom_F_14	CGTTCGCAAAGTTGACAAAGT
	Sp5prom_R_14	CAATTTTATAAGCGTGATAAAGCAA
	Sp5prom_F_15	TCAATTTCAACAAAATAAGTGTCAA
	Sp5prom_R_15	TGAAGTTTCAATCCCTTTTAAACAA
double-stranded oligos for EMSA	ds-Sp5-oligo PPA wt	TATCTTTT CCGCCT TACGTATTCTGTTTATCA CCGCCT CTTAGACCATCCCATTTGTACGTAAACAGAG
	ds-Sp5-oligo PPA mut	TATCTTTT CTTCCT TACGTATTCTGTTTATCA CTTCCT CTTAGACCATCCCATTTGTACGTAAACAGAG
	ds-Sp5-oligo PPB wt	CAGAGAAAATATGATCGCAAC GCGCCA TTTCTCAGTCAG AGGCGT GACATTAACCCCTTATCAAGAAGCCGA
	ds-Sp5-oligo PPB mut	CAGAGAAAATATGATCGCAAC GTTCCA TTTCTCAGTCAG ATTCTG GACATTAACCCCTTATCAAGAAGCCGA

SUPPLEMENTARY TABLE 2: List of plasmids

PLASMID NAME	PLASMID DESCRIPTION	REFERENCE
HYACT-1388	1'388 bp of <i>Hydra Actin</i> promoter and 5'UTR sequences	
HYSP5-3169	2'992 bp of <i>Hydra Sp5</i> promoter and 5'UTR sequences	
HYWNT3-2149	2'449 bp of <i>Hydra Wnt3</i> promoter sequences	
HYACT-1388:MCHERRY_ _HYSP5-3169:EGFP	Tandem reporter construct with ubiquitous mCherry expression and <i>Sp5</i> -driven eGFP expression	This work
HYACT-1388:DSRED_ _HYWNT3-2449:EGFP	Tandem reporter construct with ubiquitous dsRED expression and <i>Wnt3</i> -driven eGFP expression	(Nakamura et al., 2011)
PCS2-SP5	<i>Sp5</i> bacterial expression vector	(Vogg et al., 2019a)

SUPPLEMENTARY TABLE 3: List of transgenic lines

TRANSGENIC LINES	DESCRIPTION	REFERENCE
HyAct-1388:mCherry_ _HySp5-3169:eGFP_epidermal		This work
HyAct-1388:mCherry_ _HySp5-3169:eGFP_gastrodermal		This work
HyAct-1388:dsRED_ _HyWnt3-2149:eGFP_epidermal		(Vogg et al., 2019a)
HyAct-1388:dsRED_ HyWnt3-2149:eGFP_gastrodermal		(Nakamura et al., 2011; Vogg et al., 2019a)

Differential negative autoregulation of *Sp5* in the epidermal and gastrodermal epithelial layers in *Hydra*

**Laura Iglesias Ollé¹, Matthias Christian Vogg¹, Paul Gerald Layague Sanchez¹,
Chrystelle Perruchoud¹, Brigitte Galliot^{1*}**

¹Department of Genetics and Evolution, Institute of Genetics and Genomics (iGE3), Faculty of Sciences, University of Geneva; 30 Quai Ernest Ansermet, 1211 Geneva 4, Switzerland.

*Corresponding author. Email: brigitte.galliot@unige.ch

Figure 1. Epidermal-specific and gastrodermal-specific patterns of GFP fluorescence and *GFP* expression in *HySp5-3169:GFP* transgenic animals

Figure 2. Developmental regulation of epidermal and gastrodermal GFP fluorescence in budding and regenerating *HySp5-3169:GFP_ep* and *HySp5-3169:GFP_ga* animals

Figure 3. Morphological changes and *GFP*, *Wnt3* and *Sp5* ectopic expression induced by alsterpaullone (ALP) treatment in *HySp5-3169:GFP* and *HyWnt3-2149:GFP* animals

Figure 4. Modulations of GFP fluorescence and *GFP* expression in *HySp5-3169:GFP_ep* animals knocked-down for *β-catenin*

Figure 5. Ectopic GFP fluorescence and *GFP* expression in *HySp5-3169:GFP* animals knocked-down for *Sp5*.

Figure 6. CHIP-qPCR identification of *Sp5*-binding sites in the *HySp5* promoter

Figure 7. Summary view of the layer-specific regulation of *Sp5* in *Hydra*

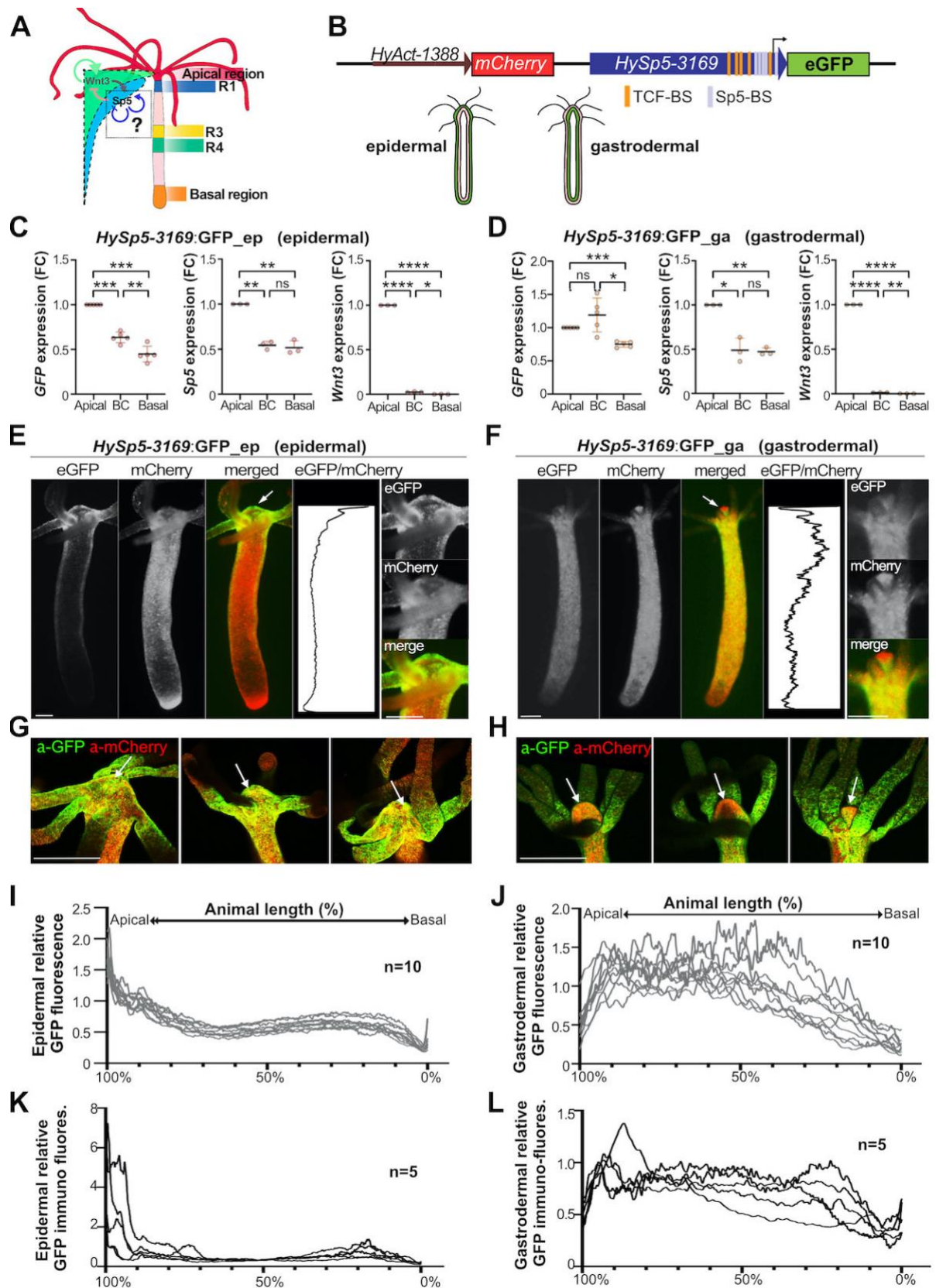


Figure 1. Epidermal-specific and gastrodermal-specific patterns of GFP fluorescence and *GFP* expression in *HySp5-3169:GFP* transgenic animals

(A) Schematic representation of the homeostatic *HySp5* RNA-seq profile measured in five regions along the body axis: Apical, R1, R2, R3, R4 and Basal regions. The cross-talk between *Wnt3* and *Sp5* is represented on the left side of the scheme (after Voggt et al., 2019). The question mark highlights

the Sp5 auto-regulation hypothesis. **(B)** Structure of the tandem reporter construct used to generate the *Sp5* transgenic lines, where 3169 bp of the *HySp5* promoter drives *eGFP* expression and 1'388 bp of the *HyActin* promoter drives *mCherry* expression (*HyAct-1388:mCherry-HySp5-3169:GFP*). Two transgenic lines were produced, *HySp5:GFP-ep* and *HySp5:GFP-ga*, which constitutively express the tandem reporter in the epidermal or the gastrodermal epithelial layer respectively as represented in the scheme below of the *Hydra*. TCF-BS : TCF binding sites (orange); Sp5-BS: Sp5 binding sites (grey). **(C, D)** Q-PCR analysis of *GFP*, *Sp5* and *Wnt3* expression in *HySp5:GFP-ep* (C) and *HySp5:GFP-ga* (D) animals dissected in three regions, apical, body column (BC) and basal immediately before fixation. P values are as follows: **** ≤ 0.0001 , *** > 0.0001 and ≤ 0.001 , ** > 0.001 and ≤ 0.01 , * > 0.01 and ≤ 0.05 , ns ≥ 0.05 . **(E, F)** Live imaging of *HySp5:GFP* animals, with eGFP green, mCherry red; the apical region of each animal is magnified on the right column. White arrows point to the tip of the hypostome. Scale bar: 250 μm . The graphs show the eGFP/mCherry fluorescence intensity ratios (Relative eGFP intensity) along the animal axis. **(G, H)** Immunodetection of GFP (green) and mCherry (red) in the apical region (white arrow) of *HySp5:GFP-ep* (G) and *HySp5:GFP-ga* (H) animals. Scale bar: 250 μm . **(I-L)** Graphs showing the relative GFP live fluorescence (I, J) or relative GFP immuno-fluorescence (K, L) measured in *HySp5:GFP-ep* (I, K) and *HySp5:GFP-ga* (J, L) animals. The apical extremity is on the left (100%), the basal one on the right (0%). See **Supplemental Figure S1**.

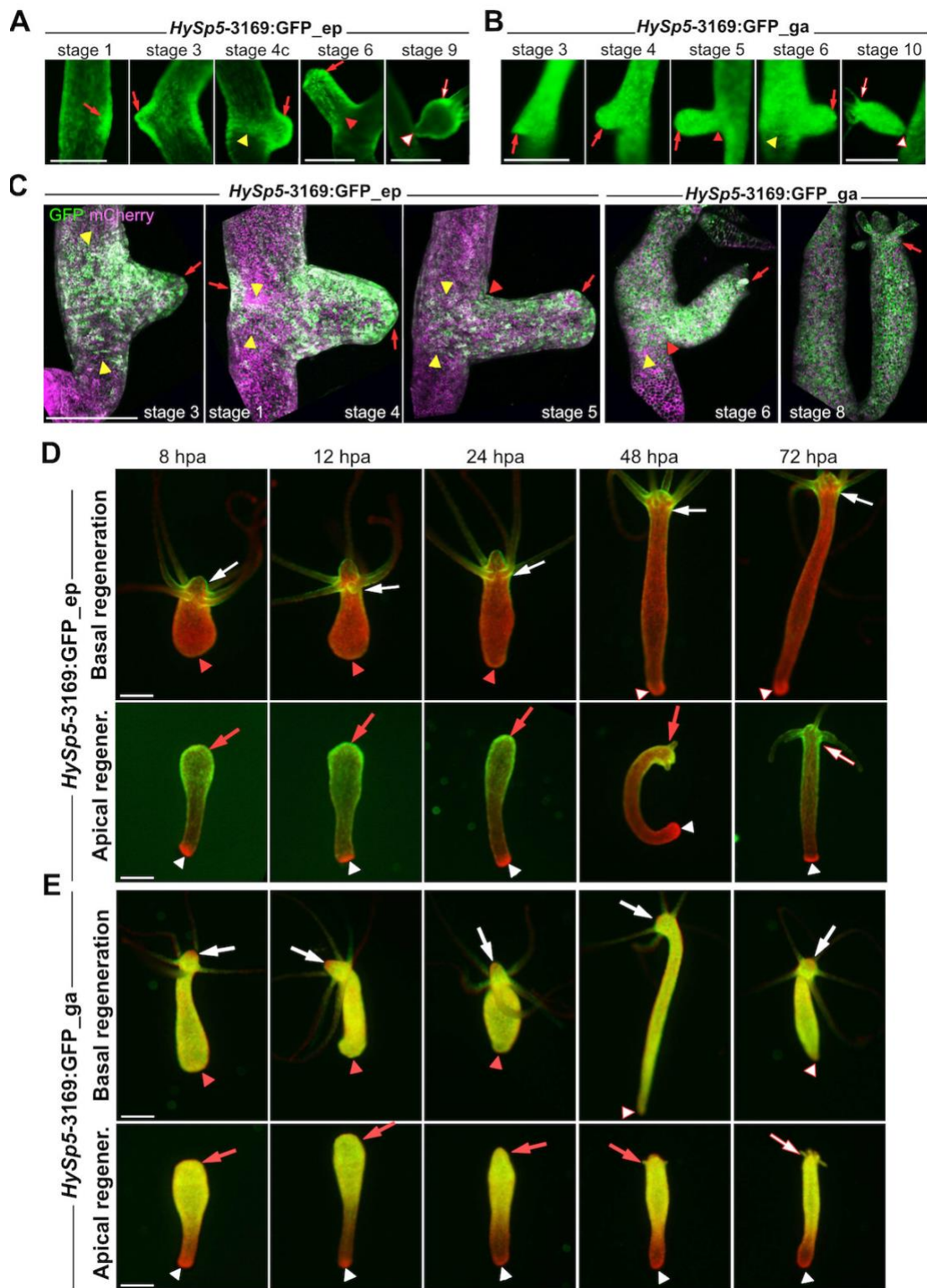


Figure 2. Developmental regulation of epidermal and gastrodermal GFP fluorescence in budding and regenerating *HySp5-3961:GFP_ep* and *HySp5-3961:GFP_ga* animals.

(A-C) Live imaging of budding animals taken at indicated stages. Red arrows point to developing apical regions; yellow arrowhead to the “budding belt” on the parental polyp, red arrowheads to the presumptive or differentiating basal region of the buds. Scale bar: 250 μ m. (D, E) GFP and mCherry fluorescence in apical-regenerating halves (D) and basal-regenerating halves (E) pictured live at 8, 12, 24, 48 and 72 hours post-amputation (hpa). White arrows point to apical regions of original polyps, red arrows to apical-regenerating regions; white arrowheads to mature basal regions from

the original polyp, red arrowheads to the basal-regenerating regions. Scale bar: 250 μm . See **Supplemental Figures S2, S3**.

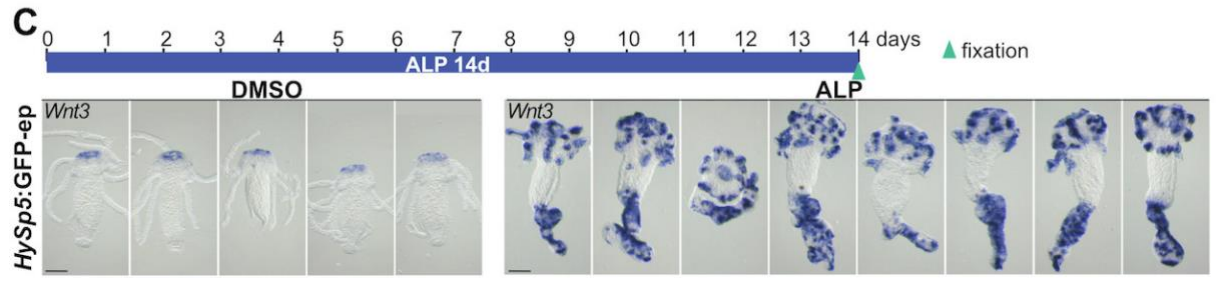
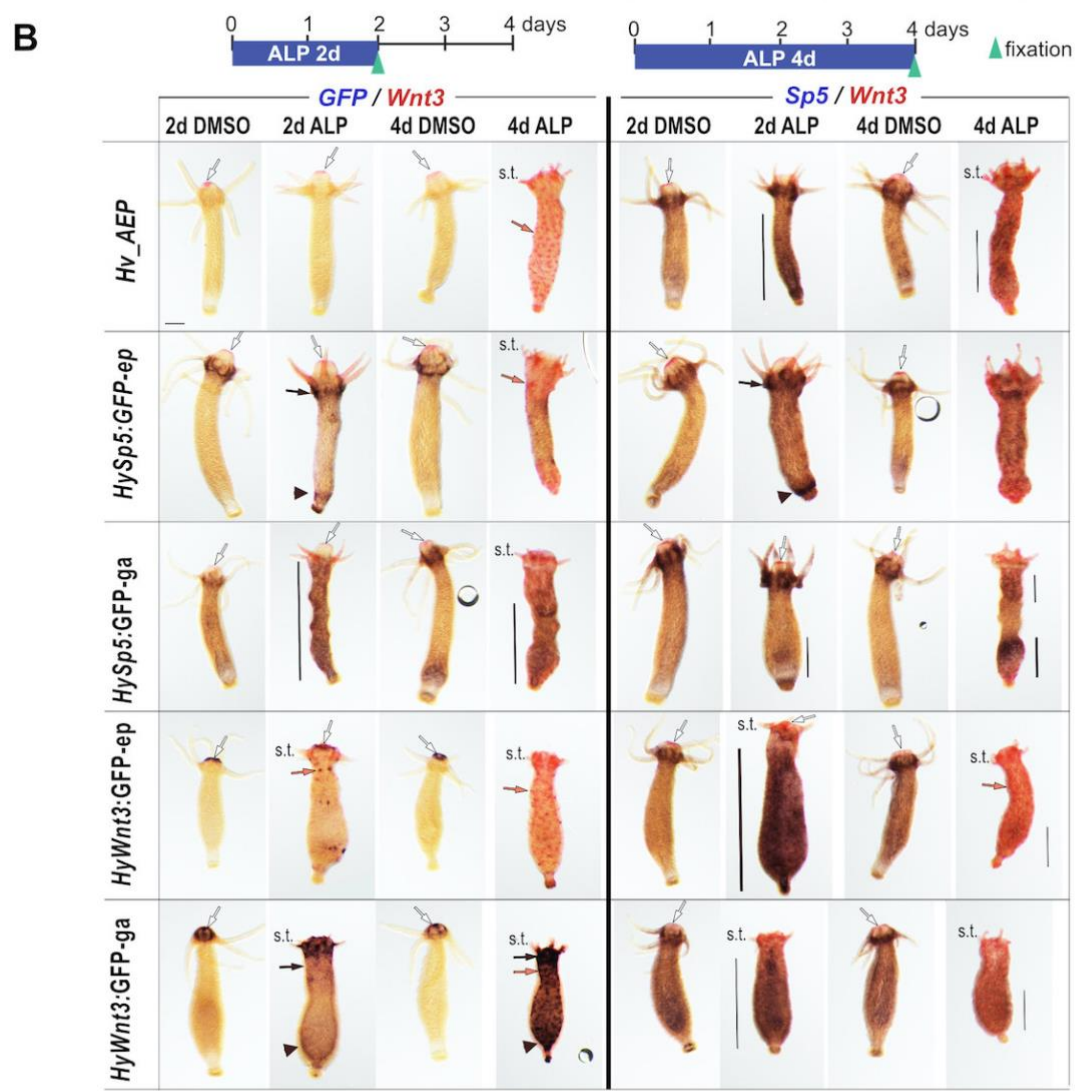
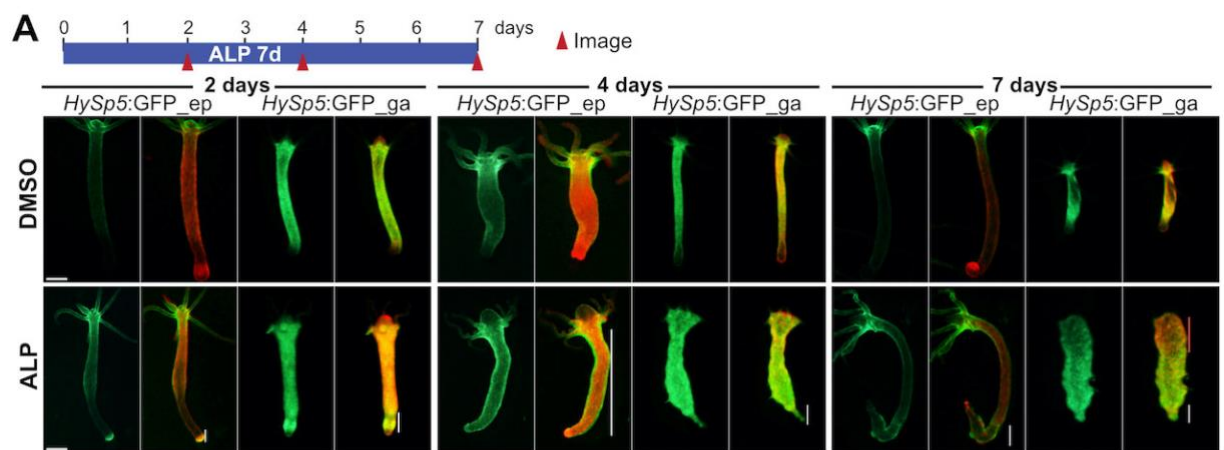


Figure 3. Morphological changes and *GFP*, *Wnt3* and *Sp5* ectopic expression induced by alsterpaullone (ALP) treatment in *HySp5-3169:GFP* and *HyWnt3-2149:GFP* animals

(A) Live imaging of *HySp5-3169:GFP_ep* and *HySp5-3169:GFP_ga* animals on day 2, 4 and 7 during the seven-days ALP treatment compared to control animals treated with DMSO as indicated in the schematic view of the procedure. For each condition, GFP fluorescence is shown on the left, and the merged GFP and mCherry fluorescence on the right. White bars indicate areas along the body column where ectopic GFP fluorescence after ALP treatment is detected. Scale bar: 250 μ m. **(B)** Double *WMISH* detecting *GFP/Wnt3* (left column) and *Sp5/Wnt3* (right column) in *Hv_AEP*, *HySp5-3169:GFP_ep*, *HySp5-3169:GFP_ga*, *HyWnt3-2149:GFP_ep* and *HyWnt3-2149:GFP_ga* animals treated with ALP during 2 days or 4 days as indicated. s.t.: short tentacles; scale bar: 200 μ m. **See Supplemental Figures S4, S5, S6.** **(C)** *Wnt3* expression in ALP-treated animals for 14 days versus control animals (DMSO). Note the two unusual *Wnt3* expression domains: apical in multiple tentacle rings, and in the lower section of the body column including the basal extremity. Scale bar: 200 μ m.

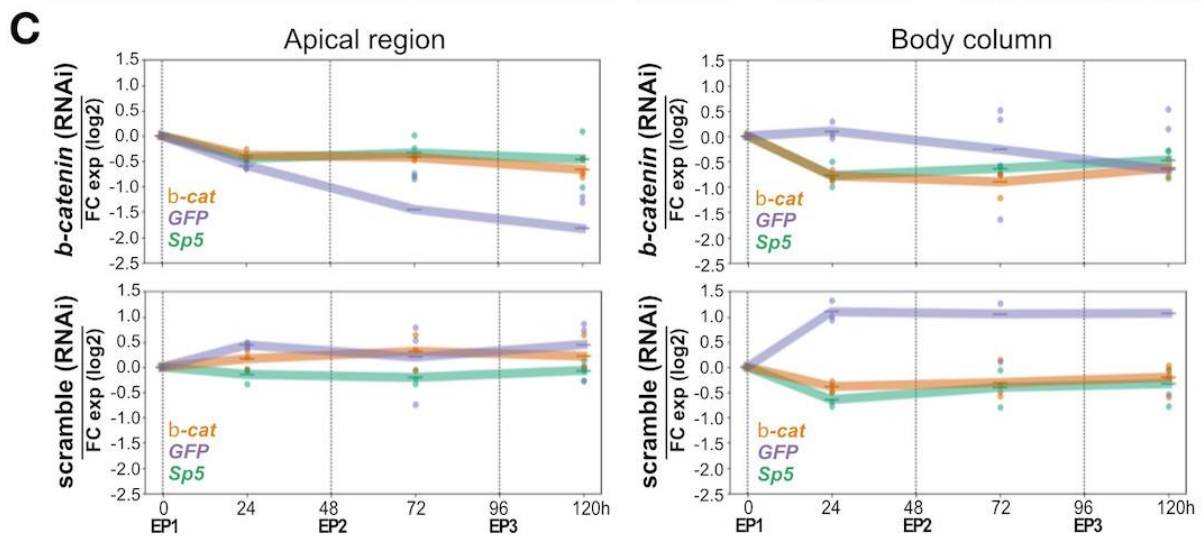
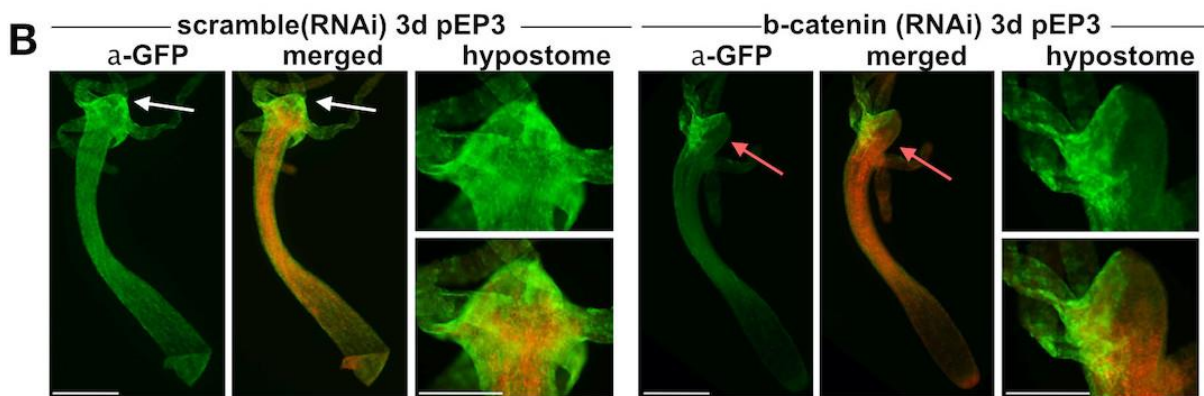
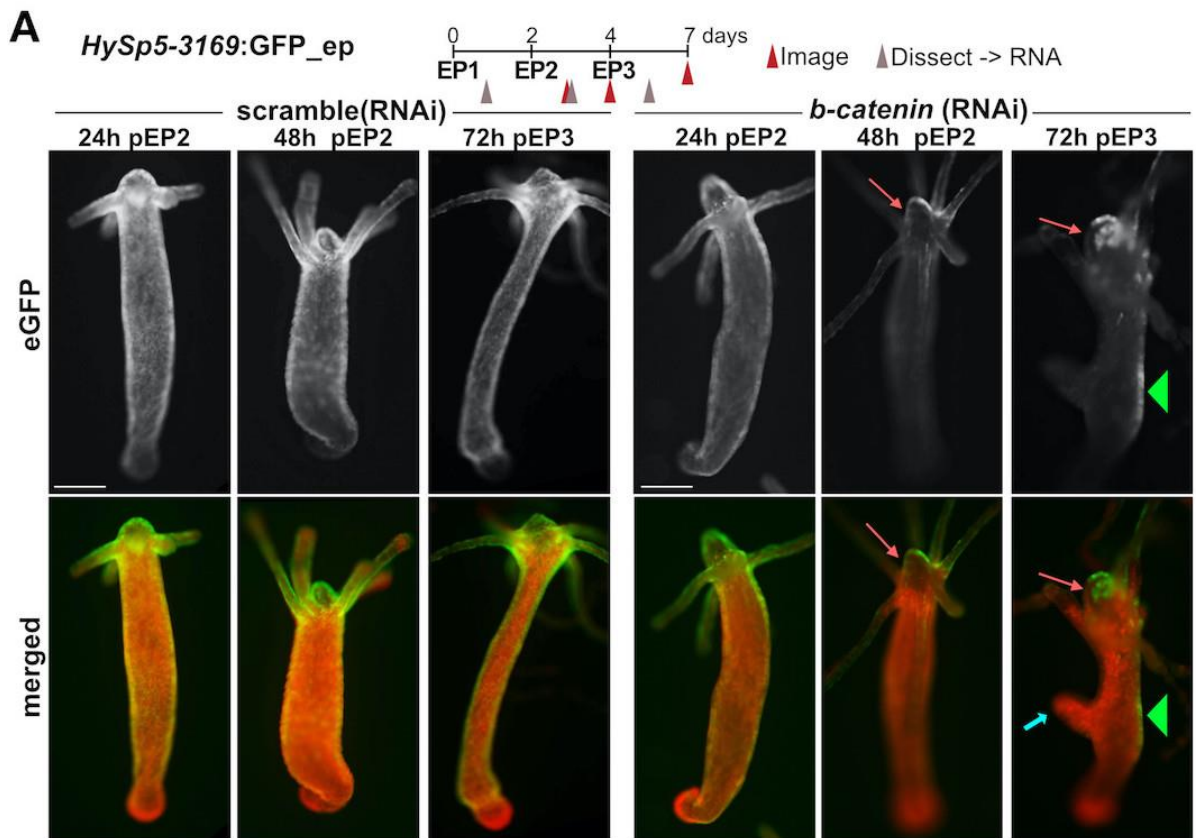


Figure 4. Modulations of GFP fluorescence and *GFP* expression in *HySp5-3169:GFP_ep* animals knocked-down for *β-catenin*

(A) Schematic view of the knock-down procedure with electroporations (EP) of *β-catenin* or scramble siRNAs performed at day 0 (EP1), day 2 (EP2) and day 4 (EP3). Red triangles: imaging of GFP and mCherry fluorescences of live *HySp5-3169:GFP_ep* animals; gray triangles: dissection of the apical and body column regions followed by immediate RNA extraction. On images, white and red arrows point to apical regions where GFP fluorescence is either normal (white) or reduced (red); blue arrow points to a “bump” structure that develops along the body axis three days post-EP3, and green triangles to ectopic GFP fluorescence. Scale bar: 250 μm. **(B)** Immunodetection of GFP and mCherry in *HySp5-3169:GFP_ep* animals three days after EP3. Magnified apical regions of *β-catenin* (RNAi) and scramble animals are shown in the right side. White and red arrows as in A **See Supplemental Figures S7, S8**. Scale bar: 250 μm. **(C)** Q-PCR values of *β-catenin*, *GFP* and *Sp5* at indicated time points after EP1, EP2 and EP3.

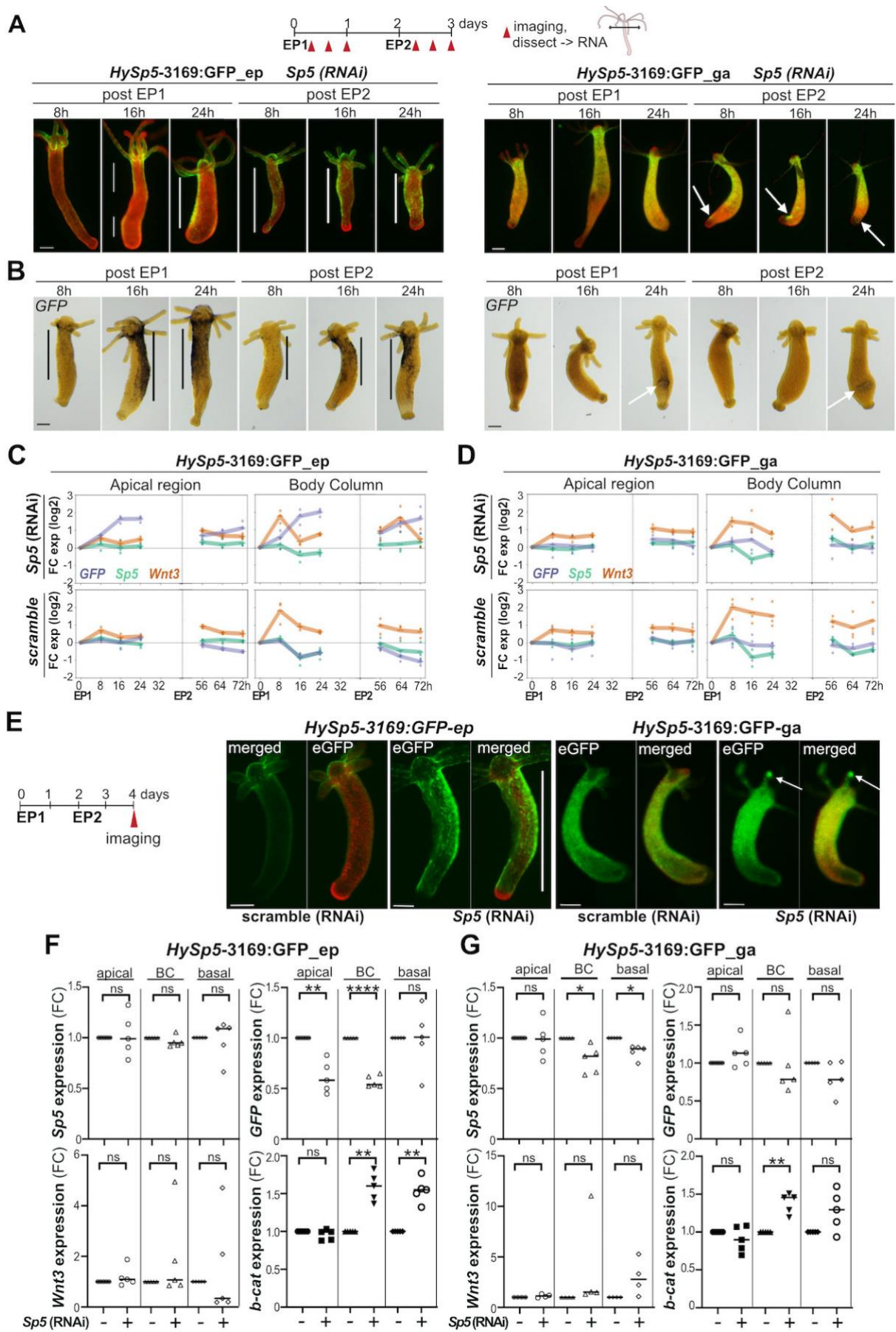


Figure 5. Ectopic GFP fluorescence and *GFP* expression in *HySp5-3169:GFP* animals knocked-down for *Sp5*

(A) Schematic view of the RNAi procedure with two electroporations (EP1, EP2) of scramble or *Sp5* siRNAs. Live imaging of intact animals and RNA extraction from the apical region and body column were performed at indicated time points (8h, 16h, 24h post-EP1, 8h, 16h, 24h post-EP2). Images show GFP and mCherry fluorescences detected in *HySp5-3169:GFP_ep* (left) and *HySp5-3169:GFP_ga* (right) animals. White bars indicate areas of ectopic GFP fluorescence along the body column of *HySp5-3169:GFP_ep* animals, white arrows spots of GFP fluorescence in the lower body column of *HySp5-3169:GFP_ga* animals. Scale bar: 250 μ m. **See Supplemental Figures S9, S11.** **(B)** *GFP* expression detected by WMISH at indicated time-points after *Sp5* (RNAi). Black bars and white arrows indicate regions where *GFP* is up-regulated along the body column of *HySp5-3169:GFP_ep* animals, or in the lower body column of *HySp5-3169:GFP_ga* animals. Scale bar: 200 μ m. **See Supplemental Figures S10, S12.** **(C, D)** Q-PCR analysis of *GFP*, *Wnt3* and *Sp5* expression measured after scramble or *Sp5* (RNAi) in the apical (100%-80%) and body column (80%-0%) regions dissected from *HySp5-3169:GFP_ep* (C) and *HySp5-3169:GFP_ga* (D) animals as indicated in (A). **See Supplemental Figure S9.** **(E)** Analysis of GFP and mCherry fluorescences in *HySp5-3169:GFP_ep* and *HySp5-3169:GFP_ga* animals electroporated twice and pictured two days post-EP2. White bar as in B; white arrows: spots of GFP fluorescence in tentacles in *HySp5-3169:GFP_ga* animals. Scale bar: 250 μ m. **Supplemental Figure S13.** **(F, G)** Q-PCR analysis of *Sp5*, *GFP*, *Wnt3* and β -*catenin* expression in *HySp5-3169:GFP_ep* (F) and *HySp5-3169:GFP_ga* (G) animals treated as in (E) and dissected 2 days post-EP2 in three regions, apical (100%-80%), central body column (BC, 80%-30%) and basal (30%-0%).

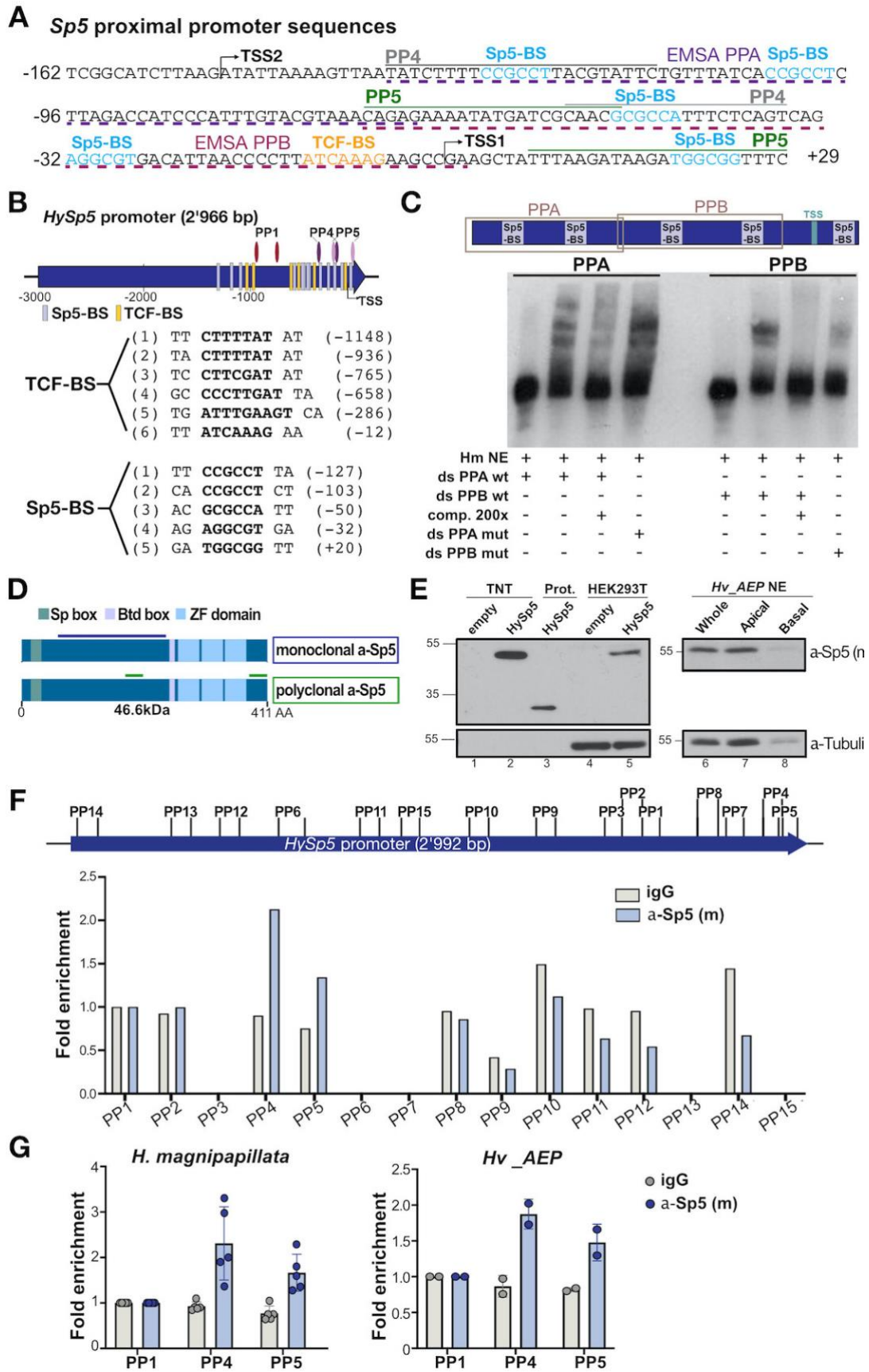


Figure 6. CHIP-qPCR identification of Sp5-binding sites in the *HySp5* promoter

(A) Proximal sequence of the *Hydra Sp5* promoter (-162 to +29), which contains the transcriptional start sites identified in *Hv_AEP* (TSS1, +1) and *Hm105* (TSS2, -149), the PPA (-135 to -67) and PPB (-

71 to +2) regions encompassing each two putative Sp5 binding sites (SP5-BS) respectively, highlighted in light blue, used in EMSA and underlined with purple (PPA) and pink (PPB) dashed lines respectively. In the same region, the PP4 and PP5 primers used for ChIP-qPCR are written grey and green respectively. **(B)** Map of the *HySp5* 2'966 bp promoter region indicating the predicted TSS1, the clustered TCF-BS and Sp5-BS in light purple and orange respectively, and the three primer pairs used for ChIP-qPCR. The TCF-BS and Sp5-BS sequences identified in the Sp5 promoter are given. **(C)** EMSA showing a shift of the PPA and PPB ds-DNAs incubated with *Hydra* NEs. Comp.: unlabelled ds-PPA (left) or ds-PPB (right) added 200x in excess during the incubation. **(D)** Structure of the *Hydra* Sp5 protein with the conserved Sp box (green), Buttonhead box (Btd, light purple) and zinc-finger (ZF) domain (light blue). A purple line covers the region used to raise the monoclonal anti-Sp5 antibody and the green lines indicated the peptides used to raise the polyclonal anti-Sp5 antibody. **(E)** Western blot using the anti-Sp5 monoclonal antibody to detect the Sp5 protein produced either with the TNT system (lanes 1, 2), or as recombinant partial protein to raise the monoclonal antibody (218 AAs, lane 3), or in HEK293T cells (lanes 4, 5), or present in *Hydra* NEs prepared from whole *Hv_AEP2* animals (lane 6) or from their apical region (100%-50% body length, lane 7), or from the body column (50%-0% body length, lane 8). **(F)** Schematic view of the 15 regions tested along the 2'992 bp-long *Sp5* promoter sequences by ChIP-qPCR using *Hv_magnipapillata* extracts and the α -Sp5 monoclonal antibody. The graph below shows a relative enrichment in regions PP4 and PP5. **(G-H)** Comparative analysis of the enrichment obtained by ChIP-qPCR in regions PP4 and PP5 compared to region PP1/PP2 when using the anti Sp5 monoclonal antibody in *Hv_magnipapillata* (G) or *Hv_AEP2* (H). **See Supplemental Figure S14.**

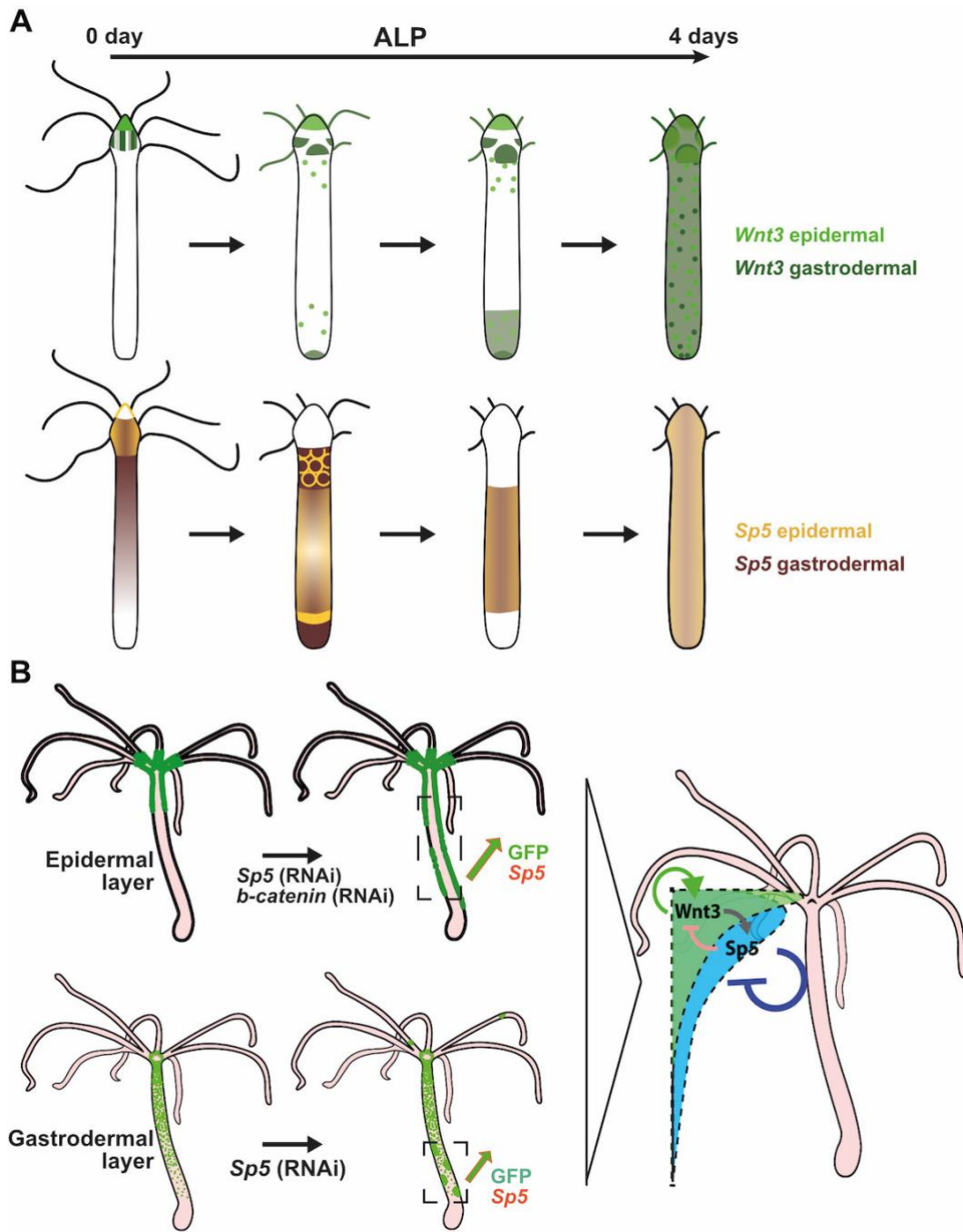


Figure 7: Summary view of the layer-specific regulation of *Sp5* in *Hydra*

(A) Scheme showing the *Wnt3* and *Sp5* expression patterns in the epidermal and gastrodermal layers after ALP treatment that leads to a constitutive activation of Wnt/ β -catenin signaling. The epidermal and gastrodermal *HyWnt3-2149:GFP* and *HySp5-3169:GFP* transgenic lines were used to discriminate their layer-specific regulation in intact animals. Epidermal and gastrodermal *Wnt3* expression patterns are shown in light green and dark green respectively; epidermal and gastrodermal *Sp5* expression patterns are shown in yellow and brown respectively. (B) Schematic view of GFP fluorescence in *HySp5-3169:GFP* transgenic animals, either maintained in homeostatic conditions (left), or knocked-down for *Sp5* (middle). Note after *Sp5* (RNAi) the extended zone of GFP fluorescence along the epidermis of the body column and, in the gastrodermis, the presence of ectopic spots of GFP fluorescence at the level of the peduncle and in the tentacles. On the right, we show the cross-talk between *Wnt3*/ β -catenin and *Sp5* and their respective auto-regulatory loops, positive for *Wnt3*/ β -catenin, negative for *Sp5*.

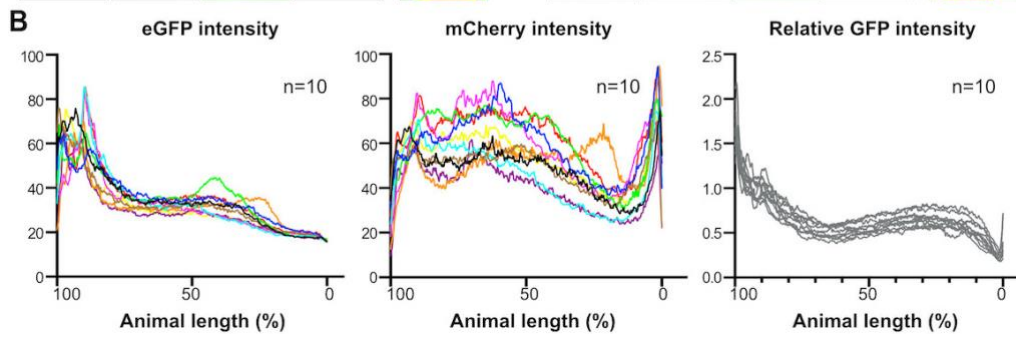
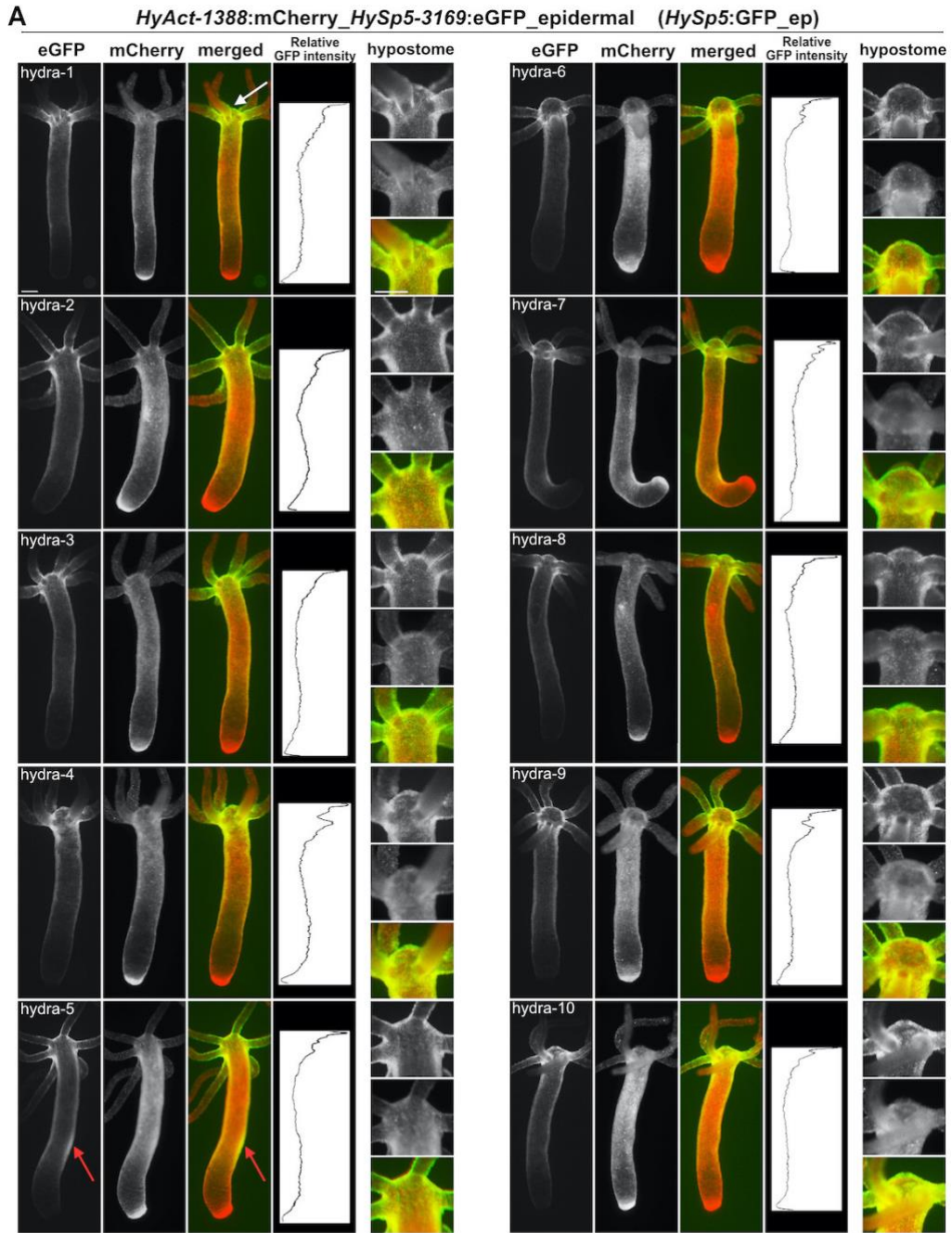
Differential negative autoregulation of *Sp5* in the epidermal and gastrodermal epithelial layers in *Hydra*

Laura Iglesias Ollé¹, Matthias Christian Vogg¹, Paul Gerald Layague Sanchez¹,
Christelle Perruchoud¹, Brigitte Galliot^{1*}

¹Department of Genetics and Evolution, Faculty of Sciences, Institute of Genetics and Genomics in Geneva (iGE3), University of Geneva; Switzerland. *Corresponding author: brigitte.galliot@unige.ch

SUPPLEMENTARY FIGURES	2
Figure S1. Epidermal and gastrodermal eGFP and mCherry fluorescences detected in live <i>HySp5-3169</i> GFP-ep and <i>HySp5-3169</i> GFP-ga transgenic animals.....	3
Figure S2. GFP fluorescence detected in live <i>HySp5-3169</i> :GFP_ep (A) and <i>HySp5-3169</i> :GFP_ga (B) animals undergoing apical or basal regeneration.....	5
Figure S3. <i>GFP</i> expression in <i>HySp5-3169</i> :GFP_ep and <i>HySp5-3169</i> :GFP_ga animals undergoing apical (A) or basal (B) regeneration.....	7
Figure S4. Alsterpaullone (ALP)-induced modulations of <i>Sp5</i> , <i>Wnt3</i> and <i>GFP</i> expression in <i>Hv_AEP</i> animals.....	9
Figure S5A,B. Co-detection of <i>Sp5</i> and <i>Wnt3</i> expression in <i>HySp5-3169</i> :GFP_ep (A) and <i>HySp5-3169</i> :GFP-ga (B) transgenic animals exposed to Alsterpaullone (ALP).....	10
Figure S5C,D. Co-detection of <i>GFP</i> and <i>Wnt3</i> expression in <i>HySp5-3169</i> :GFP_ep (C) and <i>HySp5-3169</i> :GFP-ga (D) transgenic animals exposed to Alsterpaullone (ALP).....	11
Figure S6A,B. Co-detection of <i>Sp5</i> and <i>Wnt3</i> expression in <i>HyWnt3-2149</i> :GFP_ep (A) and <i>HyWnt3-2149</i> :GFP-ga (B) transgenic animals exposed to Alsterpaullone (ALP).....	12
Figure S6C,D. Co-detection of <i>GFP</i> and <i>Wnt3</i> expression in <i>HyWnt3-2149</i> :GFP_ep (C) and <i>HyWnt3-2149</i> :GFP-ga (D) transgenic animals exposed to Alsterpaullone (ALP).....	13
Figure S7. Ectopic "bump" structures along the body column of <i>Hv-Basel</i> animals knocked-down for <i>b-catenin</i>	14
Figure S8. Ectopic epidermal GFP fluorescence in <i>HySp5-3169</i> :GFP_ep animals knocked-down for <i>β-catenin</i>	16
Figure S9. GFP fluorescence and <i>GFP</i> expression in <i>HySp5-3169</i> :GFP_ep animals knocked-down for <i>Sp5</i>	17
Figure S10. Ectopic epidermal <i>GFP</i> expression in <i>HySp5-3169</i> :GFP_ep animals knocked-down for <i>Sp5</i>	19
Figure S11. GFP fluorescence and <i>GFP</i> expression in <i>HySp5-3169</i> :GFP_ga animals knocked-down for <i>Sp5</i>	21
Figure S12. Gastrodermal <i>GFP</i> expression in <i>HySp5-3169</i> :eGFP_ga animals knocked-down for <i>Sp5</i>	23
Figure S13. Transient ectopic <i>GFP</i> expression in <i>HySp5-3169</i> :GFP <i>Sp5</i> (RNAi) animals 2 days post-EP2.....	24
Figure S14. ChIP-qPCR analysis of the <i>Sp5</i> -binding sites in the <i>Hydra Sp5</i> promoter using anti <i>Hydra Sp5</i> antibodies.....	25
APPENDIX	27
A1. Mapping the <i>Sp5</i> Transcriptional Start Sites (TSS).....	27
A2. <i>HyActin-1388</i> :mCherry- <i>HySp5-3169</i> :eGFP map and sequences (10'533 bp).....	28

SUPPLEMENTARY FIGURES



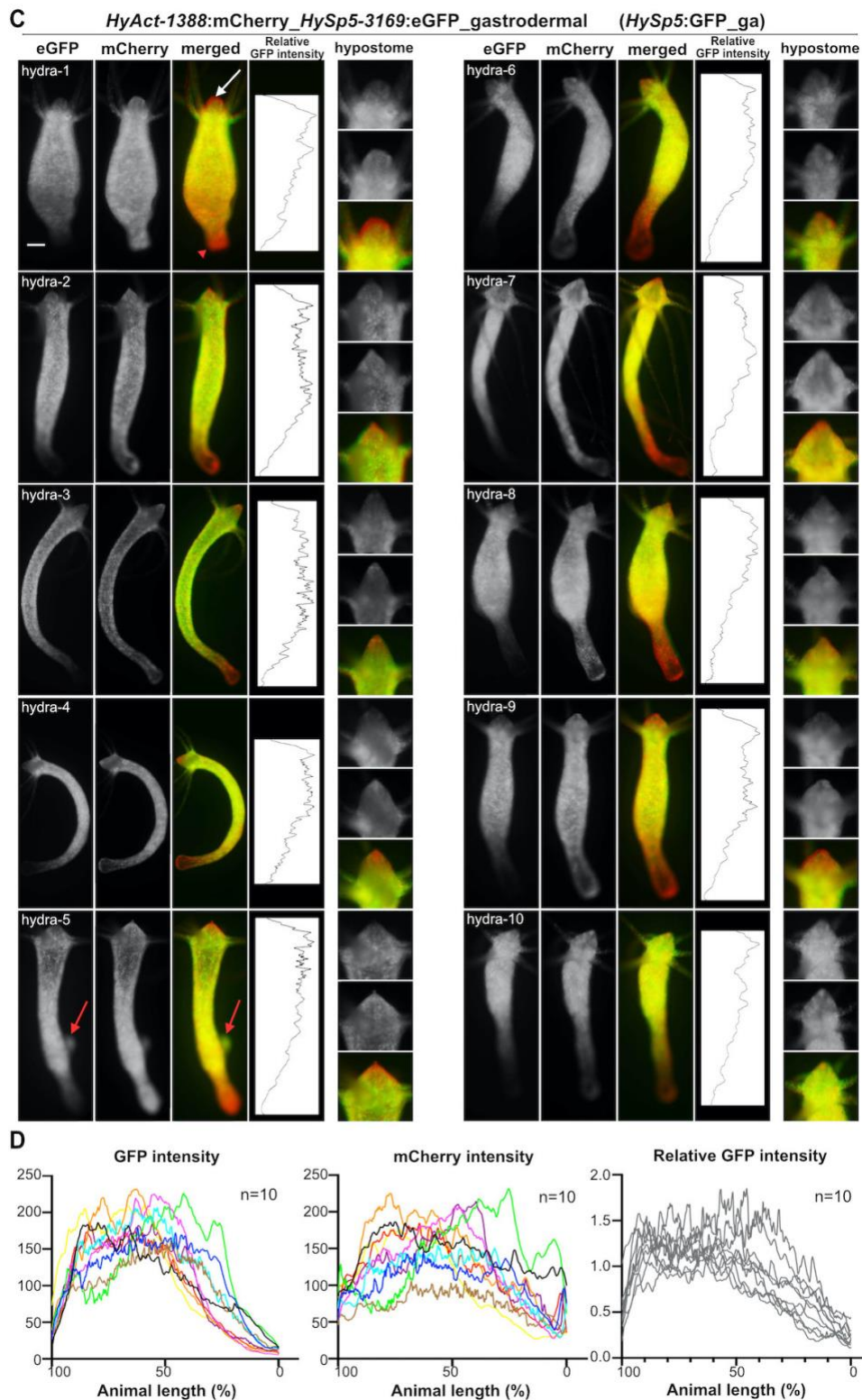


Figure S1. Epidermal and gastrodermal eGFP and mCherry fluorescences detected in live *HySp5-3169:GFP-ep* and *HySp5-3169:GFP-ga* transgenic animals.

(A, C) Live imaging of GFP (green) and mCherry (red) fluorescences in *HySp5-3169:GFP-ep* (A) and *HySp5-3169:GFP-ga* (C) transgenic animals maintained in homeostatic conditions (n=10). The ratio between the eGFP and mCherry fluorescences is shown as the relative eGFP intensity. Magnified views of the hypostome are shown on the right. White arrows indicate tips of the hypostome; red arrows point to GFP fluorescence in budding regions, red arrowheads to basal regions. Scale bar: 250 μ m. Note the lack of GFP fluorescence at the tip of the hypostome of *HySp5-3169:GFP-ga* animals. (B, D) Graph displaying the GFP (center),

mCherry (middle) and relative GFP (right) intensities along the apical (100%, left) to basal (0%, right) axis of the animals. **Supplement to Figure 1C-1F.**

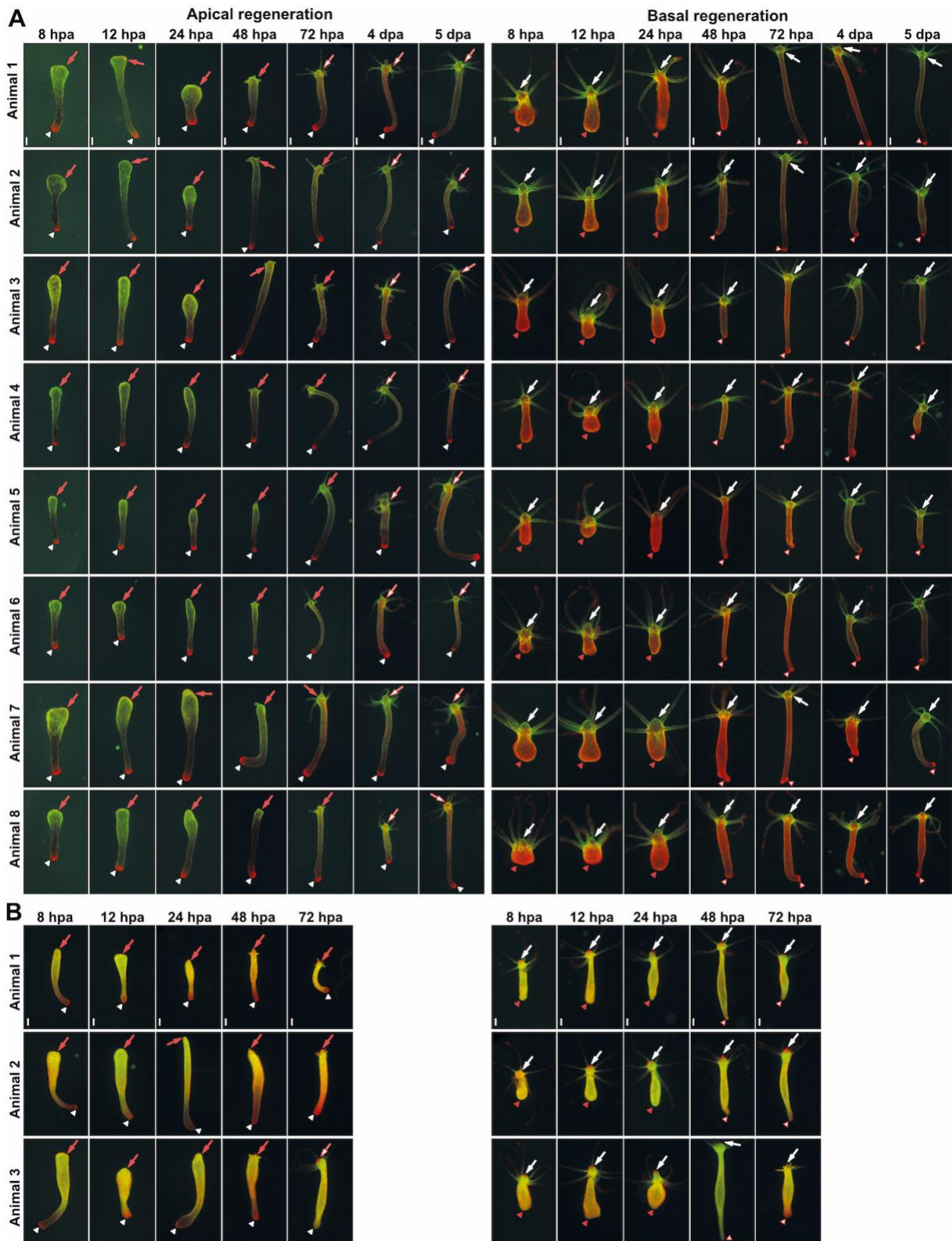


Figure S2. GFP fluorescence detected in live *HySp5-3169:GFP_ep* (A) and *HySp5-3169:GFP_ga* (B) animals undergoing apical or basal regeneration

(A-B) Live imaging of GFP and mCherry fluorescence in *HySp5-3169:GFP_ep* (A) and *HySp5-3169:GFP_ga* (B) transgenic animals in apical- and basal-regenerating halves pictured at 8, 12, 24, 48 and 72 hpa. *HySp5-3169:GFP_ep* animals are also live imaged at 4 and 5 dpa in apical- and basal-regenerating halves. White arrows indicate the apical regions of original polyps; red arrows to the apical-regenerating regions; white arrowheads to the basal-regenerating regions.

arrowheads to the basal regions of original polys and red arrowheads to the basal-regenerating regions.
Scale bar: 250 μm .

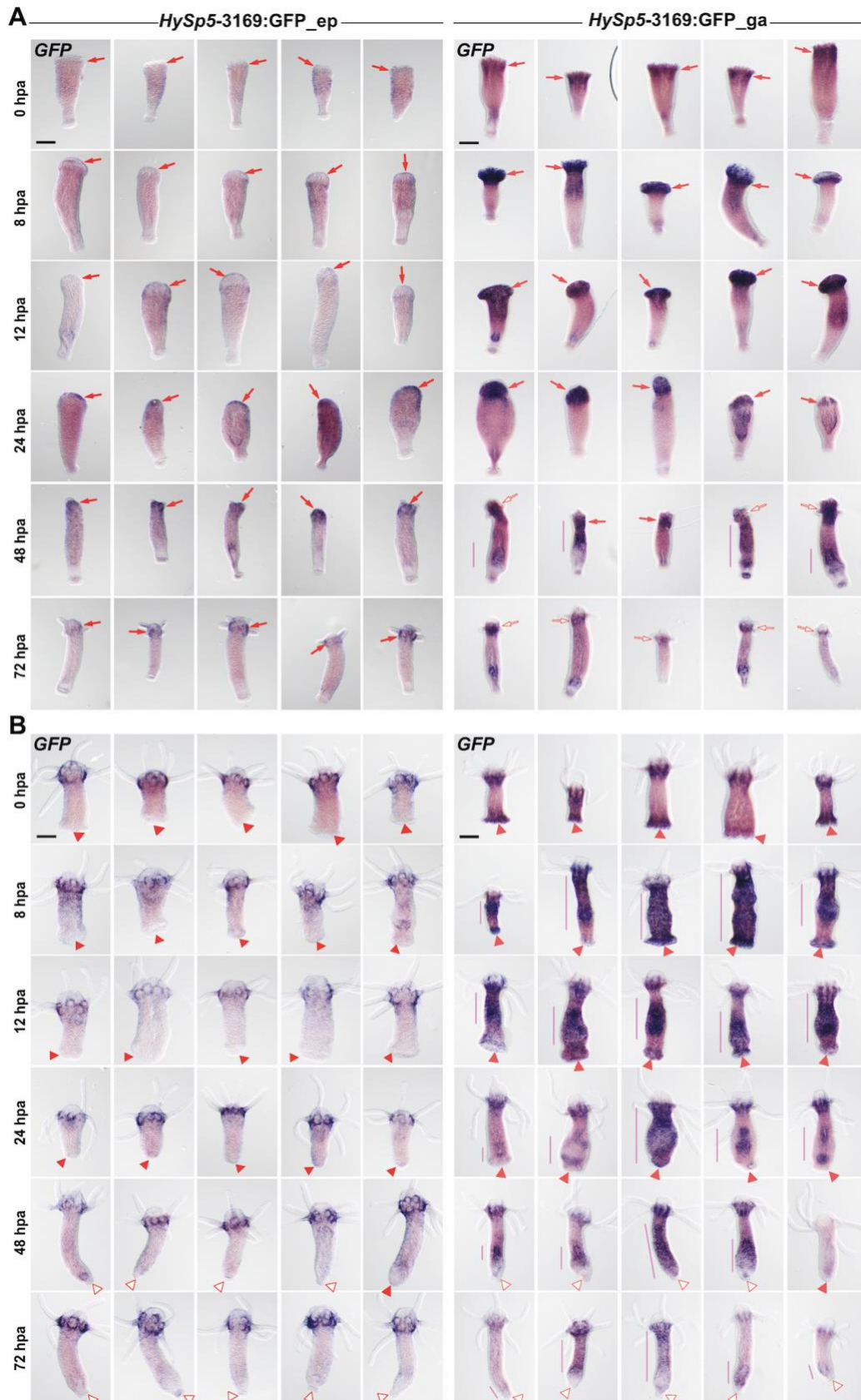


Figure S3. *GFP* expression in *HySp5-3169:GFP_ep* and *HySp5-3169:GFP_ga* animals undergoing apical (A) or basal (B) regeneration.

GFP expression in apical- (A) and basal-regenerating (B) halves taken at 0, 8, 12, 24, 48 and 72 hours post amputation (hpa). Arrows: developing apical regions of *HySp5-3169:GFP_ep* (red) or *HySp5-3169:GFP_ga*

(brown) animals; brown vertical bars: gastrodermal *GFP* expression along the body column; red triangles: basal region undergoing differentiation; white triangles: differentiated basal discs. Scale bar: 250 μm .

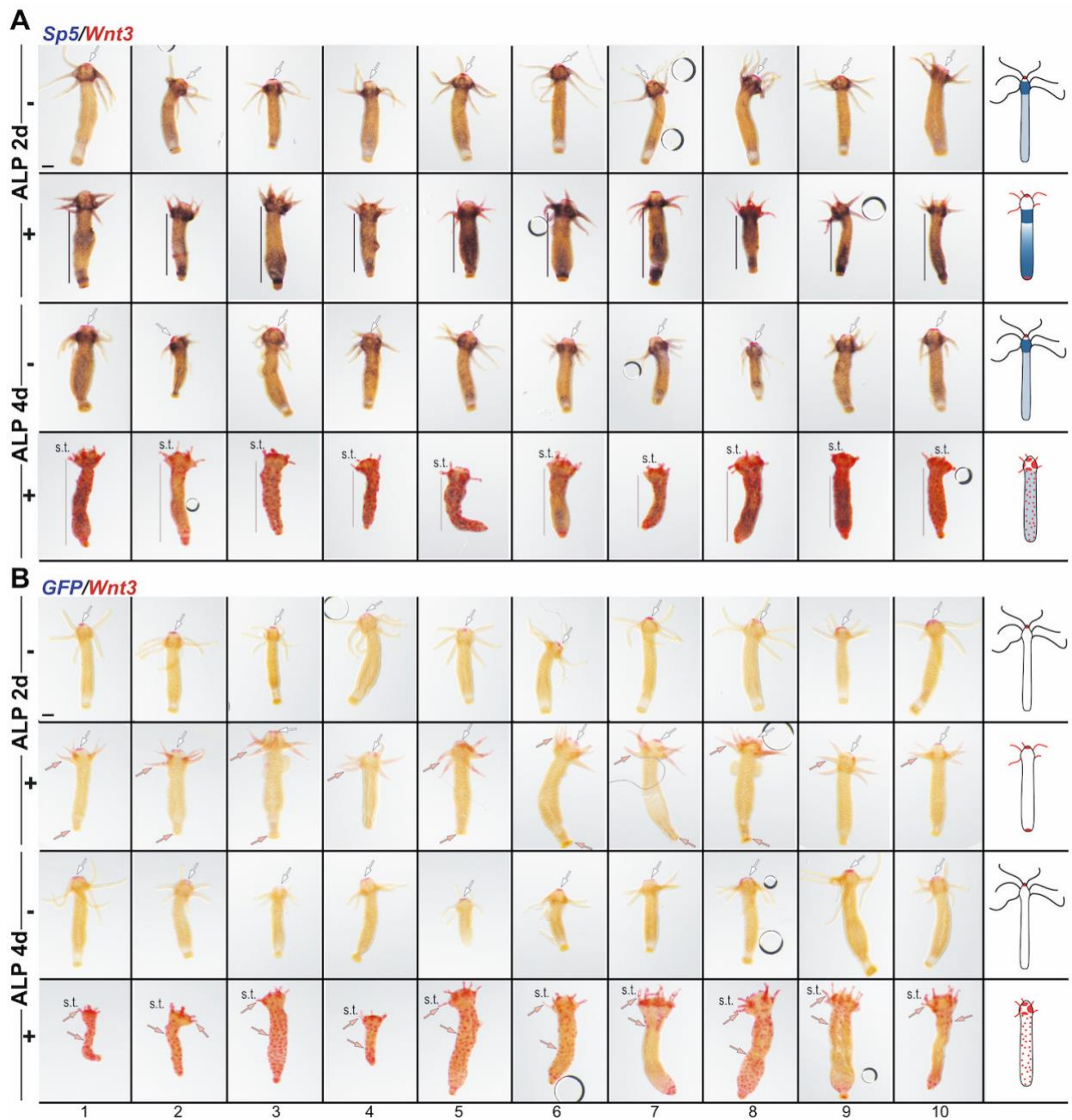


Figure S4. Alsterpaullone (ALP)-induced modulations of *Sp5*, *Wnt3* and *GFP* expression in *Hv_AEP* animals. Double WMISH detecting *Sp5* (dark blue) and *Wnt3* (red) (A), or *GFP* (dark blue) and *Wnt3* (red) (B) in animals untreated (DMSO) or treated with alsterpaullone (ALP) for 2 or 4 days. Schematic views of *Hydra* polyps on the right depict the typical expression profile of each condition. As expected, wt *Hv_AEP* animals do not express *GFP*. Scale bar: 200 μ m; s.t.: short tentacles; white arrows: apical *Wnt3* homeostatic expression domain; salmon arrows: ectopic *Wnt3* expression domains; black bars: *Sp5* expression domain along the body column.

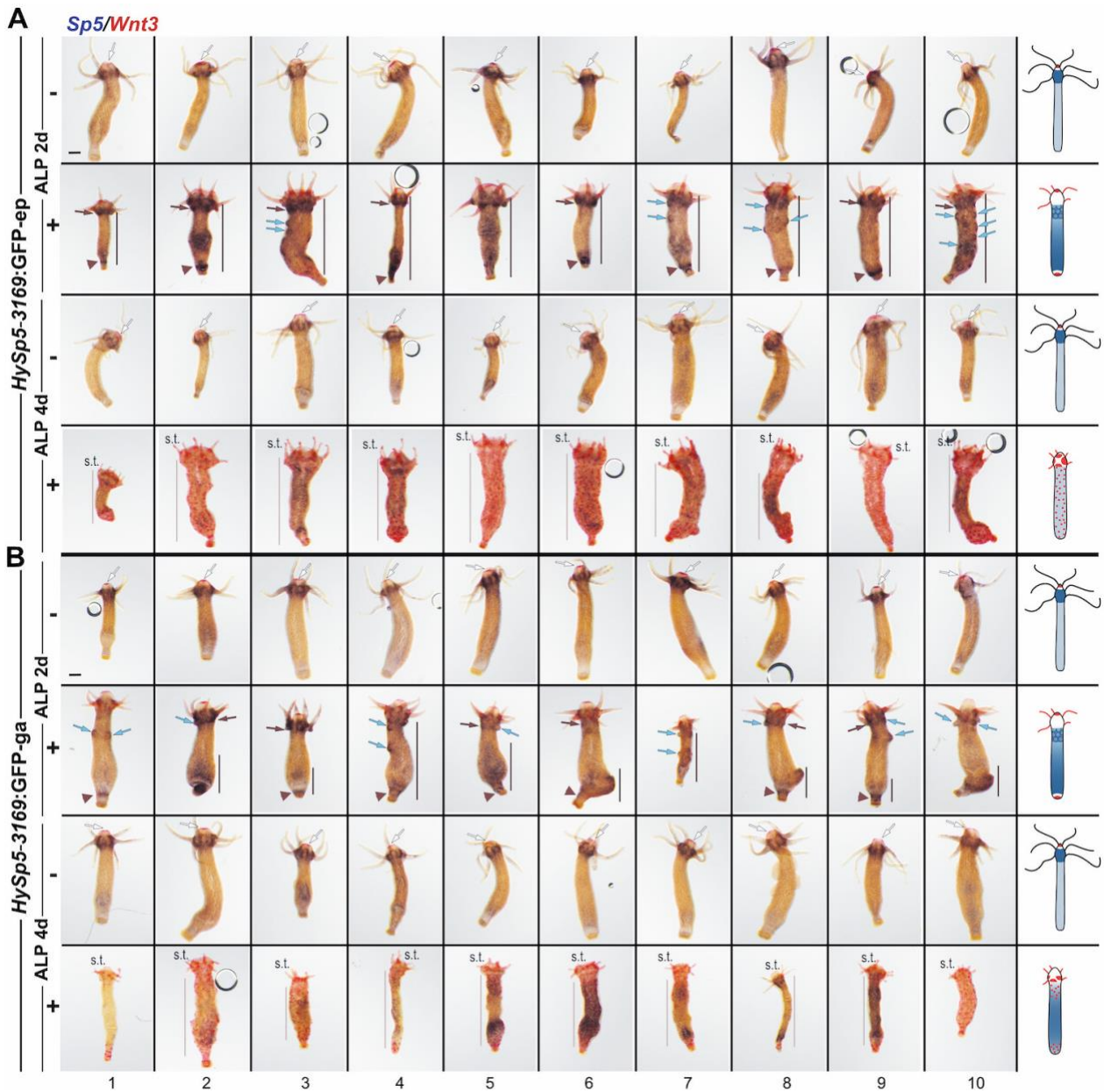


Figure S5A,B. Co-detection of *Sp5* and *Wnt3* expression in *HySp5-3169:GFP-ep* (A) and *HySp5-3169:GFP-ga* (B) transgenic animals exposed to Alsterpaullone (ALP)

Double WMISH showing *Sp5* expression (dark blue) and *Wnt3* expression (red) in animals treated with DMSO (-) or ALP (+) for 2 or 4 days. Schematic views of *Hydra* polyps on the right of each row depict the typical expression profile of each condition. Black arrows: *Sp5* apical expression domain; black bars: *Sp5* expression domain along the body column; black triangles: *Sp5* basal expression domain; light blue arrows: circular *Sp5* expression; s.t.: short tentacles; white arrows: apical *Wnt3* homeostatic expression domain; scale bars: 200 μ m.

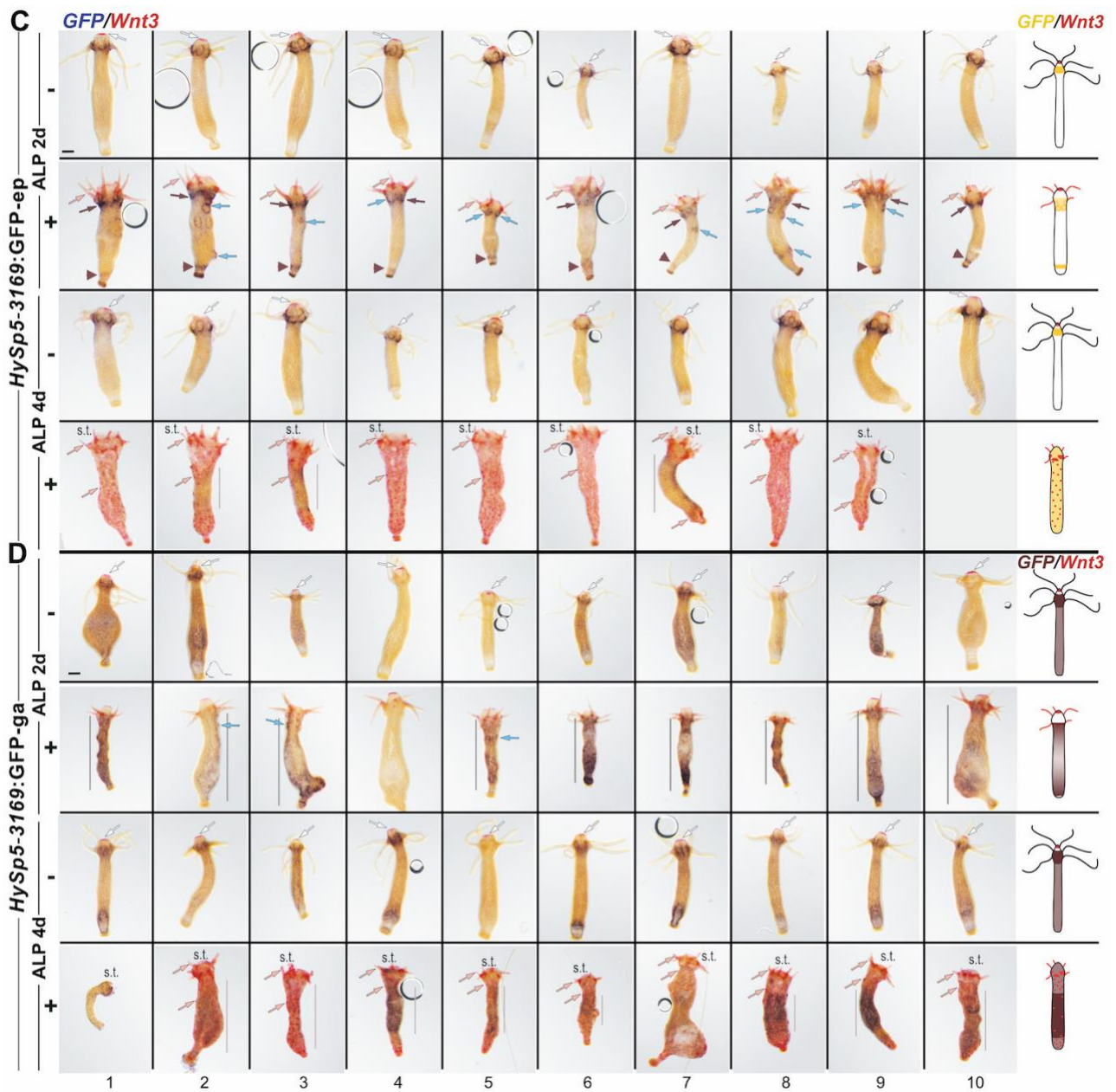


Figure S5C,D. Co-detection of *GFP* and *Wnt3* expression in *HySp5-3169:GFP-ep* (C) and *HySp5-3169:GFP-ga* (D) transgenic animals exposed to Alsterpaullone (ALP)

Double WMISH showing *GFP* (dark blue) and *Wnt3* (pink) expression in animals treated with DMSO (-) or ALP (+) for 2 or 4 days. Schematic views of *Hydra* polyps on the right of each row depict the typical expression profile of each condition. Black arrows point to the upper body column *Sp5* expression domain immediately below the tentacle ring; black bars: *Sp5* expression domain along the body column; black triangles: *Sp5* basal expression domain; light blue arrows: circular *Sp5* expression; white arrows: homeostatic *Wnt3* expression at the tip of the hypostome; salmon arrows: ectopic *Wnt3* expression in the tentacles along the body column or at the basal extremity; s.t.: short tentacles; scale bars: 200 μ m.

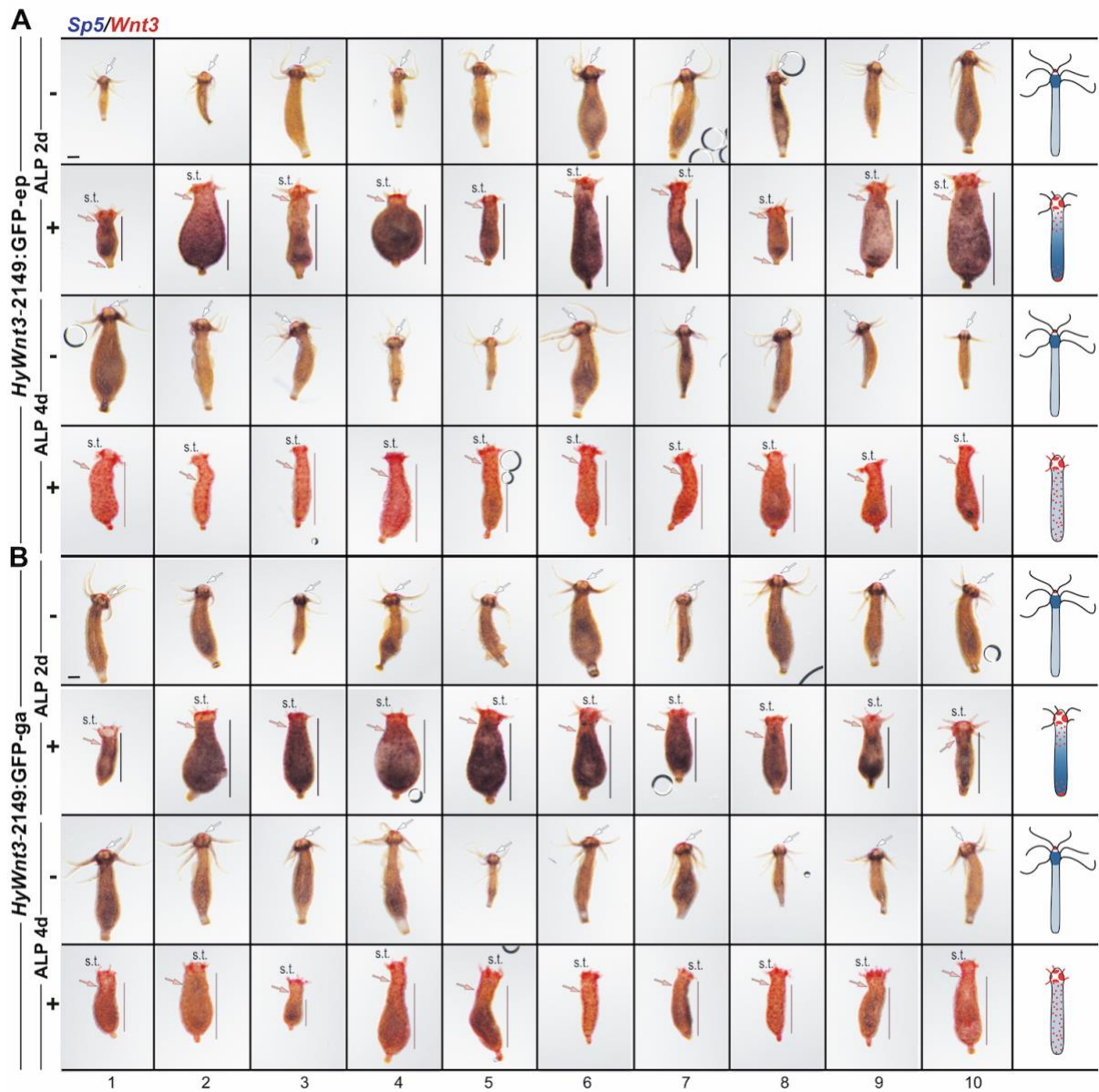


Figure S6A,B. Co-detection of *Sp5* and *Wnt3* expression in *HyWnt3*-2149:GFP-ep (A) and *HyWnt3*-2149:GFP-ga (B) transgenic animals exposed to Alsterpaullone (ALP)

Double WMISH showing *Sp5* (dark blue) and *Wnt3* (red) expression in animals treated with DMSO (-) or ALP (+) for 2 or 4 days. Schematic views of *Hydra* polyps on the right of each row depict the typical expression profile of each condition. Black bars: *Sp5* expression domain along the body column; white arrows: homeostatic *Wnt3* expression at the tip of the hypostome; salmon arrows: ectopic *Wnt3* expression in the tentacles, along the body column or at the basal extremity; s.t.: short tentacles; scale bars: 200 μ m.

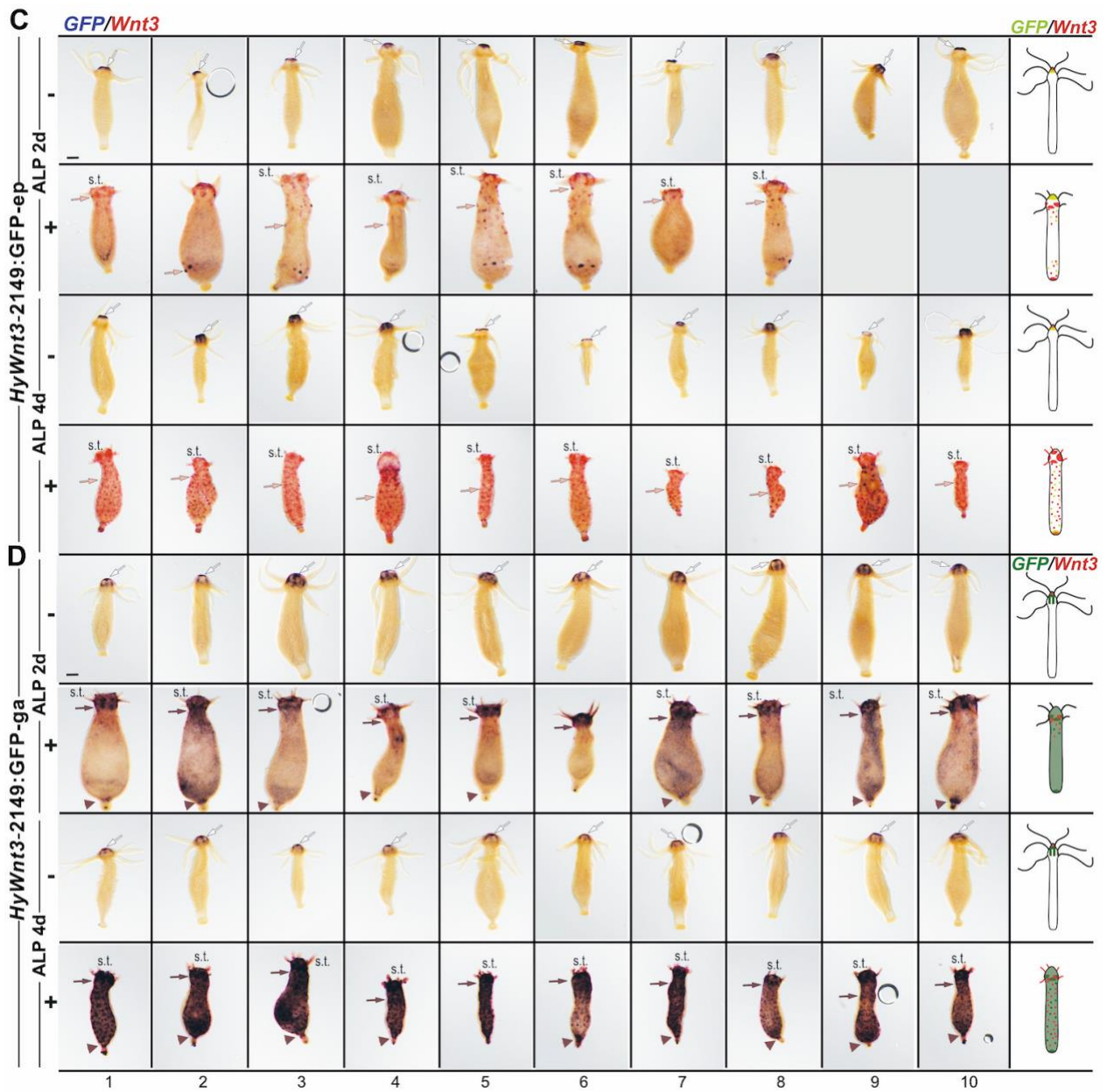


Figure S6C,D. Co-detection of *GFP* and *Wnt3* expression in *HyWnt3-2149:GFP-ep* (C) and *HyWnt3-2149:GFP-ga* (D) transgenic animals exposed to Alsterpaullone (ALP)

Double WMISH showing *GFP* (dark blue) and *Wnt3* (red) expression in animals treated with DMSO (-) or ALP (+) for 2 or 4 days. Schematic views of *Hydra* polyps on the right of each row depict the typical expression profile of each condition. White arrows: apical *GFP* expression at the tip of the hypostome; gray arrows: *GFP* expression at the base of the apical region; salmon arrows: ectopic *Wnt3* expression along the body column; gray triangles: *GFP* expression at the basal extremity; s.t.: short tentacles; scale bars: 200 μ m.

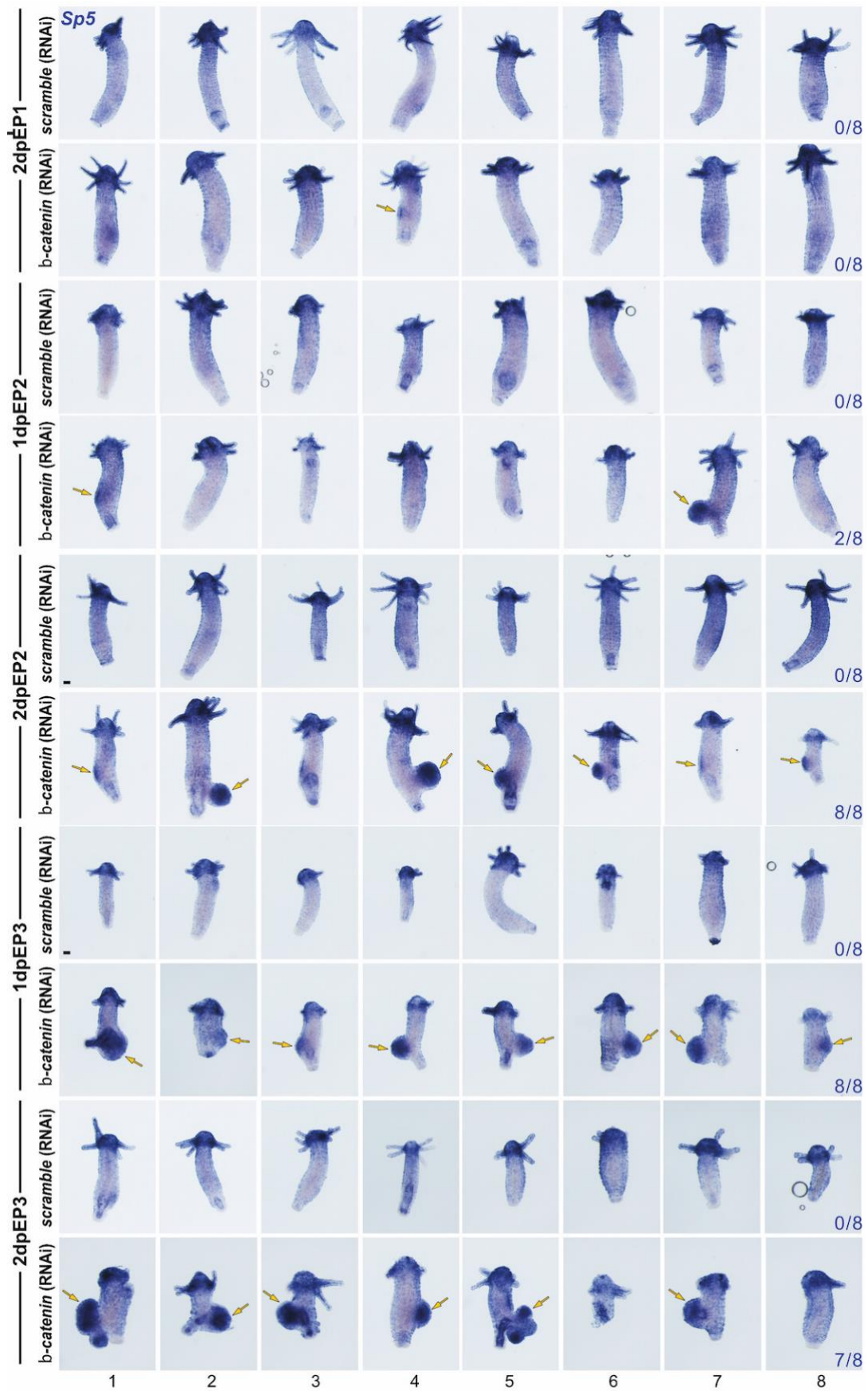
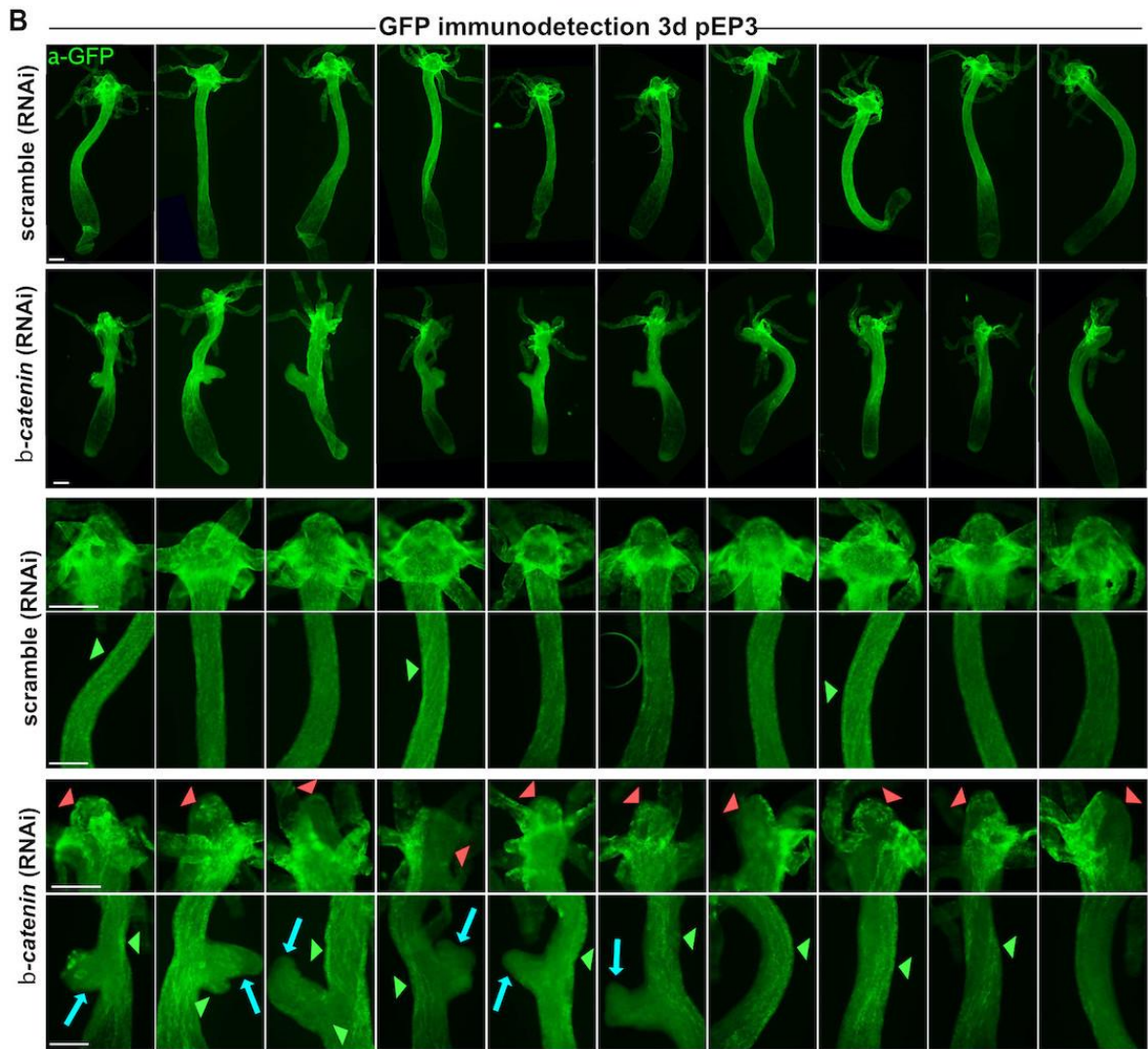
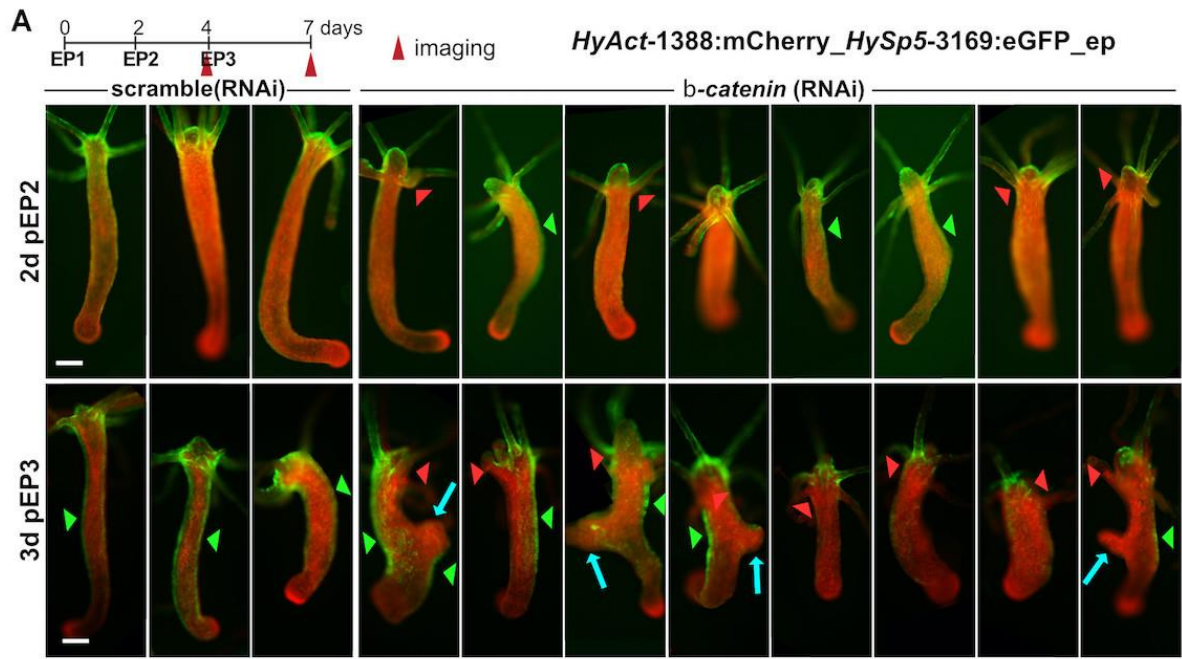


Figure S7. Ectopic "bump" structures along the body column of *Hv-Basel* animals knocked-down for *b-catenin*. *Hv-Basel* animals electroporated three times with scramble or β -*catenin* siRNAs and fixed at indicated time-points for detecting *Sp5* expression by WMISH. Yellow arrows point to presumptive (patches) or already grown bump structures that highly express *Sp5*. Scale bars: 200 μ m.



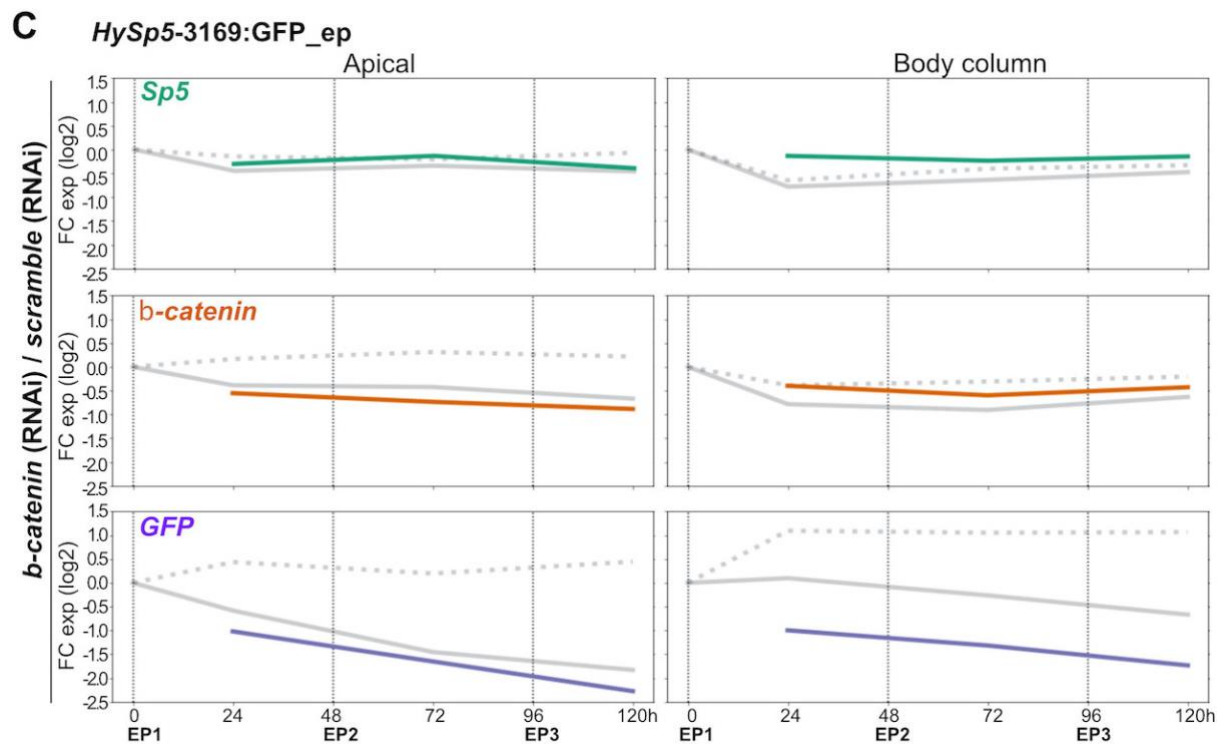


Figure S8. Ectopic epidermal GFP fluorescence in *HySp5-3169:GFP_ep* animals knocked-down for β -catenin
(A) Live imaging of GFP fluorescence in *HySp5-3169:GFP_ep* transgenic animals electroporated twice with scramble or β -catenin siRNAs, 2 days post-EP2. Red triangles indicate apical areas where GFP fluorescence is reduced, green arrows the areas where GFP is ectopically expressed along the body column and blue arrows the bump structures where GFP fluorescence is absent. Scale bars: 250 μ m. **See Figure 4A.** **(B)** Immunodetection of GFP performed on scramble (control) and β -catenin (RNAi) animals 3 days post-EP3. Enlarged views of the apical region and body column are shown below each condition. GFP fluorescence is largely reduced in apical regions (red triangles), absent from the bump structures (blue arrows) and limited along the body column (green triangles). Scale bars: 250 μ m. **See Figure 4B.** **(C)** Q-PCR analysis of *Sp5*, β -catenin and *GFP* transcript levels in apical region (100%-80%) and body column (80%-0%) of *HySp5-3169:GFP_ep* animals at indicated time-points after EP1, EP2 and EP3. Ratios between values obtained in β -catenin (RNAi) and scramble (RNAi) animals are shown. **See Figure 4C.**

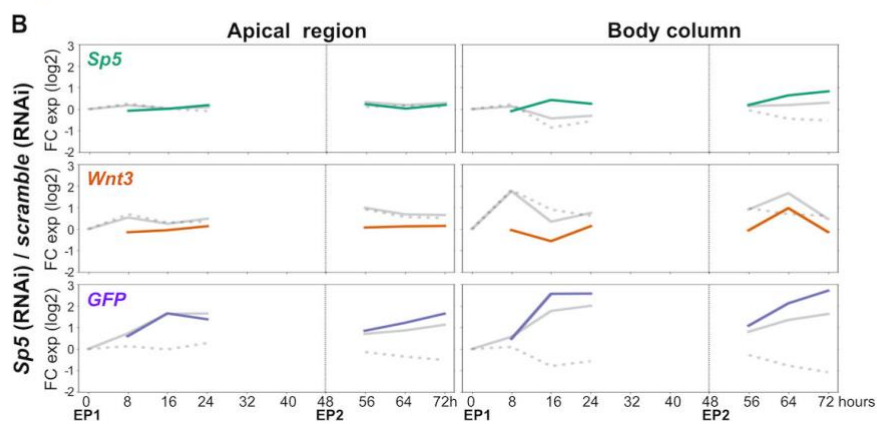
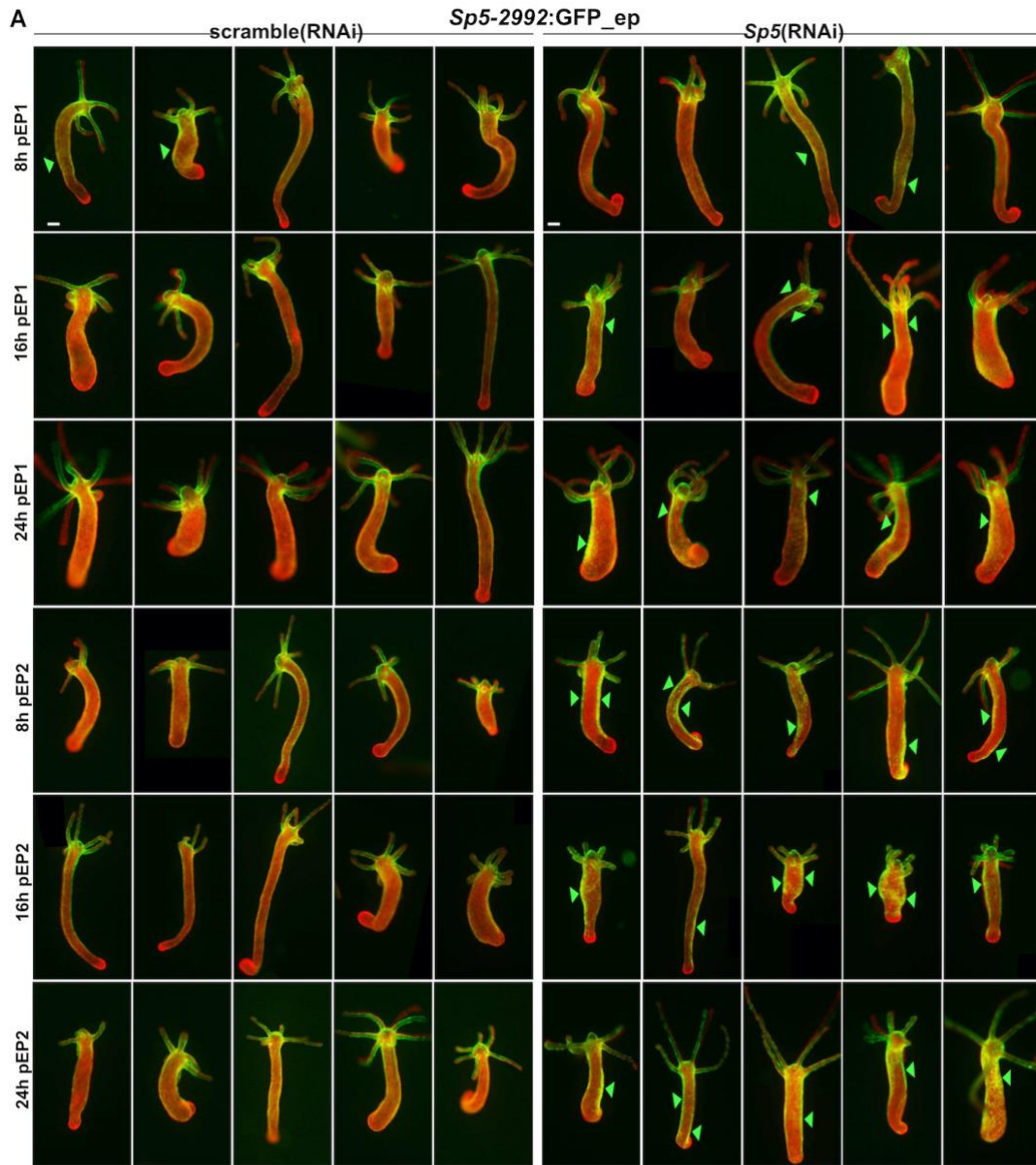


Figure S9. GFP fluorescence and *GFP* expression in *HySp5-3169:GFP_ep* animals knocked-down for *Sp5*
(A) GFP fluorescence in five representative *HySp5-3169:GFP_ep* animals electroporated with scramble or *Sp5* siRNAs and imaged at 8, 16, 24 hours post-EP1 (pEP1) and 8, 16, 24 hours post-EP2 (pEP2). Images from GFP and mCherry merged channels are shown. Green triangles indicate areas of ectopic GFP fluorescence along the body column. Scale bars: 200 μ m. **See Figure 5A, 5B left panel.** **(B)** Q-PCR analysis of *Sp5*, *Wnt3* and *GFP* transcript levels in apical region (100%-80%) and body column (80%-0%) of *HySp5-3169:GFP_ep* animals at

indicated time-points after EP1 and EP2. Ratios between values obtained in *Sp5* (RNAi) and scramble (RNAi) animals (continuous and dotted grey lines respectively) are shown. **See Figure 5D.**



Figure S10. Ectopic epidermal *GFP* expression in *HySp5-3169:GFP_ep* animals knocked-down for *Sp5* *GFP* expression in *HySp5-3169:GFP_ep* animals either untreated (wt, uppest row), or electroporated once or twice with scramble or *Sp5* siRNAs (EP1, EP2) with EP2 performed two days after EP1. Ten animals are shown per condition at six different time points, 8, 16, 24 hours post-EP1 (hpEP1); 8, 16, 24 hours post-EP2 (hpEP2).

Bars indicate ectopic *GFP* expression in the body column at 8, 16 and 24 hours post-EP1 and post-EP2. Scale bars: 250 μ m. See Figure 5C.

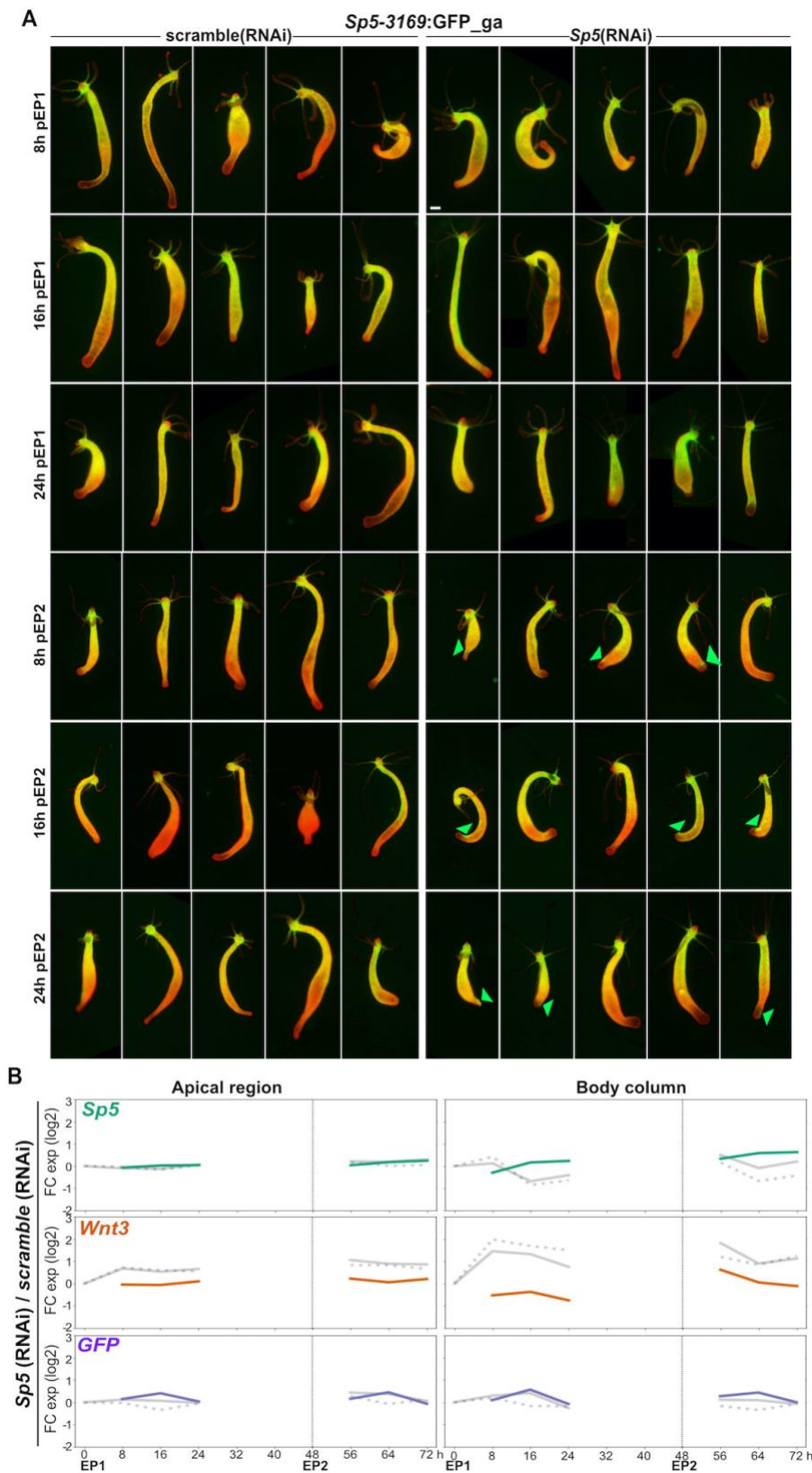


Figure S11. GFP fluorescence and *GFP* expression in *HySp5-3169:GFP_ga* animals knocked-down for *Sp5*
(A) GFP fluorescence in five representative *HySp5-3169:GFP_ga* animals electroporated with scramble or *Sp5* siRNAs and imaged at 8, 16, 24 hours post-EP1 (pEP1) and 8, 16, 24 hours post-EP2 (pEP2). Images from GFP and mCherry merged channels are shown. Green triangles indicate spots of ectopic GFP fluorescence along the body column. Scale bars: 200 μ m. See Figure 5A, 5B right panel. **(B)** Q-PCR analysis of *Sp5*, *Wnt3* and *GFP* expression levels in apical region (100%-80%) and body column (80% - 0%) of *HySp5-3169:GFP_ga* animals

at indicated time-points after EP1 and EP2. Ratios between values obtained in *Sp5* (RNAi) animals and scramble (RNAi) animals are shown. **See Figure 5E.**

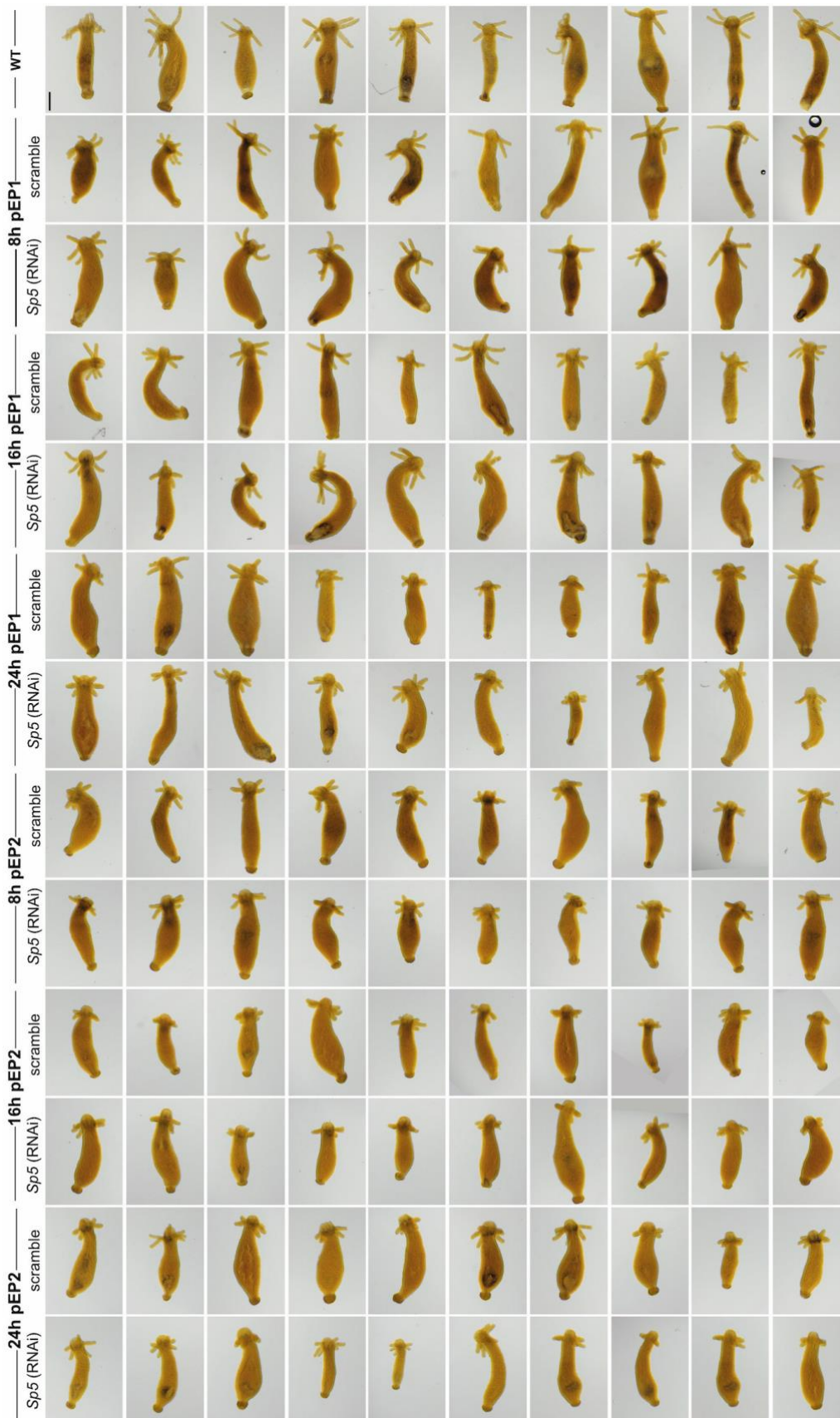


Figure S12. Gastrodermal *GFP* expression in *HySp5-3169:eGFP_ga* animals knocked-down for *Sp5*. *GFP* expression in *HySp5-3169:eGFP_ga* animals, either untreated (uppermost row) or electroporated (EP1, EP2) with scramble (control) or *Sp5* siRNAs. Ten animals are shown per condition at six different time points, 8, 16 and 24 hours post EP1 or EP2 with EP2 performed 2 days after EP1. Note the absence of significant modulations in *GFP* expression in the different conditions. Scale bars: 250 μ m. See Figure 5C.

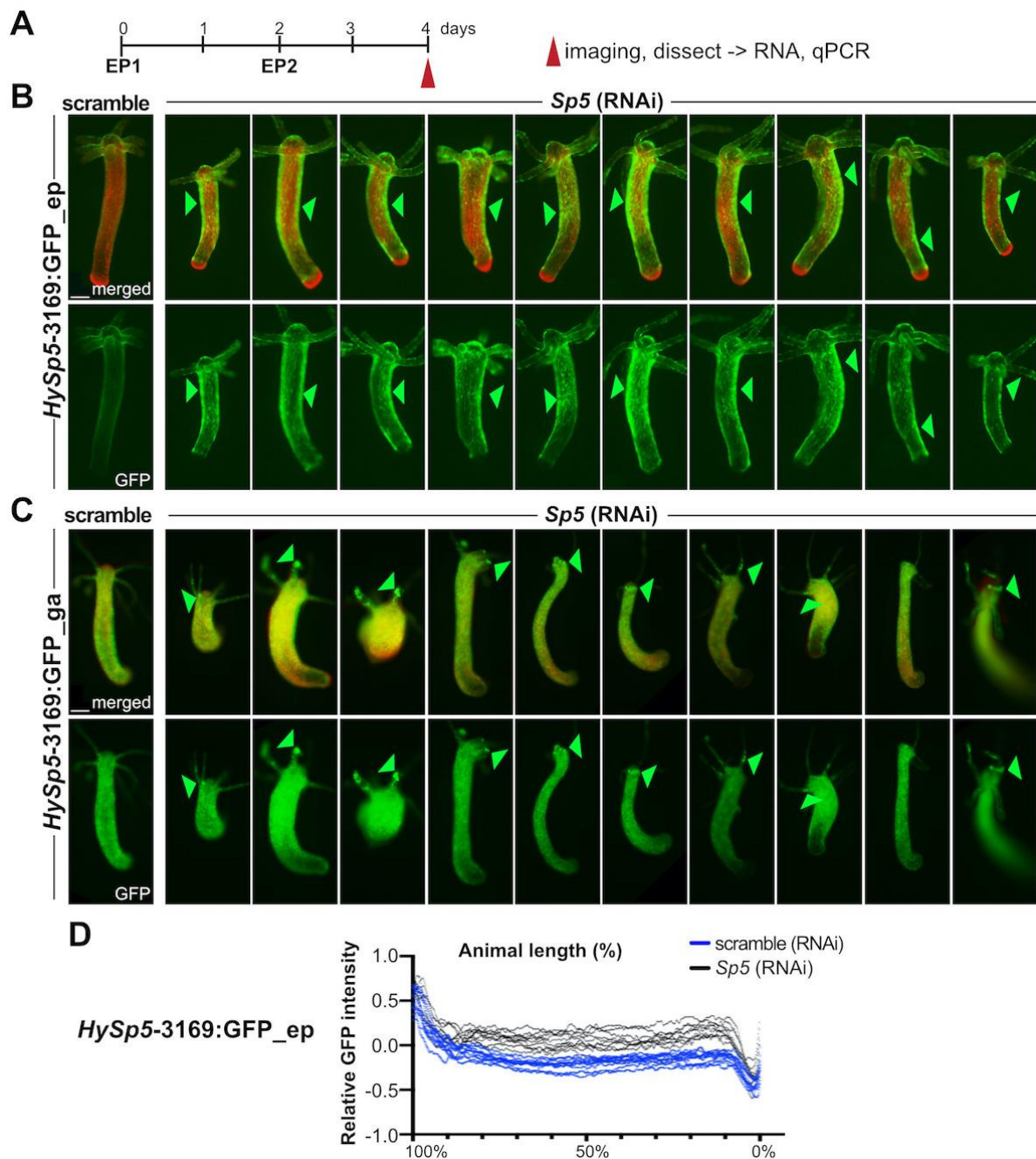


Figure S13. Transient ectopic *GFP* expression in *HySp5-3169:GFP Sp5(RNAi)* animals 2 days post-EP2

(A) Schematic view of the procedure where animals are exposed twice to scramble or *Sp5* siRNAs and pictured two days later (2d pEP2). (B, C) Live imaging of *HySp5-3169:GFP_ep* (B) and *HySp5-3169:GFP_ga* (C) on 2d pEP2. Green triangles point to ectopic areas of GFP fluorescence, along the epidermis in the body column or in the tentacles. Scale bars: 250 μ m. (D) Measurement two days post-EP2 of the relative GFP intensity in *HySp5-3169:GFP_ep* animals exposed to scramble or *Sp5* siRNAs (panel F, n=10). See Figure 5E-G.

A *Hydra Sp5* protein sequence (411aa)

Sp box IKYSP LALLAATCKKIGRP ISPLEQTS PKKIFOPWNHTFESHNYDT α-Sp5 Monoclonal

MSPPSRVPTTISP NFKSQHHCLKEH IKYSP LALLAATCKKIGRP ISPLEQTS PKKIFOPWNHTFESHNYDT
PISPNSKVRHFLETNFSLPPSPPLKSEIVKVPPTIRPMPMTNVMQEKATLNYSOKLSPPPCLACSAGOKCN

α-Sp5 Polyclonal

GINKISPVLLSPPASPISWLF PQNI IQSHPSKVS INEHHIKEYSEHSQADPTRFVN YVYKNVDSSQAKPNL

Btd Box

IIRHDNMISSSTOSYNNRIFSSSPHLTTTSHIYSMSTSI PAQSHAVIPNSVATRR CRRRCKPCNCLSGQQSEP

ZF domain ZF domain

NKPKCHVCHIPGCGKVYGKTSHLKAHLRWH AGLR FVCNWLFCNKSFTRSDELQRHLRTH TGEKRFACQDC

ZF domain α-Sp5 Polyclonal

GKRFTRSDHLSKHMKTH QNKKQENTFVKD TVIEVIKDNVDEN CDENVMELEVNVEN

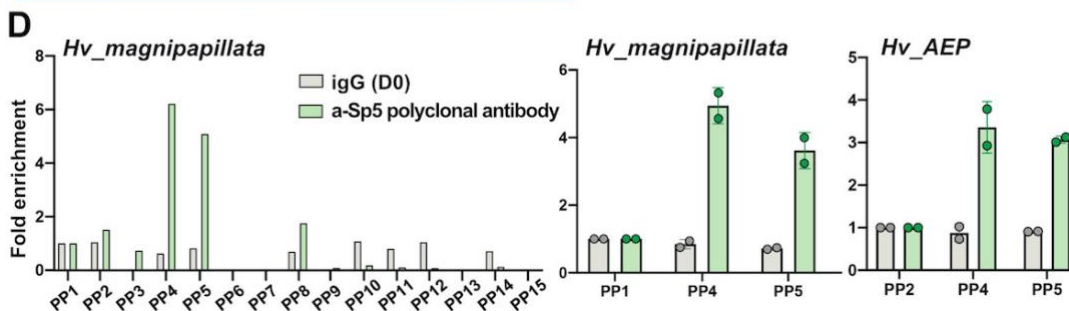
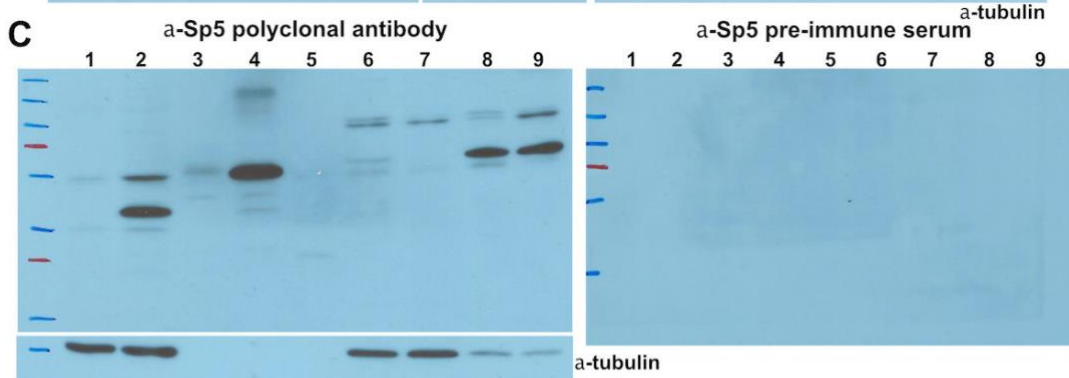
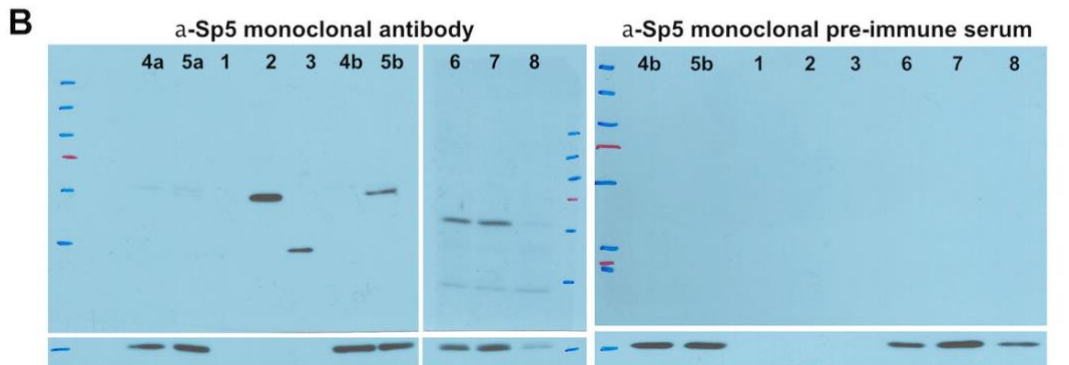
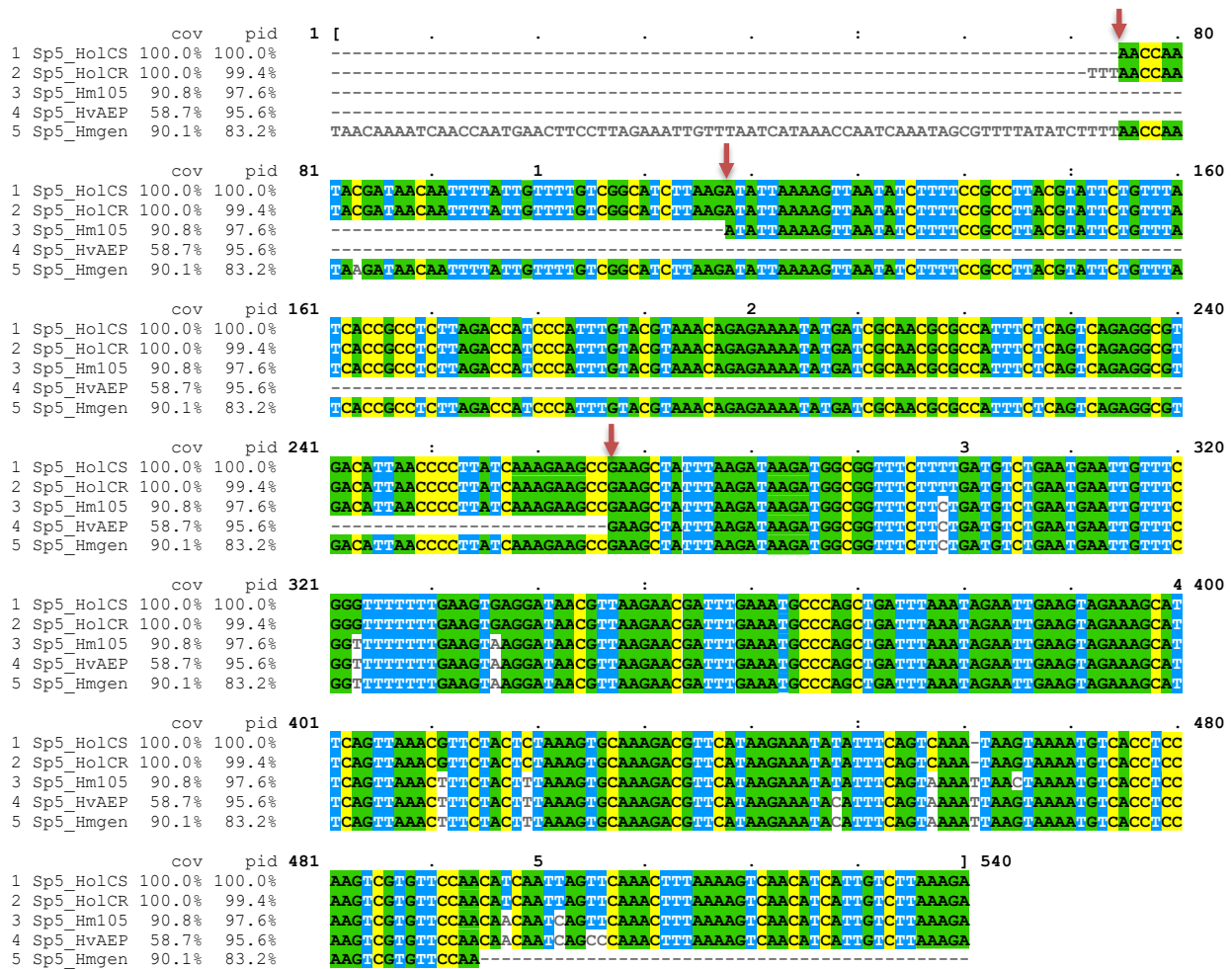


Figure S14. ChIP-qPCR analysis of the Sp5-binding sites in the *Hydra Sp5* promoter using anti Hydra-Sp5 antibodies.

(A) HySp5 protein sequence with the different domains highlighted in boxes (Sp box: green, Btd box: purple, zinc finger domains: blue). The sequence used to raise the monoclonal anti-Sp5 antibody is underlined, the peptides used to raise the polyclonal antibody are written green. (B) Western blot showing that the anti-Sp5 monoclonal antibody but not the pre-immune serum detects Sp5 protein. Conditions, identical for both films, are detailed in Figure 5E. (C) Western blot showing that the anti-Sp5 polyclonal antibody detects the HySp5 protein expressed in HEK293T cells (lane 2), produced with TNT (lane 4), or as partial recombinant protein (lane 5, 24.5kDa), in *Hydra* NEs when prepared from the body column (lane 8) or the basal region (lane 9) but not from whole animal (lane 6) or from the apical region (lane 7). (D) Graph comparing the enrichment obtained by ChIP-qPCR with *Hv_magnipapillata* extracts using the anti-Sp5 polyclonal antibody and 15 primer pairs (left). An enrichment is only found in regions PP4 and PP5. Graph comparing the

enrichment of regions PP1, PP4 and PP5 (middle) or regions PP2, PP4 and PP5 (right) after ChIP-qPCR using *Hv_magnipapillata* or *Hv_AEP* extracts with the anti-Sp5 polyclonal antibody.

APPENDIX



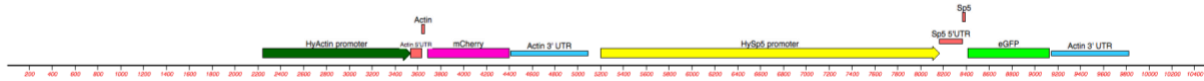
A1. Mapping the *Sp5* Transcriptional Start Sites (TSS)

Sp5 cDNAs sequences obtained on [HydrAtlas](#) (Wenger et al. 2019) for Cold Sensitive or Cold Resistant *H. oligactis* (HolCS, HolCR) and *Hv_AEP H. vulgaris* strains, on NCBI for *Hm105* were first aligned to the *Sp5 H. magnipapillata* genomic sequence (Sp5_Hmgen) with the [Muscle Align](#) software selecting a ClustalW output format, then the alignment was visualized with the [MView](#) tool (Madeira et al., 2022). The three vertical red arrows indicate the transcriptional start sites (TSS): TSS1 from *Hv_AEP* (position +1), TSS2 from *Hm105* (position -149) and TSS3 from *H. oligactis* (position -192). Accession numbers: *Sp5_HolCS*: S034511c0g1_i01; *Sp5_HolCR*: R029443c0g1_i01; *Sp5_HvAEP*: c16537_g1_i01; *Sp5_Hm105* XM_004206770.3. The *Sp5* cDNA sequence from *Hv_Jussy* (seq62049_loc 21222) was not used as its 5'UTR sequence is divergent, suggesting a distinct TSS.

Madeira F, Pearce M, Tivey ARN, et al. (2022). Search and sequence analysis tools services from EMBL-EBI in 2022. *Nucleic Acids Res* Apr;gkac240. DOI: 10.1093/nar/gkac240.

Wenger Y, Buzgariu W, Perruchoud C, Loichot G, Galliot B. (2019). Generic and context-dependent gene modulations during *Hydra* whole body regeneration. *BioRxiv* 587147; doi: [10.1101/587147](https://doi.org/10.1101/587147)

A2. HyActin-1388mCherry-HySp5-3169.eGFP map and sequences (10'533 bp)



pBSSA-AR plasmidic sequence (2'244 bp)

```

1  gtggcacttttcggggaaatgtgcgcggaaccctatttgtttatTTTTTCTAAATACATTCAAATATGTATCCGCTCATGAGACAATAACCCTGATAAAT
101 gcttcaataatattgaaaaaggaagagatgatgattcaacatttccgtgtcgccttattcccttttttgcggcattttgcttctctgtttttgctcac
201 ccagaaacgctggtgaaagttaaagatgctgaagatcagttgggtgacagagtggttacctgcaactggatctcaacagcggtaagatccttgagagtt
301 ttcccccgaagaacgttttccaatgatgagcacttttaaagtctgctatgtggcgcgggtattatccogtatgacgccgggcaagagcaactcggctg
401 ccgcatacactattctcagaatgacttgggtgagtagtaccagctcagaaaaagcatcttacggatggcatgacagtaagagaattatgacagtgctgcc
501 ataaccatgagtgataaactcgcggcaacttacttctgacaacgatcggaggaccgaaggagctaacccgcttttttgcaacaatgggggatcatgtaa
601 ctgcgcttgatcgttgggaaccggagctgaatgaagccataccaacgacgagcgtgacaccacgatgctgtagcaatggcaacaacgcttgcgcaact
701 attaaactggcgaactacttactctagcttcccggaacaatttaataagtagactggatggaggcggataaaagtgcaggaccacttctgcgctcggcctccg
801 gctggctgggttattgctgataaatctggagccggtgagcgtgggtctcgcggtatcattgcagcactggggccagatggttaagcctcccgtatcgtag
901 tatctacacgacggggagtcaggcaactatggatgaacgaaatagacagatcgctgagataggtgcctcactgatgaagcattggtaactgtcagacca
1001 agtttactcatatatacttttagattgatttaaaaacttcatttttaatttaaaggatctagggaagatcctttttgataatctcatgaccaaatacct
1101 taacgtgagtttctgctccactgagcgtcagaccccgtagaaaaagatcaaaggatcttcttgagatccttttttctgcgcgtaactctgctgcttgcaa
1201 caaaaaaacaccgctaccagcgggtggtttgtttgcccgatcaagagctaccaactccttttccgaaggtaactggcttcagcagagcgcagataccaaa
1301 tactgtccttctagtgtagccgtagtttagccaccactcaagaactctgtagcaccgctacatactcgtctgctaactctgttaccagtggtcgtc
1401 gccagtgccgataaagctgtcttaccgggttggactcaagaacgatagttaccggataaaggcgcagcggctggggtgaaacggggggttcggtgcaacagc
1501 ccagcttgagcgaacgactacaccgaactgagatactacagcgtgagctatgagaaagcgcacgctcccgaagggaagaaagcggacaggtatcc
1601 ggtaagcggcaggtcggaaacaggagagcgcagcagggagcttccaggggaaacgcctggatctttatagctctgctggttccgcaacctctgact
1701 gagcgtcgatttttggtagctgctcagggggcggagcctatggaaaaacgcccagcaacgcggccttttaccggttccggccttttgcgctggccttttg
1801 ctacatgttcttctcgtgttatcccctgattctgtggataaccgtattaccgctttgagtgagctgataccgctcggcgcagcgaacgacagcggc
1901 cagcagctcagtgagcgaagcgggaagcgcgaacacacgccaatcagcaaacgcctctcccgcgcttggccgatcatttaagcagctggcagcagcgtt
2001 cccgactggaagcgggcagtgagcgaacccaattatgtgagtagctcactcatagggaccaccagcctttacactttatgcttccggctcgtatgt
2101 tgtgtggaattgtgagcgaataacaatttcacacaggaacagctatgacctatgacctatgacctatgacctatgacctatgacctatgacctatgacctat
2201 ggtaccgggccccctcgaggtcgactctagaggtacccccat 2244
    
```

Actin promoter sequences (1'289 bp) + Actin 5'UTR (99 bp) + Actin coding sequence (27 bp) + MCS (27 bp)

```

-1289 cgatctgactaacctaaccagtgcaaaaaatttaaagatttgcattgtgaaagttagaataattataaaaaatctaaaacgagtattactcgagtaaat
-1189 gttatagcgtctatagattaaatataattaaaagtgtatagcgaattgttaaactaaatataataataaaacttgaaaacttactaaattgcaaaaactcaa
-1089 aaccgactgtatcatttttacaggaaaccgttatcaagataacttaagttgtttactacattatataaacctttgcaatttagcaagacaactcgttattt
-989 taacatcacggtatcgaaggattttgagaatttttattgaaacatttttaaacaaaaaatatcatatttagatgcaatttaagccgagatgcaggtattct
-889 gaatgaaaaagaaaaaagaagtctcggtagagtaaaagtgtcggtttgcgaactgtaaaatttattgaaagtaaccaataattttatataaaataaaactg
-789 aaataaaagttaaagttgctgttctataagtttaccgaattttaaaccattgttaacgctagagtaaatattgagttactaaagttagctcccgcactt
-689 ttttaactcaagcaataaaatcccaaacctttgcttattcaaatcaataaaccaatatactcttaaaataaagtaaaaaactctgaaattctataaaaaaaa
-589 atttaatttcgaaatatacaatgtaacttcaacaccgcactattttcttttaaacactgataatagtaattacttctcaaaaacgttatctcaaggtttg
-489 tgatgactttaaaccactcctattttgttacgcggttttaaaaaagcaaacataagttggttctattgatgaatgagaacatattcatttaaagttaaa
-389 atcctaccagtggtttcactgtacgtaaacaccgtcaaaaaaacggaacgctttttaaagattaaatgaaagtaaaaaaaatttaataccgggggtta
-289 aaaaaatccttttaaaataattataaatatataattaaattataaaatttttaaacacatttaaaatataatataagtaataaaagtaattattataa
-189 aaaaaatttaattttataaattttttatataaattttataaataataggtaaaaacttacatataccggttttttttcttaataaaaaaacccgtgcaaa
TSS +1
-89 tttttgtccatataaaagaccttttgcacaataactttttgcttagccggtttttttcttatatggtcaaaaaagcgcctcaagcgattCAccataaaaa
99
12 gcgcaattagttcagcgttctgatttaccagaagcttcagcgtttgcttgatactcagcctctctcttttaaacaaaaacacttaatacaaaATGGCCGATGAT
M A D D
GAAGTTGCCGCCCTC GCTGCAGCCCCGGTAGAAAAAGTCGAC
E V A A L
    
```

mCherry coding sequence (711 bp) + MCS (14 bp)

```

1  ATGTTAGTAAAGGAGAAGAAGATAATATGGCTATTATTAAGAATTTATGAGATTTAAAGTTCATATGGAAGGATCTGTTAATGGTCATGAATTTGAAA
101 TTGAAGGTGAAGGAGAAGGTAGACCATATGAAGGTACTCAAACGCTAAACTTAAAGTTACTAAAGGTGGACCATTACCTTTTGCATGGGATATCTTTTC
201 ACCACAATTTATGTTGGAAGTAAAGCTTATGTTAAACATCCAGCAGATATTCCTGATTTCTTAAACTTTTAACTTTCTGAAAGGTTTTAAATGGGAAGA
301 GTTATGAATTTGAAGATGGTGGAGTTGTTACTGTTACACAAGATTTCTTATTACAAGATGGAGAATTTATTTATAAAGTTAAACTTAGAGGAACTAATT
401 TTCCAAGTGATGGTCTGTTATGCAAAAGAAAACATATGGGTGGGAAGCTAGTTCTGAAAGAATGTATCCTGAAGATGGAGCATTAAAGGTGAAATTA
501 ACAAGACTTAAACTTAAAGATGGTGGACATTATGATGCTGAAGTTAAACTACATATAAAGCTAAAAAACAGTTCAATTACCTGGAGCTTATAATGTT
601 AATATTAACCTTGATATTACTTCTATAATGAAGATTATACAATTTGTAACAATATGAAAGAGCAGAAGGTAGACATTCAACAGGTGGAATGGATGAAT
701 TATAATAATAA CATTCTGATAATTC
    
```

Actin 3' UTR (677 bp) + pBSSA-AR plasmidic sequence (110 bp)

```

1  acaattcgattatatttatactggactatttttacatctgttcgggtattttccatttatttttctatatatatcttataaacgttttaaaccctatg
101 aatttttgttaagctgtaataataaaagcgtcctcaacaactctcttttactgtaatttcttataataataacaagttttaaataaaattca
201 ggcaattaaagcgcctcctgaggtactaaaattatgtaaacattttaaatttaacttggatggcttaagactgtactcgtgatttgttatactttatt
301 attagaaaagctcgtcttaacttttggcttacttctgatttctgcttatttctgcttatttatacaaatcaggttttgcgctgatttttagagaaaaaa
401 cttattagaaaaatgaataagcaaggttttaggctaacaatggttttttatttttaaatagttcaagtaacatgacgtataaaatgcatttgcaaaaaat
501 ttaagtaaacctataaacttagcaatagtagactggtgcaagcattcagtagcagcattgcatactcgtgctttacgtacaaaataacagcaaaaa
601 ttgacctttatggcttcacatcgtctgtaaacatggtttattggactgtcacaatggtttagatcacagagct 677
1  tagctcttgatggtgatcactagttctagagcggcggccaccgggtggagctcggcgcgccggtaccgggccccctcgaggtcgacgggtatcgataa
101 gcttgatatac
    
```

Hydra Sp5 promoter (2'966 bp) + Sp5 5'UTR (203 bp) + Sp5 coding sequence (25 bp) + MCS (20 bp)

```

-2966 ctagtttctaatttagctctattacgcttcgcaaaagttgcaaaagtcgcaatttttttcttttcaaaagacctccattcttttaataaaagactggttc
    
```


-2866 taattttgctttatcacgcttataaaaaattgacaaaagtcgcaagctactttgttttttaaaagacctcccattcattgagataaaactagttattttcat
-2766 gtatcattgaaatagtaaaacaattcattctagtttttttttctagggcagctatttcacacctccacaagtcgcaaacggttttatttacttgattgag
-2666 taaattaatttaaaaaataaaaaataaagaacttaagtgtgaaaaaaaaacaaaaacaaaaataaaaaaaacaatgtaaaatattttctcata
-2566 gctgttgaaatatttaaaagacggaaggaataataacggcaaaagctaaattctttctcgctattgctttttatctcttattgtctgtttgtgtgctt
-2466 ttcactgcattctattttgtgcttaataaatctcaatcgatttttaaggaatgactaggatgtttcattttgttatatacaataactgaaatataaaaaat
-2366 ctccctcagtgatccgctcgtagacaattgggggtatctaactcaattttctcgaatataaaactcaacaagtaaaaaagtttcatccgtaagcaagca
-2266 agaataacgcacttggttacatttaagaattttcttaactttatgttaaaaaacaattcttagtataaaacgaagtaaaagggttttaattttttgtttt
-2166 tagttgaaaaacaattgctaataaaaaacttaatttaaaaaaaaaaaccaataatttaaaatgataaaactggttaaaatataatagattatacaaacctt

Sp5-BS

-2066 gtaagcatttaaaaaacaatttttttttataaaaaacaacaaaaaaatttcacctaattactCCGCCTTgtgtaaaaaacctccgttttacagttaa
-1966 aagtaatgtatgaaccgtaatccctattacaaaagaaatggtatattgtttataaaagcgttttgatgattgtagcttattttatattttgtgtgcttt
-1866 gttttgttttccctgtgtgtgttttaatttgattagttatattcttacggccttaacgaccgctttgtctgttttaaatcgcgagcgttgctttgacttta
-1766 cacgaagcctctaaaaacaacataaaagagaattcatcgaaagtaaaaaaatcatgctgaccttcggtgtagccgtaattgaaattgatataattttctc
-1666 cctattttgacataataaatggttaaagttaatctttttataaactcaatcaatttcaacaaaaaagtgtaaaagtttactgcttatttcaagtaacaaa
-1566 taagcttattgttaaaataaaagttattgtttaaaagggtgaaactcaatcattattgttaaaagaagaatttcatgtaagattgtatttataaaa
-1466 ttaataaaactaaatgaaacgaagcgtacgtaaaattttatattttgattataaagaggaatttttttaactaatgtaaaactactgtaaaactcgact
-1366 gaatcaataaggtcagagagactaggtcagcgagtttggatcattaaaatcgataacaataataacgatagtttataatgataggaacttaactt

Sp5-BS

-1266 gacatttaaatgggaagtcctgaggtataacgcttctgtttgtcgtggtagataaagccaattgacaaaaccatcatcttatatttttatggtGCGCCAat

TCF-BS

-1166 gttttatcatgtttaatttCTTTTATataaatgataaaaaacatttaaccacaattattttttttatctccaatgaaatcaagaacttttaagtataaaa

Sp5-BS

-1066 aagtgccgacaGCGCCAGtataatcatagacaaggtgacacattagcttatacaaaagtagctagagtaaaagcttattgtttgtttgtgctaggata

TCF-BS

-966 tatccttctcgtaaataaattgtcctaCTTTTATatacgaatttcatatttttaggtttctgtttcgaatataatataatattcgttatgtttgtat
-866 gtatatatgtgtttgtgtatgtgtaaaaaatgaaataacttttgcgaactctttgttagaagtttaataaaataagatcaagtttaaaaatt

TCF-BS

-766 cCTTCGATatttttaaaagcttcaatttgggtggcgtagacacattagtaattgcggtaaagatcagtaagaatttcaaatagacgttaatttttaaaac

TCF-BS

-666 tggcctgcCCCTTGATtatttaatttgaaatttttaagctgtctccatttcaaccacagtatcaatgggtcggcaaaaaaagaagattgaaacttttat
-566 caattttaccacgaaaaaaccttaacaaatattgtagtacttttttaagtttaaatgtttttgtaaaaactggtatttttaaaataaaccttttacttc
-466 tttttttttttttgaaatcgtttttaactgatatttaataaaagcttaaatataaatgtgtaaaagttcgttaaaacaaatgaagcgaggtgcccggcat

TCF-BS

-366 agatgaaagtgaaagaacaatttttttttattgaaacttcaacttactgtggtattgctggaatgttttactattaagttgATTGAGTcaaaaaacaaa

TSS3 -192 (*H. oligactis*)

-266 taacaaaatcaaccaatgaacttcttagaaattgttaatacaaaacaaatcaaatagcgtttTATAtcttttAaccaataagataacaattttattgt

TSS2 -149 (Hm105) Sp5-BS Sp5-BS

-166 tttgtcggcatcttaagAattataaaagtttaaatcttttCCGCCTtaacgtattctgtttatcaCCGCCTcttagaccatcccatttgtacgtaaacagag

Sp5-BS Sp5-BS TCF-BS tss1 (H. AEP) Sp5-BS

-66 aaaaatgatcgcaacGCGCCAtttctcagtcagAGGCGTgacattaaccocctATCAAAGAagcGaaagctatttaagataagaTGGCGGtttcttctg

+204

+135 tcagttaaacttttacttttaagtgcaaaagcgttcataagaatacattttagtaaaatgaagtaaaATGTCACCTCCAAGTCGTGTTCCAA +229
M S P P S R V P

CTGCAGCACCCGGGAAAAA

eGFP coding sequence (717 bp) + MCS (14 bp)

1 .ATGAGTAAAGGAGAAGAACTTTTACATGGAGTTGTGCCAATCTTGTGAATTAGATGGTGATGTTAATGGGCACAAATTTTCTGTCAGTGGAGAGGGTG
101 AAGGTGATGCAACATACGGAACACTTACCCTTAAATTTTATTTGCACTACTGGAAACTACCTGTTCCATGGCCAACTTGTCTACTACTTTCTGTTATGG
201 TGTCAATGCTTTTCAAGATACCAGATCATATGAACGGCATGACTTTTCAAGAGTGCCATGCCGAAGGTTAFTGACAGGAAGAACTATATTTTTC
301 AAAGATGACGGGAACACAAAGACACGTGCTGAAGTCAAGTTTGAAGGTGATACCTTGTTAATAGAATCGAGTTAAAAGGTATTGATTTAAAGAAGATG
401 GAAACATCTTGGACACAAATTGGAATACAACATAACTCACACAATGTATACATCATGGCAGACAAACAAAAGAATGGAATCAAAGTTAACTTCAAAT
501 TAGACACAACATTGAAGATGGAAGCGTTCAACTAGCAGACCATTTATCAACAAAATACTCCAATTGGCGATGGCCCTGTCTTTTACCAGACAAACATTAC
601 CTGTCCACACAATCTGCCCTTTCCGAAAGATCCCAAGAAAAGAGAGACCACATGGTCTTCTTGAGTTTGTAAACAGCTGCTGGGATTACACATGGCATGG
701 ATGAACATAACAATAG CATTTCGTAGAATTC

Actin 3' UTR (677 bp)

1 acaattcgattatatttatactggactatttttacatctgttcggttattttcacatttatttttctatatatctttataaacgttttaaaaccatg
101 aatttttgttaagctgtaataataaaagacgctcctaacaacttcttttattactgaaatttcttataataataacaagtttttaaaataaattca
201 ggcaattaagggcgtcctgaggtactaaaattatgtaaacatttaaaatgaactggatggctttaaagtagtactgactcgtgattttgttatactttatt
301 attagaaaagtcgtctatttaactttttgttcttaatttactttagtaaatgtcgttatttatcaaatcagttttgtcggcgttattttagagaaaaa
401 cttattagaaaaatgaataagcaagtttaggctaacatgttttttattttaaataagttcaagtcactgacgtataaaatgcatttgcaaaaaatt
501 ttaagtaacctataaacttagcaatagtagatactggatgcaagcattcagtagcagcattgcatatctgctgtctttacgtacaaaaaacagcaaaaa
601 tggacctttattggcttcacatcgtcgttaaaactgtgttattggactgtgcacaaatgtgttaagtatcacagagct 677

pBSSA-AR plasmidic sequence (713 bp)

110.....20.....30.....40.....50.....60.....70.....80.....90.....1
1 tagctcttgatggtgatcactagagcggccgacgctggagctcggcgccagctccaattcgcctatagtgagtcgtattacgcgcgctcact
101 ggccgctggtttacaacgctgtagctgggaaaaacccctggcgttacccaacttaatcgcttgcagcacatcccccttccgagctggcgtaaatagcgaa
201 gaggccgcaccgatcgccttcccaacagttgctcagcctgaatggcgaatggaattgtaagcgttaaatattttgttaaaatcgcggttaaaattttg
301 ttaaatcagctcatttttaaccaataggccgaaatcgccaaatccctataaaataaaagaatagaccgagatagggttgagttgtgtccagtttgg
401 aacaagagtcactataaagaacgtggactccaacgtcaaaagggcgaaaaaacctctacagggcgatggcccaactacgtgaacctacacctaatcaa
501 gttttttggggtcgaggtgcccgttaaagcactaaatcgaaacccataaaggagcccccgatttagagcttgacggggaaagccggcgaaactggcgagaaa
601 ggaagggaaagaaagcgaaggagcggcgctaggggcgtggcaagtgtagcggctcagcgtgcccgttaaccaccacaccgcccgcgttaatgcccgcgta
701 caaggcgcgctcag 713

DISCUSSION

1. Challenges and limitations of the project

As previously stated, *Hydra* is a good model system for studying regeneration, the establishment of organizers and the regulation between activators and inhibitors. However, despite being very useful for this study, we encountered a number of drawbacks and challenges:

a. **Investigation of re-expressed genes in the first few hours after amputation.**

Wnt3 and *Sp5* genes are both re-expressed very early after amputation, and determining their spatiotemporal expression is critical to understanding their cross-talk during head formation. However, after amputation, the wound takes about 4-5 hours to close, and therefore the wound is still open at the critical timepoints when *Wnt3* and *Sp5* start to be re-expressed, making the comprehension of their expression more difficult to understand if the wound is not properly closed because it is difficult to distinguish between real expression pattern or an artifact expression at the wound edge (**Chapter 2, Figure S3**).

- b. **Gene knockdown in *Hydra*.** The electroporation of *siRNA* was used to gene knockdown in this study. This method however, is quite heterogeneous and it is difficult to predict which cells will be targeted. Moreover, its efficiency varies depending on the gene as well as the cell type gene expression. As seen here, targeting gastrodermal genes is more difficult than epidermal genes because they are less exposed. Finally, while this method was very effective for *Sp5* because it triggers an easily observed phenotype (**Chapter 1, Figure 2**), we have to consider that the gene knockdown is transient and thus will not be sustained over time. As a result, targeting a gene with a high turnover rate, as expected for *Sp5*, makes it more challenging. Thus, performing gene knockout using CRISPR-Cas9 would be a more definitive method to perform loss-of-function assays. This method has been established in a few cnidarian organisms including *Nematostella* (Ikmi et al., 2014) and *Hydractinia* (Gahan et al., 2017), but it is not yet established in *Hydra* although some attempts were developed (Lommel et al., 2017).

- c. **Live imaging of transgenic animals.** The generation of *Sp5* transgenic lines expressing a tandem reporter gene provided us with a significant advantage as we were able to track the fluorescence over time in the different contexts in real time. Nonetheless, despite the fact that few methods for performing live imaging in *Hydra* have been developed, such as anesthetizing them with linalool (Goel et al., 2019) or embedding them in 1-2% agarose, it was critical in this case to be able to keep the animal shape after imaging and ensure that animal regeneration was not altered. Thus, the animals were simply kept in *Hydra* medium, allowing them to move naturally and thus react to light, and make imaging of both GFP and mCherry channels more challenging.
- d. **Generation of stable transgenic lines.** The creation of stable transgenic lines in *Hydra* is a long and laborious process. As described in the Material and Methods section of Chapter 2, we only obtained three positive hatched embryos from the 330 injected eggs. Since the hatched embryos had few fluorescent positive cells, it took a long time to get the two fully positive *Sp5* transgenic lines from a single embryo each. As a result, producing transgenic lines in *Hydra* is not an easy task; otherwise, we would have created additional transgenic lines to complete this study, such as a transgenic line with putative *Sp5* binding regions deleted to observe and follow the fluorescence. Furthermore, oocyte production in females is not continuous, with usually only one or two eggs produced in each female; consequently, a limited number of oocytes is another element to consider while producing transgenic animals.
- e. **Developing an antibody for *Hydra*.** The process of developing an antibody for *Hydra* tissue is very challenging because there are usually no commercial antibodies for this model organism and customized ones are not always good, as previously experienced in the lab, and thus similar happened when developing an antibody against *Hydra Sp5*. Initially, we developed a polyclonal antibody against three peptides of the *Sp5* protein sequence; however, one of these peptides was localized in one of the zinc-finger domains, a region that is well conserved in *Hydra Sp4*, and thus the antibody was not specific for *Sp5*. While purifying this antibody against the two resting peptides located outside

of this domain, we began to develop a monoclonal antibody since they are usually highly specific. The monoclonal antibody was produced against a region of the Sp5 protein sequence that did not overlap with any previously known domains. The purpose of developing a *Hydra* α -Sp5 antibody was to use it for ChIP-seq to identify putative Sp5 target genes that could eventually contribute to the head inhibition process. A disadvantage of monoclonal antibodies is that if the epitope recognized by the antibody is masked during the process of this protocol, the chances of immunoprecipitation are very low (Wardle and Tan, 2015). Nonetheless, the ChIP-qPCR results using both monoclonal and polyclonal (2-peptide) antibodies, show an enrichment in regions PP4 and PP5 of the *Hydra Sp5* promoter (**Chapter 2, Figure 6, FigS14**) as previously reported *in vitro* (**Chapter 1, Figure 5D**). These antibodies were also tested by Western blotting and show a specific recognition of recombinant Sp5 protein. Furthermore, when using *Hydra* tissue, monoclonal antibody shows very clean and specific protein recognition, whereas polyclonal antibody shows many more unspecific bands (**Chapter 2, Figure 6, FigS14**). Several attempts were also performed to test these two α -Sp5 antibodies for immunofluorescence, but none were successful.

- f. **Establishment of ChIP with *Hydra* tissue.** A similar protocol to that used in Chapter 1 when using mammalian cells was used to perform chromatin immunoprecipitation using *Hydra* tissue in Chapter 2. Nevertheless, several steps such as the number of animals, dilution conditions, sonication conditions, the amount of chromatin for immunoprecipitation, and the amount of α -Sp5 antibody, had to be established. This was done with the kind help of Dr. Leonardo Beccari.

2. Identification of the transcription factor *Sp5* as the *Hydra* head inhibitor

Sp5 satisfy all of the criteria established for the *Hydra* head inhibitor. However, we cannot rule out the possibility that other genes play a role in the head inhibition

process during head formation. *Wnt5*, which was also identified in the screen, could as well play a role, as could other Wnts that are expressed in the head region (Lengfeld et al., 2009). Nonetheless, the knockdown of *Wnt5* does not result in a multiple headed phenotype as *Sp5* does. However, setting up the organizer is a complex process that has to be well-regulated in both place and time. As a consequence, while a head activation regulator, *Wnt3*, and a head inhibitor regulated gene, *Sp5*, have been identified, we hypothesize that many more genes have to be involved in this process. For this reason, one of the goals of this study was to identify putative Sp5 target genes in order to better understand how the head is established and regulated during development, as well as how it is maintained and regulated in homeostatic conditions. *Sp5* is positively regulated by Wnt/ β -catenin signaling in *Hydra*, as it is in developing vertebrates such as mice and zebrafish (Kennedy et al., 2016; Weidinger et al., 2005), suggesting that Wnt/ β -catenin regulation is evolutionary-conservation across eumetazoan. Thus, using the *Hydra* model organism to identify Sp5 target genes could lead to a better understanding of not only the specific genes involved in the regulation and patterning of the head of the *Hydra* and thus the head organizer, but also important genes that are evolutionarily conserved and may play a role in regulating the Wnt/ β -catenin signaling pathway.

However, because *Sp5* is transcription factor and therefore presumed to work cell-autonomously and not be diffusible, it contradicts with the expected properties for the predicted head inhibitor suggested by Gierer and Meinhardt's model (Gierer and Meinhardt, 1972). Nonetheless, this model was anticipated when transcription factors were unknown, and has been revealed that certain transcription factors can be secreted like some homeoproteins (Bernard et al., 2016), or that unidentified Sp5 target genes are diffusible proteins that contribute to exert the inhibitory effect. In addition, Wnts are secreted signaling proteins that can act as morphogens and can operate over both short and long-range distances. However, because Wnt proteins are coupled to a lipid and hence hydrophobic, it poses the question of their diffusion and distribution since they cannot freely traverse the extracellular space and thus function primarily between

nearby cells (Clevers et al., 2014; MacDonald et al., 2009). Although it is commonly considered that Wnts serve as short-range intercellular signals, some specific proteins or extracellular vesicles appear to protect the lipid section, allowing wnt signals to behave as long-range morphogens. It has been postulated that Wnts can bind lipoprotein particles, allowing them the movement through the epithelium in *Drosophila* and human cells (Neumann et al., 2009; Panáková et al., 2005). Other evidence suggests that Wnt proteins are bound by secreted wingless-interacting molecules such as Swim, to facilitate transport by maintaining the solubility (Mulligan et al., 2012), or that Wnt signaling may travel through cytonemes, which are specialized signaling filopodia that would allow signaling over longer distances within a short period of time (Stanganello and Scholpp, 2016).

Recently, a novel mathematical model involving reciprocal inhibition for *de novo* patterning formation was proposed, which included Wnt3/ β -catenin on one side and *HyDkk1/2/4* in the other side (Mercker et al., 2021). As previously stated, *HyDkk1/2/4* has already been proposed as a candidate for the *Hydra* head inhibitor (Augustin et al., 2006; Guder et al., 2006). Despite being negatively regulated by Wnt/ β -catenin signaling, the expression patterns of *Wnt3* and *Dkk1/2/4* completely exclude each other and are never expressed nearby, with *Wnt3* being expressed primarily in epithelial cells and *Dkk1/2/4* being expressed in gland cells. Furthermore, this new model does not take into account the autocatalytic loop described in the *HyWnt3* promoter (Nakamura et al., 2011), necessary to sustain the activation function in the established head and in the developing ones.

3. Spatio-temporal GFP distribution in the *Sp5* transgenic lines

The injection of the tandem reporter construct to generate a *Sp5* transgenic line, did result to obtain two transgenic lines: one in which the construct is expressed in the epidermal layer and another in which the plasmid is expressed in the gastrodermal layer, resulting in a much better and more complete understanding of *Sp5* regulation. *GFP* expression and GFP fluorescence in both *Sp5* transgenic lines mimic endogenous *Sp5* expression, which is to be mainly expressed in the head and graded down the body

column. However, there are some distinctions between the two transgenic lines that will be further explain according to the different contexts.

IN HOMEOSTATIC CONDITIONS

Endogenous *Sp5* is mainly expressed by gastrodermal epithelial cells, yet it is expressed in epidermal epithelial cells with lesser amount (**Chapter 1, FigS5**). *Sp5* is primarily expressed in the head of both epithelial cells, with apical to basal gradient (**Chapter 1, Figure 1**). Its expression in the head is excluded in the hypostome region, where *Wnt3* is expressed. However, a close inspection reveals some *Sp5* expression over the hypostome in the epidermal epithelial (**Figure 14**). This completely resembles the scenario of *Sp5* transgenic lines, where GFP fluorescence is visualized along the hypostome in *HySp5-3169:GFP_ep* animals but mostly excluded in the *HySp5-3169:GFP_ga* animals (**Chapter 2, Figure 1**).

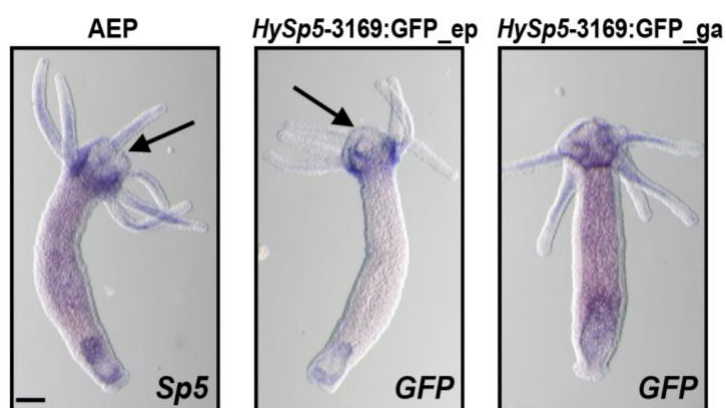


Figure 14. *Sp5* and *GFP* expression patterns by ISH.

The *Sp5* gene expression pattern in an AEP animal is shown in the left, and *GFP* expression patterns in AEP transgenic animals using *Sp5* transgenic lines are shown on the right. Arrows are pointing to *Sp5* and *GFP* expression over the hypostome. Scale bar: 200 μ m.

Regarding *GFP* expression and fluorescence in the body column, again resembles endogenous *Sp5* expression which is mostly found in the gastrodermal epithelial cells in a graded manner (**Chapter 2, Figure 1**). Furthermore, in *HySp5-3169:GFP_ga* transgenic animals, *Sp5* expression, like *GFP* expression and fluorescence, is never localized in the foot region, where inhibition levels are near zero. Thus, just above the foot region, where the budding zone is located, a minimal *Sp5* activity would still occur, but not enough to prevent the formation of a new bud, because *β -catenin* expression

is quite dynamic in this region and generates a belly expression prior the budding process (Hobmayer et al., 2000).

Despite this, we cannot completely rule out the possibility that the *GFP* expression profile and GFP fluorescence distribution is related to the number of copies of the tandem reporter construct that we assumed that have been integrated after the injection because it is a stable line, or to the location where the construct was integrated. We did, however, obtained another *Sp5* transgenic line in which the reporter construct is expressed in the epidermal layer, and the GFP fluorescence in those animals is identical to the transgenic animals used in Chapter 2. Despite the fact this transgenic line has not been used in any experiments, gain- and loss-of-function assays will be carried out to rule this out.

IN DEVELOPING CONDITIONS

During the budding process, GFP fluorescence is present in both *Sp5* transgenic lines from very early stages and continues until the bud detached, after which it persists in the newly developed polyp as in the same pattern as an adult animal. We assumed that if there is GFP fluorescence, *GFP* expression was present prior to this region. However, further exploration regarding *GFP* expression in the epidermal and gastrodermal layers during the different budding stages is needed to confirm these observations.

During regeneration, *Sp5* was found to be re-expressed in the regenerating apical tip at 8 hpa in the RNA-seq regenerating profile, which was further confirmed by *ISH* (Chapter 1, Figure 1, FigS4). Even though *ISH Sp5* data from earlier time-points are missing, *ISH* data of *Sp5* transgenic lines regarding *GFP* expression was collected. At 0 hpa, no *GFP* expression is found in the apical or basal regenerating tips of *HySp5-3169:GFP_ep* animals, but it is found in *HySp5-3169:GFP_ga* animals. However, because the animals were immediately fixed after amputation and at this time point the wound of the animals is still open, it is difficult to claim that the expression in both regenerating tips from *HySp5-3169:GFP_ga* animals is due to an upregulation of *GFP* (and thus of *Sp5*) rather than its *GFP* expression in the body column from homeostatic conditions in *HySp5-3169:GFP_ga* animals. From 8 hpa *GFP* starts to be re-expressed

in the regenerating apical tip but not in the regenerating basal tip in *HySp5-3169:GFP_ep* animals, where *GFP* is not expressed even at later time points, implying that *Sp5* plays no role in basal regeneration in the epidermis. Even though there is little *GFP* expression at the apical tip at this time point, GFP fluorescence in this region is remarkable, suggesting on one hand a likely instability of the transcripts but a high stability of the GFP protein, as previously reported (Corish and Tyler-Smith, 1999). In terms of *GFP* expression in the gastrodermis at later timepoints, we can observe that, similar to *Sp5* endogenous expression, is re-expressed during basal regeneration at the regenerating tip from 8 hpa until 24-48 hpa and then it disappears. *GFP* is broadly expressed during apical regeneration in the regenerating tip at 8 hpa and is then mostly excluded from the hypostome region at 48 hpa, similar to *Sp5* expression.

Therefore, differences in *GFP* expression and fluorescence between the two *Sp5* transgenic lines in homeostatic, budding, and regeneration conditions reflect the role that the two layers play during morphogenesis in this animal, highlighting the importance of the gastrodermis layer during head formation and the establishment of the developing structures since most of the genes responsible for the development of the head organizer are mainly expressed in the gastrodermis (Hobmayer et al., 2000).

4. The 3169bp of the *Hydra Sp5* promoter respond to Wnt/ β -catenin signaling

By transfecting a plasmid containing 2992bp of the *Hydra Sp5* promoter we were able to confirm that this length was sufficient to respond to Wnt/ β -catenin (Chapter 1, Figure 4). Following that, a reporter construct containing this length of the *HySp5* promoter together with the 5'UTR was used to generate the *Sp5* transgenic lines, and by performing gain – and loss-of-function assays we were able to confirm that it sufficient to respond to Wnt/ β -catenin signaling *in vivo* (Chapter 2, Figure 3, 4). Thus, after the silencing of *β -catenin* by RNAi, GFP fluorescence was decreased in the head region of the *HySp5-3169:GFP_ep* animals, thus in the region where GFP is mainly localized in these animals. Because *Sp5* is a downstream target of Wnt/ β -catenin signaling, it was hypothesized that *GFP* expression and fluorescence would be reduced

(Chapter 2, Figure 4). Further experiments will confirm whether a drop in GFP expression and fluorescence occurs following the silencing of β -catenin in *HySp5-3169:GFP_ga* animals.

By performing gain-of-function assays by pharmacologically activating Wnt/ β -catenin signaling with ALP, we could observe an increase in *Sp5* expression (Chapter 1, Figure 5) as well as an increase in *GFP* expression and fluorescence in regions that under normal conditions expression is not localized (Chapter 2, Figure 3). Mostly as result, it is evident that the 3169 bp of the *Sp5* promoter used to produce the *Sp5* transgenic animals are responding to perturbation of Wnt/ β -catenin signaling. Nevertheless, we cannot exclude that other regulatory sequences located out of these 3kb are not having any role.

5. The negative auto-regulation of Sp5

Although *Sp5* negatively regulates human Wnt3 target genes (Huggins et al., 2017), it varies its regulation among different species. And mostly regulated genes involved in the Wnt/ β -catenin signaling pathway (Kennedy et al., 2016) but its transcriptional regulation is not restricted only to these genes. One of the primary goals of creating the transgenic lines was to decipher *Sp5* regulation *in vivo*. However, in the Chapter 1, we used *Hv_Base1* animals to silence *Sp5* by RNAi, and first, we wanted to confirm that in the *Hv_AEP* animals used to generate the transgenic lines and for the majority of the experiments in Chapter 2, the multiple headed phenotype was as well triggered following the knockdown of *Sp5*. Despite the fact that *Hv_AEP* animals are more resistant to pharmacological treatments than *Hv_Base1*, the silencing of *Sp5* by RNAi in *Hv_AEP* animals stimulate as well the formation of multiple heads, even though three rounds of electroporations are usually required (Figure 15).

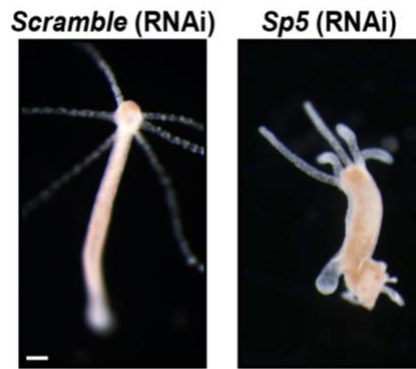


Figure 15. The knockdown of *Sp5* results in a multiple headed phenotype in *Hv_AEP* animals.

Two days after three rounds of electroporations to silence *Sp5* by RNAi, the multiple head phenotype occurs in the animals (right) when compared to control animals (left). Scale bar: 200 μ m.

From *in vitro* experiments performed in mammalian cells, we learnt that *Hydra Sp5* has a positive auto-regulation (**Chapter 1, Figure 5**); however, *in vivo* experiments using the *Sp5* transgenic lines clearly show that *Hydra Sp5* has negative auto-regulation not only on the epidermal layer but also on the gastrodermal layer (**Chapter 2, Figure 5**).

The negative *Sp5* auto-regulation in the epidermis is much easier to visualize because the *Sp5* knockdown causes a massive increase in *GFP* expression and fluorescence along the body column of the animal, where *GFP* is normally not localized in *HySp5-3169:GFP_ep* animals. In the epidermis, *GFP* expression is up-regulated at 8hpEP1 and *GFP* fluorescence rises in the body column between 16hpEP1 and 24hpEP1. Even though we can observe this rapid *GFP* up-regulation in the epidermal layer, the multiple headed phenotype that results from the knockdown of *Sp5* takes considerably longer, and in addition, no significant change in *Sp5* expression is identified at these early timepoints. This finding suggests that the epidermal layer it is not dictating the occurrence of the multiple headed phenotype, underlining the fact that it is less engaged in morphological alterations involving the head organizer structure since genes responsible for the development and maintenance of the head organizer are not predominantly expressed in the epidermis. Despite this, *GFP* up-regulation declines prior the second *Sp5* knockdown (**Chapter 2, Figure 5**) and two days pEP2 (**Chapter 2, FigS13**), which is not seen in *GFP* fluorescence due to the long stability of *GFP*. This drop in *GFP* expression implies that, despite the negative auto-regulation caused by

the silencing of *Sp5* by RNAi, it is a tightly regulated gene, and hence *GFP* expression levels return to normal expression levels in less than 48 hours pEP.

Because *GFP* expression and fluorescence is highly distributed along the body column in the gastrodermal layer, a modulation in *GFP* expression or fluorescence is considerably more difficult to detect in *HySp5-3169:GFP_ga* animals. Nonetheless, at later timepoints after the second round of electroporations, some gene expression modulations of *GFP*, *Sp5* and *Wnt3* can be perceived in the body column, as can an increase in GFP fluorescence in the lower body column and tentacles, two regions where GFP fluorescence is normally not seen in *HySp5-3169:GFP_ga* animals (**Chapter 2, Figure 5 and FigS11 and FigS13**). Aside from the amount of GFP in the body column and therefore *Sp5* in these animals under homeostatic conditions, silencing a gastrodermal gene by RNAi is significantly more challenging than knocking-down a gene expressed in the epidermis. Furthermore, because it produces severe morphological alterations in this case, it must be strictly regulated.

After analyzing *GFP* expression and GFP fluorescent pattern upon the knockdown of *Sp5*, we assumed that the targeted cells are those with increased GFP fluorescence (and thus an up-regulation of *Sp5* gene expression). However, we plan to tag the *Sp5* siRNA with a fluorophore to ensure that the cells targeted by electroporation are the ones that experience an increase in GFP due to the silencing of *Sp5* in the *Sp5* transgenic lines.

Finally, we have never noticed an increase in GFP fluorescence in the foot region of *Sp5* transgenic animals as there is rather a sharp boundary of GFP fluorescence in the region close to the foot but never going to the end of the foot region (**Chapter 2, FigS13**). Thus, we speculate that BMP signaling genes involved in foot organizer are thus preventing *Sp5* expression there (Wenger et al., 2019b).

6. Temporal expression of *Wnt3* and *Sp5*

Sp5 is re-expressed during head regeneration, however its expression occurs later than *Wnt3* re-expression (**Chapter 1, Figure 1**), allowing *Wnt3* to be expressed first before

Sp5 expression. A similar scenario must occur when the multiple headed phenotype happens caused by the silencing of *Sp5* by RNAi. This trait is often observed in the budding zone, where β -catenin is already quite dynamic (Hobmayer et al., 2000). Therefore, given the *Sp5* negative autoregulation, we hypothesize that the multiple headed phenotype can emerge as a result of one of the two situations described below. In the first scenario, the multiple headed phenotype will occur in the cells targeted by *Sp5 siRNA*, resulting in a very transient down-regulation of *Sp5* that is therefore difficult to detect but sufficient to allow *Wnt3* to be expressed and trigger the phenotype. *Sp5* will be up-regulated immediately after as a result of its negative autoregulation, resulting in a rise in GFP. In the second scenario, *Sp5 siRNA* targeted cells would experience a *Sp5* up-regulation due to its negative autoregulation, resulting in increased *GFP* expression and fluorescence. Then, the multiple headed phenotype would not occur in the cells targeted by *Sp5 siRNA*, but rather from the cells located in the opposite site of the budding region or a bit distant from the targeted cells.

These scenarios explained above, are supported by the *GFP* expression pattern and GFP fluorescence visualized specially in the epidermal *Sp5* transgenic animals after the silencing of *Sp5* by RNAi. In these animals, we usually observe that the increase of GFP is concentrated along one side of the animals rather than an increase homogeneously spread in the animal. Then, the multiple headed phenotype would occur in the budding region since it is already a competent area for the budding process, although it is possible that the method used to silence *Sp5* would also have an impact. To discard the possibility that it is not due to the approach, we could generate an inducible transgenic line with the tetracycline-sensitive promoter (Klimovich et al., 2018). Exposure to doxycycline of this transgenic line would induce the *Sp5* knockdown due to the conditional expression of *Sp5 shRNA* inserted in the genome to produce the transgenic line. After, we would examine the appearance of the multiple headed phenotype caused by the knockdown of *Sp5* with this approach and compare with the electroporation approach.

7. Generation of transgenic lines with unstable reporter genes to follow the regulation in the epidermal and the gastrodermal layer

The development of the two *Sp5* transgenic lines demonstrated that *Sp5* has different spatial regulation in the epidermis and gastrodermis layers in both intact and developing contexts. It is evidenced by the previously reported modulations of *GFP* expression and fluorescence upon silencing *Sp5*, but as well with the silencing of β -*catenin* or upon ALP treatment.

The silencing of β -*catenin* by RNAi triggers the formation of ectopic bumps (**Chapter 1, Figure 3**). These ectopic bumps express *Wnt3* (**Chapter 1, Supplementary Figure 10**) as well as *Sp5* (**Chapter 2, FigS7**). Nonetheless, GFP fluorescence is not observed in these ectopic structures in *HySp5-3169:GFP_ep* transgenic animals and GFP modulation in *HySp5-3169:GFP_ep* transgenic animals has to be further investigated. On the other hand, by using *Wnt3* and *Sp5* transgenic lines with expression in either the epidermal or gastrodermal layer, we were able to observe how the expression of these two genes behave upon Wnt/ β -catenin signaling activation (**Chapter 2, Figure 3**). In general, we could see an up-regulation of these genes, which in the epidermis causes the formation of concrete and defined expression patterns such as dotted or circular expression patterns, but an up-regulation of these genes in the gastrodermis causes a more homogeneous and diffuse expression pattern. Furthermore, a prolonged ALP treatment would reveal how the expression of *Wnt3* and *Sp5* evolves over time and what structures would emerge, particularly in the basal region of these pharmacologically treated animals. This, together with the fixation of these pharmacologically treated animals at many more timepoints and the drug treatment with iCRT14, a specific down-regulator of Wnt/ β -catenin (Gufler et al., 2018), will help in better understanding the expression patterns and deciphering its control. As a result, it is evident that the balance of the two main components of the head organizer, *Wnt/b-catenin* and *Sp5*, differs between the two epithelial layers.

To further investigate the different regulation of these two genes in the different epithelial layers, a generation of dual reporters involving the *Hydra Wnt3* and the *Hydra Sp5* promoters using reporter genes with a shorter half-life than GFP such as

Achilles (Yoshioka-Kobayashi et al., 2020) would definitely shed more light on the layer-specific regulation of *Wnt3* and *Sp5*. By using these transgenic lines, we would be able to track the expression dynamics as well as the fluorescence in real time of *Wnt3* and *Sp5* in the two epithelial layers throughout the emergence of the *Sp5* and the *β -catenin* phenotypes as well as their regulation when pharmacologically treating them with ALP. Furthermore, we would be able to follow whether *Sp5* expression oscillates in intact or developing conditions, as we observed a highly variable *Sp5* *ISH* expression pattern specially in homeostatic conditions (Chapter 1, FigS4).

8. Sp5 binds to the *Hydra Sp5* promoter

We revealed that Hydra Sp5 can bind its own promoter in two areas directly upstream of the Sp5 TSS by performing ChIP-qPCR in mammalian cells, and these findings were verified by performing ChIP-seq in mammalian cells when Hydra Sp5 was expressed (Chapter 1, Figure 5-6). The ChIP-seq analysis confirmed that Hydra Sp5 binds to the generic SP/KLF consensus sequence, allowing us to locate this motif in the regions of the *Hydra Sp5* promoter that were enriched by ChIP-qPCR. In Chapter 2, we performed ChIP-qPCR using *Hydra* tissue and we were able to confirm binding of the Hydra Sp5 in the previously reported regions of the *Hydra Sp5* promoter by using two different *Hydra* α -Sp5 antibodies (Chapter 2, Figure 6). The ChIP-seq analysis also identified putative *Hydra* Sp5 binding sites in the repressor element of the *Hydra Wnt3* promoter (Nakamura et al., 2011). Thus, the next step is to perform ChIP-seq analysis with a *Hydra* α -Sp5 antibody to confirm the putative binding sites of *Hydra* Sp5 in all of the previously identified regions and identify putative Sp5 target genes that can contribute and thus play a role during the inhibition process of head formation and maintenance. Once identified, we want to compare the genes where Sp5 binds in this analysis to the previously done ChIP-seq analysis in mammalian cells to identify binding of *Hydra* Sp5 in evolutionarily conserved genes as well as binding in *Hydra* or Cnidarian specific genes.

CONCLUSIONS AND PERSPECTIVES

From this investigation we can conclude that *Hydra* Sp5 despite the fact that its spatiotemporal regulation differs between the two epithelial layers, the epidermis and the gastrodermis has a negative auto-regulation through the binding in the proximal region of the *Hydra* Sp5 promoter (Figure 16).

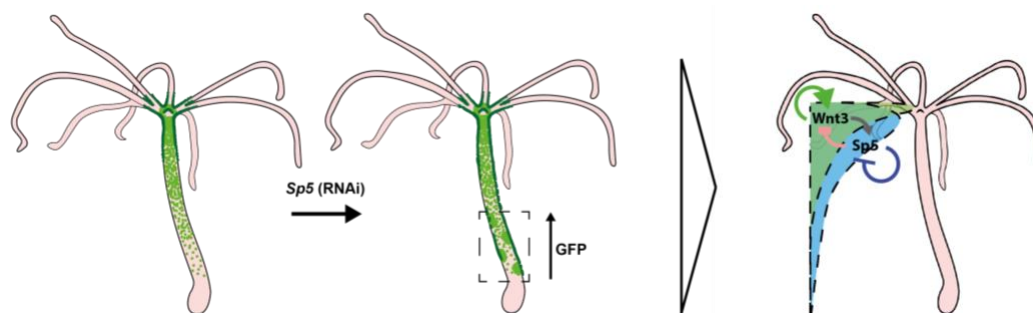


Figure 16. Sp5 functions as a transcriptional repressor on its own promoter.

The silencing of *Sp5* by RNAi causes an increase in GFP fluorescence, especially in the body column of the *Sp5* transgenic lines. As a result, *Hydra* Sp5 has a negative auto-regulation.

In addition, by using *Sp5* and *Wnt3* transgenic lines, we show for the first time that the balance of these two key components of the apical organizer is different in the two epithelial layers, suggesting that their impact may not be the same. Thus, to further understand the regulation of these genes, we plan to generate transgenic lines with the *Hydra* *Wnt3* and *Sp5* promoters using reporter genes that can better follow their dynamic expression, such as Achilles. Together with the ChIP-seq experiment that we plan to do utilizing a *Hydra* α -Sp5 antibody to identify putative Sp5 target genes, we aim to get a much deeper understanding of the complex regulation of the *Hydra* head organizer under both homeostatic and developmental conditions such as regeneration and budding.

In summary, the work presented here contributed to the identification and characterization of the *Hydra* head inhibitor *Sp5*, which had remained uncharacterized for many years despite its existence being known since 1966. Furthermore, shed some

insights on the ancestral autoregulation of a downstream target of the evolutionarily conserved Wnt/ β -catenin signaling pathway.

REFERENCES

- Abraham Trembley (1744). *Mémoires, pour servir à l'histoire d'un genre de polypes d'eau douce, à bras en forme de cornes*. Durand. Universty of Lausanne.
- Anderson, C. and Stern, C. D. (2016). Organizers in Development. *Curr. Top. Dev. Biol.* **117**, 435–454.
- Athanikar, J. N., Sanchez, H. B. and Osborne, T. F. (1997). Promoter selective transcriptional synergy mediated by sterol regulatory element binding protein and Sp1: a critical role for the Btd domain of Sp1. *Mol. Cell. Biol.* **17**, 5193–5200.
- Augustin, R., Franke, A., Khalturin, K., Kiko, R., Siebert, S., Hemmrich, G. and Bosch, T. C. G. (2006). Dickkopf related genes are components of the positional value gradient in Hydra. *Dev. Biol.* **296**, 62–70.
- Azambuja, A. P. and Simoes-Costa, M. (2021). A regulatory sub-circuit downstream of Wnt signaling controls developmental transitions in neural crest formation. *PLoS Genet.* **17**, e1009296.
- Bagaeva, T., Aman, A. J., Graf, T., Niedermoser, I., Zimmermann, B., Kraus, Y., Schatka, M., Demilly, A., Technau, U. and Genikhovich, G. (2020). *β -catenin dependent axial patterning in Cnidaria and Bilateria uses similar regulatory logic*. Developmental Biology.
- Bely, A. E. and Nyberg, K. G. (2010). Evolution of animal regeneration: re-emergence of a field. *Trends Ecol. Evol.* **25**, 161–170.
- Berking, S. (1979). Analysis of head and foot formation in Hydra by means of an endogenous inhibitor. *Wilhelm Roux Arch. Dev. Biol.* **186**, 189–210.
- Bernard, C., Vincent, C., Testa, D., Bertini, E., Ribot, J., Di Nardo, A. A., Volovitch, M. and Prochiantz, A. (2016). A Mouse Model for Conditional Secretion of Specific Single-Chain Antibodies Provides Genetic Evidence for Regulation of Cortical Plasticity by a Non-cell Autonomous Homeoprotein Transcription Factor. *PLoS Genet.* **12**, e1006035.
- Black, A. R., Black, J. D. and Azizkhan-Clifford, J. (2001). Sp1 and krüppel-like factor family of transcription factors in cell growth regulation and cancer. *J. Cell. Physiol.* **188**, 143–160.
- Bode, H. R. (2003). Head regeneration in Hydra. *Dev. Dyn. Off. Publ. Am. Assoc. Anat.* **226**, 225–236.
- Bode, H. R. (2009). Axial patterning in hydra. *Cold Spring Harb. Perspect. Biol.* **1**, a000463.

- Bode, P. M. and Bode, H. R.** (1980). Formation of pattern in regenerating tissue pieces of *hydra attenuata*. I. Head-body proportion regulation. *Dev. Biol.* **78**, 484–496.
- Boehm, A.-M., Khalturin, K., Anton-Erxleben, F., Hemmrich, G., Klostermeier, U. C., Lopez-Quintero, J. A., Oberg, H.-H., Puchert, M., Rosenstiel, P., Wittlieb, J., et al.** (2012). FoxO is a critical regulator of stem cell maintenance in immortal Hydra. *Proc. Natl. Acad. Sci. U. S. A.* **109**, 19697–19702.
- Bossert, P. and Galliot, B.** (2012). How to use Hydra as a model system to teach biology in the classroom. *Int. J. Dev. Biol.* **56**, 637–652.
- Broun, M. and Bode, H. R.** (2002). Characterization of the head organizer in hydra. *Dev. Camb. Engl.* **129**, 875–884.
- Broun, M., Gee, L., Reinhardt, B. and Bode, H. R.** (2005). Formation of the head organizer in hydra involves the canonical Wnt pathway. *Dev. Camb. Engl.* **132**, 2907–2916.
- Browne, E. N.** (1909). The production of new hydranths in Hydra by the insertion of small grafts. *J. Exp. Zool.* **7**, 1–23.
- Buzgariu, W., Al Haddad, S., Tomczyk, S., Wenger, Y. and Galliot, B.** (2015). Multi-functionality and plasticity characterize epithelial cells in Hydra. *Tissue Barriers* **3**, e1068908.
- Buzgariu, W., Wenger, Y., Tcaciuc, N., Catunda-Lemos, A.-P. and Galliot, B.** (2018). Impact of cycling cells and cell cycle regulation on Hydra regeneration. *Dev. Biol.* **433**, 240–253.
- Chapman, J. A., Kirkness, E. F., Simakov, O., Hampson, S. E., Mitros, T., Weinmaier, T., Rattei, T., Balasubramanian, P. G., Borman, J., Busam, D., et al.** (2010). The dynamic genome of Hydra. *Nature* **464**, 592–596.
- Chen, Y., Guo, Y., Ge, X., Itoh, H., Watanabe, A., Fujiwara, T., Kodama, T. and Aburatani, H.** (2006). Elevated expression and potential roles of human Sp5, a member of Sp transcription factor family, in human cancers. *Biochem. Biophys. Res. Commun.* **340**, 758–766.
- Chera, S., Ghila, L., Dobretz, K., Wenger, Y., Bauer, C., Buzgariu, W., Martinou, J.-C. and Galliot, B.** (2009). Apoptotic cells provide an unexpected source of Wnt3 signaling to drive hydra head regeneration. *Dev. Cell* **17**, 279–289.
- Clevers, H.** (2006). Wnt/beta-catenin signaling in development and disease. *Cell* **127**, 469–480.
- Clevers, H., Loh, K. M. and Nusse, R.** (2014). Stem cell signaling. An integral program for tissue renewal and regeneration: Wnt signaling and stem cell control. *Science* **346**, 1248012.

- Cohen, D. J. (2017). Sorting Things Out: Cell Sorting during Hydra Regeneration. *Biophys. J.* **113**, 2577–2578.
- Cohen, S. M. and Jürgens, G. (1990). Mediation of Drosophila head development by gap-like segmentation genes. *Nature* **346**, 482–485.
- Corish, P. and Tyler-Smith, C. (1999). Attenuation of green fluorescent protein half-life in mammalian cells. *Protein Eng.* **12**, 1035–1040.
- Croce, J. C. and McClay, D. R. (2006). The canonical Wnt pathway in embryonic axis polarity. *Semin. Cell Dev. Biol.* **17**, 168–174.
- Dailey, S. C., Kozmikova, I. and Somorjai, I. M. L. (2017). Amphioxus Sp5 is a member of a conserved Specificity Protein complement and is modulated by Wnt/ β -catenin signalling. *Int. J. Dev. Biol.* **61**, 723–732.
- David, C. N. (2012). Interstitial stem cells in Hydra: multipotency and decision-making. *Int. J. Dev. Biol.* **56**, 489–497.
- David, C. N. and Campbell, R. D. (1972). Cell Cycle Kinetics and Development of *Hydra Attenuata*. *J. Cell Sci.* **11**, 557–568.
- De Robertis, E. M. (2009). Spemann's organizer and the self-regulation of embryonic fields. *Mech. Dev.* **126**, 925–941.
- Dunty, W. C., Kennedy, M. W. L., Chalamalasetty, R. B., Campbell, K. and Yamaguchi, T. P. (2014). Transcriptional profiling of Wnt3a mutants identifies Sp transcription factors as essential effectors of the Wnt/ β -catenin pathway in neuromesodermal stem cells. *PLoS One* **9**, e87018.
- Elsy, M., Rowbotham, A., Lord, H., Isaacs, H. V. and Pownall, M. E. (2019). *Xenopus laevis* FGF16 activates the expression of genes coding for the transcription factors Sp5 and Sp5l. *Int. J. Dev. Biol.* **63**, 631–639.
- Franzenburg, S., Fraune, S., Künzel, S., Baines, J. F., Domazet-Lošo, T. and Bosch, T. C. G. (2012). MyD88-deficient Hydra reveal an ancient function of TLR signaling in sensing bacterial colonizers. *Proc. Natl. Acad. Sci. U. S. A.* **109**, 19374–19379.
- Fujimura, N., Vacik, T., Machon, O., Vlcek, C., Scalabrin, S., Speth, M., Diep, D., Krauss, S. and Kozmik, Z. (2007). Wnt-mediated down-regulation of Sp1 target genes by a transcriptional repressor Sp5. *J. Biol. Chem.* **282**, 1225–1237.
- Gahan, J. M., Schnitzler, C. E., DuBuc, T. Q., Doonan, L. B., Kanska, J., Gornik, S. G., Barreira, S., Thompson, K., Schiffer, P., Baxevanis, A. D., et al. (2017). Functional studies on the role of Notch signaling in Hydractinia development. *Dev. Biol.* **428**, 224–231.
- Galliot, B. (2012). Hydra, a fruitful model system for 270 years. *Int. J. Dev. Biol.* **56**, 411–423.

- Galliot, B. and Chera, S. (2010). The Hydra model: disclosing an apoptosis-driven generator of Wnt-based regeneration. *Trends Cell Biol.* **20**, 514–523.
- Galliot, B. and Ghila, L. (2010). Cell plasticity in homeostasis and regeneration. *Mol. Reprod. Dev.* **77**, 837–855.
- Gee, L., Hartig, J., Law, L., Wittlieb, J., Khalturin, K., Bosch, T. C. G. and Bode, H. R. (2010). beta-catenin plays a central role in setting up the head organizer in hydra. *Dev. Biol.* **340**, 116–124.
- Gierer, A. and Meinhardt, H. (1972). A theory of biological pattern formation. *Kybernetik* **12**, 30–39.
- Gierer, A., Berking, S., Bode, H., David, C. N., Flick, K., Hansmann, G., Schaller, H. and Trenkner, E. (1972). Regeneration of hydra from reaggregated cells. *Nature. New Biol.* **239**, 98–101.
- Goel, T., Wang, R., Martin, S., Lanphear, E. and Collins, E.-M. S. (2019). Linalool acts as a fast and reversible anesthetic in Hydra. *PLoS One* **14**, e0224221.
- Guder, C., Pinho, S., Nacak, T. G., Schmidt, H. A., Hobmayer, B., Niehrs, C. and Holstein, T. W. (2006). An ancient Wnt-Dickkopf antagonism in *Hydra*. *Development* **133**, 901–911.
- Gufler, S., Artes, B., Bielen, H., Krainer, I., Eder, M.-K., Falschlunger, J., Bollmann, A., Ostermann, T., Valovka, T., Hartl, M., et al. (2018). β -Catenin acts in a position-independent regeneration response in the simple eumetazoan Hydra. *Dev. Biol.* **433**, 310–323.
- Gurley, K. A., Rink, J. C. and Sánchez Alvarado, A. (2008). Beta-catenin defines head versus tail identity during planarian regeneration and homeostasis. *Science* **319**, 323–327.
- Gurtner, G. C., Werner, S., Barrandon, Y. and Longaker, M. T. (2008). Wound repair and regeneration. *Nature* **453**, 314–321.
- Hamada, M., Satoh, N. and Khalturin, K. (2020). A Reference Genome from the Symbiotic Hydrozoan, *Hydra viridissima*. *G3 Bethesda Md* **10**, 3883–3895.
- Harrison, S. M., Houzelstein, D., Dunwoodie, S. L. and Beddington, R. S. (2000). Sp5, a new member of the Sp1 family, is dynamically expressed during development and genetically interacts with Brachyury. *Dev. Biol.* **227**, 358–372.
- Hemmrich, G., Anokhin, B., Zacharias, H. and Bosch, T. C. G. (2007). Molecular phylogenetics in Hydra, a classical model in evolutionary developmental biology. *Mol. Phylogenet. Evol.* **44**, 281–290.
- Hemmrich, G., Khalturin, K., Boehm, A.-M., Puchert, M., Anton-Erxleben, F., Wittlieb, J., Klostermeier, U. C., Rosenstiel, P., Oberg, H.-H., Domazet-Loso, T., et al. (2012).

- Molecular signatures of the three stem cell lineages in hydra and the emergence of stem cell function at the base of multicellularity. *Mol. Biol. Evol.* **29**, 3267–3280.
- Hobmayer, B., Rentzsch, F., Kuhn, K., Happel, C. M., von Laue, C. C., Snyder, P., Rothbacher, U. and Holstein, T. W. (2000). WNT signalling molecules act in axis formation in the diploblastic metazoan Hydra. *Nature* **407**, 186–189.
- Huggins, I. J., Bos, T., Gaylord, O., Jessen, C., Lonquich, B., Puranen, A., Richter, J., Rossdam, C., Brafman, D., Gaasterland, T., et al. (2017). The WNT target SP5 negatively regulates WNT transcriptional programs in human pluripotent stem cells. *Nat. Commun.* **8**, 1034.
- Ikmi, A., McKinney, S. A., Delventhal, K. M. and Gibson, M. C. (2014). TALEN and CRISPR/Cas9-mediated genome editing in the early-branching metazoan *Nematostella vectensis*. *Nat. Commun.* **5**, 5486.
- Janssen, R. and Budd, G. E. (2020). Expression of the zinc finger transcription factor Sp6-9 in the velvet worm *Euperipatoides kanangrensis* suggests a conserved role in appendage development in Panarthropoda. *Dev. Genes Evol.* **230**, 239–245.
- Joven, A., Elewa, A. and Simon, A. (2019). Model systems for regeneration: salamanders. *Dev. Camb. Engl.* **146**, dev167700.
- Kaczynski, J., Cook, T. and Urrutia, R. (2003). Sp1- and Krüppel-like transcription factors. *Genome Biol.* **4**, 206.
- Kawakami, Y., Rodriguez Esteban, C., Raya, M., Kawakami, H., Martí, M., Dubova, I. and Izpisua Belmonte, J. C. (2006). Wnt/beta-catenin signaling regulates vertebrate limb regeneration. *Genes Dev.* **20**, 3232–3237.
- Kelly, C., Chin, A. J., Leatherman, J. L., Kozlowski, D. J. and Weinberg, E. S. (2000). Maternally controlled (beta)-catenin-mediated signaling is required for organizer formation in the zebrafish. *Development* **127**, 3899–3911.
- Kennedy, M. W., Chalamalasetty, R. B., Thomas, S., Garriock, R. J., Jailwala, P. and Yamaguchi, T. P. (2016). Sp5 and Sp8 recruit β -catenin and Tcf1-Lef1 to select enhancers to activate Wnt target gene transcription. *Proc. Natl. Acad. Sci. U. S. A.* **113**, 3545–3550.
- Kim, C.-K., He, P., Bialkowska, A. B. and Yang, V. W. (2017). SP and KLF Transcription Factors in Digestive Physiology and Diseases. *Gastroenterology* **152**, 1845–1875.
- Klimovich, A., Rehm, A., Wittlieb, J., Herbst, E.-M., Benavente, R. and Bosch, T. C. G. (2018). Non-senescent Hydra tolerates severe disturbances in the nuclear lamina. *Aging* **10**, 951–972.

- Klimovich, A., Wittlieb, J. and Bosch, T. C. G. (2019). Transgenesis in Hydra to characterize gene function and visualize cell behavior. *Nat. Protoc.* **14**, 2069–2090.
- Kragl, M., Knapp, D., Nacu, E., Khattak, S., Maden, M., Epperlein, H. H. and Tanaka, E. M. (2009). Cells keep a memory of their tissue origin during axolotl limb regeneration. *Nature* **460**, 60–65.
- Lapébie, P., Gazave, E., Ereskovsky, A., Derelle, R., Bézac, C., Renard, E., Houliston, E. and Borchiellini, C. (2009). WNT/ β -Catenin Signalling and Epithelial Patterning in the Homoscleromorph Sponge *Oscarella*. *PLoS ONE* **4**, e5823.
- Lengfeld, T., Watanabe, H., Simakov, O., Lindgens, D., Gee, L., Law, L., Schmidt, H. A., Ozbek, S., Bode, H. and Holstein, T. W. (2009). Multiple Wnts are involved in Hydra organizer formation and regeneration. *Dev. Biol.* **330**, 186–199.
- Lenhoff, H. M. (1991). Ethel Browne, Hans Spemann, and the Discovery of the Organizer Phenomenon. *Biol. Bull.* **181**, 72–80.
- Li, Q., Yang, H. and Zhong, T. P. (2015). Regeneration across metazoan phylogeny: lessons from model organisms. *J. Genet. Genomics Yi Chuan Xue Bao* **42**, 57–70.
- Lommel, M., Tursch, A., Rustarazo-Calvo, L., Trageser, B. and Holstein, T. W. (2017). *Genetic knockdown and knockout approaches in Hydra*. Developmental Biology.
- Lommel, M., Strompen, J., Hellewell, A. L., Balasubramanian, G. P., Christofidou, E. D., Thomson, A. R., Boyle, A. L., Woolfson, D. N., Puglisi, K., Hartl, M., et al. (2018). Hydra Mesoglea Proteome Identifies Thrombospondin as a Conserved Component Active in Head Organizer Restriction. *Sci. Rep.* **8**, 11753.
- MacDonald, B. T., Tamai, K. and He, X. (2009). Wnt/beta-catenin signaling: components, mechanisms, and diseases. *Dev. Cell* **17**, 9–26.
- MacWilliams, H. K. (1983a). Hydra transplantation phenomena and the mechanism of Hydra head regeneration. II. Properties of the head activation. *Dev. Biol.* **96**, 239–257.
- MacWilliams, H. K. (1983b). Hydra transplantation phenomena and the mechanism of hydra head regeneration. I. Properties of the head inhibition. *Dev. Biol.* **96**, 217–238.
- MacWilliams, H. K. and Kafatos, F. C. (1968). Hydra viridis: inhibition by the basal disk of basal disk differentiation. *Science* **159**, 1246–1247.
- Marcum, B. A. and Campbell, R. D. (1978). Development of Hydra lacking nerve and interstitial cells. *J. Cell Sci.* **29**, 17–33.

- Marques, I. J., Lupi, E. and Mercader, N. (2019). Model systems for regeneration: zebrafish. *Dev. Camb. Engl.* **146**, dev167692.
- Martínez, D. E., Iñiguez, A. R., Percell, K. M., Willner, J. B., Signorovitch, J. and Campbell, R. D. (2010). Phylogeny and biogeography of Hydra (Cnidaria: Hydridae) using mitochondrial and nuclear DNA sequences. *Mol. Phylogenet. Evol.* **57**, 403–410.
- Mercker, M., Kazarnikov, A., Tursch, A., Özbek, S., Holstein, T. and Marciniak-Czochra, A. (2021). *How Dickkopf molecules and Wnt/β-catenin interplay to self-organise the Hydra body axis*. Developmental Biology.
- Miller, J. R. (2002). The Wnts. *Genome Biol.* **3**, REVIEWS3001.
- Mulligan, K. A., Fuerer, C., Ching, W., Fish, M., Willert, K. and Nusse, R. (2012). Secreted Wingless-interacting molecule (Swim) promotes long-range signaling by maintaining Wingless solubility. *Proc. Natl. Acad. Sci. U. S. A.* **109**, 370–377.
- Nagasue, N., Yukaya, H., Ogawa, Y., Kohno, H. and Nakamura, T. (1987). Human liver regeneration after major hepatic resection. A study of normal liver and livers with chronic hepatitis and cirrhosis. *Ann. Surg.* **206**, 30–39.
- Nakamura, Y., Tsiairis, C. D., Özbek, S. and Holstein, T. W. (2011). Autoregulatory and repressive inputs localize Hydra Wnt3 to the head organizer. *Proc. Natl. Acad. Sci. U. S. A.* **108**, 9137–9142.
- Neumann, S., Coudreuse, D. Y. M., van der Westhuyzen, D. R., Eckhardt, E. R. M., Korswagen, H. C., Schmitz, G. and Sprong, H. (2009). Mammalian Wnt3a is released on lipoprotein particles. *Traffic Cph. Den.* **10**, 334–343.
- Nusse, R. and Clevers, H. (2017). Wnt/β-Catenin Signaling, Disease, and Emerging Therapeutic Modalities. *Cell* **169**, 985–999.
- Okamura, D. M., Brewer, C. M., Wakenight, P., Bahrami, N., Bernardi, K., Tran, A., Olson, J., Shi, X., Yeh, S.-Y., Piliponsky, A., et al. (2021). Spiny mice activate unique transcriptional programs after severe kidney injury regenerating organ function without fibrosis. *iScience* **24**, 103269.
- Orlic, D., Kajstura, J., Chimenti, S., Bodine, D. M., Leri, A. and Anversa, P. (2003). Bone marrow stem cells regenerate infarcted myocardium. *Pediatr. Transplant.* **7** Suppl 3, 86–88.
- Ossipova, O., Stick, R. and Pieler, T. (2002). XSPR-1 and XSPR-2, novel Sp1 related zinc finger containing genes, are dynamically expressed during Xenopus embryogenesis. *Mech. Dev.* **115**, 117–122.
- Otto, J. J. and Campbell, R. D. (1977). Budding in Hydra attenuata: bud stages and fate map. *J. Exp. Zool.* **200**, 417–428.

- Pallas, P. S. (1766). *Elenchus zoophytorum sistens generum adumbrationes generaliores et specierum cognitarum succintas descriptiones, cum selectis auctorum synonymis* / P. S. Pallas. Hagae-Comitum : Apud Petrum van Cleef.
- Panáková, D., Sprong, H., Marois, E., Thiele, C. and Eaton, S. (2005). Lipoprotein particles are required for Hedgehog and Wingless signalling. *Nature* **435**, 58–65.
- Park, E., Hwang, D.-S., Lee, J.-S., Song, J.-I., Seo, T.-K. and Won, Y.-J. (2012). Estimation of divergence times in cnidarian evolution based on mitochondrial protein-coding genes and the fossil record. *Mol. Phylogenet. Evol.* **62**, 329–345.
- Park, D.-S., Seo, J.-H., Hong, M., Bang, W., Han, J.-K. and Choi, S.-C. (2013). Role of Sp5 as an essential early regulator of neural crest specification in xenopus. *Dev. Dyn. Off. Publ. Am. Assoc. Anat.* **242**, 1382–1394.
- Petersen, C. P. and Reddien, P. W. (2008). Smed-betacatenin-1 is required for anteroposterior blastema polarity in planarian regeneration. *Science* **319**, 327–330.
- Petersen, C. P. and Reddien, P. W. (2009). Wnt signaling and the polarity of the primary body axis. *Cell* **139**, 1056–1068.
- Petersen, H. O., Höger, S. K., Looso, M., Lengfeld, T., Kuhn, A., Warnken, U., Nishimiya-Fujisawa, C., Schnölzer, M., Krüger, M., Özbek, S., et al. (2015). A Comprehensive Transcriptomic and Proteomic Analysis of Hydra Head Regeneration. *Mol. Biol. Evol.* **32**, 1928–1947.
- Poss, K. D. (2010). Advances in understanding tissue regenerative capacity and mechanisms in animals. *Nat. Rev. Genet.* **11**, 710–722.
- Price, J. S., Allen, S., Faucheux, C., Althnaian, T. and Mount, J. G. (2005). Deer antlers: a zoological curiosity or the key to understanding organ regeneration in mammals? *J. Anat.* **207**, 603–618.
- Ramirez, A. N., Loubet-Seneor, K. and Srivastava, M. (2020). A Regulatory Program for Initiation of Wnt Signaling during Posterior Regeneration. *Cell Rep.* **32**, 108098.
- Rand, H. W., Bovard, J. F. and Minnich, D. E. (1926). Localization of Formative Agencies in Hydra. *Proc. Natl. Acad. Sci. U. S. A.* **12**, 565–570.
- Reddien, P. W. and Sánchez Alvarado, A. (2004). Fundamentals of planarian regeneration. *Annu. Rev. Cell Dev. Biol.* **20**, 725–757.
- Reuter, H., März, M., Vogg, M. C., Eccles, D., Grífol-Boldú, L., Wehner, D., Owlarn, S., Adell, T., Weidinger, G. and Bartscherer, K. (2015). B-catenin-dependent control of positional information along the AP body axis in planarians involves a teashirt family member. *Cell Rep.* **10**, 253–265.

- Rodrigues, M., Leclère, P., Flammang, P., Hess, M. W., Salvenmoser, W., Hobmayer, B. and Ladurner, P. (2016). The cellular basis of bioadhesion of the freshwater polyp Hydra. *BMC Zool.* **1**, 3.
- Safe, S. and Abdelrahim, M. (2005). Sp transcription factor family and its role in cancer. *Eur. J. Cancer Oxf. Engl. 1990* **41**, 2438–2448.
- Sánchez Alvarado, A. (2000). Regeneration in the metazoans: why does it happen? *BioEssays News Rev. Mol. Cell. Dev. Biol.* **22**, 578–590.
- Schaeper, N. D., Prpic, N.-M. and Wimmer, E. A. (2010). A clustered set of three Sp-family genes is ancestral in the Metazoa: evidence from sequence analysis, protein domain structure, developmental expression patterns and chromosomal location. *BMC Evol. Biol.* **10**, 88.
- Seifert, A. W., Kiama, S. G., Seifert, M. G., Goheen, J. R., Palmer, T. M. and Maden, M. (2012). Skin shedding and tissue regeneration in African spiny mice (Acomys). *Nature* **489**, 561–565.
- Shimizu, H. (2012). Transplantation analysis of developmental mechanisms in Hydra. *Int. J. Dev. Biol.* **56**, 463–472.
- Shimizu, T., Bae, Y.-K., Muraoka, O. and Hibi, M. (2005). Interaction of Wnt and caudal-related genes in zebrafish posterior body formation. *Dev. Biol.* **279**, 125–141.
- Siebert, S., Farrell, J. A., Cazet, J. F., Abeykoon, Y., Primack, A. S., Schnitzler, C. E. and Juliano, C. E. (2019). Stem cell differentiation trajectories in Hydra resolved at single-cell resolution. *Science* **365**, eaav9314.
- Spallanzani, Lazzaro (1768). *Prodromo di un'opera da imprimersi sopra le riproduzioni animali*. Montanari.
- Spemann, H. and Mangold, H. (1924). über Induktion von Embryonalanlagen durch Implantation artfremder Organisatoren. *Arch. Für Mikrosk. Anat. Entwicklungsmechanik* **100**, 599–638.
- Stanganello, E. and Scholpp, S. (2016). Role of cytonemes in Wnt transport. *J. Cell Sci.* **129**, 665–672.
- Stoick-Cooper, C. L., Weidinger, G., Riehle, K. J., Hubbert, C., Major, M. B., Fausto, N. and Moon, R. T. (2007). Distinct Wnt signaling pathways have opposing roles in appendage regeneration. *Dev. Camb. Engl.* **134**, 479–489.
- Suske, G. (1999). The Sp-family of transcription factors. *Gene* **238**, 291–300.
- Suske, G., Bruford, E. and Philipson, S. (2005). Mammalian SP/KLF transcription factors: bring in the family. *Genomics* **85**, 551–556.

- Takahashi, M., Nakamura, Y., Obama, K. and Furukawa, Y.** (2005). Identification of SP5 as a downstream gene of the beta-catenin/Tcf pathway and its enhanced expression in human colon cancer. *Int. J. Oncol.* **27**, 1483–1487.
- Takano, J. and Sugiyama, T.** (1983). Genetic analysis of developmental mechanisms in hydra. VIII. Head-activation and head-inhibition potentials of a slow-budding strain (L4). *J. Embryol. Exp. Morphol.* **78**, 141–168.
- Tallafuss, A., Wilm, T. P., Crozatier, M., Pfeffer, P., Wassef, M. and Bally-Cuif, L.** (2001). The zebrafish buttonhead-like factor Bts1 is an early regulator of pax2.1 expression during mid-hindbrain development. *Dev. Camb. Engl.* **128**, 4021–4034.
- Tanaka, E. M. and Reddien, P. W.** (2011). The cellular basis for animal regeneration. *Dev. Cell* **21**, 172–185.
- Technau, U. and Holstein, T. W.** (1992). Cell sorting during the regeneration of Hydra from reaggregated cells. *Dev. Biol.* **151**, 117–127.
- Tewari, A. G., Owen, J. H., Petersen, C. P., Wagner, D. E. and Reddien, P. W.** (2019). A small set of conserved genes, including sp5 and Hox, are activated by Wnt signaling in the posterior of planarians and acoels. *PLoS Genet.* **15**, e1008401.
- Thomas Hunt Morgan** (1901). *Regeneration*. Macmillan.
- Thorpe, C. J., Weidinger, G. and Moon, R. T.** (2005). Wnt/beta-catenin regulation of the Sp1-related transcription factor sp5l promotes tail development in zebrafish. *Dev. Camb. Engl.* **132**, 1763–1772.
- Treichel, D., Becker, M. B. and Gruss, P.** (2001). The novel transcription factor gene Sp5 exhibits a dynamic and highly restricted expression pattern during mouse embryogenesis. *Mech. Dev.* **101**, 175–179.
- Turing** (1952). The chemical basis of morphogenesis. *Philos. Trans. R. Soc. Lond. B. Biol. Sci.* **237**, 37–72.
- Turner, J. and Crossley, M.** (1999). Mammalian Krüppel-like transcription factors: more than just a pretty finger. *Trends Biochem. Sci.* **24**, 236–240.
- Vogg, M. C., Beccari, L., Iglesias Ollé, L., Rampon, C., Vríz, S., Perruchoud, C., Wenger, Y. and Galliot, B.** (2019a). An evolutionarily-conserved Wnt3/ β -catenin/Sp5 feedback loop restricts head organizer activity in Hydra. *Nat. Commun.* **10**, 312.
- Vogg, M. C., Galliot, B. and Tsiarris, C. D.** (2019b). Model systems for regeneration: Hydra. *Development* **146**, dev177212.
- Wardle, F. C. and Tan, H.** (2015). A ChIP on the shoulder? Chromatin immunoprecipitation and validation strategies for ChIP antibodies. *F1000Research* **4**, 235.

- Watanabe, H., Schmidt, H. A., Kuhn, A., Höger, S. K., Kocagöz, Y., Laumann-Lipp, N., Ozbek, S. and Holstein, T. W. (2014). Nodal signalling determines biradial asymmetry in Hydra. *Nature* **515**, 112–115.
- Webster, G. (1966). Studies on pattern regulation in hydra. II. Factors controlling hypostome formation. *J. Embryol. Exp. Morphol.* **16**, 105–122.
- Webster, G. and Wolpert, L. (1966). Studies on pattern regulation in hydra. I. Regional differences in time required for hypostome determination. *J. Embryol. Exp. Morphol.* **16**, 91–104.
- Wehner, D., Cizelsky, W., Vasudevaro, M. D., Ozhan, G., Haase, C., Kagermeier-Schenk, B., Röder, A., Dorsky, R. I., Moro, E., Argenton, F., et al. (2014). Wnt/ β -catenin signaling defines organizing centers that orchestrate growth and differentiation of the regenerating zebrafish caudal fin. *Cell Rep.* **6**, 467–481.
- Weidinger, G., Thorpe, C. J., Wuennenberg-Stapleton, K., Ngai, J. and Moon, R. T. (2005). The Sp1-related transcription factors sp5 and sp5-like act downstream of Wnt/ β -catenin signaling in mesoderm and neuroectoderm patterning. *Curr. Biol. CB* **15**, 489–500.
- Wenger, Y. and Galliot, B. (2013). RNAseq versus genome-predicted transcriptomes: a large population of novel transcripts identified in an Illumina-454 Hydra transcriptome. *BMC Genomics* **14**, 204.
- Wenger, Y., Buzgariu, W. and Galliot, B. (2016). Loss of neurogenesis in Hydra leads to compensatory regulation of neurogenic and neurotransmission genes in epithelial cells. *Philos. Trans. R. Soc. Lond. B. Biol. Sci.* **371**, 20150040.
- Wenger, Y., Buzgariu, W., Perruchoud, C., Loichot, G. and Galliot, B. (2019a). *Generic and context-dependent gene modulations during Hydra whole body regeneration*. Developmental Biology.
- Wenger, Y., Buzgariu, W., Perruchoud, C., Loichot, G. and Galliot, B. (2019b). *Generic and context-dependent gene modulations during Hydra whole body regeneration*. Developmental Biology.
- Willert, K., Brown, J. D., Danenberg, E., Duncan, A. W., Weissman, I. L., Reya, T., Yates, J. R. and Nusse, R. (2003). Wnt proteins are lipid-modified and can act as stem cell growth factors. *Nature* **423**, 448–452.
- Wimmer, E. A., Frommer, G., Purnell, B. A. and Jäckle, H. (1996). buttonhead and D-Spl: a novel Drosophila gene pair. *Mech. Dev.* **59**, 53–62.
- Wittlieb, J., Khalturin, K., Lohmann, J. U., Anton-Erxleben, F. and Bosch, T. C. G. (2006). Transgenic Hydra allow *in vivo* tracking of individual stem cells during morphogenesis. *Proc. Natl. Acad. Sci.* **103**, 6208–6211.

- Yoshioka-Kobayashi, K., Matsumiya, M., Niino, Y., Isomura, A., Kori, H., Miyawaki, A. and Kageyama, R.** (2020). Coupling delay controls synchronized oscillation in the segmentation clock. *Nature* **580**, 119–123.
- Zacharias, H., Anokhin, B., Khalturin, K. and Bosch, T. C. G.** (2004). Genome sizes and chromosomes in the basal metazoan Hydra. *Zool. Jena Ger.* **107**, 219–227.
- Zhang, J. S., Moncrieffe, M. C., Kaczynski, J., Ellenrieder, V., Prendergast, F. G. and Urrutia, R.** (2001). A conserved alpha-helical motif mediates the interaction of Sp1-like transcriptional repressors with the corepressor mSin3A. *Mol. Cell. Biol.* **21**, 5041–5049.
- Zhao, J., Cao, Y., Zhao, C., Postlethwait, J. and Meng, A.** (2003). An SP1-like transcription factor Spr2 acts downstream of Fgf signaling to mediate mesoderm induction. *EMBO J.* **22**, 6078–6088.
- Ziegler, B., Yiallourous, I., Trageser, B., Kumar, S., Mercker, M., Kling, S., Fath, M., Warnken, U., Schnölzer, M., Holstein, T. W., et al.** (2021). The Wnt-specific astacin proteinase HAS-7 restricts head organizer formation in Hydra. *BMC Biol.* **19**, 120.

APENDIX 1: Construct maps

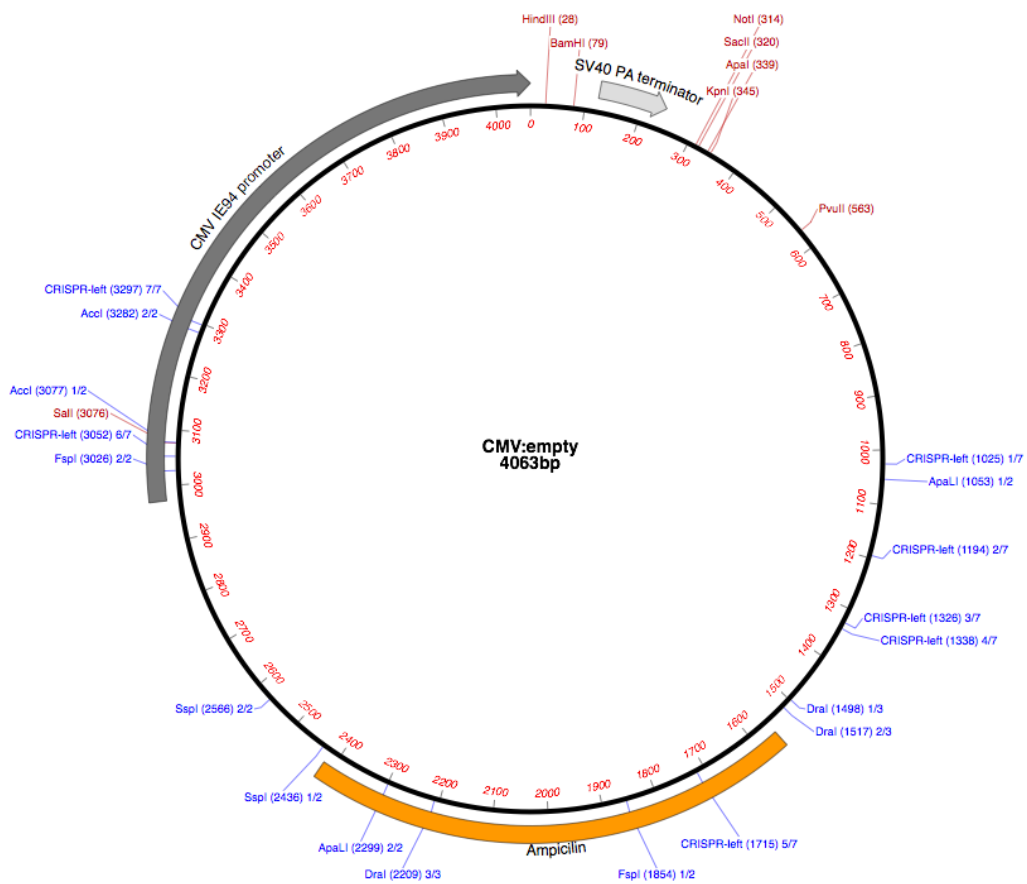
Construct name: pCS2+empty

Made by: Addgene

Backbone: pCS2+

Promoter: CMV

Insert: -



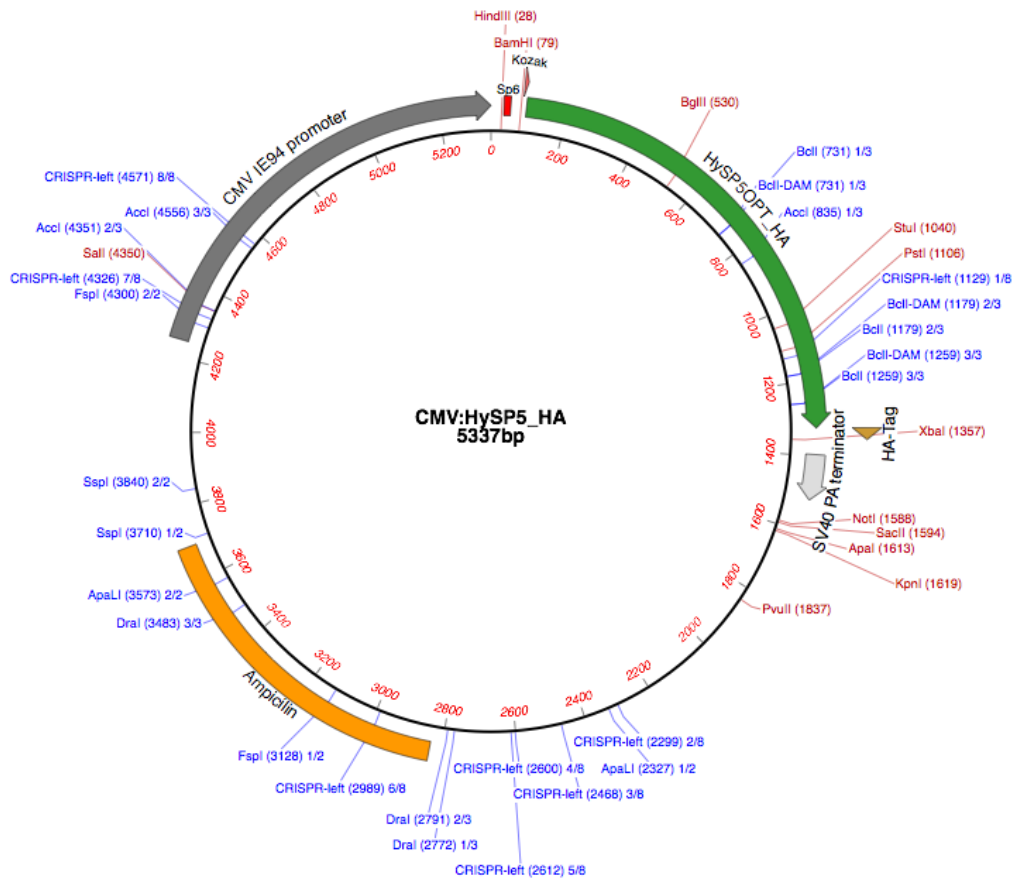
Construct name: pCS2+HySp5

Made by: GenScript

Backbone: pCS2+

Promoter: CMV

Insert: HySp5-HA



Construct name: HyActin:mCherry-HySp5:GFP

Made by: Laura Iglesias and GenScript

Backbone: pBSSA-AR (plasmid from T. Holstein lab)

Promoter: Hydra Actin and Hydra Sp5

Insert: Hydra Sp5 promoter and replacement of dsRED to mCherry

